

Deciphering the Indoleacetic Acid Biosynthesis Pathways in the Rhizobacterium *Pseudomonas* sp. UW4

by

Daiana Duca

A thesis
presented to the University of Waterloo
in fulfillment of the
thesis requirement for the degree of
Doctor of Philosophy
in
Biology

Waterloo, Ontario, Canada, 2017

©Daiana Duca 2017

Examining Committee Membership

The following served on the Examining Committee for this thesis. The decision of the Examining Committee is by majority vote.

Dr. Bernard Glick Supervisor	Professor	Ph. D.
Dr. David Rose Co-Supervisor	Professor	Ph. D.
Dr. Kirsten Muller Thesis Examination Committee Member	Professor	Ph. D.
Dr. Trevor Charles Thesis Examination Committee Member	Professor	Ph. D.
Dr. Raymond Legge Internal External Thesis Examination Committee Member Department of Chemical Engineering University of Waterloo	Professor	Ph. D.
Dr. Manish Raizada External Thesis Examination Committee Member Department of Plant Agriculture University of Guelph Guelph, ON.	Professor	Ph. D.

Author's Declaration

I hereby declare that I am the sole author of this thesis. This is a true copy of the thesis, including any required final revisions, as accepted by my examiners.

I understand that my thesis may be made electronically available to the public.

Abstract

Healthy plants host, within and on the surfaces of their tissues, diverse endophytic and epiphytic bacteria. Often, this interaction is mutualistic, leading to adaptive benefits for both partners. We refer to these beneficial microbes as plant growth-promoting bacteria (PGPB), as they can have a tremendous positive influence on plant health, yield and productivity. PGPBs can be used as natural biofertilizers to promote plant growth in an environmentally responsible manner. One of the main mechanisms used by PGPB to enhance plant growth is the production of indoleacetic acid (IAA). This compound is central to a plant's lifecycle and overall functioning. Because of the indispensable role of IAA in plant-growth promotion, there is great interest in genetic manipulation of IAA biosynthesis to maximize phytostimulation. This is a cumbersome task, as the nature of IAA biosynthesis is convoluted; multiple, independent and inter-dependent pathways operate within a single bacterium. The research reported herein strived to decipher the IAA biosynthesis pathways at the genetic and biochemical level, in a particularly effective PGPB known as *Pseudomonas* sp. UW4. This remarkable rhizobacterium has been shown to enhance plant growth in the presence of flooding, heavy metals, cold, high levels of salt, and phytopathogens. The entire genome of strain UW4 was sequenced in our lab and seven genes were implicated to encode enzymes involved in the indole acetonitrile (IAN) and indoleacetamide (IAM) pathways of IAA biosynthesis. In this work, some of these enzymes were isolated and their catalytic activity was experimentally verified through biochemical assays. Transformants of strain UW4 with increased IAA biosynthetic capacity were created by introducing a second copy of the target IAA-genes, and canola seedlings inoculated with these transformants displayed enhanced root growth. Mutagenesis experiments were undertaken to create deletions in all seven IAA-genes, in order to delineate which of the genes/pathways contribute most to IAA production in this strain. Failure to produce mutants with a reduced ability to synthesize IAA, led to speculation of a third pathway. Biochemical evidence of this pathway is based on the detection of the IPyA metabolite. The IPyA pathway appears to be predominant in strain UW4 and can compensate for disruptions in the IAN/IAM pathways. Genomic screens identified several candidate IPyA pathway genes, however the functional roles of the encoded enzymes remain to be determined. Altogether, this work describes three interconnected IAA biosynthetic pathways in strain UW4.

Acknowledgements

Yu Gu and the Ron Johnson Lab at the University of Guelph are gratefully acknowledged for their technical support with the HPLC analyses. Richard Smith is also kindly acknowledged for LC-MS-MS training. I also thank Kirsten Muller at the University of Waterloo for her guidance with the phylogenetic analyses and all my colleagues who provided insight and expertise that greatly assisted the research. Finally, I wish to recognize and thank Janet Lorv and Merium Fernando for their help with mutant screens and enzyme assays.

Dedications

To my parents and my brother - this work is dedicated to you. You have always been an unwavering source of support and encouragement during the challenges of grad school and throughout my entire life. There are no words to describe the love and immense gratitude that I feel for the three of you. Thank you for believing in me and loving me unconditionally. Thank you for the sacrifices you have made to give me every opportunity to succeed. This accomplishment would not have been possible without you.

To Bernie, thank you for your wisdom, guidance and inspiration. You have taught me to be a scientist and if I become only half the thinker, half the teacher, half the person that you are, it will surely be one of my greatest accomplishments.

To my friends, my home team, my middle-of-the-night, no-matter-what people, thank you for sticking with me all these years, for loving and understanding me throughout my sometimes weird, distant introvert phases. You know who you are- I love you.

To Kas-it is entirely possible that I would not have made it through undergrad had you not been there with me every day, every class; and that I would have drowned in the sea of grad research had you not been there to keep my head above the water. You have helped me more than you know.

Sometimes you get lucky and you find a soul that grooves with yours. ***To the Alien***- you are a monument of mind. Thank you for the sustenance when I was overwhelmed with writing this thesis and for nourishing my mind when I was starved of insight. I may have never had a moment from myself had you not been as important a part of my life, my consciousness, as you are. Lace up your shoes, I'll pack a bag and let's get lost in a worldly adventure for a while...

Table of Contents

Examining Committee Membership	ii
Author's Declaration	iii
Abstract	iv
Acknowledgements	v
List of Figures	x
List of Tables	xi
Chapter 1	1
Introduction and Literature Review	1
1.1 Plant-Microbe Interactions.....	1
1.2 Application of Plant-Growth-Promoting Bacteria.....	2
1.3 Plant Indoleacetic Acid (IAA).....	5
1.4 Bacterial IAA in Plant-Microbe Interactions	6
1.4.1 Bacterial IAA and Pathogenesis.....	7
1.4.2 Bacterial IAA and the Promotion of Plant Growth.....	11
1.5 The Biological Function of IAA in Bacteria.....	14
1.6 IAA Biosynthesis Pathways.....	20
1.6.1 The Indole-Pyruvic Acid (IPyA) Pathway.....	20
1.6.2 The Indoleacetamide (IAM) Pathway.....	25
1.6.3 The Indoleacetaldoxime (IAOx)-Indoleacetonitrile (IAN) Pathway.....	29
1.7 Factors Modulating IAA Production in Bacteria.....	31
1.8 Genetic Factors involved in the regulation of IAA Biosynthesis.....	40
1.9 Introduction to Thesis	46
1.9.1 Research Goals.....	50
1.9.2 Organization of thesis.....	52
Chapter 2	53
Biochemical Characterization of an Amidase that converts Indoleacetamide into Indoleacetic acid	53
2.1 Introduction.....	53
2.2 Materials and Methods.....	55
2.2.1 Bacterial Strains and Plasmids.....	55
2.2.2 DNA Extraction and Expression Plasmid Construction	58
2.2.3 Overexpression of Recombinant Ami in <i>E. coli</i>	58
2.2.4 Purification of the Recombinant Ami protein.....	59
2.2.5 Enzyme Assay	59
2.2.6 Temperature and pH optima for Ami activity.....	60
2.2.7 High Performance Liquid Chromatography (HPLC) Analysis	60
2.2.8 Multiple Sequence Alignment & Phylogenetic Analysis	61
2.3 Results and Discussion	61
2.3.1 Physicochemical Properties of Ami from strain UW4.....	62
2.3.2 Biochemical Characterization of Ami Catalytic Activity.....	65
2.3.3 Multiple Sequence Alignment of Amidases	68
2.3.4 Domain Analysis and Structural Comparisons of Signature Amidases	75
2.3.5 Phylogenetic Analyses of Amidases.....	77
2.3.6 Organization of Amidase Genes in Bacterial Genomes	81
2.4 Conclusion.....	84

Chapter 3	86
Construction and Characterization of IAA-Overproducing Transformants of <i>Pseudomonas</i> sp. UW4	86
3.1 Introduction.....	86
3.2 Materials and Methods.....	89
3.2.1 Bacterial Strains and Plasmids.....	89
3.2.2 DNA Amplification	91
3.2.3 Tri-Parental Mating.....	92
3.2.4 High Performance Liquid Chromatography (HPLC) Analysis	92
3.2.5 ACC Deaminase Assay.....	93
3.2.6 Bacterial Growth Curve.....	93
3.2.7 Real-Time Quantitative PCR Analyses.....	93
3.2.8 Growth Pouch Assay.....	94
3.2.9 Statistical Analyses.....	95
3.3 Results	95
3.3.1 IAA Production.....	95
3.3.2 ACC Deaminase Activity.....	96
3.3.3 Transcriptional Analyses (Real-Time qPCR)	97
3.3.4 Bacterial Growth Curves	98
3.3.5 Effect on Plant Growth.....	101
3.4 Discussion.....	102
3.5 Conclusion.....	111
Chapter 4	115
Construction and Characterization of IAA-Knockout Mutants.....	115
4.1 Introduction.....	115
4.2 Materials and Methods.....	117
4.2.1 Bacterial Strains and Plasmids.....	117
4.2.2 DNA Manipulation	117
4.2.3 Bacterial Conjugation & Gene Sequencing.....	126
4.2.4 HPLC Analysis	127
4.2.5 Liquid Chromatography-Tandem Mass Spectrometry (LC-MS-MS).....	127
4.3 Results & Discussion	129
4.3.1 IAA-Gene Knockout Mutants.....	129
4.3.2 Quantification of IAA & Identification of an alternate IAA pathway	132
4.3.3 Evidence of the IPyA Pathway	139
4.3.4 The IPyA pathway.....	142
4.3.5 Mining Genes involved in the IPyA Pathway.....	144
4.4 Conclusion.....	150
Chapter 5	152
Deciphering the Role of IaaM and Aux Proteins in <i>Pseudomonas</i> sp. UW4	152
5.1 Introduction.....	152
5.2 Methods	155
5.2.1 Bacterial Strains and Plasmids.....	155
5.2.2 DNA Extraction and Expression Plasmid Construction	157
5.2.3 Expression and Purification of Recombinant IaaM and Aux Proteins in <i>E. coli</i>	157
5.2.4 Removal of bound Indoleacetamide (IAM) from IaaM and Aux	158
5.2.5 Protein Determination and SDS-PAGE.....	159

5.2.6 UV-Absorption Spectrum	159
5.2.7 TMO Enzyme Assay.....	159
5.2.8 High Performance Liquid Chromatography (HPLC) Analysis	160
5.2.9 Liquid Chromatography-Tandem Mass Spectrometry (LC-MS-MS).....	160
5.2.10 Multiple Sequence Alignment & Phylogenetic Analyses	162
5.3 Results and Discussion	162
5.3.1 Protein Classification	162
5.3.2 UV Spectrum of IaaM and Aux.....	163
5.3.3 TMO Assay.....	168
5.3.4 Sequence Similarity.....	171
5.3.5 Sequence Analyses and Phylogenetic Tree.....	174
5.3.6 Structural Analysis.....	185
5.3.7 Genetic organization of <i>iaaM</i> and <i>aux</i> genes	191
5.4 Conclusion	195
Chapter 6	197
General Discussion.....	197
6.1 Overview.....	197
6.2 Role of amidase in IAA biosynthesis.....	198
6.3 The effect of increasing UW4's capacity to produce IAA on canola root growth	199
6.4 The contribution of each IAA gene to the production of IAA by strain UW4.....	200
6.5 The role of IaaM and Aux proteins in IAA biosynthesis.....	201
6.6 Limitations	202
6.7 Conclusion: Just the Beginning.....	205
References	207
Appendix A	240

List of Figures

Figure. 1. The Indole Pyruvic Acid (IPyA) Pathway	23
Figure. 2. The Indoleacetamide (IAM) Pathway.....	26
Figure. 3. The Indole acetaldoxime (IAOx)- Indole acetonitrile (IAN) Pathway	31
Figure. 4. Plant-growth-promoting mechanisms used by strain UW4.....	48
Figure. 5. IAA Biosynthesis Pathways in Bacteria.....	49
Figure. 6. Putative IAA Biosynthesis Pathways in UW4.....	50
Figure 7. The IAN-IAM Pathway in UW4	54
Figure 8. Plasmid map of the pET30b(+) expression vector	57
Figure 9. Temperature profile of Ami	67
Figure 10. pH profile of Ami	67
Figure 11. Multiple sequence alignment of characterized amidases.....	71
Figure 12. Molecular Phylogenetic Analysis of Characterized Amidases	80
Figure 13. Schematic representation of the physical organization of the <i>ami</i> gene cluster	83
Figure 14. Transcriptional Analysis of Wild-type and Transformant UW4 Strains.....	97
Figure 15. Growth Curve of Wild-Type and Transformed UW4 Strains.....	100
Figure 16. Growth Curve of IAA-producing Wild-Type and Transformed UW4 Strains.....	100
Figure 17. Results of the Canola Seedling Growth Pouch Assay.....	101
Figure 18. Map of pGem®-T easy plasmid	120
Figure 19. Map of pBluescript II SK(+) plasmid	121
Figure 20. Map of pK18 mobSacB plasmid.....	122
Figure 21. Gene Deletions in IAA biosynthesis pathways in strain UW4.....	132
Figure 22. Production of IAA by UW4 wild-type strain and UW4 deletion mutants	134
Figure 23. IAA production by wild-type and deletion mutants when fed IAM.....	135
Figure 24. Conversion of IAN to IAM and IAA by <i>nit</i> , <i>nthAB</i> and <i>ami</i>	135
Figure 25. IAA and IAM production by the UW4 deletion mutant <i>nit-ami</i>	137
Figure 26. IAA and IAM production by the UW4 deletion mutant <i>nit</i>	138
Figure 27. LC-MS-MS Chromatogram of IPyA pathway metabolites from wild-type UW4.....	140
Figure 28. Putative IPyA biosynthesis pathways in <i>Pseudomonas</i> sp. UW4.....	142
Figure 29. Putative IAN-IAM Biosynthesis Pathways in UW4.....	153
Figure 30. Conversion of Trp into IAM by a TMO Enzyme.....	155
Figure 31. UV Spectrum of free FAD _{OX} in aqueous solution	166
Figure 32. The UV-Absorption Spectrum of purified IaaM and Aux	166
Figure 33. Changes in absorbance of IaaM and Aux in the presence of Trp and FAD	167
Figure 34. Sequence Alignment of Flavin Amine Oxidases	175
Figure 35. Multiple Sequence Alignment of IaaM, Aux, TMO and LMO	181
Figure 36. Molecular Phylogenetic Analysis of IaaM by Maximum Likelihood Method	184
Figure 37. Predicted Secondary Structures of IaaM and LMO	187
Figure 38. Predicted Secondary Structure of Aux and PAO	189
Figure 39. Gene organization of <i>iaam</i> in the <i>Pseudomonas</i> sp. UW4 genome	193
Figure 40. Gene organization of <i>davB</i> in the genome of <i>P. putida</i> KT2440.....	193
Figure 41. Genetic organization of <i>aux</i> in the <i>Pseudomonas</i> sp. UW4 genome.....	193
Figure 42. AMV pathway for the degradation of lysine by <i>Pseudomonas</i>	194

List of Tables

Table 1 Plasmids, strains and primers used in this study	56
Table 2. Physicochemical Properties of Ami from strain UW4 and other Signature Amidases.....	64
Table 3. Sequence conservation in characterized amidases	70
Table 4. Characterized Amidases used in Phylogenetic Analysis	73
Table 5. Organization of the <i>ami</i> gene in the genome of strain UW4	83
Table 6. Expression plasmid constructs and primers used in this study	90
Table 7 Biological Activities of the UW4 Wild-Type Strain and UW4 Transformants	96
Table 8. Growth Comparison of Wild-Type and Transformant UW4 Strains	99
Table 9. Plasmid Constructs used in this study	123
Table 10. Primers and Restriction Enzymes used to make Gene Deletions	125
Table 11. <i>Pseudomonas</i> sp. UW4 IAA-gene Deletion Mutants generated in this study.....	131
Table 12. Potential UW4 Genes involved in the IPyA Pathway	144
Table 13. Plasmids, strains and primers used in this study	156
Table 14. LC-MS-MS Analysis of <i>E. coli</i> BL21 Culture Extracts	170
Table 15. Amino Acid Sequence Similarity of Flavin Monoamine Oxidases.....	173
Table 16. Conservation of Critical Residues in TMO and LMO	179
Table 17. Lysine metabolism genes in <i>P. putida</i> KT2440 and homologs in strain UW4.....	195

Chapter 1

Introduction and Literature Review

1.1 Plant-Microbe Interactions

The interactions between plants and microbes can include both mutualism and pathogenicity. The outcome depends on a set of abiotic and biotic factors including, the genotypes of both the plant and microbe, environmental conditions, and the complex network of interactions within the plant microbiome (1). This literature review focuses mainly on the intimate association between plants and beneficial bacteria, where the mutualistic interaction leads to adaptive benefits for both partners.

Healthy plants host, within and on the surfaces of their tissues, diverse endophytic and epiphytic bacteria (2). We refer to these beneficial microbes as plant growth-promoting bacteria (PGPB) and can generally classify them into three major groups: i) microbes that alleviate abiotic stress on the host plant; ii) microbes that defend hosts from biotic stress such as phytopathogens; and iii) microbes that support the growth of the host plant (2). The specific mechanisms used by PGPB to enhance plant growth include: (i) the ability to produce a vital enzyme, 1-aminocyclopropane-1-carboxylate (ACC) deaminase to reduce the level of stress ethylene in the plant (3); (ii) the ability to produce hormones (4); (iii) symbiotic nitrogen fixation (5)(6); (iv) antagonism against phytopathogenic bacteria by producing siderophores, β -1, 3-glucanase, chitinases, antibiotics, fluorescent pigments and cyanide (7)(8)(9); (v) solubilization and mineralization of nutrients (10); (vi)

enhanced resistance to drought, salinity, waterlogging and oxidative stress (11)(12)(13)(14); (vii) production of water-soluble B-vitamins niacin, pantothenic acid, thiamine, riboflavine and biotin (15)(16). A single PGPB can employ one or several of these modes of action (17).

Relationships between PGPB and their hosts can be categorized into two groups: (i) rhizospheric and (ii) endophytic. The soil immediately surrounding the root system is known as the rhizosphere and is a hot spot of microbial abundance and activity. A single gram of soil may contain 10^7 - 10^9 CFU of culturable bacteria and sustain more than 30,000 species (18). Rhizosphere colonization is supported by root exudation; the microbial population benefits from root secretion of vitamins, sugars, proteins, carbohydrates, organic acids, amino acids and mucilage (19). In endophytic relationships, PGPB reside within the tissues of the host plant and may be found in all parts of plants (seed, roots, stems, leaves and fruit) (17).

1.2 Application of Plant-Growth-Promoting Bacteria

The global population faces three incredible challenges: ensuring that the 7+ billion people alive today are adequately fed; dramatically increasing food production in the next 30 years to sustain the projected increase in the global population; and achieving both goals in a truly environmentally sustainable manner (20). We could boost food production by clearing more land for agriculture or using more chemical pesticides and fertilizers. However, this will only exacerbate environmental problems (21). What is more, emerging and endemic phytopathogens are decimating crop biomass worldwide, costing crop producers billions of dollars (22)(23). It is for these reasons, that the quest

for environmentally benign bacterial inoculants with positive impacts on plant yield that can lead to reduced agrochemical inputs is gaining great momentum. Considering that some PGPB began interacting with flowering plants around 80-100 million years ago, the deliberate use of PGPB in agriculture merely mimics what has already been successful in nature (24).

Despite a large number of patents using PGPB as inoculants, few have materialized in a register for agricultural application (25). This is because the development of commercial PGPB products is a complex process, requiring the concerted action of many specialists in various fields. Once the product is developed, the hurdle of approval and registration must be overcome. Variable and inconsistent national or regional rules can apply to this process, making it expensive and time consuming (25). Nevertheless, among the microbial inoculants that are currently commercialized, strains of *Bacillus* and *Pseudomonas* make up most of the market for biocontrol of pests and phytopathogens (21)(26). In 2011, the global market for biopesticides in terms of revenues was ~ 5 billion US, which is about 2.5% of the global market for chemical pesticides. The biofertilizer market share is projected to reach 1.7 billion US by 2022. The current biofertilizer market represents about 5% of the chemical fertilizers market. North America is expected to dominate the global biopesticide/biofertilizer market in terms of demand between now and 2023. Nitrogen-fixing bacteria occupy most of the global biofertilizer market, since nitrogen is an essential nutrient for plants. Species of *Rhizobium*, *Mesorhizobium*, *Bradyrhizobium*, *Azorhizobium*, *Allorhizobium*, *Sinorhizobium*, *Azotobacter* and *Azospirillum* are used commercially to establish the nitrogen-fixing symbiosis with leguminous crops, rice and sugarcane (27). In North America, the biofertilizer market is

monopolized by two major players; Novozymes and Becker Underwood, which together have a market share of ~85% (25).

Developed countries such as The Netherlands, France, Australia, Canada and the United Kingdom enforce standards for inoculant quality such as having a threshold number of cells, in order to obtain the intended positive plant response. However, in developing countries where these inoculants are most needed, such standards are not always met and the inoculants produced are often of poorer quality (27). The efficacy of PGPB inoculants must be improved with respect to the commercial delivery of the microbe, manufacturing at an industrial scale, longevity of shelf-life and improved survival and stability upon release into the environment (28). Another challenge is the potential for some PGPB to be opportunistic human pathogens. For example, some species of *Burkholderia*, *Enterobacter*, *Herbaspirillum*, *Serratia* and *Staphylococcus*, that are root-associated, can interact with both plant and human hosts (21)(29).

The practical aspect of how to apply the PGPB to the target plant is addressed in two ways: (i) direct inoculation on the seed surface or; (ii) direct inoculation into the soil. Seed applications are more popular than soil applications because inoculation is easier and requires a relatively small amount of inoculant (27). To ensure that every seed is coated with enough bacteria, adhesives are used. The inoculant is mixed with seeds either by hand, rotating drums, large cement mixers, or mechanical tumbling machines. The drawbacks of seed inoculation include; insufficient bacterial adhesion, disturbance of the seed coat causing desiccation and seed release of anti-bacterial compounds that inhibit the inoculant (27).

Soil inoculation involves placing granular inoculants in the seedbed or alongside the seed during sowing. This technique does not damage seed coats and protects the inoculant from inhibition by pesticides/fungicides that the seeds may be treated with (27). Liquid inoculants can also be applied directly to soil or hydroponic systems. The drawback of soil inoculation include the need for specialized equipment, large quantities of inoculant, more storage space, transport and higher costs (27).

1.3 Plant Indoleacetic Acid (IAA)

Like teenagers, plants are full of raging hormones. These include steroids and peptides, as well as the five classical phytohormones- auxins, abscisic acid, cytokinins, ethylene and gibberellins (30). Auxin is the umbrella term for a group of important molecules found in plants, humans, animals, and microorganisms. Indoleacetic acid (IAA) is the predominant and most indispensable auxin in plants (30). IAA is a weak organic acid with an indole ring and a carboxylic acid function. It is a fundamental compound that modulates a plethora of plant developmental processes from early embryogenesis and organogenesis to cambial growth, vascular development and fruit ripening (31)(32). Its far-reaching effects are beyond just regulating plant-growth, and extend to being central to a plant's lifecycle and overall functioning. As Paque and Weijers refer to it, IAA is the plant molecule that **Influences Almost Anything** (33). Many studies on IAA have been undertaken to elucidate its biological function, biosynthesis, metabolism, transport, and signal transduction pathways. These aspects are reviewed herein, with a significant portion of the text taken from a review (Duca et al., 2014) that I previously wrote and published on this topic (4).

Plants produce IAA and unevenly distribute it throughout their body. This heterogeneity in the distribution of IAA is imperative for proper development (33). It is produced in the shoots and subsequently transported from source organs (young leaves) to sink organs (meristems) where it accumulates (34)(35). The hydrophobic protonated form (IAAH) can diffuse freely across cell membranes, however the hydrophilic anionic form (IAA⁻) requires active transport by specific influx carriers and efflux transporters (36). Typically, the IAA concentration is 10–100 times lower in roots than in shoots (38). Within the root, the highest levels of IAA are seen in the center of the root meristem, where stem cells are located. From this zone the IAA concentration tends to decrease and a gradient forms that governs a specific developmental pattern (34)(37). Even at super low concentrations (picograms), IAA is a master regulator of plant development.

Establishing the proper IAA concentration gradient requires strict regulation of many different cellular processes. The concentration of IAA within a plant cell is regulated by the rate of biosynthesis, conjugation/deconjugation, degradation and transport between cellular compartments (39). A disturbance in its homeostasis can incite dramatic phenotypic changes, as demonstrated by plant mutants that overproduce IAA (e.g. *superroot1*)(40), that are depleted in IAA (e.g. *weil8 tar2*) (41) or in which IAA transport is hindered (e.g. *pin1*)(42).

1.4 Bacterial IAA in Plant-Microbe Interactions

Bacteria that can produce IAA have a tremendous influence on plant health and productivity. Many different bacteria are capable of synthesizing IAA, including soil, epiphytic, endophytic,

methylotrophs, marine, and cyanobacteria (43)(44). IAA is a reciprocal signaling molecule between plants and bacteria, both in stimulation of growth and in pathogenesis (45).

1.4.1 Bacterial IAA and Pathogenesis

Initially, bacterial IAA was associated with pathogenesis, specifically with bacteria that cause neoplastic plant diseases. Tumor- and gall-inducing bacteria were the first plant-associated bacteria in which IAA biosynthesis pathways were studied (46). Tumor formation induced by *Agrobacterium tumefaciens* involves transfer of the T-DNA-located IAA biosynthesis genes from the bacterium into the host genome (47). The local overproduction of IAA by the transformed plant cells (together with the overproduction of cytokinin) results in the proliferation of tumor tissue (48). Gall-forming strains of *Pantoea agglomerans* pv. *gypsophilae* carry the IAA biosynthesis genes on the pPATH plasmid, but they do not transfer DNA into host cells (49). Instead, the bacteria must be in constant association with the plant to secrete IAA and induce disease.

IAA-deficient mutants can no longer elicit disease symptoms indicating that the virulence of some bacterial strains may be attributed to IAA. For instance, removing the Ti –plasmid IAA biosynthesis genes from *Agrobacterium*, results in an inability to produce tumors. Similarly, the symptoms and knot sizes developed upon infection of olive trees with IAA⁻ mutants of *Pseudomonas savastanoi* pv. *savastanoi* were less severe than those induced by the wild-type strain (50). IAA metabolism, not just its biosynthesis, was found to be an essential virulence determinant for *P. savastanoi* pv. *nerii*. A mutation in the *iaaL* gene, involved in the conjugation of IAA to IAA-Lys, led to elevated levels of

free IAA, which in turn caused the bacteria to be hypervirulent on its oleander host. The mutant strain was able to reach higher in plant population densities and cause more extended hyperplastic symptoms than the wild-type. Conversely, hyperplastic symptoms and bacterial growth were drastically reduced or completely abolished in a *P. savastanoi* pv. *nerii* mutant impaired in IAA biosynthesis (51).

In the phytopathogen *Dickeya dadantii* 3937, a mutation in the IAA biosynthesis pathway reduced symptoms of rot disease on African violet. IAA is known to play a signaling role for upregulation of the type III (T3SS) and type VI (T6SS) secretion system in the bacterial phytopathogen *Dickeya dadantii*. It also positively regulates the production of pectinases that are used to attack the plant cell wall. When the IAA biosynthesis pathway was mutated, there was a parallel decrease in the production of pectate lyase and in the expression of T3SS genes (52). Conversely, in *P. savastanoi* pv. *nerii*, the addition of exogenous IAA reduced the expression of T3SS genes (51). Similarly, in *P. savastanoi* pv. *savastanoi* NCPPB 3335, IAA had a negative effect on the expression of T3SS genes (*brpA* and *brpL*) and a positive effect on a T6SS gene (*vglG*) (53). Considering that T3SS genes are required to establish infection, to guarantee bacterial fitness, the level of biologically active IAA must be carefully modulated during the phases of interaction between the phytopathogen and the host (51).

Native plant IAA biosynthesis genes are induced upon infection by an IAA-producing pathogen, augmenting endogenous IAA and amplifying the virulence effect caused by supra-optimal IAA levels (54). Plant pathogenic bacteria use a type III secretion system to inject bacterial effector

proteins directly into the host cell cytoplasm (55). Effector proteins secreted by *Pseudomonas syringae* have been shown to hijack the host plant systems for IAA biosynthesis, signaling and transport (51)(56). One such bacterial effector is AvrRpt2. When this effector protein is delivered into plant cells it induces native IAA biosynthesis and suppresses plant defenses mediated by salicylic acid (SA)(57). Transgenic *Arabidopsis thaliana* plants that overexpress AvrRpt2, have elevated levels of free IAA and are more susceptible to *P. syringae* compared with wild-type plants (58). Indeed, IAA has also been shown to increase the susceptibility of tobacco, sweet orange and rice to bacterial infection (59)(60)(61). For example, pre-treatment of *Arabidopsis thaliana* with synthetic IAA analogs promoted the growth of the pathogen and resulted in more severe disease symptoms (54). Similarly, pre-treatment of rice plants with exogenous IAA increased the disease symptoms of the phytopathogen *Xanthomonas oryzae* (54). It was not determined whether *X. oryzae* uses IAA as a virulence factor to invade rice, but the IAA secreted by the bacterium contributes to the accumulation of deleterious levels of IAA in rice plants, and exacerbates the disease symptoms (54). It is important to note that many soil bacteria, including *Pseudomonas* spp., can use IAA as a source of carbon and nitrogen (62). As such, it is possible that pre-treating plants with these compounds prior to phytopathogen inoculation leads to increased bacterial biomass, which in turn aggravates plant disease symptoms. Therefore, it is important to measure the number of infecting cells.

One of the proposed virulence mechanisms of IAA is through the impediment of the salicylic acid (SA) pathway which serves as a critical signal for activating disease resistance in plants (63). Studies show that the IAA-producing *P. syringae* promotes disease in *Arabidopsis thaliana* by suppressing pathogenesis-related (PR) gene expression, which is naturally induced as part of systemic acquired

resistance and SA-dependent defense. This suppression is paralleled by an increase in endogenous IAA levels (64). Other studies have also observed that plants treated with exogenous IAA had reduced expression of the pathogenesis related gene 1, PR1, a marker gene of SA-mediated defense (65)(66). Kazan and Manners (2009), report that plants deficient in salicylic acid also show increased IAA levels (67). In contrast to this, Mutka et al. (2013) suggest that the increased susceptibility is not primarily due to suppression of SA-mediated defenses. They observed that the expression of a SA biosynthesis gene increased to the same degree in both wild-type and IAA-overproducing *Arabidopsis thaliana* plants infected with *P. syringae* DC3000. Moreover, SA levels were not significantly altered in infected IAA-overproducing plants relative to the wild-type plant (68). Instead, they suggest that high IAA levels promote pathogenesis through the hypersensitive response (HR), a mechanism used by plants to prevent the spread of infection by the rapid death of cells in the local region surrounding an infection (69). Earlier studies reported that induction of hypersensitive cell death response by a bacterial elicitor could be reversed by IAA (70). Similarly, Mutka et al., (2013) found that treatment of plants with the bacterial elicitor alone, induced plant cell death. However, co-infiltrating with IAA prevented the elicited cell death, allowing the pathogen to spread. When wild-type plants were inoculated with non-pathogenic *P. syringae* pv. *phaseolicola*, expressing type-III effector protein AvrRpm, they displayed a strong HR with 70% of leaves exhibiting tissue death. Conversely, when IAA-overproducing plants were inoculated with the same strain, only 23% of inoculated leaves exhibited tissue death (68). Thus, it appears that elevated IAA levels impede the progression of the HR response.

Bacterial IAA also compromises the integrity of the plant cell wall, the first barrier of defense against pathogens. IAA promotes the release of hydrogen ions into the cell wall, causing acidification. This

process stimulates the activities of glycosidases that hydrolyze polysaccharides in the cell wall, leading to cell wall loosening and membrane leakiness (71)(72)(73). Through this loosening, pathogens gain easier access to host cells for the delivery of type III secreted effector proteins and other virulence factors and receive more nutrients via root exudation (68). IAA also induces the expression of proteins responsible for decreasing cell wall rigidity. For example, IAA is reported to induce the expression of expansins, which are responsible for extending the cell wall, allowing phytopathogens to intrude in the process (74)(75)(76)(77). Overexpression of expansin in rice has been shown to increase its susceptibility to the bacterial pathogen *X. oryzae* (60).

1.4.2 Bacterial IAA and the Promotion of Plant Growth

IAA produced by PGPB plays a pivotal function in triggering lateral and adventitious root formation, root elongation and the development of root hair. A well-developed root system helps to anchor plants in soil and increases the surface area through which water, minerals and nutrients can be taken up (78)(43). The effect of bacterial IAA depends on its concentration- that is, low concentrations of exogenous IAA can promote, whereas high concentrations can inhibit growth (79). For instance, lateral and adventitious roots are generally induced by higher concentrations of exogenous IAA, whereas primary root elongation is stimulated by application of much lower levels of IAA (78). Each plant and plant organ, has a unique capacity for IAA; some being more sensitive, while others can tolerate higher concentrations. The plant already has an existing internal pool of IAA that it produces independently of soil bacteria. This endogenous level of IAA can vary depending on the tissue type, the amount of tryptophan precursor available and the environmental

conditions to which the plant is exposed. Therefore, the amount of exogenous IAA that a plant needs can vary at different times throughout the plant's life cycle (80)(81).

Since IAA is one of the main mechanisms of plant growth promotion by bacteria, there is great interest in genetic manipulation of IAA biosynthesis to maximize phytostimulation. It is imperative that we understand the biological and ecological impact of modified bacterial phytostimulators in order to determine ideal usage conditions for these inoculants (82). IAA-producing PGPB from genera such as *Pseudomonas*, *Rhizobium*, *Azospirillum*, *Enterobacter*, *Azotobacter*, *Klebsiella*, *Alcaligenes*, *Pantoea* and *Streptomyces* have been described (45)(46)(83). It is difficult to establish a direct relationship between enhanced root growth and bacterial IAA because no one has been able to create bacterial mutants that are completely devoid of IAA. Nonetheless, the effect of rhizobacteria has been attributed to bacterial IAA by observing the phenotypic outcome of inoculating plants with bacterial mutants that either over or under-produce IAA. Mutants with significantly reduced levels of IAA have been generated with the phytopathogens *P. syringae* (84), *A. tumefaciens* (85), *Erwinia herbicola* pv. *gypsophylae* (49) and with plant growth-promoting bacteria such as *Azospirillum* spp. (86)(87) and *Pseudomonas* spp. (88). For example, a mutant of *Azospirillum brasilense* Sp6 that produces ~90% less IAA, is unable to promote root development to the same extent as the wild-type strain (89). Insertional mutagenesis of an IAA biosynthesis gene in *Pseudomonas putida* GR12-2 reduced its ability to promote primary root growth in canola seedlings (78).

Modifying bacterial strains to produce more IAA, can lead to enhanced plant-growth. For instance, introducing recombinant plasmid-based copies of an IAA biosynthesis gene into *Azospirillum*

brasilense Sp245, resulted in higher IAA production. The recombinant plasmids were maintained in all inoculant cells and had no negative effect on the rhizosphere fitness of the bacterium. Winter wheat inoculated with the IAA-overproducing Sp245 displayed enhanced shoot biomass compared to inoculation with the wild-type strain. This is a demonstration that IAA-overproducing inoculants are ecologically viable and are functional as phytostimulators (82). An IAA-overproducing mutant of *P. putida* GR12-2 stimulated the formation of adventitious roots of canola better than the wild-type strain (33). Similarly, an IAA-overproducing mutant of *Pseudomonas fluorescens* CHA0 increased the root growth of cucumber up to 36% more than the wild-type strain (90). Barrelclover plants inoculated with IAA-overproducing mutant of *Sinorhizobium meliloti* RD64 showed significant weight increase in shoots and roots under phosphorus starvation (91). The length of the roots of *Arabidopsis thaliana* seedlings treated with an IAA-overproducing mutant of *P. savastanoi* pv. *nerii* was extremely reduced, yet lateral root formation was massively enhanced. This effect was not observed in *Arabidopsis thaliana* seedlings treated with a *P. savastanoi* pv. *nerii* mutant which is unable to synthesize IAA (51). Improving IAA levels in *A. brasilense* SM by introducing heterologous IAA synthesis genes, led to a superior effect on the lateral branching of sorghum grass roots as well as the dry weight of the plants when compared with the wild-type strain (92).

On the other hand, several studies have demonstrated that bacteria modified to overproduce IAA can also have a root growth-inhibiting effect (93)(94). A *P. putida* GR12-2 mutant that overproduced IAA (4-times the amount produced by the wild-type) inhibited root elongation of canola (95). A mutant strain of *P. fluorescens* BSP53a that overproduced IAA imparted a stimulatory effect on the root growth of black currant softwood cuttings but had an inhibitory effect on cherry tree plant

cuttings (96). Green gram seedlings treated with the IAA-overproducer *Pseudomonas* sp. MPS90 showed no significant difference in root length when compared to the control, whereas black gram seedlings showed an inhibition of growth (97).

Many legume-associated *Rhizobium* species produce IAA and this compound has been shown to positively affect nodule organogenesis and nitrogen-fixation (98)(99)(100)(101). Non-legume endophytic diazotrophs such as *Klebsiella variicola* RCA26, *Enterobacter cloacae* RCA25 and *Herbaspirillum seropedicae* z67 were genetically modified to increase their IAA production capacity. Consequently, the activity of the nitrogenase enzyme responsible for nitrogen fixation increased by 30, 40, and 70% in the IAA-overproducing strains respectively, compared to the wild-type (102).

1.5 The Biological Function of IAA in Bacteria

Considering that the vast majority of bacteria that associate with plants are IAA-producers, from an evolutionary perspective, having the ability to produce this hormone must give the bacteria a selective advantage in that environment (103). However, having the ability to produce IAA is not limited to bacteria that interact with plants. For instance, bacteria isolated from unvegetated sediments (104), thermo-acidophilic archaea isolated from a hot spring and bacteria inhabiting the human intestine also produce IAA (105)(106). The broad distribution of IAA biosynthetic capacity and the broad substrate specificity of the enzymes implicated in IAA biosynthesis, suggests a role beyond the plant interactions for which it has been mostly studied (43). IAA plays a role in the regulation of bacterial physiology, adaptation to stress conditions and microbe-microbe communication (43).

Recent studies have shown that IAA protects bacterial cells against environmental stresses. Wild-type *Sinorhizobium meliloti* 1021 and its derived IAA-overproducing mutant (RD64) were both exposed to various stress conditions such as acidity, osmotic shock, UV-irradiation and heat shock. Viable bacterial cell counts were higher for the IAA-overproducing strain (RD64) than for the wild-type strain under all of the conditions tested (107). Under conditions of stress, bacterial cells activate general protective systems such as the production of lipopolysaccharide (LPS), exopolysaccharide (EPS) and biofilm. The IAA-overproducer RD64 cells contained higher levels of LPS and produced more biofilm compared to wild-type cells (107). Quantitative analysis of EPS, a major factor in adherence of cells to surfaces, revealed the same trend, with higher levels produced by RD64 than the wild-type strain. Enhanced production of LPS, EPS and biofilm leads to better adherence of cells to surfaces, protection from desiccation in soil, protection from attack by antimicrobial compounds of plant origin, cryoprotection for growth at low temperatures and to a more communal life with other microbes (108)(109)(110)(111). The RD64 cells also produced ~3 times more trehalose than the wild-type strain. Bacteria can use trehalose as a source of carbon and as an osmolyte that confers protection against freezing and desiccation. Indeed, RD64 cells survived longer at cold temperatures (4°C) and as dry pellets compared to wild-type cells. The same protective effect was observed when IAA was added exogenously (107)(112).

IAA also affects the central metabolism pathways which function to generate energy in *S. meliloti*. Results showed an activation of the tricarboxylic acid (TCA) cycle in the IAA over-producing strain and when exogenous IAA was added (107). Moreover, the production of polyhydroxybutyrate (PHB) was also increased in response to IAA. Polyhydroxybutyrate (PHB)

plays a role in stress tolerance in many bacteria. Bacteria use PHB granules as a carbon source during starvation conditions, especially in the soil where nutrient stress is prevalent. They also provide the carbon and energy sources required to convert free-living bacteria into the differentiated bacteroids that carry out nitrogen fixation (107).

Donati et al. (2013) examined the effects of IAA pre-treatment on the ability of *Bradyrhizobium japonicum* to tolerate oxidative stress, heat shock, cold shock, osmotic stress and desiccation (113). The results show that under heat shock conditions, 84 % of IAA-treated cells survived, whereas only 47 % of non-treated cells survived. Similarly, under cold-shock conditions 98 % of IAA-treated cells survived, compared to 72 % survival for non-treated cells. IAA-treated cells exposed to oxidative, osmotic and desiccation stress had 96, 86 and 89 % survival, respectively, whereas the non-treated cells had 67, 49, 84 % survival, respectively. Altogether, these cell viability assays indicate that IAA enhances *B. japonicum*'s ability to tolerate abiotic stresses. This study also revealed that EPS production and biofilm formation increased significantly (1.7 and 2.5-fold, respectively) in response to IAA treatment (113).

Interestingly, IAA plays a key role in modulating the level of the bacterial alarmone (ppGpp) in the chloroplasts of plant cells. Plant chloroplasts conserve many bacterial systems, implicating its origin from the symbiosis of a photosynthetic bacterium (114). As such, the role of IAA in modulating ppGpp levels in plant chloroplasts may also extend to bacterial cells. Bacterial cells can become tolerant to antibiotics by entering a dormant state known as persistence. The key intracellular metabolite that has been linked to this persister state is ppGpp (115). This compound is a key factor in bacterial physiology because it can shut down cell growth and prime cellular defensive and

adaptive processes (116). The ppGpp binds to RNA polymerase, alters its promoter specificity and therefore modulates the expression of more than 80 different genes (117). When environmental conditions become favourable, the ppGpp levels decrease and the stringent response is reversed (118). IAA has been shown to confer antibiotic tolerance in *E. coli*, although the effect on ppGpp was not investigated specifically (119). Cerbonechi et al. (2016) used phenotype microarray technology to test the chemical sensitivity patterns of wild-type *P. savastanoi* pv. *nerii* and its respective IAA-overproducing or IAA-knockout mutant. Both mutants were more sensitive than the wild-type towards some antibiotics and biocides, especially the quinolone 8-HQ. This quinoline derivative is naturally secreted by plants and used as an antimicrobial agent in agriculture. However, the IAA-deficient mutants were more sensitive to oxytetracycline compared to the wild-type, suggesting that IAA contributes to oxytetracycline resistance (51). These findings suggest that IAA can have a fitness cost for survival of this bacterium under the presence of certain antimicrobials produced by the host plant during infection (51).

IAA is secreted and can diffuse into neighbouring cells, acting as a cell–cell communication signal (43). Scott et al. (2013) were the first to observe bacterial chemotaxis towards IAA by the IAA-degrader *P. putida* 1290 (120). Chemotaxis is mediated by methyl-accepting proteins (MCPs), which recognize a specific attractant and transmit a signal to the flagellar machinery to stimulate movement toward it (121). It is possible that *P. putida* 1290 possesses specific MCPs that attract the cells towards IAA, however, these have not yet been identified. The genome of a non-IAA-degrading bacterium *P. putida* KT2440 contains 27 MCPs (122), however, none of them confer chemotaxis toward IAA when this bacterium is transformed with the full IAA-degradative gene cluster. Many

chemotactic behaviors are linked to metabolism of the attractant (121). Bacteria that can actively chemotaxi toward IAA to degrade it, would have a competitive advantage over IAA-degrading bacteria that lack this chemotactic ability. IAA can serve as a carbon and nitrogen source and confers protection against environmental stresses, thus having the ability to chemotaxi towards IAA may improve survival in the plant environment. In nature, bacteria coexist in multispecies communities and compete for resources and space (123). Plants are biological sources of IAA and perhaps bacteria also use this attractant to outcompete others in plant colonization (124).

In *Rhizobia*, IAA was shown, using transposon mutagenesis and gene expression analyses, to have a definitive role in motility, signaling and plant root attachment, (125). IAA is suggested to play a critical role in the ability of bacteria to colonize host plants. Fitness attenuation has been described in IAA-mutants of *Pseudomonas savastanoi* isolated from olive trees (50). Similarly, the IAA-mutant of *Pseudomonas savastanoi* NCPPB 3335 was outcompeted by the wild-type strain *in planta*, showing that the IAA biosynthesis operon is required for the full fitness of this strain. The IAA-overproducing *S. meliloti* RD64 is less competitive than the wild-type strain under normal conditions, but is more competitive under stress conditions (112). The phytopathogen *P. savastanoi* pv. *nerii* achieved higher cell densities *in planta* when it was mutated to over-produce IAA than the wild-type (51). Studies using a transgenic *Arabidopsis thaliana* line with suppressed IAA signaling (miR393), showed that endophytic colonization by *Burkholderia phytofirmans* was grossly impaired. Similar results were found with miR393 plants inoculated with the pathogen *P. syringae* DC 3000, where repression of auxin signaling restricted the bacterium's growth inside plants (126)(59).

Matsukawa et al. (2007) found that IAA plays a role in regulating cellular differentiation and secondary metabolism in *Streptomyces* that are often associated with plant roots or tubers. These researchers investigated the effect of exogenously applied IAA on aerial mycelium formation and antimicrobial activity in several *Streptomyces* species. Low concentrations of IAA were observed to significantly stimulate aerial mycelium formation and antimicrobial activity against various other bacteria (127). Plant-associated *Streptomyces* spp. are well known for their ability to produce antibiotics, which can be used to protect plant roots from fungal and bacterial pathogens. IAA can be prevalent in the rhizosphere as it is produced and secreted by both plants and bacteria. In the rhizosphere, it may act as a signal for *Streptomyces* spp. to upregulate antibiotic production; inhibiting the growth of competing microbes, while simultaneously protecting plants from pathogens (127).

In *Agrobacterium*, IAA (25 μM) was found to inhibit *vir* gene induction; *vir* genes are required for the transfer of T-DNA and proteins into the plant cell. IAA may signal *Agrobacterium* that the plant environment is changing from a pre-tumorous to a post-tumorous state, and that the bacterium should modify its *vir* gene expression accordingly. For instance, when *Agrobacterium* is in the vicinity of a host, the bacteria recognize plant signals that activate the *vir* genes and start the transformation process. Once the tumour is established and is exuding high levels of IAA, the *vir* regulon is inhibited. Since the *vir* genes are dedicated to plant cell transformation, it is wasteful for the bacteria to continue to synthesize *vir* proteins when their function is no longer necessary. Moreover, at very high levels of IAA (200 μM), *Agrobacterium* cell growth is inhibited but the cells are not killed, as growth is resumed once the IAA is removed. The ability of IAA to inhibit the growth of other plant-associated and non-plant-associated bacteria, was also assessed in this study. The findings show a

bias toward inhibition of plant-associated bacteria, while the non-plant-associated bacteria are not affected by IAA. The underlying basis for this observation and whether this IAA-mediated bacterial growth inhibition occurs naturally in the rhizosphere is not known (128).

1.6 IAA Biosynthesis Pathways

Bacterial IAA biosynthesis may be tryptophan-dependent, or independent of tryptophan. Neither genes nor enzymes involved in the tryptophan-independent pathway have been identified to date. However, several genes, enzymes and co-factors have been studied in the tryptophan-dependent pathways (45). The production of tryptophan is the most energy intensive of any amino acid and comes at a high cost to the bacterial cell. As such, endogenous tryptophan levels are low, therefore high levels of IAA are only produced when excess tryptophan is supplied exogenously (43). Low levels of IAA may be produced from endogenous tryptophan, but only if it does not compromise protein synthesis (43). In bacteria, at least three principal pathways for the biosynthesis of IAA exist. These are classified as; the indole-3-pyruvic acid (IPyA) pathway, indole-3-acetamide (IAM) pathway and the indole-3-acetonitrile (IAN) pathway (46).

1.6.1 The Indole-Pyruvic Acid (IPyA) Pathway

Both plants and bacteria can synthesize IAA via the indole-3-pyruvic acid (IPyA) pathway. Initially, L-tryptophan is deaminated to IPyA by an aminotransferase. Subsequently, a decarboxylase enzyme converts IPyA into indole-3-acetaldehyde (IAAld), which is then oxidized to IAA by aldehyde dehydrogenase/oxidase (45).

A bacterium may possess several different isoforms of aminotransferase, each able to utilize multiple amino acid substrates, including all three aromatic amino acids (129). This suggests that these general enzymes likely function within diverse metabolic pathways in addition to IAA synthesis (129)(130). The second step in the IPyA pathway is the non-oxidative decarboxylation of IPyA to IAAlD by indolepyruvate decarboxylase, encoded by the *ipdC* gene (78). The *ipdC* gene has been cloned from several bacteria and disruptions in this gene have shown significant IAA-deficiency (88)(131)(87)(132)(133). The *ipdC*-encoded enzyme is a thiamine diphosphate-dependent, α -keto acid decarboxylase. These enzymes have been demonstrated to have broad substrate specificity, acting on indolepyruvate, phenylpyruvate, pyruvate and benzoylformate. Thus, while they can incidentally catalyze the decarboxylation of IPyA to IAAlD, their main catalytic function may not be the production of IAA (43). IPyA can also be non-enzymatically converted into IAAlD (134). As a side reaction, IPyA may be reduced to indole-3-lactic acid (ILA) by indole lactate dehydrogenase. This is a reversible reaction and NAD^+ is used as a cofactor. This enzyme has been isolated from *Rhizobium meliloti* (135). Indole-3-ethanol (IEt) is the product of a side reaction from IAAlD (25, 33).

The final step in the IPyA pathway is the oxidation of IAAlD to IAA. The gene responsible for the aldehyde oxidation remains somewhat elusive in bacteria. Putative NADP-dependent IAAlD dehydrogenase genes were identified in the genomes of *Bacillus amyloliquefaciens* FXB42 and *Bacillus subtilis* 168 (136). However, disruption of this gene in *B. amyloliquefaciens* FXB42 did not significantly affect its IAA production, suggesting that the encoded enzyme does not play a role in IAA synthesis

(136). Xie et al. (2005) identified an aldehyde dehydrogenase (*aldA*) gene in *Azospirillum brasilense* Yu62 that had significant homology to an aldehyde dehydrogenase from *Bradyrhizobium japonicum* USDA110 and *Mesorhizobium loti* MAFF303099. The *aldA* gene was disrupted by transposon mutagenesis and the resulting mutant produced less IAA, implicating the encoded enzyme in the production of IAA (137). Aldehyde dehydrogenase was identified in *Gluconacetobacter diazotrophicus*, however this enzyme showed narrow substrate specificity toward aliphatic aldehydes and was not tested with the aromatic IAAl substrate (138). Enzymatic conversion of IAAl to IAA and IET was shown with the cell-free extracts of *P. fluorescens* ATCC 29574. Pyridine nucleotides were required for this conversion, indicating that aldehyde dehydrogenase was involved in the reaction. Moreover, when arsenite, an inhibitor of aldehyde dehydrogenase, was added to the cells, the formation of IAA from L-tryptophan decreased significantly with the concomitant increase in IET (139).

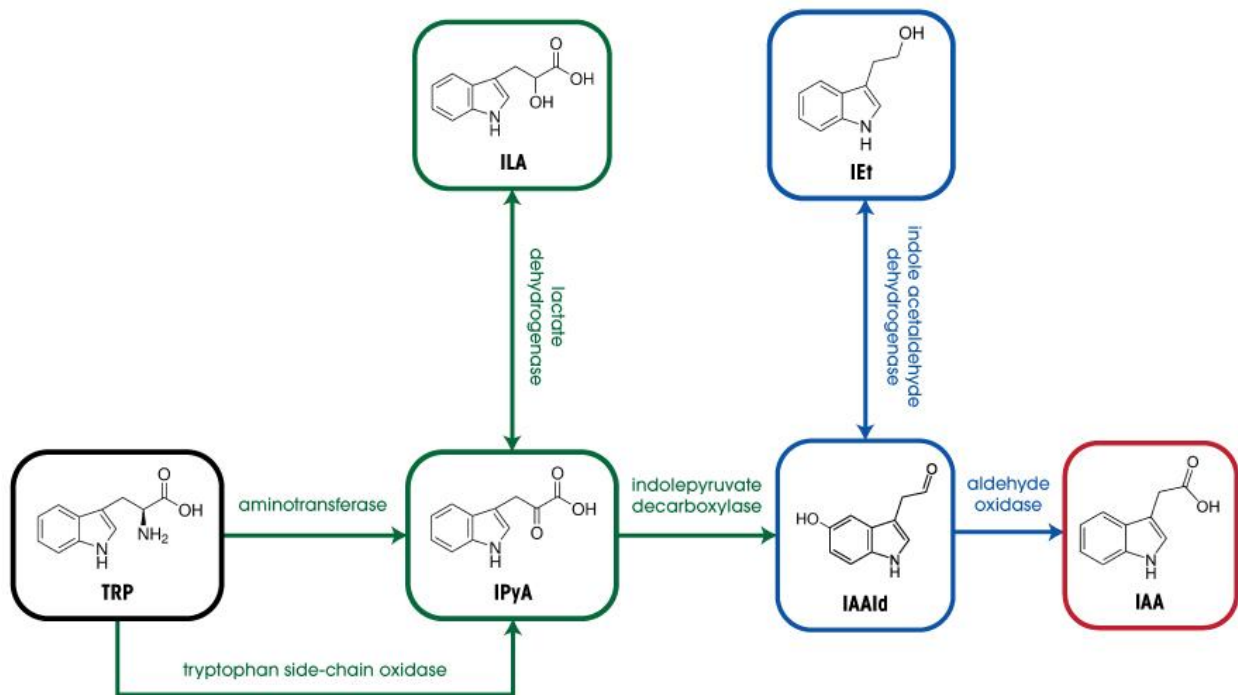


Figure. 1. The Indole Pyruvic Acid (IPyA) Pathway

TRP= tryptophan, IPyA= indole pyruvic acid, IAAld= indole acetaldehyde, IAA= indole acetic acid, ILA= indole lactic acid, IEt= indole-3-ethanol

An interesting finding and the first of its kind, came from the transposon mutagenesis of the sugarcane endophyte *Gluconacetobacter diazotrophicus*, which resulted in the isolation of a mutant strain that produced only 6% of the amount of IAA excreted by the parent strain. This study revealed a surprising discovery; the mutation causing the IAA⁻ phenotype was linked to genes involved in cytochrome c biogenesis (*ccmCEF*). More specifically, this study revealed that cytochrome c biogenesis genes are required for a large proportion, (~90%) of the IAA produced in *G. diazotrophicus*. This was the first report of *ccm* gene products being involved in IAA production in any bacteria. In *G. diazotrophicus* IAA is produced via the IPyA pathway. The side-product of this pathway, ILA, was also reduced significantly in the *ccm* mutant compared with the wild-type. A

plasmid containing the functional *cym* operon restored the ability to produce IAA; reinforcing the notion that a defect in cytochrome c production is responsible for the IAA mutant phenotype (140). Cytochrome c proteins are involved in respiration, oxidase and dehydrogenase activities; therefore these activities were measured in the wild-type and mutant strains. In the case of the *cym* mutants, no ethanol, acetaldehyde, or lactate oxidase activities were detected. Moreover, the acetaldehyde, ethanol and lactate dehydrogenase activities of *cym* mutants were significantly decreased compared to the wild-type. There are no reports describing the relationship between IAA production and cytochrome c in the literature. However, it is possible that cytochrome c is involved in a novel IAA biosynthetic pathway, as no known intermediates of IAA accumulated in the mutant. If the *cym* mutation resulted in defects in a known IAA biosynthetic pathway such as the IPyA pathway, we would have expected to see some corresponding intermediates accumulate. Alternatively, cytochrome c may play a role in the regulation of IAA production in *G. diazotrophicus*. Further biochemical characterization of the enzymes involved in the IAA biosynthetic pathway is required to reveal whether cytochrome c is directly involved in IAA synthesis or acts by regulating other IAA synthesis enzymes (140).

Although the IPyA pathway has mainly been observed in PGPB, it has also been suggested to occur in phytopathogens such as *Agrobacterium tumefaciens*, *Pseudomonas syringae* pv. *savastani* and *Erwinia herbicola* pv. *gypsophilae* (141)(142)(143). The presence of the IPyA pathway in these phytopathogens was proposed based on the identification of the corresponding intermediates or based on the ability of the cells to metabolize the intermediates of this pathway. However, it is necessary to identify

IPyA pathway genes and biochemically characterize the encoded enzymes in order to definitively confirm their involvement in IAA biosynthesis (43).

An alternative pathway exists in which tryptophan is directly converted into IAAlD bypassing the IPyA intermediate (Fig.1). This pathway is referred to as the tryptophan side-chain oxidase (TSO) pathway (46). A hemoprotein labelled as tryptophan side-chain monooxygenase catalyzes the oxidation of the side chain of tryptophan (139)(144). The TSO pathway has been reported in *P. fluorescens* HP72, *P. fluorescens* CHA0, *P. fluorescens* Pf-5 and *P. fluorescens* ATCC 29574 (94)(144)(145)(139).

1.6.2 The Indoleacetamide (IAM) Pathway

The IAM pathway has been characterized mainly in phytopathogenic bacteria, although it does occur in symbiotic bacteria as well (76). In this two-step pathway, tryptophan is first oxidatively decarboxylated to IAM by the enzyme tryptophan-2-monooxygenase (TMO), encoded by the *iaaM/tms1* gene. In the second step IAM is deaminated oxidatively to IAA by an IAM-hydrolase/amidase, encoded by the *iaaH/tms2* gene (Fig. 2) (146)(48). These genes have been cloned and characterized from *Agrobacterium tumefaciens*, *Pseudomonas syringae*, *Pantoea agglomerans*, *Rhizobium* and *Bradyrhizobium* (147)(49)(148). In some cases, the IAM-pathway genes are present on the chromosome and in other cases they reside on plasmids (149)(150)(151). The identification of this pathway in bacteria is generally based on (i) chemical identification of the IAM intermediate during metabolism of Trp into IAA; (ii) production of IAA following infiltration of the bacterial cells with IAM; and (iii) incorporation of radioactive carbon from Trp into IAM and IAA (152).

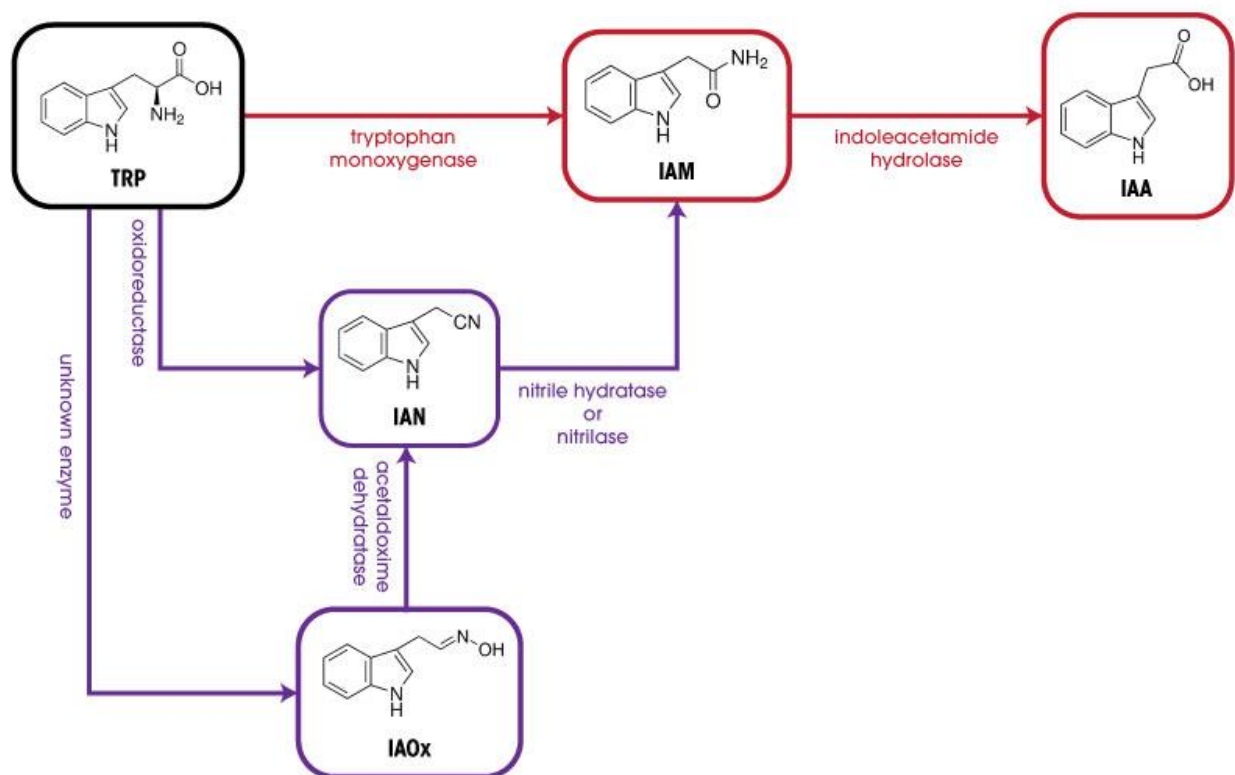


Figure. 2. The Indoleacetamide (IAM) Pathway

TRP= tryptophan, IAM= indole acetamide, IAA= indoleacetic acid, IAN= indole acetonitrile, IAOx= indole acetaldoxime.

Patten et al. (2013) performed a phylogenetic analysis of the genes of the IAM pathway and found that homologues of the *iaaM* gene exist in few bacterial genera. The *iaaM*-like sequences clustered into two distinct groups. Group I sequences are known tryptophan 2- monooxygenases that participate in IAA synthesis, such as those in the plant pathogens *A. tumefaciens*, *P. syringae pv. savastanoi*, *P. agglomerans* and *D. dadantii* (43). The Group II sequences exist within more diverse bacteria, however their functions are not well characterized and their involvement in IAA biosynthesis has not been determined experimentally (43).

Homologs of the IAM-hydrolase/amidase occur in a large number of different bacterial genera. Lehmann et al. (2010) inferred the evolutionary relationships among amidases from plants and bacteria, finding that the bacterial IAM-hydrolases (IaaH) cluster together on the phylogenetic tree and underwent a functional diversification from more general amidases that metabolize various amide substrates (153). In another phylogenetic analysis, Patten et al., (2013) found that amidases such as mandelamide hydrolase, aspartate/glutamate tRNA-dependent amidotransferase, 5-aminovalelamide hydrolases and arylpropionamide hydrolases cluster with the known IAM-hydrolases that have been described in phytopathogens (43). These findings suggest that bacterial IAM-hydrolases may in fact be wide-spectrum amidases that can catalyze the oxidative deamination of various amides in addition to IAM.

Nitrile hydratase enzymes link the IAN and IAM pathways by catalyzing the hydration of IAN into IAM, which is then converted to the final product IAA by IAM-hydrolase/amidase (Fig. 2)(154). Nitrile hydratases have been reported in several bacteria; however few studies have characterized this enzyme with respect to its direct involvement in IAA biosynthesis (155)(43). These enzymes are mostly studied for their application in the industrial production of acrylamide, nicotinamide, and 5-cyanovalelamide. They act on various nitrile substrates including aliphatic, aromatic and heterocyclic nitriles, converting them into the corresponding amides (156)(157). Although they may be involved in IAA biosynthesis, their catalytic role likely extends beyond that. Asano et al. (1980), were among the first to purify a nitrile hydratase and amidase from *Arthrobacter* sp. J1 (158). The nitrile hydratases of *P. chlororaphis* B23 and *R. rhodochrous* J-1 are strongly induced by amides (159), although that of *Rhodococcus* sp. N-774 (23) is formed constitutively (160).

Amidase genes are often located adjacent to nitrile hydratase genes as they convert the amide product of the nitrile hydratase to the corresponding carboxylic acid (161). This type of genetic organization has been observed in the genomes of some *Pseudomonas* spp., *Bacillus* sp., *Rhodococcus* spp., *Brevibacter* sp., *Agrobacterium radiobacter*, *Bradyrhizobium japonicum*, and *Ruegeria pomeroyi* (162)(163)(164)(165). The coupled enzymatic activity of nitrile hydratase and amidase has been described in *Rhodococcus* spp., *A. tumefaciens*, *P. putida*, *Microbacterium imperiale*, *Nocardia globerula* and *Bacillus subtilis* (166)(167)(168)(169)(170)(171)(172). However, the concerted action of these two enzymes specifically in the conversion of IAN→IAM→IAA has not been investigated.

Xie et al. (2003) demonstrated a genetic relationship between nitrile hydratase, amidase and a third enzyme- an aldoxime dehydratase, in *Rhodococcus globerulus* A-4 (173). The aldoxime dehydratase produces the nitrile substrate for the nitrile hydratase, while the nitrile hydratase produces the amide substrate for the amidase. A similar gene cluster is found in *Pseudomonas* sp. UW4, *Rhodococcus* sp. N-771 and *Rhodococcus* sp. YH3-3 (162)(174). The organization of these three genes in a putative operon reflects their concerted action. The coupling of aldoxime dehydratase and nitrile hydratase activity has been reported in *Aureobacterium testaceum*, *Nocardia asteroides*, *Kocuria varinus*, *Bacillus subtilis*, *Rhodococcus erythropolis* JCM 3201, *Brevibacterium butanicum* ATCC 21196 and *Pseudomonas* sp. K-9 (175)(176)(174). However, this activity was not tested with the substrates indoleacetaldoxime and indoleacetonitrile but rather with phenylacetaldoxime and phenylacetonitrile. Vega-Hernandez et al. (2002) showed that in *Bradyrhizobium* cultures, nitrile hydratase rather than tryptophan monooxygenase is responsible for the production of IAM (154). Kobayashi et al. (1995) also observed that IAA is produced by the sequential action of nitrile hydratase and amidase

in *Agrobacterium tumefaciens* and *Rhizobium* spp. (177). Altogether these results suggest that the presence of the IAM intermediate does not necessarily implicate the traditional IAM pathway (i.e. via tryptophan monooxygenase) as the IAM could be formed from the IAN intermediate via nitrile hydratase.

1.6.3 The Indoleacetaldoxime (IAOx)-Indoleacetonitrile (IAN) Pathway

Relatively little is known about the indoleacetaldoxime (IAOx)-indoleacetonitrile (IAN) pathway in bacteria. The first step of this pathway is the conversion of tryptophan into IAOx (Fig. 3). The enzyme responsible for this conversion is likely an oxidoreductase, however this enzyme has not yet been identified in bacteria. This speculation is based on plant studies in which cytochrome p450 oxidoreductases catalyze this step (178). In the second step, the IAOx intermediate is converted into IAN by an acetaldoxime dehydratase (EC 4.2.1.29) (Fig. 3). The ability to degrade acetaldoxime is widely distributed in bacteria (179). Aldoxime dehydratase enzymes are encoded by *oxd* genes and are generally induced by aldoximes (179). Most aldoxime dehydratase activities have been characterized using phenyl acetaldoxime or pyridine-3-acetaldoxime as the substrate (179). It is possible that these enzymes can also convert IAOx into IAN. However pure enzyme assays must be performed to reveal the substrate specificity of these enzymes. In the third step, the IAN intermediate is converted to IAA by a nitrilase enzyme (Fig. 3). In bacteria, nitrilase enzymes have roles in hormone synthesis, nutrient assimilation and detoxification of exogenous and endogenous nitriles (180). Nitrilases are part of a large superfamily with over 180 known members, classified into 13 branches, of which only branch I (EC 3.5.5.1) can convert nitriles to their corresponding carboxylic acids, releasing ammonia in the process (181). Nitrilases isolated from various bacteria

reveal diverse substrate specificities and the ability of a single nitrilase to act upon multiple nitriles (i.e., aromatic, aliphatic and aryl acetonitriles). The nitrilases belonging to branch I have been implicated in IAA biosynthesis. However, there are very few reports that biochemically characterize nitrilase with respect to its direct role in IAA biosynthesis. The majority of nitrilases have been biochemically characterized for their role as biofactories in the production of commercially important carboxylic acids such as acrylic, glycolic, mandelic and nicotinic acid, as well as to detoxify toxic nitrile compounds in waste treatment. Most nitrilases are inducible by the nitrile substrates and amide or carboxylic acid products, although a few constitutive nitrilases have also been described in *Brevibacterium* R312, *Klebsiella. ozaenae*, *B. subtilis* ZJB-063, and *Alcaligenes* sp. ECU0401. *Bacillus* sp. strain OxB-1 was shown to metabolize phenyl acetaldoxime (PAOx) into phenyl acetontirile (PAN), by the action of PAOx-dehydratase, which is successively hydrolyzed to phenylacetic acid (PAA) by the action of nitrilase (182). Kobayashi et al., (1995) characterized an IAN-specific nitrilase from *Alcaligenes faecalis* JM3 (183). Howden et al., (2009) also identified an aryl acetonitrilase that was capable of hydrolyzing IAN to IAA in the plant pathogen *P. syringae* B728a (184). (185).

In some bacteria, nitrilase genes are found next to acetaldoxime dehydratase genes and their enzymatic activities are linked. This genetic organization was observed in *Rhodococcus* sp. NCIMB 11216, *Rhodococcus* sp. AK32, *Bacillus* sp. OxB-1 and *Corynebacterium* sp. C5 (175)(186). The genomes of the plant-associated bacteria *P. syringae* B728a and *P. syringae* DC3000 also encode a putative phenyl acetaldoxime dehydratase upstream of the nitrilase gene (187). In some instances, bacteria can possess acetaldoxime dehydratase and both nitrilase and nitrile hydratase. Both nitrile-

hydrolyzing enzymes can act on the same substrate, but perhaps each is induced under different conditions.

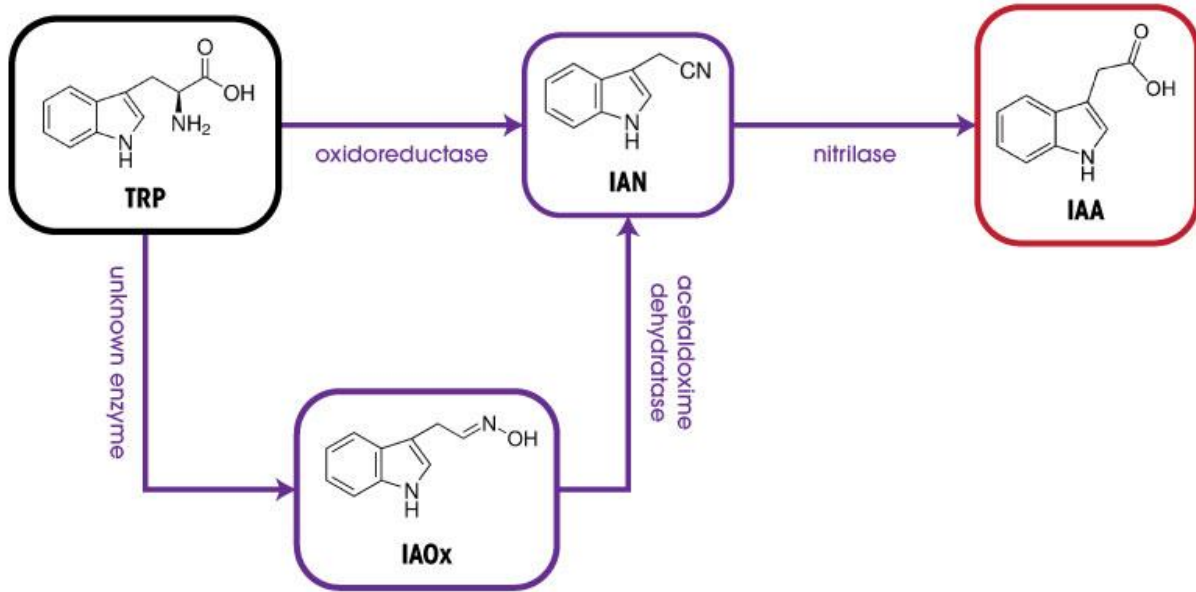


Figure. 3. The Indole acetaldoxime (IAOx)- Indole acetonitrile (IAN) Pathway

TRP= tryptophan, IAN= indole acetonitrile, IAA= indoleacetic acid, IAOx= indole acetaldoxime

1.7 Factors Modulating IAA Production in Bacteria

Both genetic and environmental factors affect the production of microbial IAA. The concentration of IAA acts as a crucial information cue to trigger and modulate various aspects of plant and bacterial physiology (188). Therefore, endogenous levels of IAA are very finely regulated in both plants and bacteria.

The IAA secreted by rhizospheric and endophytic bacteria acts in conjunction with the plant's endogenous IAA supply. Thus, the impact of bacterial IAA on plants can either be positive or negative, depending on the level of IAA produced and secreted (189). The production of IAA by bacteria, is affected by both abiotic and biotic factors that can lead to distinct expression patterns in space and time, with different effects on host plants. By determining the factors that control the microbial synthesis of IAA, we can maximize the beneficial effects of IAA-producing PGPB and perhaps reduce the virulence of IAA-producing phytopathogens. A microbe may selectively employ a particular IAA biosynthesis pathway of the multiple pathways of which it is capable, according to its environment (45). For instance, *Rhizobium* spp. appear to utilize the IAM pathway only when associated with the host plant (190) and the IPyA pathway when it is in the free-living state (191). Brandl and Lindow (1997) suggest that plant-associated bacteria have each evolved mechanisms to induce conditional expression of IAA genes based on environmental cues specific for that plant habitat, whether it be the internal or external surfaces of plants (192).

Plants have IAA regulatory systems in place that maintain IAA at nontoxic physiologically appropriate levels (193). Converting free IAA to conjugated forms is part of this regulatory system. Inside the plant, free IAA can be inactivated through conjugation to sugars, amino acids, or peptides (193). In a manner similar to plants, bacteria may also conjugate IAA to other moieties. Oleander strains of *Pseudomonas syringae* pv. *savastanoi* have IAA-lysine synthetase activity, which catalyzes the formation of an amide bond between the carboxyl group of IAA and the amino group of lysine to form IAA-Lys (194). Olive strains of *P. syringae* pv. *savastanoi*, cannot convert IAA to IAA-lysine and accumulate twice as much free IAA when fed with tryptophan. When this strain was conferred with

IAA-lysine synthetase activity, IAA accumulation was reduced to half that of the wild-type strain. Similarly, strains with deletions in the IAA-lysine synthetase gene accumulated five times more free IAA than the parental strains (194)(195). IAA conjugates may vary among bacteria and can occur as storage forms of IAA (IAA–Ala, –Leu, –Asp, –Glu)(196). A group of bacterial aminoacylases that specifically hydrolyze acetylated amino acids, including an IAA-Asp hydrolase, has been purified from *P. agglomerans* (197). When IAA is secreted by the cell, it can be readily degraded by chemical or enzymatic oxidation or metabolized by other microbes (96). However, IAA conjugates appear to be protected from such degradation (198)(199)(200). Therefore, conjugation may be a way for the bacteria to deliver continuous and effective levels of IAA to host tissues (45).

Several bacteria are able to degrade IAA and use it as a sole carbon and energy source. However, knowledge is scarce on both the biochemical and genetic aspects of IAA degradation. An anaerobic IAA degradation pathway has been proposed in *Azoarcus evansii* (201)(202), while aerobic degradation has been reported in *Bradyrhizobium* (203)(202), *Pseudomonas* (62), *Burkholderia*, *Rhodococcus*, *Sphingomonas* (204) and *Acinetobacter* (205). The cluster of genes (*iac*) responsible for IAA degradation was first described in *Pseudomonas putida* 1290. Since then, *iac* gene homologues have been identified in several Proteobacteria and Actinobacteria but with different genetic organizations (204). Recently, the plant-growth-promoting bacterium *Paraburkholderia phytofirmans* PsJN was found to possess a cluster of *iac* genes related to those described in *P. putida* 1290, but with additional genes encoding regulatory, transport, and enzymatic functions (206). It is evident that complex IAA regulatory mechanisms exist that control the expression/coordination of IAA degradation and synthesis in natural environments (206). Zuniga et al. (2013) observed that bacterial degradation of IAA plays a

key role in plant-growth-promotion by *Paraburkholderia phytofirmans* PsJN and is necessary for efficient rhizosphere colonization. In wild-type *Paraburkholderia phytofirmans* PsJN the synthesis of IAA occurs before IAA degradation, suggesting that IAA turnover is carefully controlled in this bacterium. Moreover, IAA regulates its own degradation and is able to significantly induce *iac* gene expression. In plants inoculated with the *P. phytofirmans iac*⁻ mutant, the IAA levels in roots are higher than in those inoculated with the wild-type, because the mutant cannot degrade IAA. Consequently, plants inoculated with the *iac* mutant showed a shortening of root growth, in comparison to inoculation with the wild-type (126).

Endophytic bacteria secrete IAA directly to plant cells, often inducing tumorous growths (146). Conversely, secretion of IAA by rhizobacteria exposes the plant to lower concentrations as the hormone may be degraded in the rhizosphere before it ever reaches the plant cell. The cell density of the bacteria also reflects the amount of microbial IAA imposed upon the plant (207)(45).

Production of IAA by microbial isolates varies between different species and among strains of the same species. It appears that IAA biosynthesis is finely tuned to adapt to different environmental conditions and stresses that may be encountered by the bacteria in the environment(46).

Tryptophan, vitamins, salt, oxygen, pH, temperature, carbon source, nitrogen source and growth phase are all contributing factors in the regulation of IAA biosynthesis.

The plant flavonoid luteolin causes a significant increase in the production of IAA in *Rhizobia* (208). Plant roots also release compounds such as vitamins (e.g., pyridoxine and nicotinic acid) and organic

acids (e.g., phenylacetic acid) All of these compounds increased IAA production significantly in *Azospirillum brasilense* Sp245 (209).

Not surprisingly, tryptophan is a major effector of IAA biosynthesis, considering most IAA biosynthesis pathways begin with this precursor (83). Sergeeva et al. (2007) observed that the ideal concentration of tryptophan needed for maximum IAA production differed significantly between six legume-associated *Pantoea agglomerans* isolates (210). For *Rhizobium* sp., there appears to be no linear correlation between the amount of tryptophan and IAA production. In fact, in some strains, higher concentrations of tryptophan actually reduced IAA production (211). Different bacteria require different amounts of exogenous tryptophan supplementation to obtain maximum IAA production. This likely corresponds to each bacterium's inherent ability to synthesize tryptophan and to metabolize tryptophan-derived compounds. Acquisition of nitrogen by transamination of tryptophan yields carbonyl intermediates that are toxic when they accumulate (212)(213)(45). When the concentration of tryptophan is too high, production of IAA may serve as a way to detoxify these toxic intermediates (43). In nature, tryptophan concentrations in root exudates vary with plant species and as such, the amount of IAA by a rhizobacterium can be regulated by the plant with which it is associated (45).

Different microbes vary in their preferential carbon and nitrogen sources for IAA production. Organic nitrogen sources have been observed to stimulate IAA production better than inorganic nitrogen sources (214). Perhaps this is due to increased availability of tryptophan from proteins. *Rhizobium* strains isolated from various host plants had different carbon preferences; some preferred

mannitol, while others preferred glucose. Likewise, for the nitrogen source some strains preferred KNO_3 , NaNO_3 or glutamic acid (215). Shokri and Emtiazi (2010) report that the most important factor that impacts IAA production is the nitrogen source (211). Omay et al. (1993) observed that the IAA content in the supernatant of *Azospirillum brasilense* Cd was more than 10 times higher in ammonium-containing nutrient media than in nitrogen-free medium (216). Similarly, Malhotra and Srivastava (2009) report that *Azospirillum brasilense* SM had lower IAA levels in nitrogen-free conditions (214). Perhaps the carbon/nitrogen preference of each strain is a reflection of their adaptation to what is naturally most available to them in that specific plant environment.

Dimkpa et al. (2012) demonstrated that CuO and ZnO nanoparticles affect the amount of IAA produced in vitro by the soil isolate *Pseudomonas chlororaphis* O6. The levels of copper (200 mg/L) and zinc (500 mg/L) released from the nanoparticles were relevant to those reported for contaminated soils, which ranged from 100 -1,000 mg/kg of Cu and 2,000 mg/kg of Zn. The presence of copper resulted in higher IAA levels in the culture supernatant than in control cultures, while the presence of zinc lowered the levels of IAA. This study found that 23% more tryptophan was utilized by culture amended with copper compared to the unamended control. The presence of zinc did not impact the amount of tryptophan utilized. Neither of the two metals had an effect on the expression of the IAA biosynthesis genes *iaaM/iaaH* (217). Bhattacharyya et al. (2006) investigated the effect of the metals Hg, Pb, Cd and Ba on IAA production by *Rhizobium* and observed that all metals had an inhibitory effect. Dimkpa et al. (2008) also observed that the presence of Fe, Al, Cd, Cu and Ni significantly reduced the levels of IAA produced by *Streptomyces* spp., without affecting the growth of the bacteria (218). Similarly, Kamnev et al. (2005) observed that adding Cu or Cd to the culture

medium of *Azospirillum brasilense* resulted in significantly lower levels of IAA without affecting the bacterial growth rate (219). Therefore, heavy metal-polluted soils may compromise the beneficial effects of IAA-producing PGPR.

Acidic pH, osmotic stress, oxygen stress and temperature changes are environmental circumstances frequently encountered by bacteria. Each of these abiotic factors alters IAA biosynthesis. The optimum temperature for IAA production is strain specific and is not necessarily correlated with the optimum temperature for growth of that bacterium. For example, *Azospirillum brasilense* SM grows best at 30°C, yet maximum IAA production occurs at 37°C. The optimum temperature for IAA production was 30 °C for *Bacillus* spp. and *Streptomyces viridis*, and 37 °C for *Rhizobium* (220)(221). The differential uptake of NO_3^- and NH_4^+ ions absorbed by plants roots, can affect the pH of the rhizosphere. Absorption of NH_4^+ reduces the pH by releasing H^+ ions in the rhizosphere, whereas absorption of NO_3^- increases pH by releasing OH^- ions (222). In *Azospirillum brasilense* Sp245, the expression of the IAA biosynthesis gene *ipdC* is pH dependent. Maximum induction of *ipdC* biosynthesis gene was observed at pH 5.5, a threefold increase in transcriptional activity as compared with that at pH 7. Consequently, growth of strain Sp245 at pH 6.3 resulted in a 40-fold increase in IAA production capacity, as compared with that at pH 6.8 (223). The optimal temperature and pH for IAA production may be a reflection of the niche that the bacterium occupies, be it at the slightly acidic conditions of the rhizosphere or at the physiological conditions inside a plant. The enzyme systems in these bacteria evolve to operate best within these temperature and pH ranges (224)(225). Therefore, the optimal temperature and pH for IAA production is likely a function of what is optimal for the enzymes that carry out IAA biosynthesis. A reduction in pH

caused *Pseudomonas fluorescens* CHA0 to preferentially utilize the tryptophan side chain pathway for IAA biosynthesis (144). An acidic environment can also reduce IAA production in some *Pseudomonas* species (226). Oxygen is also an important factor in the production of IAA. In *Enterobacter cloacae*, microaerobic conditions activate enzymes catalyzing the reduction of the IAA biosynthesis intermediates IPyA and IAAld to the storage compounds ILA and IET, respectively. In contrast, *Azospirillum brasilense* cells under microaerophilic conditions were found to preferentially catalyze the conversion of IPyA to IAA (227). *Azospirillum brasilense* inhabits areas of low oxygen content so when cells were cultured under aerobic conditions, IAA production was greatly reduced, while the bacterial biomass remained unaffected (228). Lowering the oxygen pressure progressively in *A. brasilense* cultures, reduced the *ipdC* expression level up to 15-fold as compared with aerobically grown cells (223). In *Erwinia herbicola*, *ipdC* is expressed independently of culture medium pH and oxygen availability, however it is induced up to 36-fold by osmotic stress. Low water availability is a feature common in the natural environment of bacterial epiphytes; thus *ipdC* expression in response to low water availability may be an adaptation to conditions experienced on plant surfaces (192). The possibility remains that *ipdC* is not directly under osmotic control, but that its rate of transcription is dependent on other factors that are affected by osmotic stress (192).

IAA-production is typically observed when the cells enter the stationary growth phase (45)(229)(230)(231)(216). This may be because in stationary phase, the ideal nitrogen sources have been depleted from the culture medium, and so the nitrogen required for biosynthetic processes can be obtained by deamination of tryptophan via induction of IAA biosynthetic pathways (43). Alternatively, IAA production may be regulated by the stationary-phase sigma factor RpoS (88)(232).

This sigma factor is referred to as a general stress regulator in bacteria; controlling the expression of genes involved in morphological changes, resistance to various stress conditions (e.g. oxidative stress, heat shock, osmotic stress, near-UV irradiation or pH changes), metabolic processes, virulence, synthesis of quorum sensing molecules and production of secondary metabolites (118). Recombinant *P. putida* that constitutively produced RpoS also produced IAA earlier and maintained a high level of production longer compared with wild-type cells (88). Contrastingly, RpoS-deficient mutants of *Serratia plymuthica* G3 had significantly enhanced IAA production. By complementing the *rpoS* mutation, IAA production decreased to wild-type levels (233). Beyond the stationary phase, IAA levels begin to decrease, likely due to the release of enzymes that degrade or conjugate IAA to amino acids (211).

IAA biosynthetic genes may also be induced in response to a cell-density dependent signal.

Quorum-sensing signals such as N -acylhomoserine lactones (AHLs) have been shown to positively regulate bacterial IAA production in *Azospirillum lipoferum* B518 (234). Conversely, inactivation of AHLs in two *Serratia plymuthica* strains resulted in a significant increase in IAA concentration in the culture supernatant, suggesting that in this bacterium the QS systems suppress IAA production (235)(236). These findings suggest that QS-mediated IAA regulation may be strain-specific and perhaps tailored to the life-style of each bacterium to promote competence and adaptation in that specific environment (235).

1.8 Genetic Factors involved in the regulation of IAA Biosynthesis

The molecular mechanisms that regulate IAA biosynthesis at the transcriptional and translational level in bacteria are not well understood. The variances in the IAA levels produced by different bacteria can be attributed to; variations in the regulatory regions flanking IAA biosynthesis genes, the number of functional pathways in each bacterium and the location of the IAA biosynthesis genes, whether on the chromosome or on a plasmid.

The bulk of the work on the regulation of IAA biosynthetic pathways is based solely on the IPyA pathway. Although this pathway is common and perhaps predominant in some bacteria, there are several alternative pathways that may be equally important in IAA production. Therefore, it is imperative that we develop an understanding of the regulation of all the IAA biosynthetic pathways (IPyA, IAM, IAN-IAOx). This is especially important since multiple pathways often co-exist within the same organism and may be differentially or co-regulated.

Having IAA biosynthesis genes on a high copy number plasmid within the bacterial cell provides more gene copies to be transcribed as compared with those located on the chromosome (45). For example, the phytopathogen *P. savastanoi* pv. *savastanoi* has plasmid-borne IAA biosynthetic genes and produces more IAA than *P. syringae* pv. *syringae*, whose homologous genes are on the chromosome (237). Introducing IAA biosynthesis genes on a low-copy number plasmid into the latter strain increases the IAA levels dramatically (237)(46).

During the exponential growth phase, the major sigma factor, $\sigma 70$ (RpoD), is responsible for transcription of most of the highly expressed constitutive genes. When the bacteria stop growing due to deprivation of nutrients, the second principal sigma subunit, $\sigma 38$ (RpoS), begins to be synthesized. Guanosine 3',5'-bispyrophosphate (ppGpp) activates RpoS, acting as a signal of imminent stationary phase and as a signal of perturbations in steady-state growth (238). When environmental conditions are favourable, the ppGpp levels decrease. In *E. coli*, the levels of ppGpp strongly increase in response to amino acid limitation, or starvation for carbon, nitrogen, and phosphorus. Mutants that are ppGpp-deficient contain highly reduced RpoS levels. On the other hand, RpoS accumulation can be triggered by artificially stimulating ppGpp accumulation (64)(112). However, it is also unclear whether this ppGpp effect is direct or indirect (239). *Serratia plymuthica* G3 possesses two *ipdC* genes. Inactivation of *ipdC1* resulted in a 2.5-fold reduction in IAA levels, while inactivation of *ipdC2* led to an ~100-fold reduction in IAA levels, suggesting that IPCD2 contributes more to the IAA pool. The sigma factor RpoS was found to positively control expression of *ipdC1* at the transcriptional level, but negatively regulates transcription of *ipdC2* (233). A previous report also showed that production of IAA in the rhizobacterium *Pseudomonas chlororaphis* O6 was negatively regulated by RpoS (240). It has been suggested that a two component regulatory system composed of a GacS sensory kinase and a GacA response regulator may be involved in controlling the synthesis of IAA in some bacteria (241)(242). This system has been known to regulate an array of genes involved in the production of secondary metabolites (243). Saleh and Glick (2001) observed that when *Enterobacter cloacae* CAL2 and *Pseudomonas* sp. UW4 were transformed with a plasmid harboring either RpoS or GacS genes from *Pseudomonas fluorescens*, there was a 10- and 2-fold increase in IAA levels, respectively (232). This finding implies that both RpoS

and GacS work together in the regulation of IAA synthesis. Whistler et al. (1998) report that the GacS system actually up-regulates RpoS, therefore perhaps the observed increase in IAA production is due to RpoS accumulation (145). Kang et al. (2006) report the opposite effect, the GacS system down-regulated IAA synthesis in *P. chlororaphis* O6 (243). A GacS mutant produced 10-fold more IAA than the wild-type when supplemented with tryptophan in stationary phase (243). The level of RpoS was not measured in this study, therefore, it is unknown whether in this strain GacS regulates IAA levels via RpoS or acts together with other regulators.

Some studies suggest that IAA biosynthesis is induced when the bacterium is in contact with a host plant. For example, *ipdC* promoter activity increased dramatically when *A. brasilense* Sp7 was associated with wheat roots (244). Similarly, the *iaaM* gene of *Dickeya dadantii* 3937 was upregulated when associated with host spinach plants (245). Studies using *ipdC*-driven reporter gene fusion have shown that the *ipdC* gene in *E. herbicola* 299R is plant inducible. Expression of *ipdC* increased by 32-fold on bean and tobacco leaves, and 1000-fold on pear flowers compared to induction in culture medium (192)(246). Manulis et al., (1998) suggest that different IAA biosynthesis pathways are employed in different microenvironments by the same bacterium. This idea came from a study on the plant pathogen, *E. herbicola* pv. *gypsophylae* where the plasmid-borne IAM pathway genes are highly transcribed when the bacteria is inside the plant stems as opposed to when it is on the leaf surfaces (151). However, it is unclear which plant-specific signal is responsible for this induction. Tryptophan is not only a precursor for IAA synthesis but it also induces the expression of IAA biosynthetic genes. In the rhizosphere, bacteria acquire tryptophan from plant root exudates, thus to some extent, the host plant controls microbial IAA production by supplying this inducer (131).

Perhaps it is the release of tryptophan through plant exudates that serves as the signal to induce IAA production when the bacterium is in contact with the plant. In *P. syringae* pv. *syringae* and *D. dadantii* 3937, IAA production via the IAM pathway increased upon addition of tryptophan to the culture medium (247)(248). On the other hand, in *P. syringae* pv. *savastanoi*, the IAM pathway genes are constitutively expressed and do not require an exogenous supply of tryptophan (249). In *Enterobacter cloacae* the *ipdC* gene is transcribed constitutively at a basal level but is inducible by tryptophan. Expression of this gene is also increased by phenylalanine and tyrosine. Similarly, in *Rhizobium* spp. and *Azospirillum brasilense*, the IPyA pathway was also induced by tryptophan and in the latter strain by other aromatic amino acids as well (131)(133)(216)(250)(251)(252)(191). The expression of *ipdC* in *E. herbicola* 299R is not influenced by exogenous tryptophan (192)(228).

The end product IAA induces *ipdC* gene expression in a positive feedback manner in *A. brasilense* Sp245 and *A. brasilense* SM, while in *A. brasilense* Sp7 there was no increase in expression upon addition of IAA (223)(87). Differences in regulation of *ipdC* expression between the *Azospirillum* strains may be due to regulatory elements in the promoter regions of the gene. Phenylacetic acid (PAA) is a weak auxin with similar plant growth promoting properties to IAA and a similar structure. It is also able to induce *ipdC* gene expression in some *Azospirillum* strains in a concentration range similar to that of IAA (253). Early studies on the *P. savastanoi* tryptophan monooxygenase (TMO) enzyme that converts Trp into IAM, showed that activity was inhibited by both IAM (the reaction product) and by IAA in a feedback mechanism (146)(254). In *Agrobacterium* and *Rhizobium* the nitrile hydratase which converts IAN into IAM, is induced by the end product IAM (177).

In order to understand the regulation of IAA-biosynthesis genes at the transcriptional level, the promoters and regulatory sequences of these genes must be investigated. Ryu and Patten (2008) discovered that the promoter region of the *ipdC* gene of *E. cloacae* UW5 contained a sequence that is highly similar to the TyrR recognition sequence of *E. coli*. The *tyrR* gene encodes a regulatory protein that is both an activator and a repressor of genes involved in aromatic amino acid transport and metabolism. To test whether TyrR regulates IAA biosynthesis in *E. cloacae*, a *tyrR*⁻ mutant was constructed. The *tyrR*⁻ mutant did not produce detectable IAA in the presence of tryptophan in the stationary phase, indicating that the encoded protein is required for IAA production. Real-time Q-PCR revealed that *ipdC* transcript levels in the *tyrR* mutant were very low in the stationary phase even in tryptophan-supplemented cultures. Electrophoretic mobility shift assays confirmed that TyrR binds to the predicted TyrR box in the *ipdC* promoter region and induces expression (131).

The 5' upstream regions of the *ipdC* gene of *A. brasilense* strains SM, Sp45 and Sp7 were also analyzed to determine regulatory elements in the *ipdC* promoter. A conserved cis element similar to the auxin responsive elements in plants (TGTCNC) was identified in the promoters of the *ipdC* gene (255)(244)(214)(223). This element is essential for *ipdC* expression, as point mutations within this region completely abolished expression (100). Furthermore, an 8-bp inverted repeat separated by a 4-bp spacer was also identified in the upstream region of the *ipdC* gene. Site-directed mutagenesis of this dyadic sequence as well as deletion mutations demonstrated that this element is also required for full activation of the *ipdC* promoter and for its IAA inducibility (223). Vande Broek et al. (2005) further identified an open reading frame, known as *iaaC*, immediately downstream of *ipdC* that is co-

transcribed in an operon. The role of *iaaC* in *ipdC* transcription was analyzed by transferring an *ipdC-gusA* fusion plasmid into an *iaaC* mutant. GusA activity was assayed when the cells were grown in stationary phase, IAA-induced and uninduced. The growth rate of the *iaaC* mutant was similar to the parent strain under all the conditions tested. Furthermore, there was no difference in *ipdC* expression between the parent strain and the *iaaC* mutant. However, the IAA levels in the *iaaC* mutant were dramatically increased. These findings suggest that the protein encoded by *iaaC* reduces the levels of IAA but not by repressing *ipdC* expression (223). Malhotra and Srivastava (2008) compared levels of IAA produced by the three *A. brasilense* strains Sp245, SM and Sp7. Their findings revealed that Sp245 with *iaaC* produces 40% less IAA than strains Sp7 and SM which both lack *iaaC*. The effect of introducing this gene into a strain that lacks it was investigated. Heterologous over-expression of *iaaC* resulted in a ~50 % decrease in IAA. The *iaaC* gene either encodes a regulatory protein that down-regulates some step of the IAA biosynthesis pathway, or it is directly involved in degrading or conjugating IAA. In some *A. brasilense* strains IAA levels seem to be more strictly controlled than in others, perhaps as a function of the extent of their interaction with a plant (87).

For some time, the *A. brasilense ipdC* gene was the only bacterial gene reported to possess an auxin response element (AuxRE) in its promoter, as is typically observed in plants (255). The plant AuxRE is a promoter DNA sequence that confers inducibility to auxin response genes. Recently, a sequence resembling the AuxRE of IAA-inducible plant promoters was also identified in *P. savastanoi* Psn23, located at the 5' end of the *iaaM/iaaH* operon and the 5' end of the *iaaL* gene. This study suggests that in *P. savastanoi*, IAA synthesis (*iaaM/iaaH* operon) and IAA conjugation to IAA-lys

(*iaaL*) are regulated by IAA. The DS element associated with the AuxRE of *iaaL*, but not with that of the *iaaM/iaaH* operon, allows differential IAA-inducible expression of these genes in *P. savastanoi*, based on their function in IAA metabolism. At high IAA concentrations, the DS element of *iaaL* would guarantee its IAA inducibility and consequently, excess IAA is conjugated to IAA-lys (51).

An AraC-type transcriptional regulator (*nitR*) is found downstream of the nitrilase gene in *Rhodococcus rhodochrous* J1 and is essential for nitrilase expression (175)(256). A similar transcriptional regulator is found upstream of the nitrilase genes of *Bacillus* sp. OxB-1, *P. syringae* B728a and *P. syringae* DC3000 (173)(184). In *Pseudomonas* sp. UW4, a predicted LysR transcriptional regulator is located upstream of the nitrilase gene that is involved in IAA biosynthesis and a predicted AraC transcriptional regulator is directly upstream of a gene cluster containing aldoxime dehydratase, nitrile hydratase and amidase (162). These transcriptional regulators may provide insight into the regulation of the IAN and IAM pathways.

1.9 Introduction to Thesis

A plethora of studies can be found in the literature, where stimulation of plant growth is reported following inoculation with a putative PGPB; however, the specific mode of action of the PGPB is rarely described. The research reported herein strived to design and execute experimentation that describes a fundamental mode of action at the physiological and genetic level in a particularly effective PGPB known as *Pseudomonas* sp. UW4. This bacterium was originally isolated from the rhizosphere of reeds growing in Waterloo, Ontario, Canada (1)

Pseudomonas sp. UW4 is a highly remarkable rhizobacterium, able to establish a beneficial association with a wide variety of plants. It also has the ability to adapt successfully to different and changing environmental conditions. This is reflected in its genome, which shows traits of a versatile metabolism, including the production of polyhydroxyalkanoates (PHAs) carbon storage compounds, degradation of various aromatic compounds, heavy metal resistance, antibiotic resistance, cold tolerance and high salinity tolerance (Fig. 4). This psychrotolerant bacterium is able to grow in soil at low temperatures (4°C), typical of those encountered in the spring in Canada; thus providing the plant with a significant advantage under these conditions (257). Strain UW4 has been shown to enhance plant growth in the presence of flooding, heavy metals, cold, high levels of salt, and phytopathogens (162).

The fundamental objective in PGPB application is the delivery of beneficial products or biological activities to the target plant. The major mechanisms employed in plant-growth-promotion by UW4 include: ACC deaminase, siderophore secretion, trehalose synthesis and IAA synthesis. Because of the indispensable role of IAA in plant-growth promotion, a crucial component to the advancement of the development of highly effective PGPB inoculants is to delineate IAA biosynthesis pathways by characterizing the gene(s) involved.

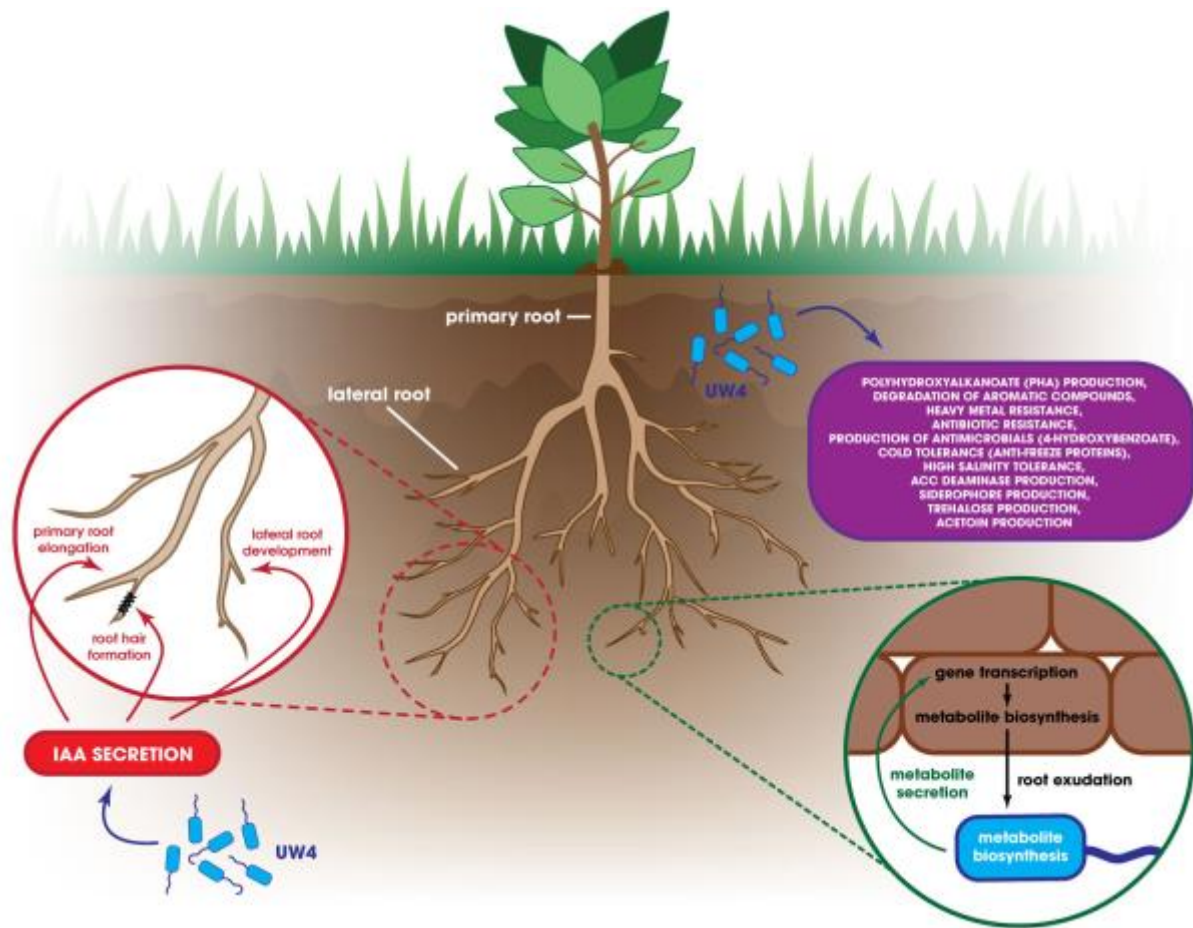


Figure 4. Plant-growth-promoting mechanisms used by strain UW4

IAA biosynthesis is often highly complex in nature as multiple intersecting pathways may operate within a single bacterium such as strain UW4, creating a robust IAA biosynthetic network (Fig. 5). This complex multi-route biosynthetic system provides IAA-insurance to the bacterium; this occurs because the loss of any particular pathway can be compensated by the activation of an alternate pathway. It also stresses the importance to PGPB of having the ability to produce IAA.

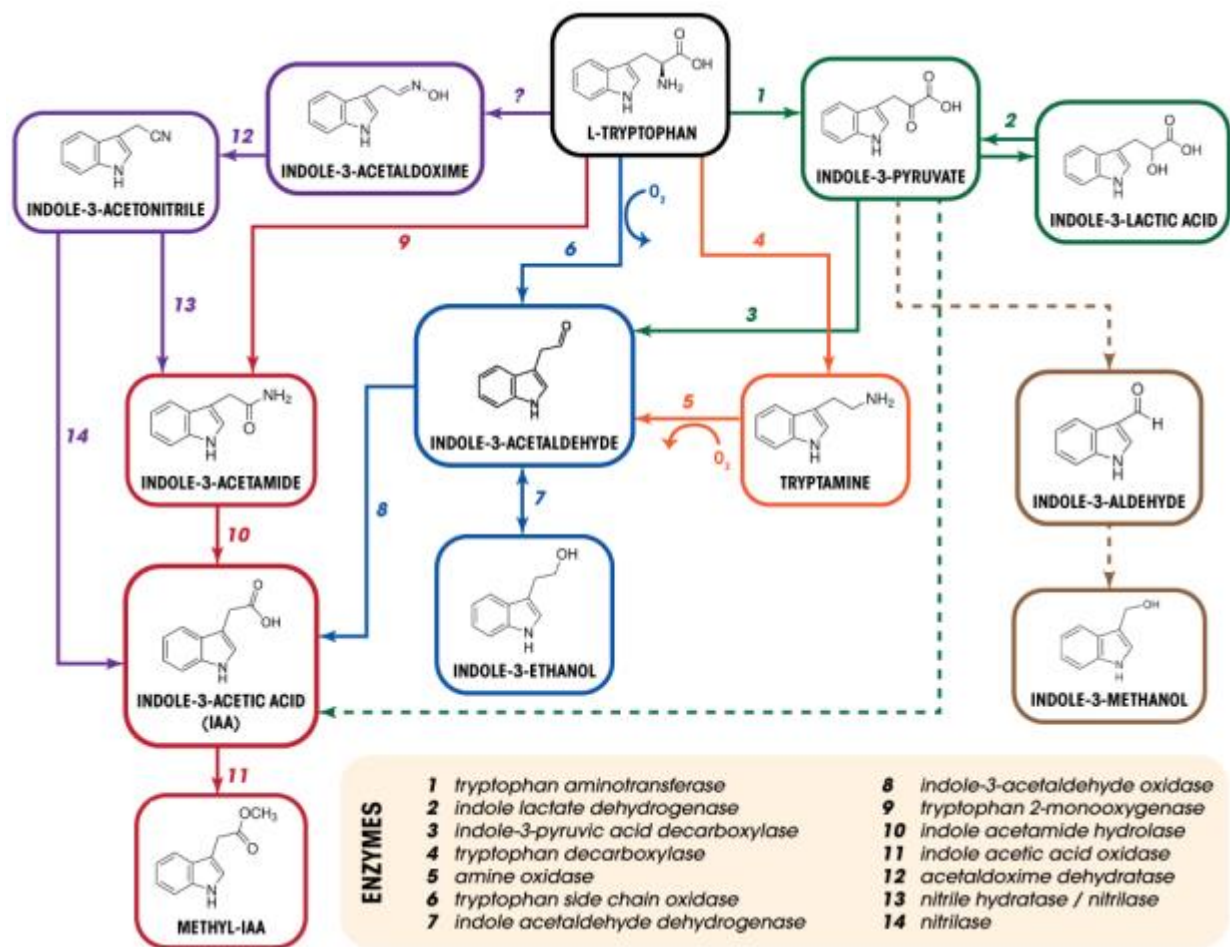


Figure 5. IAA Biosynthesis Pathways in Bacteria

Dashed lines represent reactions that occur non-enzymatically. Enzymes are labeled with respective numbers.

The entire genome of strain UW4 was sequenced in our lab, allowing us to unravel some of the complex biological mechanisms that this bacterium uses to promote plant growth. The genome contains 5,423 predicted coding sequences (CDSs) and biological roles were assigned to 4,158 (76.7%) genes of the predicted coding sequences based on sequence similarity searches and experimental evidence (162). Two potential IAA biosynthesis pathways- the IAN and IAM pathway,

and at least seven marker genes for these pathways were identified in the genome (Fig. 6) (162). Based on this sequence information, it was hypothesized that in the IAN pathway, the tryptophan precursor is first converted to the IAOx intermediate by an unknown enzyme. Subsequently, a phenyl acetyldoxime dehydratase (*pheD*) converts the IAOx intermediate into the IAN intermediate. This IAN is either directly converted into IAA by nitrilase (*nit*) or it may be converted into IAM by either nitrilase (*nit*) or nitrile hydratase (*nthAB*). Alternatively, tryptophan can be directly converted into IAM by tryptophan monooxygenase (*iaaM/aux1*). The IAM intermediate would then be converted into the final product, IAA, by amidase (*ami*). Figure 6 summarizes the putative pathways operating in strain UW4 and the genes mediating each step of the pathway.

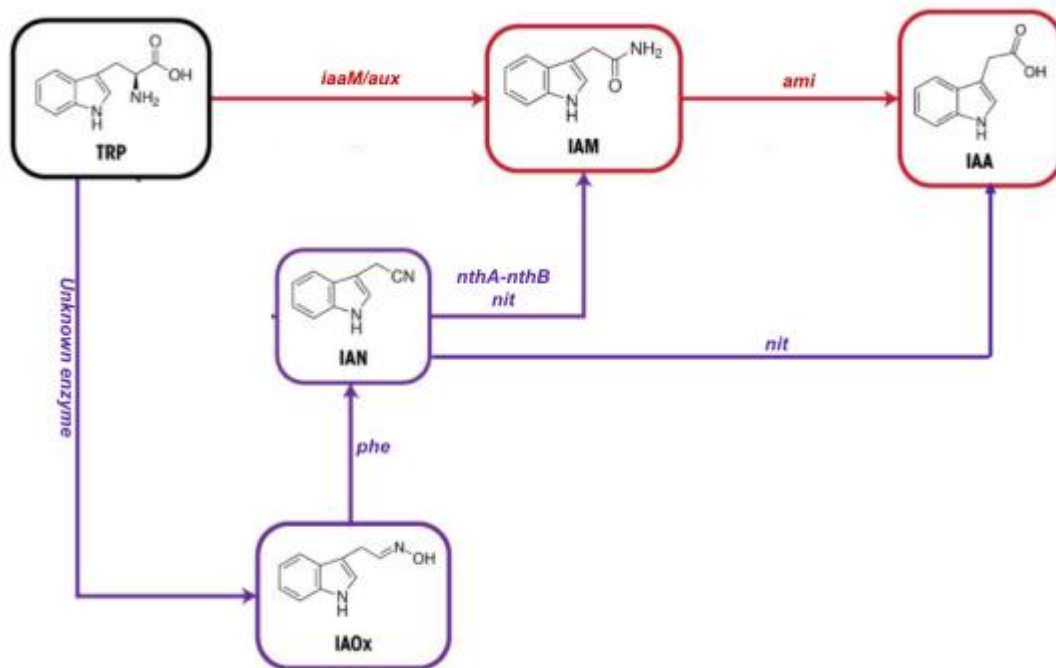


Figure 6. Putative IAA Biosynthesis Pathways in UW4

iaaM, aux= tryptophan monooxygenase, *ami*= IAM-hydrolase/amidase, *nit*= nitrilase
nthA-nthB= nitrile hydratase, *phe*= indole acetyl oxime dehydratase

1.9.1 Research Goals

The central aim of the research reported herein was to decipher the IAA biosynthesis pathways in strain UW4. My previous research elucidated a fraction of the IAA biosynthetic network in this strain by biochemically characterizing three of the seven implicated genes (*nit*, *ntbA* and *ntbB*) (258). To gain a more complete understanding of how this pivotal hormone is produced, a mechanistic functional analysis of all seven target genes was undertaken, to determine the contribution of each gene to the overall IAA pool and how their expression is regulated.

The first objective was to biochemically characterize the amidase protein encoded by the *ami* gene. The enzymatic activity of Ami is proposed to be coupled with that of the previously characterized nitrile hydratase (*ntbA*, *ntbB*) and nitrilase (*nit*). Altogether these genes complete the proposed IAN-IAM pathway. Regulatory effects were taken into consideration by performing transcriptional analysis in order to determine whether the expression of these genes is regulated by the tryptophan, IAA-intermediates (i.e., IAM and IAN) or by IAA. To date, the bulk of the information on the genetic regulation of IAA is based studies of the IPyA pathway. Although this pathway has been described in various PGPB, based on DNA sequence similarity searches, it is not found in strain UW4. The work reported herein is among the first attempts to explore the regulation of the IAOx-IAN-IAM pathways in a PGPB.

The effect of bacterial IAA on plant growth, be it stimulatory or inhibitory, is concentration-dependent. As such, the performance level of PGPB may need fine-tuning to avoid production levels too small or too great (259). The second objective of this research was to increase the IAA biosynthetic capacity of strain UW4 by overexpressing target IAA genes in a transformed UW4

strain, and to examine the biological effect of inoculating plants with these transformants. The third objective was to create IAA-mutants by knocking out the seven target genes involved in IAA biosynthesis, in order to delineate which genes/pathways contribute most to IAA production. By inoculating plants with the IAA knockout mutants, we may be able to better assess the contribution of the bacterially-derived IAA to the growth of the plant. It is expected that the mutants will not promote plant growth to the same extent as the wild-type strain. On the other hand, it is expected that inoculating plants with the IAA over-producing transformants, may promote plant growth to a greater extent than the wild-type strain. Considering that UW4 harbors multiple plant-beneficial properties, which may or may not be co-regulated; the cross-talk between IAA and other plant-growth-promoting factors such as ACC deaminase activity and siderophore production was also considered. The final objective of this work was to characterize the putative tryptophan monooxygenase genes (*iaaM* and *aux*) and determine whether they play a role in the IAM pathway.

1.9.2 Organization of thesis

Each chapter of this thesis is written in manuscript-style that should be suitable for subsequent publication. Each chapter includes a brief introduction that outlines the theme and objectives of that chapter, methods, results, discussion and a conclusion that draws out its overall implications. All of the chapters contribute to the general aim of deciphering IAA biosynthesis pathways in UW4, however each chapter focuses on a different approach to achieving this goal.

Chapter 2

Biochemical Characterization of an Amidase that converts Indoleacetamide into Indoleacetic acid

2.1 Introduction

Bacterial provision of IAA to plants was first described as a mechanism used by phytopathogens to invoke plant disease in the 1980's (260)(45). Since then, it was discovered that many plant growth-promoting bacteria (PGPB) also produce IAA, and consequently, this compound has been designated as one of the most important plant growth regulators. PGPB promote plant growth by secreting IAA, which is subsequently taken up and used by the host plant (45). This hormone is so crucial to plant development, that PGPB often possess multiple biosynthesis pathways to ensure the production of a sufficient amount of IAA (4). The effect of microbial IAA on the plant phenotype depends mainly upon the IAA concentration, which in turn is affected by the extraordinary complexity of several other processes such as IAA biosynthesis, conjugation, de-conjugation, degradation, and intercellular transport (261).

The promotion of plant root development by *Pseudomonas* sp. UW4 is dependent in large part on IAA production. Several genes that encode enzymes putatively involved in the biosynthesis of IAA were identified in strain UW4 (162). These genes appear to be part of at least two different IAA biosynthesis pathways (Fig. 6) (258). In this bacterium, the indole acetonitrile (IAN) and indoleacetamide (IAM) pathways appear to be linked (Fig. 7).

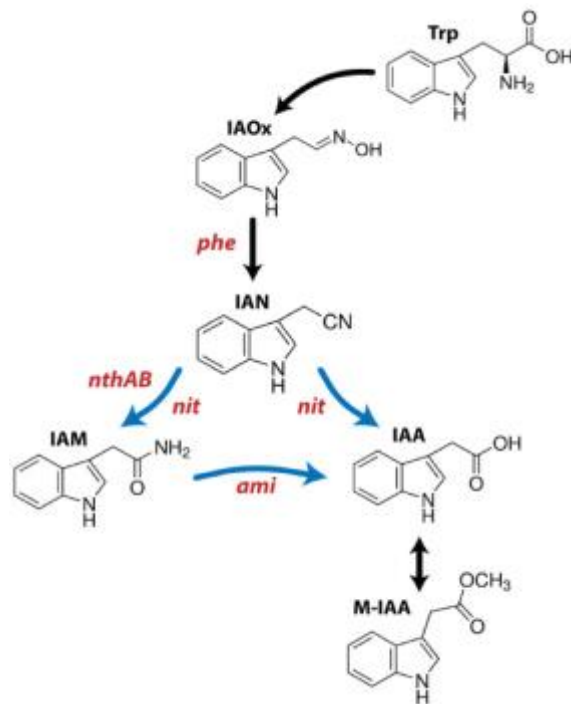


Figure 7. The IAN-IAM Pathway in UW4

Trp = tryptophan, IAOx = indole acetaldoxime, IAN = indole acetonitrile, IAM = indole acetamide, IAA = indoleacetic acid, M-IAA= methyl indoleacetic acid. The genes are labeled in red above each arrow (*phe*, *nthAB*, *nit*, *ami*). Arrows that are shaded blue represent enzymes that have been biochemically characterized in our lab.

The traditional IAM pathway was first described in phytopathogenic bacteria and involves a two-step reaction; (I) Trp is first converted to IAM by the enzyme tryptophan monooxygenase, (II) IAM is deaminated oxidatively to IAA by IAM hydrolase/amidase.

Very few studies have characterized the IAN pathway in bacteria (258)(175)(182)(174). In this pathway, Trp proceeds to IAA through the intermediates indoleacetaldoxime (IAOx) and IAN. The

enzyme that catalyzes the conversion of Trp to IAOx has not been characterized in bacteria; however, in plants cytochrome P450 monooxygenases carry out this reaction (178). The IAOx is dehydrated to IAN by an aldoxime dehydratase (176). The IAN can be converted to IAA either directly by a nitrilase or via a two-step pathway in which the IAN is first hydrated to IAM by nitrile hydratase or nitrilase and then to IAA via an IAM-hydrolase/amidase (258)(43)(185).

In our laboratory, we have previously purified and biochemically characterized a nitrilase (*nit*) and nitrile hydratase (*nthAB*) from strain UW4 that converts IAN into IAM (258). In this chapter, the gene encoding an IAM-hydrolase (*am*) has been expressed at high levels in *E. coli* and the recombinant protein has been purified and shown to be involved in the conversion of IAM to IAA.

2.2 Materials and Methods

2.2.1 Bacterial Strains and Plasmids

E. coli DH5 α (InvitrogenTM) was used as an initial cloning host, and *E. coli* BL21(DE3) (Novagen/Merck, KGaA) was used as the host for recombinant protein expression. This expression host is designed for expression directed by pET vectors and contains an IPTG (isopropyl-D-thiogalactopyranoside)-inducible T7 RNA polymerase (Novagen/Merck, KGaA). *Pseudomonas* sp. UW4 (262) was grown and maintained aerobically at 30°C in tryptic soy broth (TSB) (Becton-Dickinson) supplemented with 100 $\mu\text{g mL}^{-1}$ of ampicillin. *E. coli* strains were maintained aerobically at 37°C in Luria-Bertani (LB) broth. When appropriate, 50 $\mu\text{g mL}^{-1}$ of kanamycin and 0.1 mM IPTG

were added. The plasmid pET30b+ (Fig. 8) was used for the expression of the Ami protein. The plasmid construct generated in the present study is described in detail in Table 1.

Table 1 Plasmids, strains and primers used in this study

Plasmid, Strain or Primer	Sequence (5'-3') or Gene Accession Number	Description
Plasmids		
pET-Ami	PputUW4_03350	pET30b(+) vector with the <i>ami</i> gene from UW4 inserted between NcoI and HindIII sites
Strains		
<i>Pseudomonas sp.</i> UW4	CP003880	Wild-type <i>Pseudomonas sp.</i> UW4 plant-growth-promoting bacterium
<i>E. coli</i> DH5 α □□		F- Φ 80 <i>lacZ</i> ΔM15 Δ(<i>lacZYA-argF</i>)U169 <i>recA1 endA1 hsdR17</i> (rK-, mK+) <i>phoA supE44</i> λ- <i>thi-1 gyrA96 relA1</i>
<i>E. coli</i> BL21 (DE3)		<i>fbuA2 [lon] ompT gal</i> (λ DE3) [<i>dcm</i>] Δ <i>hsdS</i> λ DE3 = λ <i>sBamHI</i> Δ <i>EcoRI</i> -B <i>int::(lac::PlacUV5::T7 gene1) i21</i> Δ <i>nin5</i>
<i>E. coli</i> BL2::pET-Ami		<i>E. coli</i> BL21 (DE3) carrying pET-Ami vector
Primers		
ami-F	TAATCCATGGATGGCCATTGTTTCGC	ami (NcoI)-fwd
ami-R	ATTAAAGCTTTTACAACGTCTTCCAGTCG	ami (HindIII)-rev
F= forward primer, R= reverse primer		

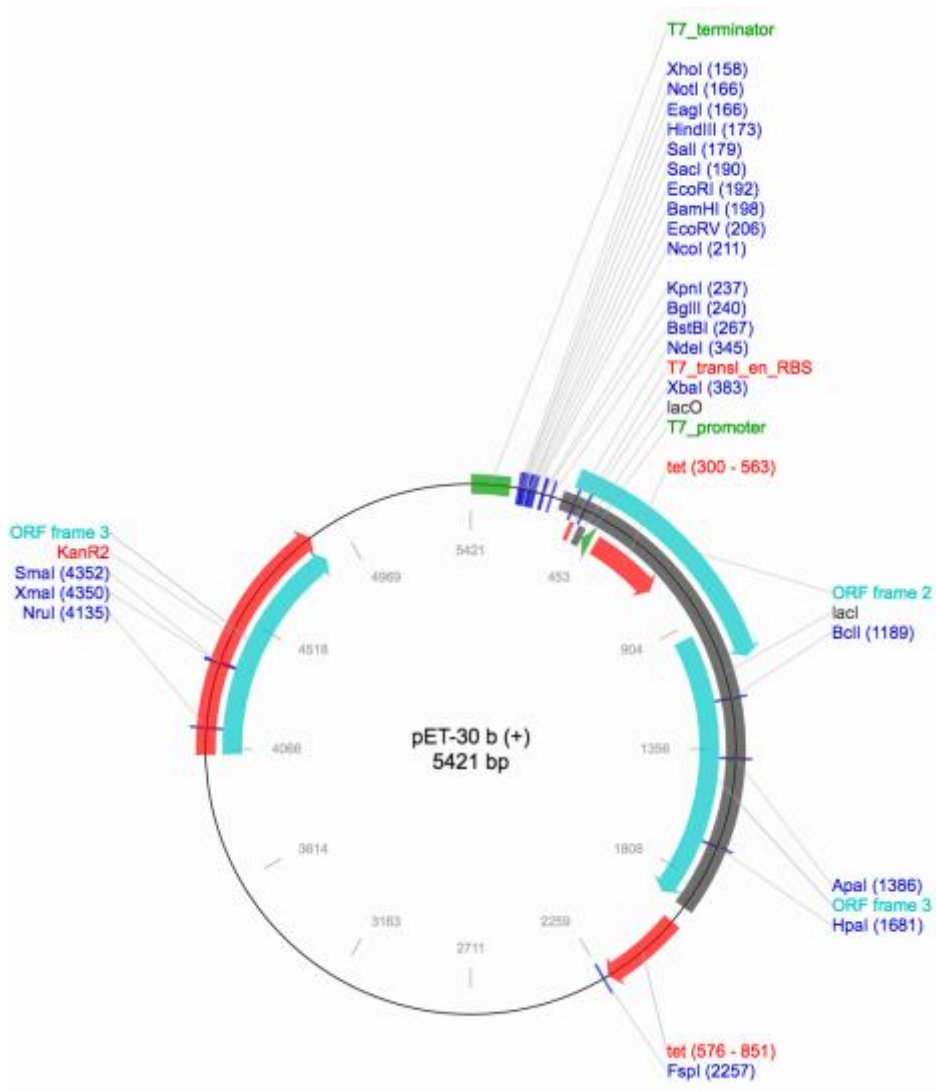


Figure 8. Plasmid map of the pET30b(+) expression vector

The *ami* gene was cloned between the NcoI and HindIII sites. Vector Map was taken from the AddGene© plasmid repository, Cambridge, MA.

2.2.2 DNA Extraction and Expression Plasmid Construction

Genomic DNA from *Pseudomonas* sp. UW4 was isolated using the Wizard® Genomic DNA purification kit (Promega Catalog No. A1120). The primer sequences used to amplify the UW4 *ami* gene are given in Table 1. Both the forward and the reverse primer sequences were based on the fully sequenced UW4 genome. The amplified fragments were subcloned between the NcoI and HindIII sites of pET30b+, resulting in the pET-Ami construct. Hot-start PCR was performed with KOD Hot Start DNA polymerase (Novagen). The reaction mixture was set up on ice and included 5 μ l of KOD hot start buffer, 3 μ l of 25 mM MgSO₄, 5 μ l of 2M of each of the deoxynucleoside triphosphates (final concentration, 0.2 mM), 1.5 μ l of forward and reverse primer (final concentration, 0.3 mM), 100 ng of template genomic DNA, 1 μ l of KOD hot start polymerase and PCR grade water up to the final volume of 50 μ l. The PCR was performed in an Eppendorf Master Cycler gradient machine using the following amplification conditions: 95°C for 2 min, 95°C for 20 s, 71°C for 10 s, 70°C for 15 s, 70°C for 5 min, and ending at 4°C.

2.2.3 Overexpression of Recombinant Ami in *E. coli*

The expression plasmid pET-Ami was initially transformed into *E. coli* DH5 α to maintain the recombinant plasmid without any background basal protein expression. For expression of the recombinant protein, the plasmid was transformed into *E. coli* BL21(DE3) using the calcium chloride method described by Sambrook and Russell (2001). Cells transformed with pET-Ami were grown in 500 ml of Luria-Bertani medium containing kanamycin (50 μ g ml⁻¹) at 37°C with shaking, until the optical density at 600 nm reached \sim 0.5. At this point, the cultures were induced with 0.1

mM IPTG and incubated at room temperature overnight. The following day, the cells were collected by centrifugation at 2,000 x g for 20 min at 4°C. The cell pellet was washed with 20 ml of 50 mM KH_2PO_4 (pH 7.5) with gentle vortexing, followed by centrifugation at 2,000 x g for 10 min at 4°C. This wash step was repeated twice more. The washed pellet was re-suspended in 50 ml of binding buffer (20 mM NaH_2PO_4 , 500 mM NaCl, 20 mM imidazole [pH 7.4]), and the cells were disrupted by sonication 30 times for 30 s each time with 10 s pauses between each round. The lysate was kept on ice at all times during sonication. After sonication, the lysate was centrifuged at 8,000 x g for 30 min at 4°C to separate the soluble and insoluble fractions. The soluble fraction was saved at 4°C for purification.

2.2.4 Purification of the Recombinant Ami protein

The recombinant Ami protein, which has a N-terminal His₆ tag, was purified under native conditions, using a His GraviTrap prepacked, single-use gravity-flow column containing precharged Ni Sepharose 6 Fast Flow, according to the manufacturer's instructions (GE Healthcare, United Kingdom). The purified protein samples were analyzed by SDS-PAGE (Fig. A1, Appendix A). Protein concentrations were determined using the Quick Start™ Bradford Protein Assay (BioRad) with bovine serum albumin (BSA) as the reference standard (263).

2.2.5 Enzyme Assay

The purified recombinant Ami protein was tested for the ability to convert the amide substrate IAM into the acid product IAA. The enzyme activity was assayed in a 1ml reaction mixture containing 50 µg of purified enzyme, 1 mM IAM substrate, and 50 mM KH_2PO_4 buffer (pH 7.5). Reaction

mixtures were allowed to proceed for 1 h. Samples were analyzed by high pressure liquid chromatography (HPLC).

2.2.6 Temperature and pH optima for Ami activity

To determine the ideal temperature conditions for Ami activity, a 1 ml enzyme assay reaction mixture was set up as described above. The tubes were incubated at various temperatures: 5, 10, 20, 30, 35, 40 and 50°C. Reaction mixtures were allowed to proceed for 3 h. To determine the ideal pH, the following buffers were used: sodium acetate at pH 5, sodium citrate at pH 6, potassium phosphate at pH 7.5, Tris-HCl at pH 8, and glycine at pH 9. The 1-ml enzyme assay reaction mixture was set up in the corresponding pH buffers. The tubes were incubated at 30°C for 1 h. Samples were analyzed by high pressure liquid chromatography (HPLC).

2.2.7 High Performance Liquid Chromatography (HPLC) Analysis

HPLC analysis was performed using a Waters Alliance 2695 HPLC separation system (Mississauga, Ontario, Canada), which includes a Waters 2996 photodiode array detector. The system was connected to a PC with Empower 2 software (Waters) for data collection and processing. A Sunfire C18 column (50 by 4.6 mm [inner diameter], 2.5 µm pore size; Waters, Ireland) was connected with a Security Guard C18 guard column (4 by 3.0 mm [inner diameter]; Phenomenex, Torrance, CA). Gradient HPLC was performed at room temperature using a mobile phase containing water-acetic acid (1% [vol/vol]) (A) and acetonitrile-acetic acid (1% [vol/vol]) (B). Starting with 80% A, the gradient began at 2 min and reached 60% A at 15 min. The flow rate was 1 ml/min. A 100 µl sample injection volume was used, and the eluent was monitored at 280 nm.

2.2.8 Multiple Sequence Alignment & Phylogenetic Analysis

A global multiple sequence alignment was constructed for amidase proteins using MEGA 7.0 software (264). Protein BLAST searches were performed using the amino acid sequence of Ami as a query to identify homologous sequences in the National Center for Biotechnology (NCBI) protein database. Only non-redundant coding sequence hits that shared at least 50% identity with the UW4 Ami were included in the alignment. Each alignment was manually refined, and the regions that could not be aligned reliably were removed. The evolutionary history of Ami was inferred by using the Maximum Likelihood method based on the JTT matrix-based model (286). Initial tree(s) for the heuristic search were obtained automatically by applying Neighbor-Join and BioNJ algorithms to a matrix of pairwise distances estimated using a JTT model, and then selecting the topology with superior log likelihood value. One thousand bootstrap replicates were performed to assess the statistical confidence for each clade of the tree. The tree is mid-point rooted; the root is placed at the mid-point of the longest distance between two taxa in a tree. Evolutionary analyses were conducted in MEGA7 (264).

2.3 Results and Discussion

Amidases exhibit broad substrate specificity and belong to a group of C-N hydrolyzing enzymes that make up the nitrilase superfamily (181). The common biochemical trait of amidases is the hydrolysis of the amide bond. Amidases can be divided into two types; aliphatic amidases hydrolyzing only short-chain aliphatic amides and aliphatic amidases that hydrolyze mid-chain aliphatic amides (266). In this study, the focus is on the second type, which are characterized by a highly conserved central region rich in glycine, serine and alanine residues, known as the amidase signature (AS) (267). The

AS family comprises more than 200 proteins found across a great diversity of bacterial genera (267). It is important to note that one microorganism may contain several different signature amidases, with wide substrate specificities. Only in a few cases have the proteins been biochemically characterized, thus there are many predicted amidases with unknown biochemical function in the sequence databases.

For the most part, the activity of amidases has been studied either for the production of D/L amino acids or for the enantioselective synthesis of methyl and methoxyarylacetic acids used in pharmaceuticals or herbicides (268)(269)(270). Little attention has been given to amidases involved in the biosynthesis of the phytohormone IAA. The few IAM-amidases/hydrolases that have been experimentally characterized include; *iaaH* from the pathogens *P. syringae* pv. *savastanoi* (84), *P. syringae* pv. *syringae* Y30 (237), *Pantoea agglomerans* (49) and *Dickeya dadantii* 3937 (52); *tms2* from *A. tumefaciens* C58 (48), *aux2* from *Agrobacterium rhizogenes* A4 (271); and *bam* from *Bradyrhizobium japonicum* (147).

2.3.1 Physicochemical Properties of Ami from strain UW4

The physicochemical properties of the UW4 Ami were deduced from an *in silico* analysis of the amino acid sequence using the ProtParam subroutine of the Expert Protein Analysis System (ExPASy) from the proteomic server of the Swiss Institute of Bioinformatics. These properties were compared to the average consensus values of signature amidases as reported by Gopal et al., (2013). (Table 2). All of the physicochemical parameters for Ami listed in Table 2, are close to the consensus values reported for general amidase signature proteins, supporting the prediction that the UW4 Ami is a broad-spectrum amidase. The InterPro software program provides functional analysis of proteins by classifying them into families and predicting domains and important sites (272). The

UW4 Ami sequence was analyzed in an attempt to further characterize the protein. This search also classified Ami into the amidase family (IPR000120) with the specific Amidase Signature domain (IPR023631). The CATH database, EMBL-EBI Pfam database and the SUPERFAMILY database (273) were all unanimous in this classification.

The instability index provides an estimate of the stability of the protein in vitro. A protein whose instability index is smaller than 40 is predicted as stable (274). The aliphatic index of a protein is defined as the relative volume occupied by aliphatic side chains (274). The amidase of UW4 has an instability index of 33.23 and a high aliphatic index of 86.41, suggesting that it is a thermostable enzyme. It also has low grand average hydropathicity value of -0.068 and is considered a hydrophilic protein (

Table 2) (275). The software package PROSO, a sequence-based protein solubility evaluator, predicted that the Ami protein is soluble upon heterologous expression in *E. coli* (276). In this study, most of the over-expressed Ami protein was indeed in the soluble form.

Based on the amino acid sequence, the predicted size of the UW4 Ami is 54 kDa. This was confirmed by SDS-PAGE, which showed a single band corresponding to this size (Fig.A1, Appendix A). In comparison, enantioselective-amidases generally have subunits with molecular masses of ~55 kDa (277)(278)(165)(279). The amidase from *P. chloraphis* B23, the closest characterized homolog to UW4 Ami (87% sequence identity), had a subunit molecular mass of 54 kDa (277). The wide-spectrum amidase of *Rhodococcus* sp. N771 (49% sequence identity to UW4

Ami) had a molecular mass of 54.7 kDa, while the amidase from *Rhodococcus erythropolis* MP50 (39% sequence identity to UW4 Ami) was approximately 61 kDa (280).

Table 2. Physicochemical Properties of Ami from strain UW4 and other Signature Amidases

Parameter	Amidase (Ami) from strain UW4	^a Consensus for Signature Amidases
Number of amino acids	504	490
Molecular weight (kDa)	54	52.3
Theoretical pI	5.3	6.0
Instability index (II)	33.23	35.6
Aliphatic index	86.41	89.6
Grand average of hydropathicity (GRAVY)	-0.068	-0.042
Total number of negatively charged residues (Asp + Glu)	55	53
Total number of positively charged residues (Arg + Lys)	38	38
Amino acid composition		
Ala (A) 61	12.1%	13.1%
Arg (R) 24	4.8%	6.9%
Asn (N) 17	3.4%	2.2%
Asp (D) 31	6.2%	6.3%
Cys (C) 8	1.6%	1.1%
Gln (Q) 19	3.8%	2.9%
Glu (E) 24	4.8%	4.5%
Gly (G) 53	10.5%	9.2%
His (H) 15	3.0%	2.6%
Ile (I) 22	4.4%	3.9%
Leu (L) 48	9.5%	9.5%
Lys (K) 14	2.8%	2.0%
Met (M) 17	3.4%	2.2%
Phe (F) 14	2.8%	2.6%
Pro (P) 30	6.0%	6.7%
Ser (S) 23	4.6%	5.6%
Thr (T) 24	4.8%	6.5%
Trp (W) 5	1.0%	1.1%
Tyr (Y) 20	4.0%	2.8%
Val (V) 35	6.9%	8.4%

^a Average consensus values for the following Bacterial Signature Amidases: *Pseudomonas chlororaphis* B23, *Pseudomonas putida*, *Rhodococcus rhodochrous*, *Rhodococcus erythropolis* N-774, *Mycobacterium tuberculosis*, *Mycobacterium bovis* (Copal et al., 2013).

2.3.2 Biochemical Characterization of Ami Catalytic Activity

The conversion of IAN into IAM, and further IAM into IAA, has been experimentally demonstrated in strain UW4 in our previous study (258). The former step is catalyzed by a nitrile hydratase, nitrilase or both (258). The latter step is catalyzed by Ami, an amidase that has the catalytic function of IAM-hydrolase. Optimal activity for the UW4 amidase was observed at a temperature of $\sim 35^{\circ}\text{C}$ and a pH of ~ 7.5 , however, the enzyme retained $>50\%$ activity at 5°C and 50°C , and at a pH of 6-8 (Fig. 9 and Fig. 10). The pH profile is comparable to other biochemically-characterized amidases; however, the temperature optimum is considerably lower. Generally, wide-spectrum enantioselective amidases show a temperature optimum in the range of 55 to 65°C . For example, the optimum for amidase activity of *R. rhodococcus* J1 was found to be 55°C and pH 7.9 (278), while the *P. chloraphis* B23 amidase exhibited maximal activity at 50°C and the optimum pH was between 7.0 and 8.6 (277)(164). Amidase from *Rhodococcus* sp. R312 had an optimum pH of 7 with neutral amides and 8 with α -aminoamides (266)(281). Amidase from *R. erythropolis* MP50 displayed maximum activity at 55°C , however the enzyme maintained 75% activity at 60°C and 65% of maximal activity at 30°C . The MP50 enzyme also showed maximal activity at pH 7.5, with about 50% of the activity still maintained at pH 6 and 9 (280). *Pseudomonas* sp. UW4 has an optimal growth temperature of 30°C , but is psychrotolerant and can proliferate at temperatures as low as 4°C (257). The inescapable influence of temperature on biological systems necessitates temperature-compensatory adaptations. Since UW4 is an inhabitant of Canadian soils, which typically experience cold conditions for a large portion of the year, it must produce enzymes that can efficiently perform their catalysis under these conditions. In UW4, Ami is predicted to have coupled enzymatic activity with nitrile hydratase (NHase) (i.e., NHase converts IAN into IAM, which is then converted to IAA

by Ami). The NHase from strain UW4 displays maximum activity at 4°C and a pH of 7.5 (258). Moreover, the nitrilase (Nit) enzyme of UW4 also produces IAM and lower temperatures were found to promote the production of more amide (i.e., Nit produced more IAM at 30°C and pH 8 than at 60°C and pH 5) (258). The ability of all three of these enzymes (Ami, NHase and Nit) to function together within the same temperature and pH range, gives strain UW4 the potential to produce and secrete IAA into the plant rhizosphere in the spring, when Canadian soil temperatures are low and new plants require IAA for growth.

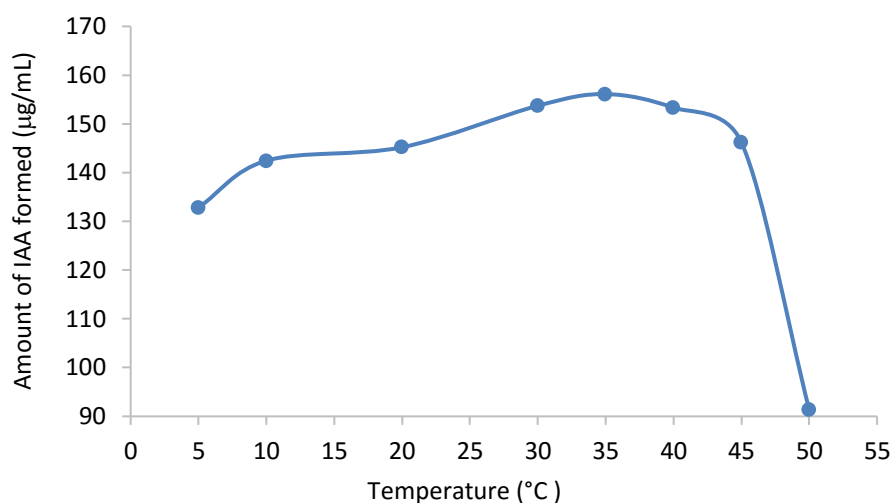


Figure 9. Temperature profile of Ami

The purified recombinant Ami was tested for the ability to convert IAM into IAA. Enzyme activity was assayed in a 1ml reaction mixture containing 50 µg of purified enzyme, 1 mM IAM substrate, and 50 mM KH₂PO₄ (pH 7.5) buffer. Reaction mixtures were allowed to proceed for 1 h. Samples were analyzed by high pressure liquid chromatography (HPLC).

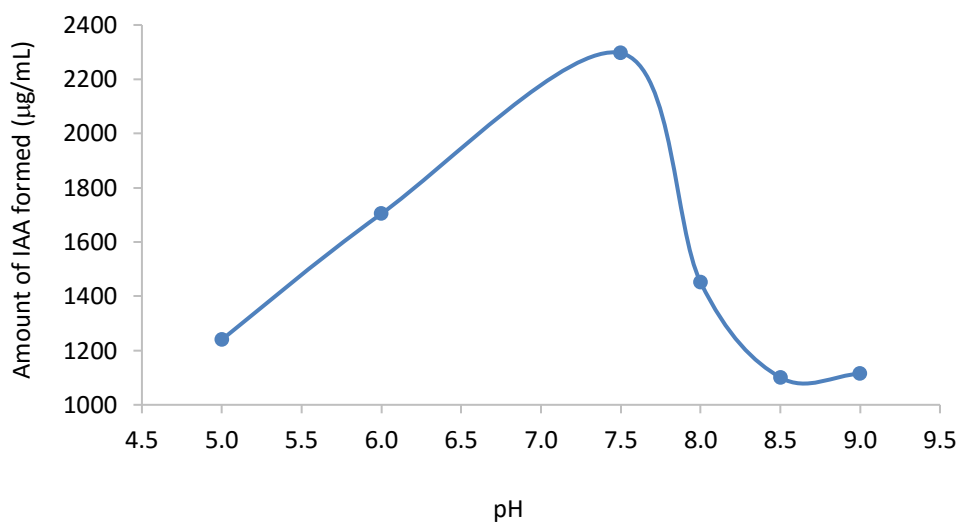


Figure 10. pH profile of Ami

The purified recombinant Ami was tested for the ability to convert IAM into IAA. Enzyme activity was assayed in a 1ml reaction mixture containing 50 µg of purified enzyme, 1 mM IAM substrate. Reaction mixtures were allowed to proceed for 3 h. Samples were analyzed by high pressure liquid chromatography (HPLC).

2.3.3 Multiple Sequence Alignment of Amidases

Chebrou et al. (1996), compared the amino-acid sequences of aliphatic amidases and classified them into four subfamilies: (i) AMD-bacterial aliphatic amidases; (ii) IAAH-indoleacetamide hydrolases; (iii) EA-eukaryotic amidases; and (iv) AH-6-aminohexanoate-cyclic-dimer hydrolases (267). The second subfamily (IAAH) contains the enzyme responsible for the production of IAA. In bacteria that cause neoplastic plant diseases, the IAAH genes are typically carried by a plasmid and can be transposed to plant hosts (i.e., *A. tumefaciens* [P25016], *A. tumefaciens* [PO3868], *Erwinia herbicola* [L33866], *A. vitis* [QO4557] (282)(267)(249)(283), and *A. rhizogenes* [409102]) (267)(43). However, the genes may also reside on the chromosome (i.e., *P. syringae* (PO6618), *B. japonicum* (PI9922), *Rhodococcus erythropolis* strains AJ270 and AJ300 and *Microbacterium* sp. AJ115 (284)(147) (157)(283). The chromosomic IAAH genes are homologous to those found on plasmids, but have lost their transposability (267).

The NCBI protein database was screened for amidase homologs by performing a Delta-Blast search using the amino acid sequence of the UW4 Ami as the query. Only non-redundant coding sequence hits that shared at least 50% sequence identity with the UW4 Ami protein and had very low probabilities (E-value =0) of random matching were retained for a global multiple sequence alignment. In total, 445 sequences ranging from 55-98% identity to the UW4 Ami protein were aligned. High sequence conservation was observed between all of the proteins, with most blocks of amino acids being 100% conserved between positions 74 – 256. The amidase signature sequence (AS) was conserved in all protein sequences (Table A1, Fig. A2, Appendix A). The proteins included in this comprehensive alignment are annotated as amidases, however genome annotations are

typically based on general relation to the closest homologous sequence, rather than precise functional analysis. The catalytic function of most of these amidases has not been experimentally determined.

To provide some insight into the catalytic function of the UW4 Ami protein, another alignment was constructed that included only protein sequences from biochemically characterized amidases. A total of 20 sequences were aligned, including IAM-hydrolases, wide spectrum enantioselective amidases, Glutamyl-tRNA(Gln) amidotransferase and 6-aminohexanoate-cyclic-dimer hydrolase (Fig. 11). Upon analyzing the multiple sequence alignment of the characterized amidases, two blocks of amino acids were highly conserved (Table 3). Block 1 is a conserved stretch of approximately 208 amino acids, containing the signature motif GGSS (S/G) G and the catalytic triad of Ser-171, Ser-195, and Lys-96 which are not position-specific. The active site residue Asp191 is also conserved in all of the proteins analyzed, while Cys203, another presumptive active site residue was retained in 80% of the sequences (Table 3, Fig. 11). Block 2 is a conserved stretch of approximately 38 amino acids located at the C-terminal extremity (Table 3, Fig. 11). Blocks 1 and 2 are similar to the blocks identified in the multiple sequence alignment of the amidase family reported by Chebrou et al., 1996.

Table 3. Sequence conservation in characterized amidases

Alignment Block	Consensus Sequence
<p style="text-align: center;">1 (amidase signature sequence)</p>	<p>L-x-G-x5-K-x25-A-x2-V-x2-L-x3-G-A-x3-G-x22-N-P-x7-<u>G-G-S-S</u>-x-G-x4-V-A-x8-G-x-D-x-G-G-S-x-R-x-P-A-x2-C-G-x2-G-x2-P-T-x-G-x5-G-x8-D-x2-G-x3-R-x-V-x-D-x9-G-x28- R-x-G-x15-V-x6-A-x3-L-x3-G</p>
<p style="text-align: center;">2 (C-terminal extremity)</p>	<p>G-x-P-x2-S-x-P-x6-L-P-x-G-x13-L-x6-E</p>

Conserved sequence blocks from global multiple sequence alignment of 20 characterized amidase proteins. Conserved sites toggled at 80% level. Amino acid residues highlighted in grey are 100% conserved in all sequences. The GGSS motif is underlined. Boldface letters represent the catalytic triad. “x” represents variable residues.

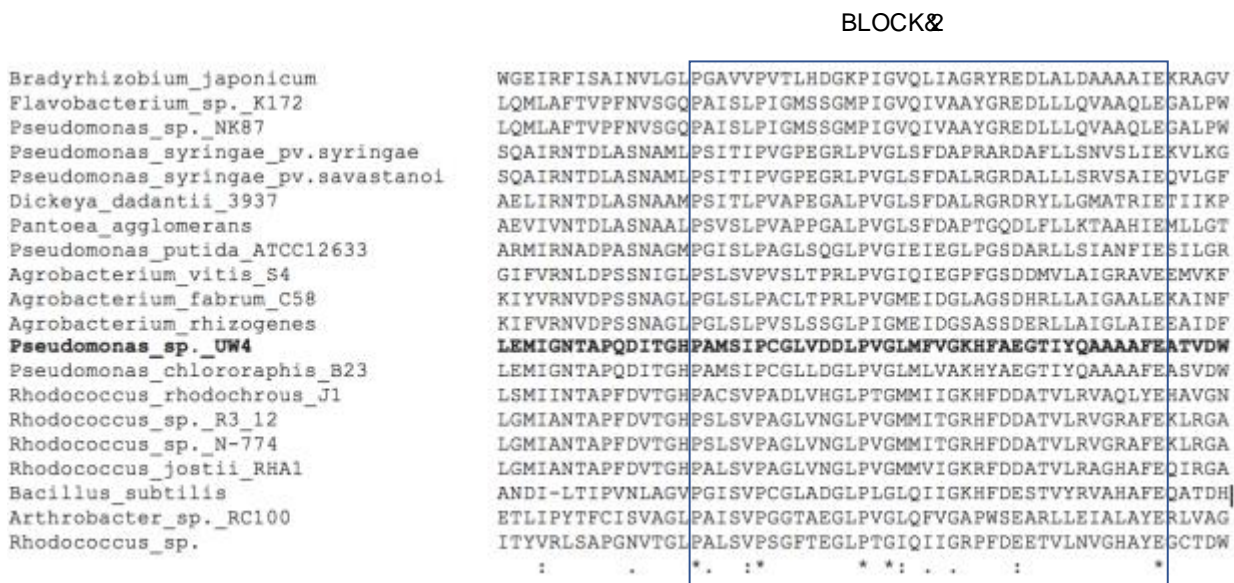


Figure 11. Multiple sequence alignment of characterized amidases

The GGSS motif is boxed in red. The catalytic triad is shown in blue boxes. An * (asterisk) indicates positions which have a single, fully conserved residue. A : (colon) indicates conservation between groups of strongly similar properties. A . (period) indicates conservation between groups of weakly similar properties.

The UW4 Ami protein shared the highest sequence identity (87%) with the amidase of *P. chlororaphis* B23, followed by 39-51% identity to wide-spectrum amidases from several different *Rhodococcus* spp. When compared to the characterized IAM-hydrolases, sequence identity ranged from 26-41% (Table 4). Finally, less than 35% identity was observed with all other amidases in the alignment, including glutamyl-tRNA(Gln) amidotransferase and 6-aminohexanoate-cyclic-dimer hydrolase (Table 4). The amidase of *R. erythropolis* R312, *R. erythropolis* MP50, *R. rhodochrous* J1, *Rhodococcus* sp. N-774 and *P. chlororaphis* B23 can hydrolyze multiple aliphatic and aromatic amides (Table 4). The amidase enzymes from *R. rhodochrous* J1 and *Rhodococcus* sp. N-774 were also shown to hydrolyze IAM. Since UW4 Ami shares significant sequence similarity with these enzymes, it is possible that it is also a broad-spectrum amidase that can hydrolyze various amides, including IAM.

Table 4. Characterized Amidases used in Phylogenetic Analysis

Organism (Protein Accession No.)	Enzyme Annotation	Gene	% Sequence identity to UW4 Ami	% Query Coverage	Biochemical Characterization
<i>Pseudomonas syringae</i> pv. <i>syringae</i> Y30 (AAA17679)	IAM hydrolase	<i>iaaH</i>	41	51	
<i>Pseudomonas syringae</i> pv. <i>savastanoi</i> (AAA2585)	IAM hydrolase	<i>iaaH</i>	41	37	
<i>Dickeya dadantii</i> 3937 (ADM96600)	IAM hydrolase	<i>iaaH</i>	30	81	
<i>Erwinia herbicola</i> pv. <i>gypsophilae</i> (AAC17186)	IAM hydrolase	<i>iaaH</i>	33	57	hydrolyzes indoleacetamide (IAM)
<i>Agrobacterium tumefaciens</i> C58 (AAK90968)	IAM hydrolase	<i>tms2</i>	26	85	
<i>Agrobacterium rhizogenes</i> (AAA22079)	IAM hydrolase	<i>aux2</i>	26	84	
<i>Agrobacterium vitis</i> S4 (Q04557)	IAM hydrolase	<i>iaaH</i>	26	87	
<i>Bradyrhizobium japonicum</i> (CAA33213)	IAM hydrolase	<i>bam</i>	27	79	
<i>Arthrobacter</i> sp. RC100 (BAC15598)	carbaryl hydrolase	<i>cabA</i>	34	85	hydrolyzes 1-naphthylacetamide and isobutyramide
<i>Pseudomonas putida</i> ATCC 12633 (AAO23019)	mandelamide hydrolase	<i>mdlY</i>	28	84	hydrolyzes mandelamide
<i>Bacillus subtilis</i> (O06491)	Glutamyl-tRNA(Gln) amidotransferase subunit A	<i>gatA</i>	32	95	transamidation of Glu-tRNA-Gln into Gln-tRNA-Gln
<i>Rhodococcus rhodochrous</i> J1 (BAA03744)	amidase	<i>amdA</i>	48	96	hydrolyzes propionamide, butyramide,

Organism (Protein Accession No.)	Enzyme Annotation	Gene	% Sequence identity to UW4 Ami	% Query Coverage	Biochemical Characterization
					isobutyramide, valeramide, hexanamide, benzamide, nicotinamide, thiophenecarbox-amide, toluamide, aminobenzamide, indoleacetamide
<i>Rhodococcus</i> sp. AJ270 (CAC08204)	amidase	<i>ami</i>	50	92	hydrolyzes acetamide
<i>Rhodococcus jostii</i> RHA1 (ABG92195)	amidase	<i>ambC</i>	51	95	hydrolyzes acetamide
<i>Rhodococcus</i> <i>erythropolis</i> R312 (P22984)	amidase	<i>amdA</i>	49	85	hydrolyzes formamide, acetamide, propionamide, butyramide, valeramide, hexanoamide, isobutyramide, pivalamide, diacetamide, malonamide, succinamide, adipamide, acrylamide, methacrylamide, benzamide, nicotinamide, isonicotinamide, aminoamides
<i>Rhodococcus</i> sp. N-774 (S15070)	amidase	<i>amdA</i>	49	85	hydrolyzes propionamide, aminobenzamide, acetamide, acrylamide, indoleacetamide
<i>Rhodococcus</i> <i>erythropolis</i> MP50 (AAK11724)	amidase	<i>amdA</i>	39	85	hydrolyzes phenylacetamide, ketoprofen amide, naproxen amide

Organism (Protein Accession No.)	Enzyme Annotation	Gene	% Sequence identity to UW4 Ami	% Query Coverage	Biochemical Characterization
<i>Pseudomonas chlororaphis</i> B23 (P27765)	amidase	<i>amdA</i>	87	100	hydrolyzes propionamide, n-butyramide, isobutyramide, acrylamide, methacrylamide, crotonamide, nicotinamide and phenylalanine amide
<i>Rhodococcus</i> sp. (AAA26183)	amidase	<i>amdA</i>	31	85	hydrolyzes 2-aryl propionamides
<i>Flavobacterium</i> sp. K172 (P13397)	6- aminohexanoate- cyclic-dimer hydrolase	<i>nylA</i>	28	81	Catalyzes the first step in 6-aminohexanoic acid degradation
<i>Pseudomonas</i> sp. NK87 (P13398)	6- aminohexanoate- cyclic-dimer hydrolase	<i>nylA</i>	28	81	
<i>Stenotrophomonas maltophilia</i> (CAC93616)	peptide amidase	<i>pam</i>	32	80	hydrolyzes C-terminally amidated peptides
<i>Bradyrhizobium japonicum</i> USDA 6 (BAL09882.1)	malonamidase E2	BJ6T_46150	28	82	hydrolyzes malonamate

2.3.4 Domain Analysis and Structural Comparisons of Signature Amidases

Sequence analyses have shown that the large N-terminal domain of amidases is conserved and includes the AS sequence (267). This observation was consistent in the sequence alignments made herein (Fig. 11). However, a correlation between the N-terminal domain and the functional

properties of these amidases has not been examined. Instead, the substrate specificities of amidases are reported to depend on the substantial variation in the number and composition of amino acids in a small domain containing the active site (285). The amidase (RhAmidase) from *Rhodococcus* sp. N771 has been biochemically and structurally characterized and so it was used to compare against UW4 Ami and other AS family amidases from our sequence alignment. Crystallographic studies of the RhAmidase complexed with the benzamide substrate, have shown that three residues are essential for substrate hydrolysis- Ser171, Ser195 and Lys96. These catalytic residues are conserved in all of the amidases in our alignment (Fig. 11). The active site of RhAmidase is located in the middle of the highly conserved core structure (G169-G170-S171-S172-G173-G174)(285). This region is part of the amidase signature sequence and is conserved in all of the amidases in our alignment (Fig. 11). The hydrophobic residues Phe146, Ile227, Trp328, Leu447 and Ile450 surround the active site of RhAmidase, making the entrance to the active site narrow. In Ami, only Ile227 is conserved. The Trp328, Leu447 and Ile450 residues are involved in benzamine substrate recognition and are not conserved among AS family enzymes. They are also not conserved in Ami. The four backbone nitrogen atoms of Gln192, Gly193, Gly194 and Ala195 form the oxyanion hole and interact directly with the amide oxygen of the benzamide substrate. These residues are essential for benzamide recognition. In Ami, only Gly193, Gly194 are conserved.

Ohtaki et al., (2009) report that despite the low amino acid sequence identity between different AS family proteins, the overall folding of these enzymes is similar. The Phyre2 web portal for protein modeling was used to predict the 3D protein structures of Ami and to search for other structural homologs in the fold library (397). The Phyre2 analyses ranks the closest matches to our protein based on the number of aligned residues and the quality of alignment. This in turn is based on the similarity of

residue probability distributions for each position, secondary structure similarity and the presence or absence of insertions and deletions (397). Our Ami protein had the highest ranked match with RhAmidase from *Rhodococcus* sp. N771. The predicted secondary structure of Ami was compared against the secondary structure of RhAmidase and the positions of α -helices and β -strands were similar between the two sequences (Fig A3, Appendix A). The substrate-binding pocket of RhAmidase is narrow due to the presence of a helix (residues 438-450). This helix is also present in the predicted secondary structure of Ami. In both *Bradyrhizobium japonicum* malonamidase (MAE2) (354-359) and *Stenotrophomonas maltophilica* peptide amidase (Pam) (463-468), this is a loop region. The wide, open substrate-binding pocket of Pam accounts for its substrate specificity for large peptide amides. In MAE2, Tyr183, His273 and Gln277 form a hydrophilic, narrow active site that recognizes malonamate.

2.3.5 Phylogenetic Analyses of Amidases

The Ami protein shared 55-98% sequence identity with 445 other amidases deposited in the NCBI database, most of which have not been experimentally characterized. All of these sequences were globally aligned to determine conserved domains and a phylogenetic analysis was undertaken to determine evolutionary relationships. The maximum likelihood (ML) tree for the 445 amidases shows distinct clusters based on the bacterial class, order, family and species (Fig. A4, Appendix A). Overall, the γ -proteobacteria make up the upper portion of the tree, a few β -proteobacteria are found in the central portion of the tree and the α -proteobacteria comprise the lower portion of tree. The UW4 Ami sits within the large pseudomonadaceae clade at the top of the tree, which makes up the majority of the γ -proteobacteria group (Fig. A4, Appendix A). Interestingly, a single *Comamonas*

sp. sequence (β -proteobacteria) also groups within the pseudomonad clade with good bootstrap support (78%) (Fig. A4, Appendix A). This grouping suggests that this amidase gene may have been subject to horizontal transfer, a common phenomenon among prokaryotes.

The enterobacteriaceae family members (γ -proteobacteria) *Serratia* spp., *Kosakonia* spp., *Erwinia* spp., *Pantoea* spp. group together with high boot strap support (100%), while *Klebsiella* spp. form their own separate clade. The moraxellaceae family, *Acinetobacter* spp. also form a distinct clade (99% bootstrap support) (Fig. A4, Appendix A). Moving toward the bottom of the tree, the α -proteobacteria cluster by order. Marine rhodobacterales such as *Sulfitobacter* spp. *Phaeobacter* spp. and *Roseobacter* spp. group together (99% bootstrap support). The burkholderiales order form another large clade with strong bootstrap support (100%). Interestingly one *Pseudomonas* sp. groups within the *Burkholderia* clade with strong bootstrap support (97%), suggesting a lateral gene transfer event (Fig. A4, Appendix A). The largest rhizobiales clade, comprised mostly of *Bradyrhizobium* spp. forms a clade at the bottom of the tree. However, not all of the *Bradyrhizobium* spp. amidases are closely related. Within the rhizobiales group, there are several well supported sub-groupings, while others do not share significant bootstrap support (Fig. A4, Appendix A). In the cases where weak statistical support (<60%) is given for a particular branch, we are unable to clearly separate these sequences into distinct groups or infer their phylogeny reliably.

The maximum likelihood (ML) tree generated for biochemically characterized signature amidases contains several enzyme subfamilies (i.e., IAM-hydrolases, wide spectrum amidases, Glutamyl-tRNA(Gln) amidotransferase and 6-aminohexanoate-cyclic-dimer hydrolase) (Fig. 12). The tree is separated in halves, the upper half consisting of multi-substrate amidases and the bottom half

consisting of the IAM-hydrolases. This junction between the IAM-hydrolase and wide-spectrum amidase subfamilies suggests a divergence of these two subfamilies from a common but distant origin. The UW4 Ami groups with the wide-spectrum amidases and seems to be more distantly related to IAM-hydrolases (Fig. 12). It is sister to the wide-spectrum amidase of *P. chlororaphis* B23 and together this clade is sister to the amidases of the rhodococci clade. The next most closely related clade is that of the *Bacillus subtilis* Glutamyl-tRNA(Gln) amidotransferase, followed by the 6-aminohexanoate-cyclic-dimer hydrolases of *Flavobacterium* sp. K172 and *Pseudomonas* sp. NK87 (Fig. 12). The amidase of *Rhodococcus* sp. which has been characterized as an arylpropionamide hydrolase also groups in this cluster but is more distantly related. In the bottom half of the tree, the known IAM-hydrolases from phytopathogens cluster together on the tree. The *Agrobacterium* spp. form a well supported clade (99%) and *Pantoea*, *Dickeya* and *Pseudomonas syringae* together form another well supported clade (100%). Both clades branch off from a common ancestor with high bootstrap support (99%), however the latter clade has a more recent evolution (Fig. 12). A *Pseudomonas putida* mandelamide hydrolase also clusters within the IAM-hydrolase group, however the support for this association is weak (36%). The carbaryl hydrolase from *Arthrobacter* sp. RC100 groups within the bottom half of the tree as well, however there is no bootstrap support for this position. This enzyme was shown to catalyze the hydrolysis of phenylacetamide in addition to carbaryl (267). Although indoleacetamide was not tested as a substrate, the similarity in structure to phenylacetamide likely also makes it a substrate. Interestingly, the *B. japonicum* IAM-hydrolase appears to be more closely related to the 6-aminohexanoate-cyclic-dimer hydrolases (78% support), rather than to the IAM-hydrolases. Chebrou et al., (1996) report a similar tree structure in which the amidase of *B. japonicum* has the catalytic function of the IAM-hydrolase subfamily, yet it groups with the 6-aminohexanoate-

cyclic-dimer hydrolase subfamily on the phylogenetic tree (267). Given the promiscuity of amidase enzymes, the primary function of the *Bradyrhizobium* amidase may not be the production of IAA, even though it can utilize IAM. Similarly, the UW4 Ami protein likely acts on a wide-spectrum of amide substrates but it can incidentally deaminate IAM.

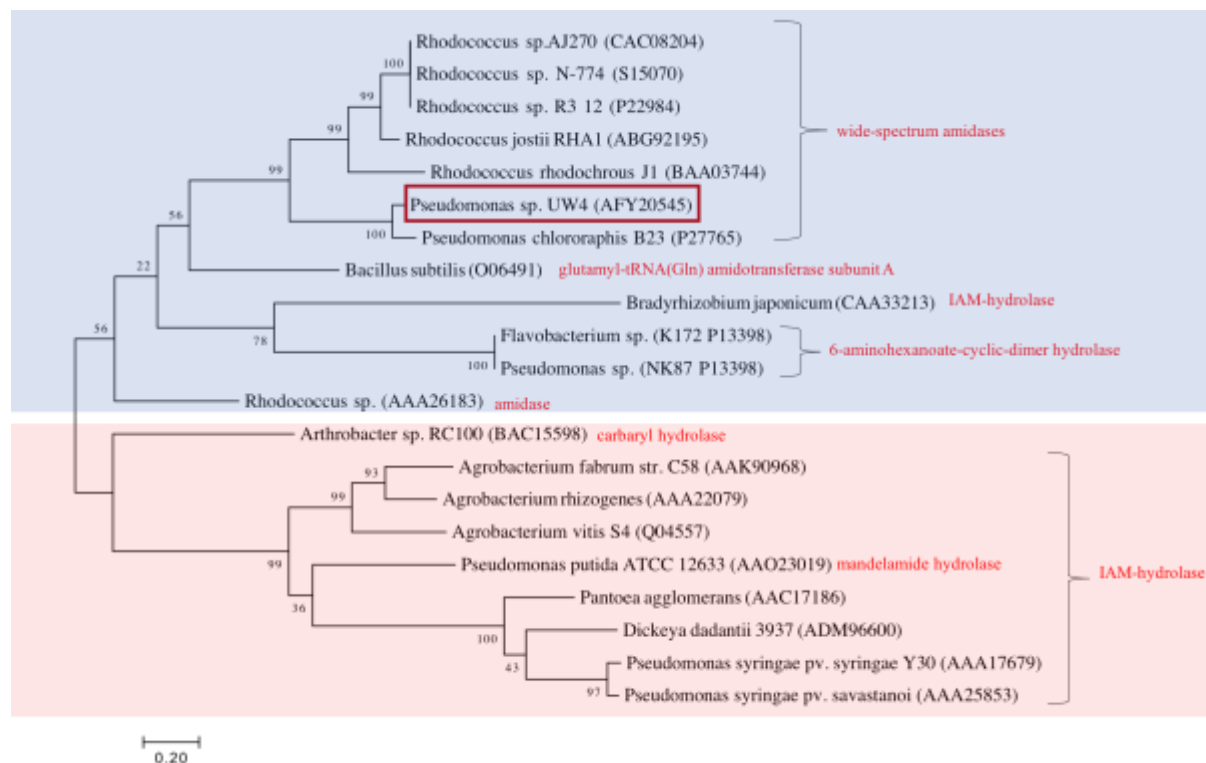


Figure 12. Molecular Phylogenetic Analysis of Characterized Amidases

The evolutionary history was inferred by using the Maximum Likelihood method based on the JTT matrix-based model (286). The tree with the highest log likelihood (-7024.6663) is shown. The percentage of trees in which the associated taxa clustered together is shown next to the branches. Initial tree(s) for the heuristic search were obtained automatically by applying Neighbor-Join and BioNJ algorithms to a matrix of pairwise distances estimated using a JTT model, and then selecting the topology with superior log likelihood value. The tree is drawn to scale, with branch lengths measured in the number of substitutions per site. The tree is mid-point rooted; the root is placed at the mid-point of the longest distance between two taxa in a tree. The analysis involved 21 amino acid sequences. All positions containing gaps and missing data were eliminated. There was a total of 219 positions in the final dataset. Evolutionary analyses were conducted in MEGA7 (265).

2.3.6 Organization of Amidase Genes in Bacterial Genomes

Examination of the genomic region surrounding an amidase gene may provide some insight into substrate preference and enzyme activity. In some cases, IAM-hydrolase genes are found adjacent to the genes for IAM-synthesizing enzymes (i.e. tryptophan monooxygenase). The coupling of tryptophan monooxygenase (TMO) and IAM-hydrolase describes the traditional IAM pathway of IAA biosynthesis. This genetic organization is seen in *P. syringae* pv. *savastanoi* and *P. agglomerans* where the *iaaH* and *iaaM* genes of the IAM pathway are transcribed together in a bicistronic operon on plasmids (249)(49)(254)(84)(146). Amidase and tryptophan monooxygenase genes are also adjacent in the genomes of *P. syringae* B728a and *D. dadantii* 3937, and in the T-DNA region of *A. tumefaciens* and *A. rhizogenes* plasmids (48)(85)(287)(52). All of these strains are phytopathogenic in nature.

In other cases, amidases that are homologous to characterized IAM-hydrolases are found adjacent to genes encoding a nitrile hydratase enzyme. It has been suggested that amidase and nitrile hydratase activities are coupled and the genes are co-expressed in an operon. Aldoxime dehydratase was also found to be linked physiologically and genetically with nitrile hydratase (174). Asano and Kato, (1998), were the first to report the enzymatic synthesis of nitriles from aldoximes by an aldoxime dehydratase from *Bacillus* sp. strain OxB-1 (182). The coexistence of all three genes (aldoxime dehydratase, nitrile hydratase and amidase) in a cluster has been described in the genome of several bacteria exhibiting nitrile-degrading activity, but none in relation to IAA-biosynthesis (288). For instance, in *A. radiobacter* K84, *B. japonicum* USDA 110 and *Ruegeria pomeroyi* DSS-3, an amidase that is homologous to the IAM-hydrolase from *A. tumefaciens* and *P. syringae*, is encoded upstream of a

predicted nitrile hydratase regulatory subunit. Amidase-nitrile hydratase gene clusters have also been described in *Rhodococcus* sp. R312, *Rhodococcus. erythropolis* JCM6823, *Rhodococcus. globerulus*, *Rhodococcus. jostii* RHA1, *P. fluorescens* SBW25, *P. chlororaphis* B23 and *Burkholderia. cenocepacia* MCO-3 (278)(157)(174)(289)(173). Moreover, the amidase-nitrile hydratase operon is identical in *Rhodococcus. sp.* N774, *Rhodococcus. sp.* N771 and *Rhodococcus sp.* R312 and biochemical characterization of these amidases showed that they hydrolyzed propionamide and benzamide efficiently, but their activities for acetamide, acrylamide and indoleacetamide were weak (285)(43). Similarly, in strain UW4, the *ami* gene is found in a cluster with phenyl acetaldoxime dehydratase and nitrile hydratase genes (Table 5, Fig. 13).

Table 5. Organization of the *ami* gene in the genome of strain UW4

Gene I.D.	Protein I.D.	Protein Annotation	Location on Chromosome	Size of Coding Sequence (no. of base pairs)
PputUW4_03347	AFY20541.1	AraC family transcriptional regulator	3903525...3904460	935
PputUW4_03348	AFY20543.1	phenylacetaldoxime dehydratase	3905050...3906108	1058
PputUW4_03349	AFY20544.1	COG4313 Protein involved in meta-pathway of phenol degradation	3906238...3907107	869
PputUW4_03350	AFY20545.1	Amidase/COG0154 Asp-tRNAAsn/Glu-tRNA ^{Gln} amidotransferase A subunit	3907318...3908832	1514
PputUW4_03351	AFY20546.1	nitrile hydratase alpha subunit	3908924...3909523	599
PputUW4_03352	AFY20547.1	nitrile hydratase beta subunit	3909566...3910228	662
PputUW4_03353	AFY20548.1	COG0523 Putative GTPases (G3E family) cobalamin synthesis protein, P47K	3910225...3911448	1223

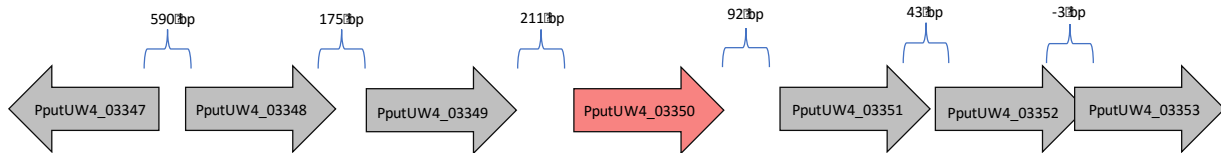


Figure 13. Schematic representation of the physical organization of the *ami* gene cluster

PputUW4_03347= AraC family transcriptional regulator, PputUW4_03348= phenylacetaldoxime dehydratase, PputUW4_03349= COG4313 protein involved in meta-pathway of phenol degradation, PputUW4_03350=amidase, PputUW4_03351= nitrile hydratase α -subunit, PputUW4_03352= nitrile hydratase β -subunit, PputUW4_03353= COG0523 Putative GTPase (G3E family)

Findings suggest that in phytopathogens, IAA is produced via IAM by a coupling of tryptophan monooxygenase and amidase activity. Conversely, a route involving nitrile hydratase and amidase may be more common in plant-associated bacteria that are not pathogenic in nature. However, one study found that eight IAA-producing *A. tumefaciens* strains exhibited both nitrile hydratase and amidase activities. Moreover, two strains of *Rhizobium leguminosarum* exhibited amidase activity, but no nitrile hydratase activity, suggesting that the amidase may be coupled with tryptophan monooxygenase (177). Dudnik et al., (2014) found that out of eight IAA-producing *P. syringae* isolates, none of them had homologs of tryptophan monooxygenase (*iaaM*) and indoleacetamide hydrolase (*iaaH*) genes from *P. syringae* pv. *savastanoi* (*Psv*). The majority of *P. syringae* genomes encode another gene annotated as tryptophan monooxygenase at a different genomic location with an amidase-like protein encoded immediately downstream of this gene (290). This putative operon is likely responsible for IAA production via IAM in strains lacking the traditional *iaaM^{Psv}/iaaH^{Psv}* homologs. A similar putative operon was identified in the UW4 genome, however the encoded proteins, annotated as aromatic aminotransferase (AFY18151) and nitrilase/cyanide hydratase/ apolipoprotein/N-acyltransferase (AFY18152) have not been functionally characterized. As such, the Ami protein characterized herein may hydrolyze IAM produced by nitrile hydratase, while a different amidase that is coupled to a potential tryptophan monooxygenase may constitute the traditional IAM pathway in UW4.

2.4 Conclusion

IAA is not only synthesized and secreted by bacteria, but it also enters host root cells in sufficient quantities to orchestrate precise phenotypic effects on plant growth and development. Strain UW4 produces IAA via two proposed pathways-the IAN pathway and the IAM pathway. These pathways

are driven by the concerted action of nitrilase and nitrile hydratase--both of which produce IAM, and an amidase which converts the IAM into IAA. Here, a gene (*ami*) encoding a putative amidase, was cloned, over-expressed, purified, and biochemically characterized. The Ami enzyme was confirmed to catalyze the conversion of IAM into IAA, with optimal activity at 35°C and a pH of 7.5. The enzyme contains the conserved catalytic triad as well as the amidase signature sequence. Phylogenetic analysis of this enzyme revealed that it is more closely related to wide-spectrum amidases than to known IAM-hydrolases. This suggest that Ami is capable of hydrolyzing various amides besides IAM; therefore, it likely has or previously had a role beyond IAA biosynthesis. In addition, the *ami* gene is co-located with genes encoding nitrile hydratase and aldoxime dehydratase on the chromosome of UW4, an arrangement typical of nitrile-hydrolyzing bacteria. Altogether, these findings suggest that this gene cluster is responsible for IAA production via IAN and IAM and possibly also for other nitrile-degrading activities.

Chapter 3

Construction and Characterization of IAA-Overproducing Transformants of *Pseudomonas* sp. UW4

3.1 Introduction

The majority of rhizobacteria produce IAA and secrete it into the rhizosphere, where plants can take up this hormone through the roots. The levels of IAA inside the plant are precisely regulated by means of a variety of mechanisms including degradation, conjugation, rate of synthesis, sequestering in different regions and shuffling back and forth between the pools where it is stored (i.e. the cytosol and chloroplast) (291)(292). For a plant to thrive, a delicate balance of this hormone must be maintained at all times.

There are several reports of soil bacteria (*Alcaligenes*, *Enterobacter*, *Acetobacter*, *Azospirillum*, *Pseudomonas* and *Xanthomonas*) that secrete IAA at low levels and as a consequence stimulate plant growth (45)(293)(95)(96). Conversely, there are also reports in which bacteria secrete IAA at high levels that are detrimental to plant growth. The question becomes; at which level does IAA transcend the stimulatory threshold and become inhibitory? This concept remains elusive as each plant and plant organ, has a unique capacity for IAA; some being more sensitive, while others can tolerate higher concentrations. Each plant already has an existing internal pool of IAA that it produces independently of soil bacteria. This endogenous level of IAA can vary depending on the tissue type,

the amount of tryptophan precursor available and the environmental conditions to which the plant is exposed. The need for additional IAA may be temporal; throughout the plant's lifecycle, endogenous IAA levels typically alternate between optimal and suboptimal. Roots are most sensitive to IAA, concentrations above $>10^{-6}$ M can inhibit root elongation, while very low levels ($\sim 10^{-8}$ M) promote root elongation (294)(295). Thus, the effect that exogenous IAA will have on a given plant depends on the total amount of IAA (from both plant and bacteria) and the plant's response or sensitivity to it.

Another key plant-growth-promoting mechanism used by bacteria is the regulation of ethylene—a plant synthesized stress hormone that is detrimental at supra-optimal levels. Some bacteria can act as a de facto sink for the ethylene precursor, 1-aminocyclopropane-1-carboxylate (ACC), sequestering it from the plant and degrading it before it has a chance to form ethylene (3). The bacterial enzyme ACC deaminase accomplishes the degradation of ACC. Interestingly, IAA and ethylene signaling pathways interact at the molecular level, although the details of these complex interactions are not completely understood. One interaction mode occurs at the hormone biosynthesis level, where IAA induces ethylene biosynthesis by upregulation of the transcription of 1-aminocyclopropane-1-carboxylate (ACC) synthase, a key enzyme in ethylene production (296)(297). As such, it might be thought that IAA works against ACC deaminase, inhibiting plant growth by promoting the synthesis of excess ethylene. However, as plant ethylene levels increase, the ethylene itself feedback inhibits IAA signal transduction thereby limiting the effect that IAA has on stimulating ACC synthase transcription (298)(299)(300). Ethylene feedback inhibition of IAA signal transduction also limits the extent to which IAA can promote plant cell proliferation and elongation (299)(301). However, the

presence of ACC deaminase, by lowering ethylene levels allows IAA to continue to promote plant growth rather than inhibit it (302).

Strain *Pseudomonas* sp. UW4 utilizes the indole acetaldoxime- indole acetonitrile (IAOx-IAN) and indole acetamide (IAM) pathways for the synthesis of IAA (Fig. 7). The tryptophan precursor is first converted to the indole acetaldoxime (IAOx) intermediate by an unknown enzyme (31).

Subsequently, a phenyl acetaldoxime dehydratase (Phe) converts the IAOx into indole acetonitrile (IAN). The IAN is directly converted into IAA or IAM by nitrilase (Nit), or it may be converted into IAM by nitrile hydratase (NthAB) (31). The IAM intermediate is then further converted into IAA by amidase (Ami) (Refer to Fig. 5)

Despite the potential that bacterial IAA has in facilitating plant growth, especially under environmentally stressful conditions, it is not a well understood aspect of the plant-microbe interaction. The aim of this chapter was to develop a deeper understanding of how bacterially synthesized IAA affects plant growth. To do this, target IAA genes were selected and used to construct transformants of *Pseudomonas* sp. UW4 that overproduce IAA. The transformants were characterized with respect to the amount of IAA that they produce, growth rate, and ACC deaminase activity, all in comparison to the wild-type strain. Plant growth assays were also undertaken to determine whether the transformants inhibit or promote the growth of canola seedlings *in vitro*.

3.2 Materials and Methods

3.2.1 Bacterial Strains and Plasmids

E. coli DH5 α (InvitrogenTM) was used as an initial cloning host and was maintained aerobically at 37°C in Luria-Bertani broth. The wild-type *Pseudomonas* sp. UW4 (262) was grown and maintained aerobically at 30°C in tryptic soy broth (Becton-Dickinson) supplemented with 100 $\mu\text{g mL}^{-1}$ ampicillin. The broad-host-range plasmid, pRK415 (35) was used to over-express the following UW4 genes; *ami*, *nit*, *nthAB*, and *phe*. All of the plasmid constructs used in this study are described in detail in Table 6. Transconjugant forms of *Pseudomonas* sp. UW4 (carrying pRK ami , pRK nit , pRK $nthAB$, or pRK phe) were grown and maintained aerobically at 30°C in tryptic soy broth supplemented with 100 $\mu\text{g mL}^{-1}$ of ampicillin and 15 $\mu\text{g mL}^{-1}$ tetracycline, where the ampicillin selects for strain UW4 and tetracycline selects for the plasmid.

Table 6. Expression plasmid constructs and primers used in this study

Plasmid, Strain or Primer	Sequence (5'-3') or Gene I.D.	Description
pRK-ami	PputUW4_03350	pRK415 vector with the <i>ami</i> gene from UW4 inserted between HindIII and KpnI
pRK-nit	PputUW4_02461	pRK415 vector with the <i>nit</i> gene from UW4 inserted between HindIII and KpnI
pRK-nthAB	PputUW4_03351 PputUW4_03352	pRK415 vector with the <i>nthAB</i> gene from UW4 inserted between HindIII and KpnI
pRK-phe	PputUW4_03348	pRK415 vector with the <i>phe</i> gene from UW4 inserted between HindIII and KpnI
Strains		
Wild-type (WT)		Wild-type <i>Pseudomonas</i> sp. UW4
UW4-ami		<i>Pseudomonas</i> sp. UW4::pRK-ami
UW4-nit		<i>Pseudomonas</i> sp. UW4::pRK-nit
UW4-nthAB		<i>Pseudomonas</i> sp. UW4::pRK-nthAB
UW4-phe		<i>Pseudomonas</i> sp. UW4::pRK-phe
Primers		
ami-F	TAATAAGCTTATGGCCATTGTTCCG	ami (HindIII)-fwd
ami-R	ATTAGGTACCTTACAACGTCCTCCAGTCCG	ami (KpnI)-rev
nit-F	TAATAAGCTTATGCCCAAATCAATCGTTG	nit (HindIII)-fwd
nit-R	ATTAGGTACCTCAGGAAGTGAAGCGCAC	nit (KpnI)-rev
nthAB-F	TAATAAGCTTATGAGCGCCACTGTATCCCCA	nthAB (HindIII)-fwd
nthAB-R	ATTAGGTACCTCATGCGGCCACCGTTTT	nthAB (KpnI)-rev
phe-F	TAATAAGCTTATGGAATCTGCGATCGATAAGCA	phe (HindIII)-fwd
phe-R	ATTAGGTACCTCAGGTTTCAGGGATCACCG	Phe (KpnI)-rev

F= forward primer, R=reverse primer

3.2.2 DNA Amplification

Genomic DNA from *Pseudomonas* sp. UW4 was isolated using the Wizard Genomic DNA purification kit (Promega, catalog no. A1120). The primer sequences used to amplify the *ami*, *nit*, *nthAB* and *pbe* genes from strain UW4 are given in Table 6. Both the forward and the reverse primer sequences were based on the fully sequenced UW4 genome (GenBank accession number CP003880). For the NthAB protein, which is composed of one α and one β subunit, the forward primer was designed starting from the first codon of the α subunit, while the reverse primer was designed starting from the last codon of the β subunit. The α -subunit, the short intergenic region (42 bp), and the β -subunit were amplified as a single fragment. The amplified genes were subcloned between the HindIII and KpnI sites of pRK415 (303). Hot-start PCR was performed with high fidelity KOD Hot Start DNA polymerase (Novagen, Mississauga, Ontario, Canada). The reaction mixture (50 μ l) was set up on ice and included 5 μ l of KOD hot start buffer (10X), 3 μ l of 25 mM MgSO₄ (final concentration, 1.5 mM), 5 μ l of 2 M deoxynucleoside triphosphates (final concentration, 0.2 mM each), 1.5 μ l each of forward and reverse primers (final concentration, 0.3 mM each), 100 ng of template genomic DNA, 1 μ l of KOD hot start polymerase and PCR-grade water up to a final volume of 50 μ l. The PCR was performed in an Eppendorf MasterCycler gradient thermocycler using the following amplification conditions for *ami*: 95°C for 2 min, 95°C for 20 s, 59°C for 10 s, 70°C for 15 s, 70°C for 5 min, and ending at 4°C; for *nit*: 95°C for 2 min, 95°C for 20 s, 63°C for 10 s, 70°C for 15 s, 70°C for 5 min, and ending at 4°C; for *nthAB*: 95°C for 2 min, 95°C for 20 s, 70°C for 10 s, 70°C for 23 s, 70°C for 5 min, and ending at 4°C; for *pbe*: 95°C for 2 min, 95°C for 20 s, 67°C for 10 s, 70°C for 23 s, 70°C for 5 min, and ending at 4°C

3.2.3 Tri-Parental Mating

Plasmids pRK-ami, pRK-nit, pRK-nthAB and pRK-phe were transformed into *E. coli* DH5 α using the calcium chloride method described by Sambrook and Russell (2001) (304). The plasmids were then individually transferred from *E. coli* DH5 α into wild-type *Pseudomonas* sp. UW4 by triparental mating using the helper plasmid pRK2013 in *E. coli* HB101 (305). Transconjugants were selected following growth on tryptic soy agar (TSA) medium supplemented with 100 $\mu\text{g mL}^{-1}$ ampicillin and 15 $\mu\text{g mL}^{-1}$ tetracycline for 24 h at 30°C. To ascertain that no rearrangement had taken place, plasmids were extracted from transconjugant UW4 strains, digested with HindIII and KpnI and compared to the empty pRK415 plasmid (digested with the same enzymes) purified from *Escherichia coli* DH5 α on an agarose gel.

3.2.4 High Performance Liquid Chromatography (HPLC) Analysis

HPLC analysis was used to determine the quantity of free IAA (unconjugated) and IAA-intermediates (IAM, IAN, indole lactic acid (ILA), methyl-IAA (M-IAA)) produced by the bacteria. The analyses were performed using a Waters Alliance 2695 HPLC separation system (Mississauga, Ontario, Canada), which includes a Waters 2996 photodiode array detector. The system was connected to a PC with Empower 2 software (Waters) for data collection and processing. A Sunfire C18 column (50 by 4.6 mm [inner diameter], 2.5 μm pore size; Waters, Ireland) was connected with a Security Guard C18 guard column (4 by 3.0 mm [inner diameter]; Phenomenex, Torrance, CA). Gradient HPLC was performed at room temperature using a mobile phase containing water-acetic acid (1% [vol vol]) (A) and acetonitrile-acetic acid (1% [vol vol]) (B). Starting with 80% A, the gradient began at 2 min and reached 60% A at 15 min. The flow rate was 1 mL^{-1} min. A 100 μl

sample injection volume was used, and the eluent was monitored at 280 nm. All analytical standards were purchased from Sigma-Aldrich. Stock solutions of the individual standards at a concentration of 0.1 mg mL⁻¹ were prepared by dissolving the compounds in acetonitrile and were stored at 4°C. Working solutions of all the standards were prepared immediately before analyses by diluting the stock solution with mobile phase, to attain the required concentrations for calibration measurements.

3.2.5 ACC Deaminase Assay

ACC deaminase activity was determined according to the protocol described by Penrose and Glick (2003) with a standard curve of α -ketobutyrate between 0.1 and 1.0 mM (306). The ACC deaminase activity was expressed as μ mole of α -ketobutyrate mg⁻¹ h⁻¹. Protein concentrations were determined using the Quick Start™ Bradford Protein Assay (BioRad) with bovine serum albumin (BSA) as the reference standard (263)(307).

3.2.6 Bacterial Growth Curve

Bacterial growth was monitored in tryptic soy broth (400 μ l) at 30°C, by measuring the optical density of the cultures at 600 nm at intervals of 1 hour, over the course of 64 hours. This assay was performed using a Microbiology Reader Bioscreen C (Bioscreen©, Helsinki, Finland) according to the User's Manual: Version 2.1.5, 2009 (Oy Growth Curves Ab Ltd).

3.2.7 Real-Time Quantitative PCR Analyses

Total RNA was extracted from the equivalent of \sim 3 OD mL⁻¹ of bacterial culture using the Aurum™ Total RNA Mini Kit (BioRad) following the manufacturer's instructions. Approximately

100 ng of total RNA was used for cDNA synthesis using iScript™ Reverse Transcription Supermix for RT-qPCR (Bio Rad). Primers were designed using Primer3 software (<http://frodo.wi.mit.edu/primer3>). Real-time quantitative PCR analyses were performed with ~10 ng of cDNA mixed with the appropriate primers (Table 1) in 10 µl of SYBR Green Supermix (Bio-Rad) using a CFX96 Touch™ Real-Time PCR Detection System. Relative quantification was performed using 16S rRNA as a reference gene. Expression of 16S rRNA did not differ between groups as ascertained by one-way ANOVA. All samples were run in duplicate. The run protocol for all genes of interest was the following: Denaturation: 95°C, 30 sec; Amplification: 40 cycles: 95°C for 10 sec, 60°C for 30 sec, Melting Curve: 60-95°C, at a rate of 0.1°C per second. Data was analyzed using the Livak ($\Delta\Delta C_t$) method (308).

3.2.8 Growth Pouch Assay

The protocol for assessing the effect of wild-type *Pseudomonas* sp. UW4 and its derivative strains on the elongation of canola seedling roots and shoots is based on the method described by Lifshitz et al. 1987 (309)(306). After growth for approximately 24 h at 30°C, the bacterial cells were centrifuged at 4000 x g for 10 min at 4°C. The bacterial cell pellets were washed twice with 100 mM MgSO₄ before being resuspended in 100 mM MgSO₄ and the optical density of the suspension was adjusted to approximately 0.5 at 600 nm. Canola (*Brassica campestris*) seeds were stored at 4°C. Immediately before use, the seeds were soaked for 5 min in a 2% solution of bleach and then rinsed thoroughly with sterile deionized water. The seeds were immersed either in suspensions of wild-type or transformant bacterial cultures in 100 mM MgSO₄, for one hour at room temperature. Ten canola seeds with the same treatment were placed at evenly spaced distances in each growth pouch (Northrup King Co., Minneapolis, MN). The pouches were placed upright in a rack in a randomized

fashion, with two empty pouches at each end of a row. The box containing the growth pouches was covered with Saran WrapTM and was kept at 25°C for ten days. Primary root lengths were measured on the tenth day of growth following imbibition.

3.2.9 Statistical Analyses

All quantitative statistical analyses were performed using the GraphPad PRISM 6.01 software (GraphPad Software Inc., California, USA). Unless otherwise stated, references to any significant differences are at an alpha level of 0.05. A one-way analysis of variance (ANOVA) test was used to verify the null hypothesis of no differences between measured biological parameters.

3.3 Results

3.3.1 IAA Production

All four UW4 transformants produced ~2-3 times more free IAA than the wild-type, when the growth medium was supplemented with 500 $\mu\text{g mL}^{-1}$ Trp (Table 7). These transformants were designated as UW4-ami, UW4-nit, UW4-nthAB, UW4-phe, reflecting each of the four IAA genes that are expressed from the introduced plasmid. Indole-lactic acid (ILA), indole acetonitrile (IAN), indole acetamide (IAM) and methyl-IAA (M-IAA) were also detected in the growth medium (Table 7). The wild-type strain produced the largest amount of ILA (3.58 $\mu\text{g mL}^{-1}$), ~3-4 times more than the transformants (0.45-1.06 $\mu\text{g mL}^{-1}$). Conversely, the transformants produced M-IAA (0.82- 1.87 $\mu\text{g mL}^{-1}$) although this compound was not detected in the wild-type culture. Similarly, IAN (1.9-3.09 $\mu\text{g mL}^{-1}$) and IAM (0.09 -0.87 $\mu\text{g mL}^{-1}$) were detected in the transformant cultures, but not in the

wild-type.

3.3.2 ACC Deaminase Activity

The UW4 transformants were assessed for ACC deaminase activity, relative to the wild-type strain (Table 7). ACC deaminase activity was always higher in the wild-type strain than in the IAA transformants, regardless of whether or not Trp was added to the culture. Moreover, the overall ACC deaminase activity was lower in the bacterial strains (wild-type and transformants) in the absence of exogenous Trp supplementation. The addition of tryptophan led to higher levels of ACC deaminase activity for all the strains (Table 7).

Table 7 Biological Activities of the UW4 Wild-Type Strain and UW4 Transformants

Strain	^a Concentration of indole compound (ug mL ⁻¹)					^b ACC deaminase activity (mol mg ⁻¹ h ⁻¹)	^b ACC deaminase activity (mol mg ⁻¹ h ⁻¹)
	[IAA]	[ILA]	[IAN]	[IAM]	[M-IAA]	(+Trp)	(No Trp)
UW4 wild-type	2.88	3.58	ND	ND	ND	21.00	15.20
UW4-ami	6.01	1.06	1.90	0.19	0.82	14.90	5.10
UW4-nit	8.51	0.92	2.73	0.61	1.87	16.20	8.10
UW4-nthAB	9.22	0.97	3.09	0.87	1.84	15.00	10.50
UW4-phe	7.22	0.45	2.75	0.09	1.50	8.30	5.70

^a HPLC analysis of indole compounds after 72 hours of growth in DF salts minimal medium plus 500 µg mL⁻¹ of L-Trp. IAA= indoleacetic acid, ILA=indole lactic acid, IAN= indole acetonitrile, IAM= indole acetamide, M-IAA= methyl indoleacetic acid, ND= not detected.

^bACC deaminase activity of cell-free extracts prepared after growth in DF salts minimal medium plus ACC

3.3.3 Transcriptional Analyses (Real-Time qPCR)

Real-time quantitative RT-PCR analyses showed increased abundance of mRNA transcripts for all four IAA genes (*ami*, *nit*, *nthAB*, and *phe*) in the transformants compared to the wild-type strain (Fig. 14). These results indicate that each of the transformed strains were successfully expressing the introduced copy of the target gene from the pRK415 plasmid.

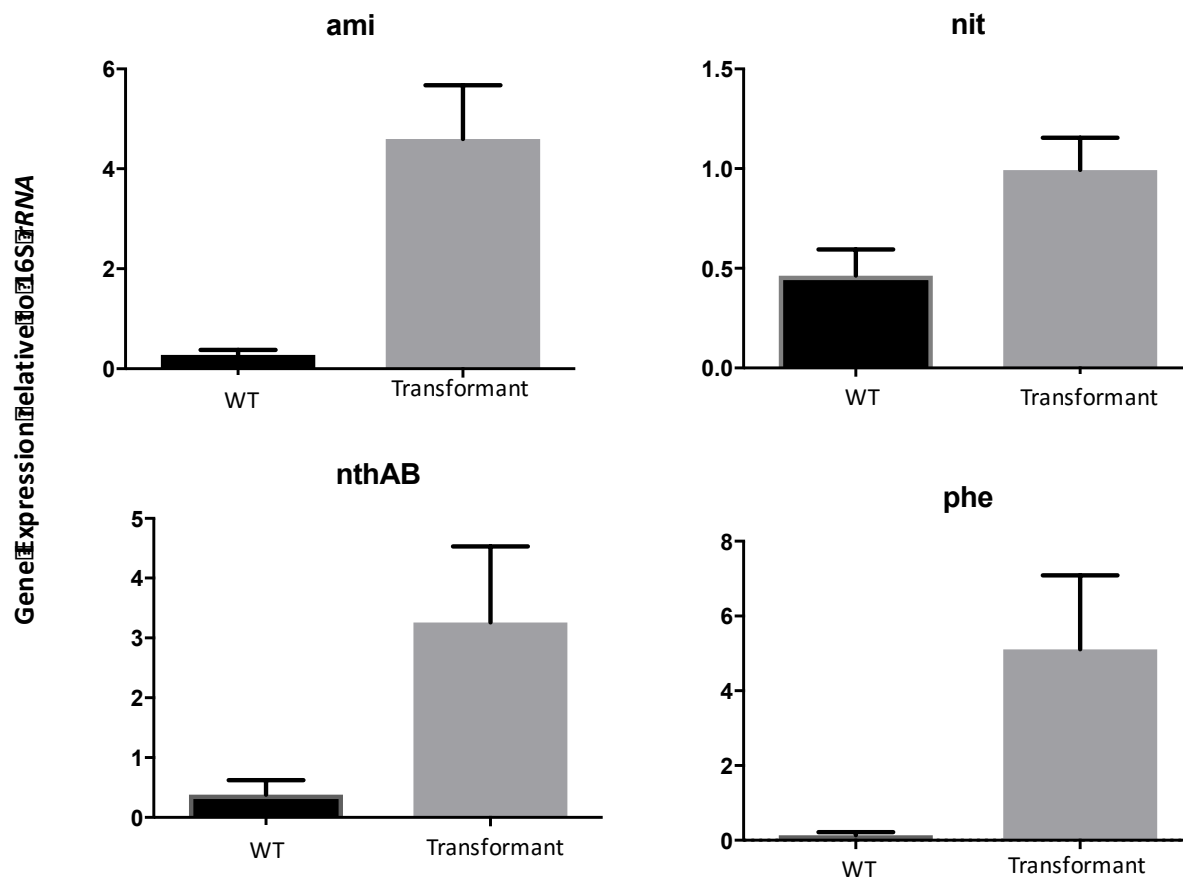


Figure 14. Transcriptional Analysis of Wild-type and Transformant UW4 Strains

Results are shown as fold changes of expression of the four IAA genes (*ami* (n=8), *nit* (n=7), *nthAB* (n=8), *phe* (n=8)) in either the wild-type (WT) or the transformant. All data was normalized and expressed relative to the 16S rRNA reference gene. Expression data illustrated as mean \pm SEM. P-values for WT vs. Transformant were < 0.05 for all four genes.

3.3.4 Bacterial Growth Curves

The growth rates of the UW4 transformants and wild-type strain were measured over the course of 64 hours. In the first assay, the strains were grown in nutrient media without any exogenous Trp supplementation to assess the effect of the plasmid on growth (Fig. 15). In the second assay, Trp ($500 \mu\text{g mL}^{-1}$) was supplemented into the growth media to determine whether the extent to which each strain produces IAA and related metabolites, affects the growth rate in rich medium (Fig. 16). The wild-type strain was able to attain a slightly higher cell density than the transformants, regardless of whether exogenous Trp was added to the media, suggesting that there is small metabolic load (310) imposed by the plasmid (Figs. 15-16). This metabolic load could be a consequence of the presence of the plasmid or a consequence of the overexpression of the IAA gene. All four transformants maintained a similar growth rate and reached a similar maximum optical density throughout the measured growth period. Bacterial IAA production generally occurs in the stationary growth phase (45-51). The maximum optical density of the wild-type strain and UW4-ami, UW4-nit, UW4-nthAB and UW4-phe transformants in the stationary phase without any exogenous Trp was 0.59, 0.45, 0.42, 0.47 and 0.43 respectively. With Trp supplementation, the maximum optical density of the wild-type strain and the UW4-ami, UW4-nit, UW4-nthAB and UW4-phe transformants in stationary phase was 0.57, 0.43, 0.39, 0.45 and 0.41, respectively (Table 8).

Table 8. Growth Comparison of Wild-Type and Transformant UW4 Strains

Strain	Maximum optical density (OD₆₀₀) in Exponential phase (2- 24 hours)		Maximum optical density (OD₆₀₀) in Stationary phase (24-64 hours)	
	+ Trp	No Trp	+ Trp	No Trp
UW4 wild-type	0.46	0.49	0.57	0.59
UW4-ami	0.34	0.36	0.43	0.45
UW4-nit	0.30	0.33	0.39	0.43
UW4-nthAB	0.37	0.38	0.45	0.49
UW4-phe	0.33	0.35	0.41	0.43

Bacterial growth was monitored in TSB medium at 30°C. The OD₆₀₀ was measured at 1 hour intervals for 64 hours. Four biological replicates were performed, each done in triplicate. The values in the table represent the mean of these replicates. L-Tryptophan was supplemented at 500 µg/mL.

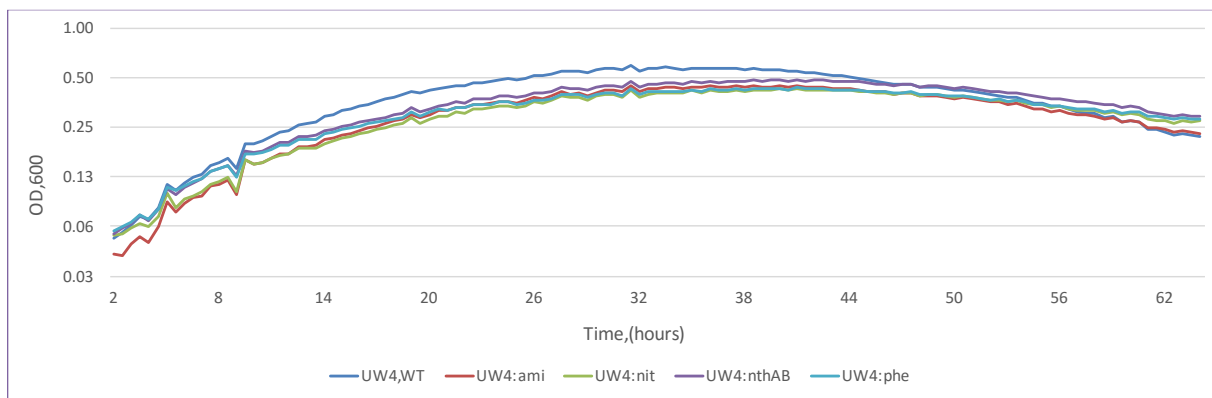


Figure 15. Growth Curve of Wild-Type and Transformed UW4 Strains

Growth was monitored in TSB medium at 30°C. The OD₆₀₀ was measured at 1 hour intervals for 64 hours. Four biological replicates were performed, each done in triplicate. No exogenous tryptophan was added to the culture media.

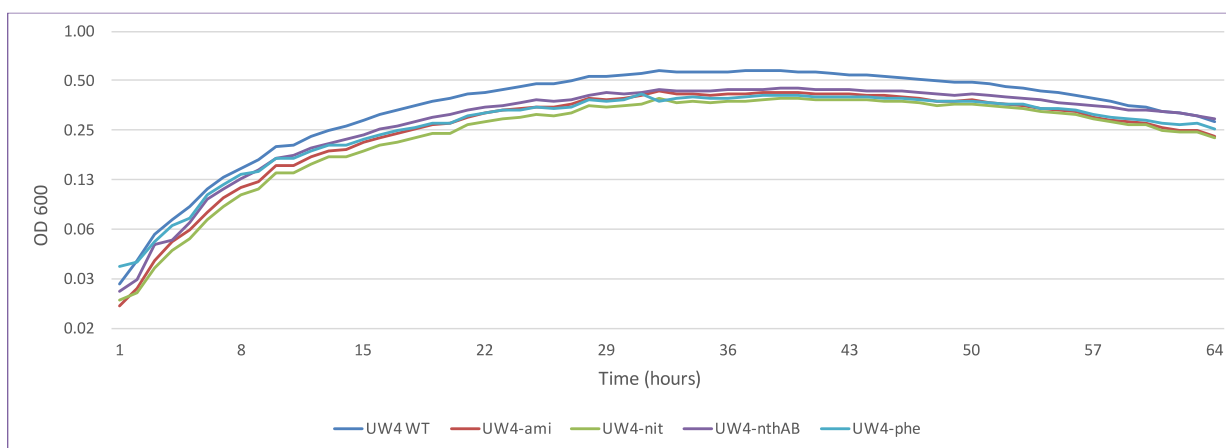


Figure 16. Growth Curve of IAA-producing Wild-Type and Transformed UW4 Strains

Growth was monitored in TSB medium at 30°C. The OD₆₀₀ was measured at 1 hour intervals for 64 hours. Four biological replicates were performed, each done in triplicate. Exogenous tryptophan (500 µg/mL) was added to the culture media.

3.3.5 Effect on Plant Growth

The results of the growth pouch assay showed that treatment of canola seeds with any of the four bacterial transformants yielded seedlings with primary roots that were longer than the roots of plants inoculated with the wild-type bacterium. Treatment of seeds with the transformant UW4-nit resulted in the longest roots; statistically-significant differences in primary root length were noted for UW4-nit *vs.* UW4-ami, UW4-nthAB and wild-type (WT). Treatment of seeds with the wild-type displayed the shortest roots overall, approximately 30% shorter than UW4-nit. There was no statistically significant difference in shoot length between any of the treatments. In all treatments, the roots were longer than the shoots by 47-63% (Fig. 17).

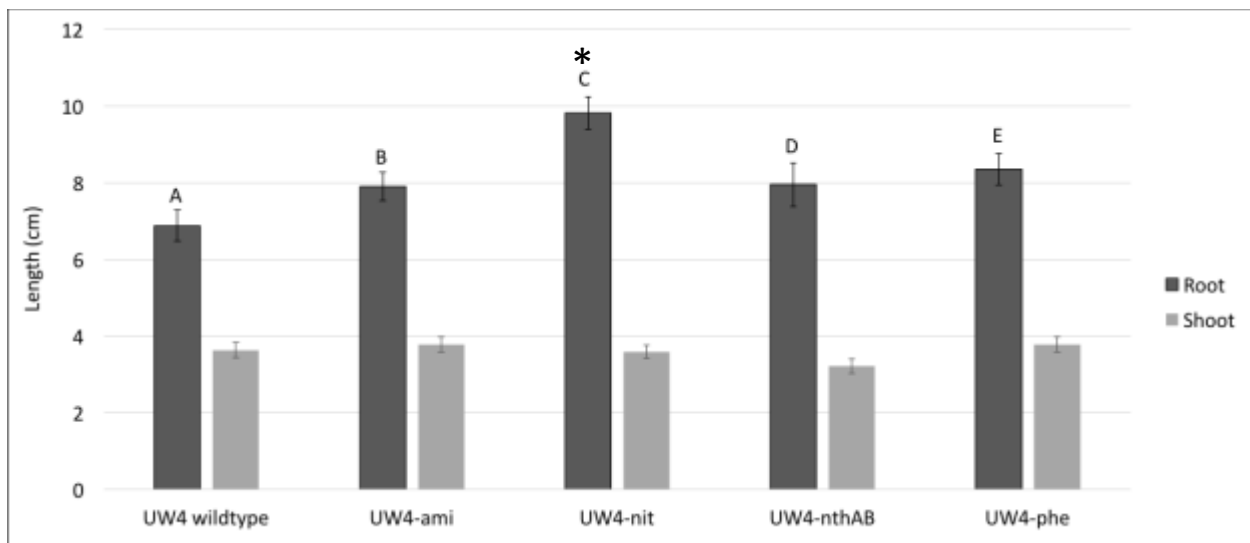


Figure 17. Results of the Canola Seedling Growth Pouch Assay

The growth of canola seedlings 10 days post-inoculation with: UW4 wild-type (n=55), UW4-ami (n=52), UW4-nit (n=55), UW4-nthAB (n=52), UW4-phe (n=53). Data illustrated as mean \pm SEM. Statistically significant ($p < 0.05$) difference in primary root length was noted between: A-C, B-C and D-C. No significant differences in shoot length. An asterisk * denotes statistical significance between wild-type and mutant.

3.4 Discussion

Pseudomonas sp. UW4 is a free-living soil bacterium, originally isolated from the rhizosphere of reeds growing in Waterloo, Ontario, Canada (262). This bacterium can promote plant growth both directly and indirectly using various mechanisms. Several studies have shown that strain UW4 is particularly efficient at enhancing plant growth in conditions of stress such as flooding, heavy metals, cold, high salt and phytopathogens (262). In this study, the focus relates to the direct promotion of plant growth by bacterial IAA.

Having multiple IAA biosynthetic pathways and several isoenzymes participating in these pathways poses a challenge in obtaining transformants with significantly altered levels of IAA (311)(312). Most reported IAA-overproducing strains have been constructed using Tn5 mutagenesis or by expressing IAA biosynthesis genes from a heterologous host on a plasmid in the desired strain (95)(92). In this study, four native IAA biosynthesis genes from strain UW4 were individually cloned into plasmid pRK415 and transformed into wild-type UW4. The UW4 transformants have two copies of the corresponding IAA gene; the original copy on the chromosome and a second copy being expressed from the introduced low copy number plasmid. To the best of our knowledge, this is the only report on the over-expression of autologous IAM-IAN pathway genes in any bacterium. This vector was chosen because it is a stable expression vector in pseudomonads (303)(313). Moreover, it was demonstrated that a transformed *Pseudomonas* strain carrying the pRK415 plasmid grew at the same rate as the wild-type, arguing that this plasmid does not impose a large metabolic load on the bacterium (314). Indeed, a similar observation was made herein, where the growth rates and optical densities of the wild-type and transformant cultures were very similar (Table 9, Fig 18). In fact, the

addition of tryptophan to the culture media did not result in any significant growth differences, suggesting that the level of IAA produced from the precursor does not significantly affect cell growth rate (Table 9, Fig 19). Sun et al., (2009) similarly observed that the growth of the wild-type *Burkholderia phytofirmans* PsJN in comparison to a mutant that produced 6-fold more IAA was identical in rich medium (315). In addition, growth of an IAA-overproducing mutant of *P. putida* GR12-2 was identical to the growth of the wild-type in rich medium (293)(95). Moreover, both IAA-underproducing and IAA-overproducing mutants of *Azospirillum lipoferum* exhibited normal growth rates when compared with that of the wild-type (229). However, it is important to note that the UW4 strains produced other indole intermediates besides IAA (Table 7) and there is no information regarding the extent that ILA, IAM, IAN and M-IAA may each affect bacterial growth.

The observed change in the level of IAA and related metabolites produced by the transconjugant UW4 strains compared to the wild-type, is attributable to the overexpression of the IAA biosynthetic genes from the plasmid. Each of the four UW4 transformants was able to produce more IAA and related metabolites (Table 7) than the wild-type strain, with the highest level being produced by UW4-nthAB (9.22 µg/mL). These genes (*nthA* and *nthB*) code for the enzyme nitrile hydratase, which is composed of one α and one β subunit (258). The UW4 NthAB enzyme specifically converts indole acetonitrile (IAN) to indole acetamide (IAM) (258). The UW4-nit transformant produced the second largest amount of IAA (8.51 µg/mL) and related metabolites, and the encoded nitrilase enzyme has also been shown to convert IAN to both IAM and IAA (258). Out of the four transformants, UW4-ami produced the least amount of IAA (6.01 µg/mL); the overexpressed gene (*ami*) codes for an amidase enzyme that converts IAM into IAA (Refer to

Chapter 2). Finally, the UW4-phe transformant produced 7.22 µg/mL (~2.5 times more IAA than the wild-type strain (2.88 µg/mL), however the enzyme encoded by the *phe* gene has not yet been biochemically characterized. The over-production of IAA resulting from the over-expression of this gene, suggests its involvement in IAA biosynthesis in strain UW4. Based on sequence similarity to other characterized enzymes and its location on the UW4 chromosome (i.e., in a gene cluster with *nthA*, *nthB* and *ami*) this enzyme is predicted to be an aldoxime dehydratase that converts IAOx into IAN.

The compound ILA, is a naturally occurring indole derivative found in some bacteria and plants (316). It is reported that ILA is reversibly formed from indole-pyruvic acid (IPyA), acting as a transient storage product to regulate IAA biosynthesis (316)(260). Indole-lactic acid (ILA) was detected in all culture supernatants; however, concentrations were much higher (3- to 8-fold) in the wild-type than in the transformant cultures, suggesting that there is an inverse relationship between the amount of IAA and the amount of ILA. Due to its similar structure to IAA, it is possible that ILA might act as an IAA analog or as an IAA antagonist (316)(317). In tomato plants, ILA was reported to exhibit weak auxin activity at concentrations below 500 µM, while at levels greater than that, it became toxic (318). In *Agrobacterium tumefaciens*, reporter gene assays have demonstrated that ILA is capable of autoregulation, while repressing auxin-induced expression of the reporter genes. In the *A. tumefaciens* system, ILA is thought to modulate the auxin response by sensing the concentration of IAA and antagonizing its action as needed (317). ILA competes with labeled-IAA for binding to auxin binding proteins that are implicated in cellular auxin transport. Koga et al. (1991) reported that under aerobic conditions, *Enterobacter cloacae* produced more IAA than ILA;

however, under less aerobic conditions, the opposite was observed (133). These results suggest that the ratio of IAA to ILA may depend on the amount of oxygen in the cultures. Under microaerobic conditions, ILA is reductively produced from IPyA. In the rhizosphere of plants, the levels of oxygen naturally fluctuate and so too will the levels of IAA and ILA (133). Kaper and Veldstra (1958) reported that *Agrobacterium tumefaciens* produced mainly IAA in the first 23 hours of growth, and that ILA only started to accumulate after 38 hours. Here, UW4 cultures were grown for 72 hours before the indole compounds were analyzed, possibly providing a sufficient amount of time for the accumulation of ILA.

Methyl- IAA (M-IAA) is an inactive IAA storage form which can be converted to free IAA as needed. The methylation of IAA has not been studied in bacteria; however, in plants IAA is methylated by a carboxyl methyltransferase (319) and M-IAA is hydrolyzed back into active IAA by esterases belonging to the methyl ester transferase family (319). M-IAA was detected in all of the transformant cell cultures, but not in cultures of the wild-type strain. A positive correlation between the amount of IAA and M-IAA was observed in the transformants; thus, the wild-type, which produced the least IAA, also had the lowest amount of M-IAA, below the limit of detection. M-IAA is scarce in plants, likely due to its rapid turnover, and therefore its function remains elusive. In plants, methylation of IAA may enhance its transport, being that it is more nonpolar than IAA and could more readily diffuse across membranes (319). M-IAA may be efficiently transported throughout a plant and subsequently hydrolyzed to active IAA by esterases belonging to the MES family (319). In bacteria, M-IAA and its respective biosynthetic and hydrolytic enzymes have not

been studied, however, a methyltransferase and esterase functionally similar to those reported in plants likely also exists in strain UW4.

Understanding and quantifying the impact of IAA-producing PGPB on plants is challenging. One strategy is to inoculate roots with a wild-type and corresponding mutant (or transformant) PGPB *in vitro* and monitor the resulting effects on the plant. Such studies reveal that some strains inhibit the elongation of the primary root but increase the number and/or length of lateral roots and stimulate root hair formation *in vitro* (45). In this study, we examined the impact of increasing UW4's capacity to produce IAA, on its ability to promote root elongation in growth pouches. The results revealed that seedlings displayed the longest primary roots when inoculated with the transformant UW4-nit, followed by UW4-phe, UW4-nthAB, and UW4-ami respectively. Treatment with wild-type UW4 resulted in the shortest roots, 30% less than those inoculated with UW4-nit (Fig. 20). In addition, IAA is known to promote the growth of root hairs, which are important for plant mineral nutrition (320)(259). Canola seedlings treated with the transformants had noticeably more root hairs than seedlings treated with the wild-type, however the density of root hairs was not quantified (Fig. A5, Appendix A).

While low levels of IAA generally stimulate root elongation, higher levels of bacterial IAA, whether from IAA-overproducing mutants or strains that naturally secrete high levels or from high-density inocula, stimulate the formation of lateral and adventitious roots. However, levels that exceed some threshold value (specific to each plant) will have growth inhibitory effects. Xie et al. (1996) report that six mutants of *Pseudomonas putida* GR12-2 which produced 2- to 3-times more IAA (4.3-6 μg

mL⁻¹) than the wild-type (2 µg mL⁻¹), stimulated canola root elongation to the same extent as the wild-type in growth pouches. However, one GR12-2 mutant that produced 4-times more IAA (8.3 µg mL⁻¹) than the wild-type, inhibited canola root elongation by ~58% (95). Several studies have noted correlations between a high level of IAA synthesis in vitro and deleterious effects of these bacteria on root growth (93)(207). The UW4-nit and UW4-nthAB transformants produced IAA within a similar range (8.51 and 9.22 µg mL⁻¹, respectively) to the deleterious rhizobacteria reported by Xie et al. (1996), however we did not see any inhibition of root growth. It is possible that the two rhizobacteria species have different levels of ACC deaminase activity, another important factor in determining root length. In another study, a *Pseudomonas fluorescens* BSP53a transformant that overproduced IAA, imparted a stimulatory effect on the adventitious root growth of black currant softwood cuttings but had an inhibitory effect on root growth of cherry tree cuttings (96). Green gram seedlings treated with the IAA-overproducer *Pseudomonas* sp. MPS90 showed no significant difference in primary root or shoot length when compared to the control, whereas black gram seedlings treated in the same manner showed an inhibition of growth (97). This data is consistent with the notion that each plant has a certain threshold level of IAA, above which the roots are unable to develop normally. Whether IAA has a stimulatory or inhibitory effect on plant growth varies over a range of concentrations, the plant species and the sensitivity of the plant tissue to IAA.

Ethylene is a gas naturally produced by plants and is considered a 'stress hormone' involved in multiple molecular and physiological plant responses. The production of ethylene by a tissue is closely linked to the level of IAA; generally, the higher the IAA level, the higher is the rate of ethylene production. Synergistic effects of IAA and ethylene have been shown in the regulation of

hypocotyl elongation (321)(322), root hair growth and differentiation (323), apical hook formation (324), root gravitropism (325)(326) and root growth (327)(328). These two signaling pathways interact at the molecular level and the extent of the crosstalk between IAA and ethylene may be plant –specific (297). Some plants and even tissue types may be more responsive to ethylene and produce the gas at a different rate than others when exposed to certain levels of IAA (297). These variances will affect the phenotypic outcome of the plant (i.e., growth promotion or inhibition). In *Arabidopsis thaliana*, it has been shown that the two hormones act synergistically in inhibiting primary root elongation (297). The two hormones affect each other’s synthesis in a feedback manner. IAA induces the transcription of the ethylene biosynthesis gene for ACC synthase, causing an increase in the level of ethylene. In turn, ethylene also has a stimulatory effect on IAA biosynthesis, as demonstrated by increased IAA responses and direct IAA measurements in the root tip in response to ethylene (297). Ethylene stimulates the biosynthesis of IAA that is transported toward the root tip. Subsequently, basipetally transported IAA activates the local auxin response that is regulated by the auxin receptor (TIR1) and inhibits cell elongation. IAA efflux carriers PIN1, PIN2, PIN4, and the influx carrier AUX1, are transcriptionally upregulated in response to ethylene. Increased expression of these carriers enhances the capacity of the main IAA transport pathway from the shoot toward the root tip (acropetal) and through the lateral root cap and epidermis (basipetal). Ethylene has also been shown to upregulate the expression of two genes (*wei2* and *wei7*) that encode subunits of anthranilate synthase, a rate-limiting enzyme in Trp biosynthesis (329). Tryptophan is the precursor from which IAA is derived (330). Upregulation of these genes by ethylene results in an increased Trp level and consequently the accumulation of IAA in the tip of the primary root (297).

On the other hand, ethylene may also reduce the levels of IAA by interfering with auxin signaling. The exact mechanism of this interaction is unknown, however it has been suggested that ethylene may stimulate the degradation of IAA, inhibit its polar transport by regulating the transcription of IAA-efflux and influx-carriers, and reduce its rate of synthesis (297)(331)(332)(333)(334). In *Arabidopsis thaliana*, studies have shown that ethylene modulates the development of adventitious roots by negatively affecting IAA synthesis but by positively enhancing the conversion of the IAA-precursor indole-3-butyric acid (IBA) into active free IAA (335). The functional relationship between ethylene and IAA for plant development can be both positive and counteractive depending on the plant and tissue type. However, both hormones are in a positive relationship with respect to the development of root hair. Bruex et al. (2012) found that 90% of genes related to root hair development were up-regulated by ethylene and IAA based on transcriptome sequencing data analysis (336). Moreover, studies showed that a root hair defect mutant was rescued both by IAA and by ACC (the ethylene precursor)(337). The long-haired phenotype of the ethylene overproducing *eto1* mutant was suppressed by the *aux1* mutation (338). Finally, the auxin and ethylene-insensitive double mutant (*aux1 ein2*) showed an additive root hair defect (328). In instances where excess ethylene is produced (either by a stress response or by excess IAA), bacteria that have ACC deaminase activity can sequester and degrade ACC, lowering ethylene and ameliorating the inhibitory effect on plant growth (3).

Given the importance of ACC deaminase in the promotion of plant growth by rhizosphere bacteria, this activity was measured in the wild-type and transformed UW4 strains to determine whether IAA and ACC deaminase activity levels might be linked. The four UW4 transformants described herein

have 1.3 – 3 times lower ACC deaminase activity than the wild-type, regardless of whether or not tryptophan was present (Table 7).

An ACC deaminase-negative mutant of *P. putida* GR12-2 which cannot reduce ethylene levels in plants stimulated the formation of more small adventitious roots than the wild-type strain (293). The increase in the number of roots on the cuttings correlated with an increase in ethylene production. Fewer adventitious roots were initiated on the cuttings when they were inoculated with an IAA-deficient mutant; this may be because the mutant is not able to stimulate the formation of ACC synthase and therefore ethylene in the plants (78).

The only studies that we are aware of that describe how IAA levels may affect the regulation of ACC deaminase in bacteria relate to changes in the level of the stationary phase sigma factor RpoS (232)(315). In the field, bacteria spend most of their life cycle in the stationary phase where a significant fraction of cellular transcription is regulated by RpoS. This stationary phase/stress sigma factor regulates a large cohort of genes that are important for the cell to overcome suboptimal conditions and ensure survival (339)(340). Most of the IAA production by plant growth-promoting bacteria takes place in the stationary phase. Saleh et al, created a UW4 transformant that overproduces RpoS and observed a 2-fold increase in IAA production and a ~20% decrease in ACC deaminase activity. Conversely, an *Enterobacter cloacae* CAL2 transformant that overproduces RpoS, yielded 10-fold more IAA while ACC deaminase activity increased by ~ 30% compared to the non-transformed strain. There was an increase of ~ 40% in root lengths of canola seedlings treated with *E. cloacae* CAL2 overproducing *rpoS* compared with the non-transformed strain. On the other hand, the UW4 transformant that overproduced RpoS did not promote root elongation significantly even

though it produced higher levels of IAA than the non-transformed strain (232). Perhaps growth promotion driven by the increase in IAA was offset by the negative effect that RpoS had on ACC deaminase transcription and activity in UW4. In addition, Sun et. al., (2009) observed that an ACC deaminase mutant of *Burkholderia phytofirmans* PsJN lost the ability to promote the elongation of canola roots (341). Concomitant with the creation of this ACC deaminase mutant, a 6-fold increase in IAA synthesis and an 8-fold increase in the cellular level of RpoS was observed (341).

Interestingly, when the mutation was complemented by the wild-type *acdS* gene and ACC deaminase activity was restored, the strain produced the same amount of IAA as the *acdS*⁻ mutant (i.e. ~5.5-fold more than the wild-type) and RpoS levels were 5-fold higher than wild-type (341). These findings suggest that RpoS is responsible for controlling the transcription of IAA biosynthesis genes.

Moreover, the level of IAA is not dependent on ACC deaminase activity and *vice versa*. It seems that RpoS controls both IAA production and ACC deaminase independently and regulation can be either positive or negative in different bacteria. To further complicate the interplay between RpoS, IAA and ACC deaminase (ACCD), the regulation of RpoS itself is affected by multiple factors including: reduction in growth rate, starvation, osmolarity, temperature, cell density and pH (339). The complexity of RpoS regulation is consistent with its role as a master regulator at the genome level and strictly correlates to the need to express the *rpoS* gene solely in response to specific environmental and physiological cues (342).

3.5 Conclusion

While it is easy to measure the level of IAA produced by a bacterium *in vitro*, it is difficult to determine the levels that are produced in the rhizosphere, as expression of the many biosynthesis and regulatory genes is controlled by both genetic and environmental factors. By manipulating the

levels of IAA produced by bacteria through genetic engineering, it is possible to improve the beneficial effects of PGPB in the rhizosphere. IAA-overproducing transformants of *Pseudomonas* sp. UW4 were constructed by introducing a second copy of a target IAA biosynthesis gene on a plasmid. Five different genes were targeted for over-expression, four of which have been functionally characterized (*ami*, *nit*, *nthA*, *nthB*) and one which has not been experimentally characterized (*phe*). All transformants produced more IAA than the wild-type bacterium, reinforcing the putative involvement of each of the respective genes in IAA production by strain UW4. Although these data do not enable us to define the specific catabolic role of the uncharacterized Phe enzyme in IAA biosynthesis, over-expression of *phe* by addition of exogenous Trp and consequent overproduction of IAA, strongly suggests the involvement of this gene in IAA synthesis by UW4. One of the transformants (UW4-nit) promoted canola root growth significantly better (30%) than the wild-type bacterium in growth pouch assays. The other three transformants (UW4-nthAB, UW4-ami, and UW4-phe), which produced either more or less IAA than UW4-nit, did not significantly alter root elongation compared to the wild-type strain. It is important to note that the amount of IAA produced by the UW4 strains *in vitro*, is a result of the exact conditions under which those cells were cultured at that time (i.e., temperature, pH, growth-phase, oxygen levels, Trp concentration). These *in vitro* conditions are not necessarily representative of the amount of IAA that the plant cells are exposed to upon inoculation with the bacteria under growth pouch assay or field conditions. It is difficult to determine the amount of IAA that the seeds are exposed to during the growth pouch assay, as this depends on the number of bacterial cells that successfully attach to the seed, the rate of IAA production/secretion by each strain under the growth pouch conditions and over the duration of the assay, and finally the extent of IAA uptake by each seed. For instance, one study reports that

inoculation of *Arabidopsis thaliana* with *B. megaterium* resulted in a stimulation of growth in vitro when seedlings were placed at a distance of 5 cm from the inoculation site, whereas repressing effects were found at a distance of 2 cm (343). Results suggest that IAA-a diffusible bacterial metabolite, alters growth depending on the concentration that actually reaches the plant cell. As such, a proportional correlation between the measured IAA concentration in each strain culture and the resulting plant growth effect upon inoculation with that strain cannot be made precisely. However, the general trend observed in this study is that a 2-3 fold improvement in UW4's capacity to produce IAA, leads to enhanced primary root growth, while shoot growth remains unaffected. In nature, the complexity of the rhizosphere environment and the intricacies of plant-bacterial interactions alter the outcome that bacterial IAA will have on the plant. From the data presented here, one can speculate that root growth is governed not only by IAA but also by other IAA-related compounds. For example, ILA may counteract the effect of IAA to some extent. There is also interaction between IAA and ethylene; therefore, ACC deaminase activity when present, likely also plays a role in the effect of bacterial IAA on plant growth and development. Additionally, our understanding of the effect of bacterial IAA on plants is confounded by the production of cytokinins by UW4. It is recognized that IAA and cytokinins interact to regulate a variety of physiological processes in plants and that these interactions may be antagonistic, as in the case of control of apical dominance, or synergistic, for example, in the activation of cell division (344). An increase in the concentration of either one of IAA or cytokinin, whether by endogenous overproduction or exogenous application, can decrease the levels of the other in plant tissues (345)(346). Moreover, some studies report a stabilizing effect of cytokinin and IAA on key ethylene biosynthesis enzymes (296)(347)(348).

UW4 displays a combination of different modes of plant-growth-promoting actions; therefore, we cannot exclude the possibility that a combination of different mechanisms, besides or in addition to increased IAA production, may account for the enhanced plant growth promotion by the transformed strains. The crosstalk between the multiple interdependent plant-growth-promoting mechanisms including IAA and its derivatives, ethylene and ACC deaminase remain to be elucidated in detail for strain UW4.

Chapter 4

Construction and Characterization of IAA-Knockout Mutants

4.1 Introduction

Production of IAA by bacterial isolates varies greatly among different species and strains and depends on regulation by genetic and environmental factors (45). Several different biosynthetic pathways for IAA production exist, sometimes in parallel in the same organism. However, the relative activity of each pathway in a given organism remains elusive. Some of these pathways are constitutively expressed, while others are inducible (45).

Generally, two different approaches have been taken to test for the effect of bacterial IAA on plant growth. In one approach, the phenotypic effects of inoculating plants with bacterial mutants that produce different levels of IAA are compared (45)(88). In the second approach the size of the inoculum of a single bacterial strain is varied; assuming that the inoculum density is proportional to the amount of IAA that will be supplied to the plant (4). Studies have shown that bacterial mutants that overproduce IAA can have both a root growth-promoting or inhibiting effect (43), however, establishing a direct relationship between altered root growth and bacterial IAA has proven to be more elusive, due to the difficulty of isolating bacterial mutants that are completely deficient in IAA synthesis (78)(45). In fact, despite many efforts, to date there are no bacterial isolates which have been successfully manipulated to be completely devoid of the ability to produce IAA. Nevertheless,

mutants with significantly reduced levels of IAA have been generated for the phytopathogens *P. syringae* (349), *A. tumefaciens* (85), and *E. herbicola* pv. *gypsophilae* (49) and for the plant growth-promoting bacterium *Azospirillum lipoferum* (89) and *Pseudomonas putida* GR12-2 (78) by targeting specific genes for mutation.

The rhizobacterium *Pseudomonas* sp. UW4 is a strong candidate for development as a soil inoculant to enhance crop yields. Inoculation of canola, tomato, and other agriculturally important plants with this strain results in substantial promotion of seedling root growth (162). One of the main characteristics that contributes to the ability of this strain to enhance plant growth is the capacity to synthesize and secrete IAA. In strain UW4, IAA is produced through at least 2 different biosynthesis pathways (the IAN and IAM pathways). Functional annotation of the complete sequenced genome of this strain (162) based on protein sequence similarity, led to the identification of seven putative IAA-biosynthesis genes in the genome of strain UW4, four of which have since been biochemically characterized.

To assess the specific function of IAA produced by strain UW4 in the plant-bacterial interaction, a directed approach was taken, in which individual IAA-biosynthesis genes were knocked. The seven putative IAA biosynthesis genes encoding enzymes that catalyze steps in the IAN/IAM pathway for IAA synthesis, were isolated, and a portion of each gene was deleted in order to obtain an IAA⁻ mutant with reduced ability to produce IAA compared to the wild-type. This approach revealed a surprising discovery- a third pathway functioning via the IPyA intermediate seems to be operating in strain UW4, and compensating for any disruption in the IAN/IAM pathways.

4.2 Materials and Methods

4.2.1 Bacterial Strains and Plasmids

E. coli DH5 α (InvitrogenTM) was used as an initial cloning host and was maintained aerobically at 37°C in Luria-Bertani broth. Wild-type *Pseudomonas* sp. UW4 and UW4 mutants (described below) were grown and maintained aerobically at 30°C in tryptic soy broth (Becton-Dickinson) supplemented with 100 $\mu\text{g mL}^{-1}$ ampicillin. The DF salts minimal medium of Dworkin and Foster (1958)(350) was used for propagation of wild-type UW4 and derivative strains where indicated. The full-size IAA-target genes were initially cloned into the pGEM[®]-T Easy vector (Promega) or the pBluescript II SK+ (reference) vector and the truncated genes were cloned into the suicide plasmid pK18 mobSacB. All of the plasmid constructs used in this study are described in Table 9.

4.2.2 DNA Manipulation

Genomic DNA from *Pseudomonas* sp. UW4 was isolated using the Wizard Genomic DNA purification kit (Promega, catalog no. A1120). The primer sequences used to amplify the seven target IAA genes are given in Table 10. Both the forward and the reverse primer sequences were based on the fully sequenced UW4 genome (GenBank accession no. CP003880).

Four of the genes (*ami*, *iaaM*, *aux*, *pbex*) were subcloned into the pGEM[®]-T Easy vector (Promega) (Fig. 18). The pGEM[®]-T Easy Vector Systems are convenient systems to clone PCR products generated by GoTaq thermostable polymerase. This polymerase adds a single deoxyadenosine, in a template-independent fashion, to the 3'-ends of the amplified fragments. The pGEM[®]-T Easy pre-

linearized Vector contains 3'-T overhangs at the insertion site to provide a compatible overhang for PCR products. Successful cloning of each insert into the pGEM®-T Easy Vector interrupts the coding sequence of β -galactosidase; therefore, recombinant clones were identified by blue/white color screening on indicator plates containing 5-bromo-4-chloro-3-indolyl-galactopyranoside (X-gal). The remaining three genes (*ntbA*, *ntbB*, *nit*) were amplified using KOD Hot Start polymerase (Sigma Aldrich) and subcloned into the pBluescript II SK+ vector (Fig. 19). KOD Hot Start polymerase (Sigma Aldrich) has high fidelity, fast extension speed and generates blunt-ended PCR products suitable for blunt-end ligation into a cloning vector. The pGemTeasy vector was not a suitable cloning plasmid for these three genes because the sequence contains restriction enzyme sites that will later facilitate the removal of a portion of these genes. Prior to cloning these genes into pBluescript II SK+, the vector was purified and double digested with SacI and HindIII to remove a portion of the multiple cloning site that contained the restriction enzyme sites used for IAA-gene deletion (Fig. 19). The resultant sticky ends of the vector were filled in with T4 DNA polymerase to produce blunt ends that were compatible with blunt-end ligation of the three KOD-amplified inserts (*ntbA*, *ntbB*, *nit*).

All recombinant cloning plasmids were transformed into *E. coli* DH5 α by the standard heat shock method described in Sambrook and Russell (2001)(304). The recombinant pGEM®-T Easy or pBluescript II SK+ carrying the full-length IAA-genes were isolated from *E. coli* DH5 α using the PureYield™ Plasmid Miniprep System (Promega, Catalog No. A1223) and digested with a set of restriction enzymes (Table 10) to remove a significant portion of the middle of each IAA biosynthesis gene insert. The digestion products were analyzed on 1% agarose gels and the target

fragments (i.e., the linearized plasmid containing the deleted gene) were purified from the gel using the Wizard® SV Gel and PCR Clean-Up System (Promega, Catalog No. A928). Upon purification, the linearized plasmids were re-ligated using T4 DNA ligase and each of the truncated IAA biosynthesis genes was PCR amplified from the plasmid using KOD Hot Start polymerase (Sigma Aldrich).

The KOD-amplified truncated IAA-genes were cloned into the pK18 mobSacB vector via blunt end ligation (Fig. 20). The small mobilizable vector pK18 mobSacB has the broad-host-range transfer machinery of plasmid RP4 and a modified *sacB* gene from *Bacillus subtilis*. This vector can be transferred by conjugation into a wide range of Gram⁻ bacteria, facilitating gene disruption and allelic exchange by homologous recombination (351). Gene *sacB* encodes levansucrase, which catalyzes the hydrolysis of sucrose and synthesizes levans. Levans are high molecular weight fructose polymers that are fatal to most Gram⁻ bacteria (352). Therefore, the pK18*mobsacB* vector is suicidal in strain UW4 in the presence of sucrose and can be used as a counter-selectable marker. The pK18 mobSacB replacement vector was digested with SmaI to linearize it and produce compatible ends for blunt end ligation with the KOD polymerase PCR products. The KOD-amplified genes (with deletions) were blunt-end ligated into the SmaI site of pK18 mobSacB, and the vector was maintained in *E. coli* DH5 α . To confirm the correct insert sizes (i.e., deletion of the target IAA biosynthesis gene), the recombinant pK18 plasmids were isolated from *E. coli* DH5 α , purified and subjected to PCR amplification using KOD polymerase. The PCR products were analyzed on a 1% agarose gel and fragment sizes were compared to a DNA-ladder of known sizes.

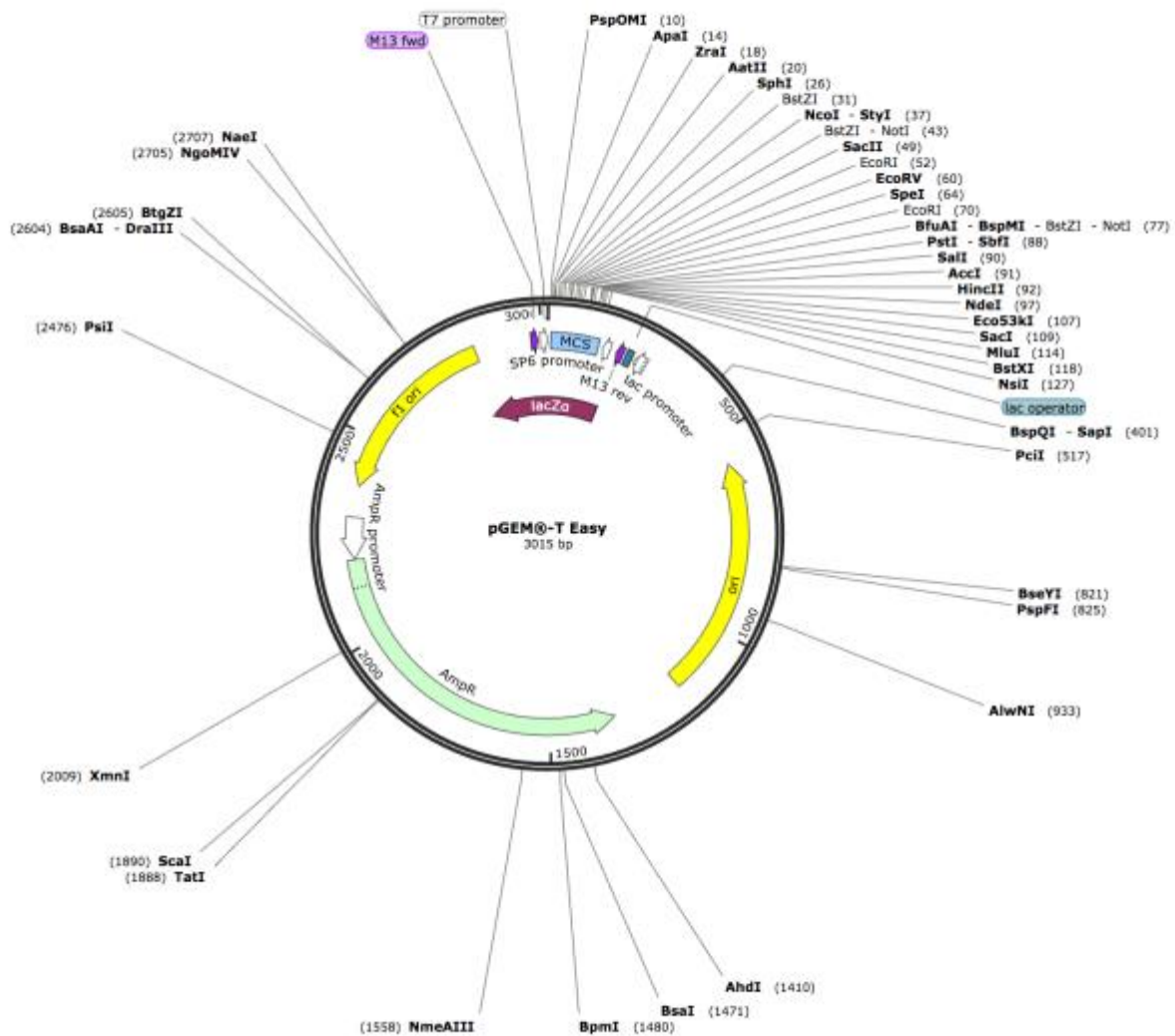


Figure 18. Map of pGem®-T easy plasmid

The genes *ami*, *iaaM*, *aux*, *pbex* generated by PCR using GoTaq thermostable polymerase were subcloned into the pGem®-T Easy vector. This polymerase adds a single deoxyadenosine (A) to the 3'-ends of the amplified fragments. The pre-linearized vector contains 3'-T overhangs at the insertion site to provide a compatible overhang for the PCR products.

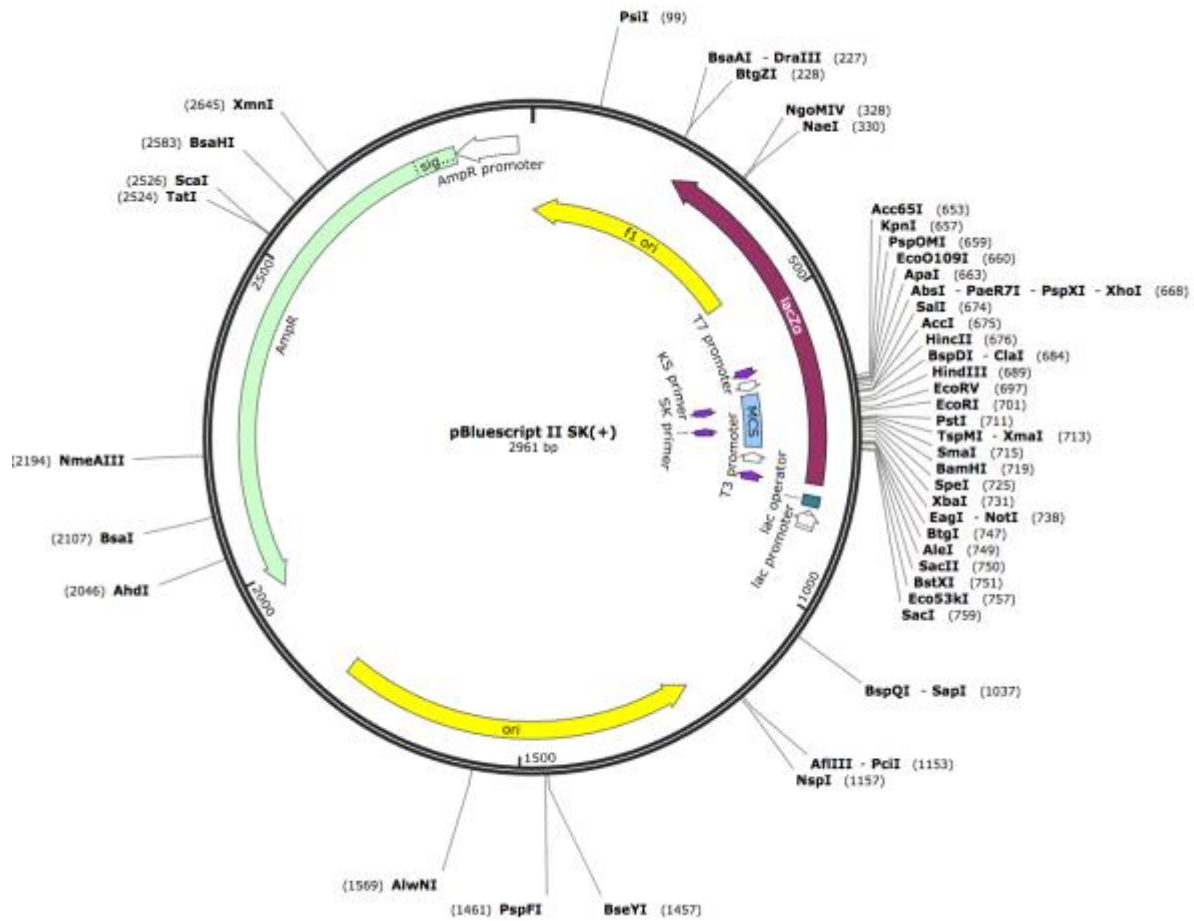


Figure 19. Map of pBluescript II SK(+) plasmid

The *nthA*, *nthB* and *nit* were amplified using KOD Hot Start polymerase and subcloned into the pBluescript II SK+ vector. Prior to cloning these genes into pBluescript II SK+, the vector was digested with SacI and HindIII to remove a portion of the multiple cloning site. The resultant sticky ends of the vector were filled in with T4 DNA polymerase to produce blunt ends that were compatible with blunt-end ligation of the KOD-amplified genes.

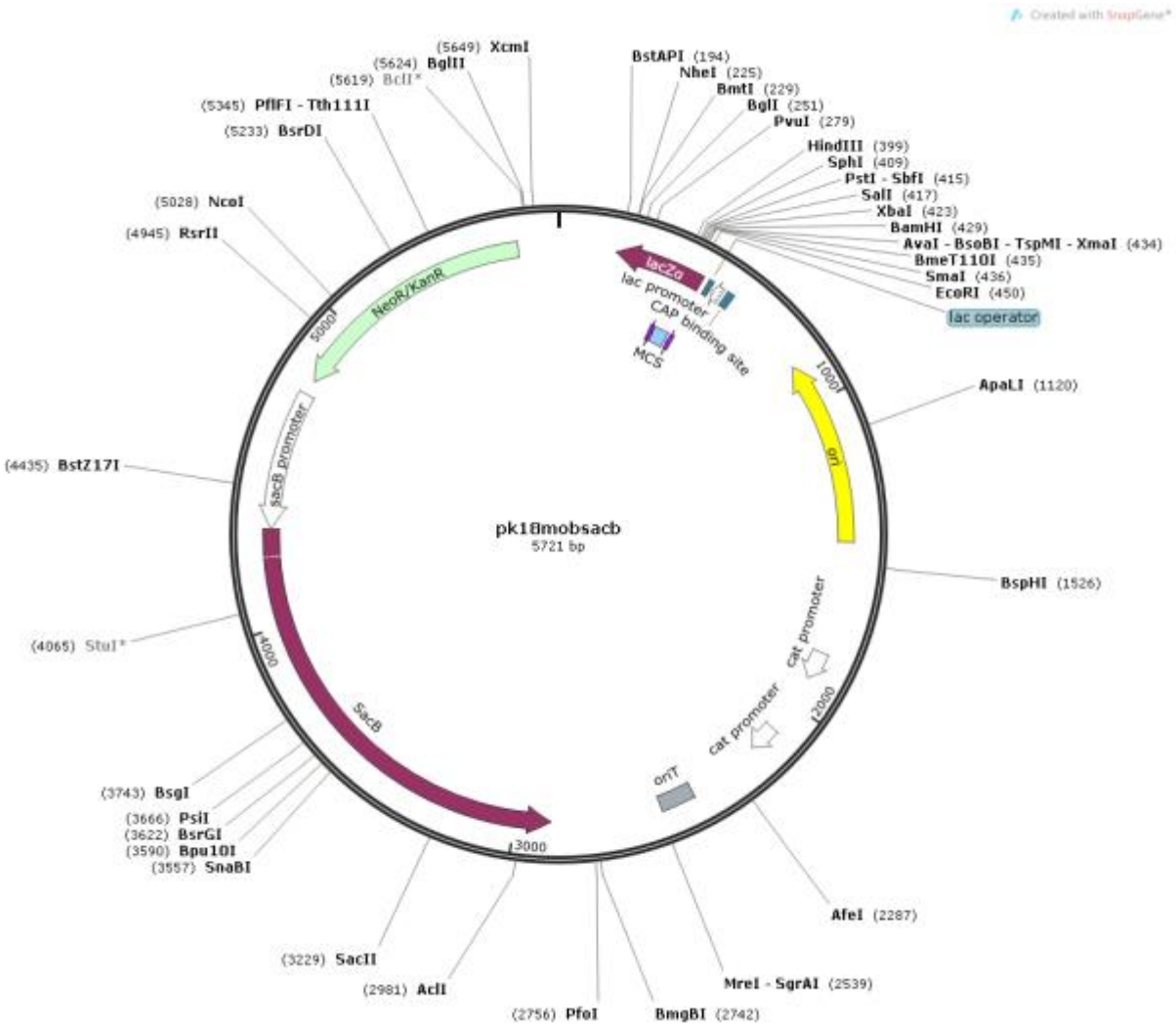


Figure 20. Map of pK18 mobSacB plasmid

The vector was digested with SmaI to linearize it and produce blunt ends for ligation. The truncated genes *iaaM*, *aux*, *ami*, *nit*, *nthA*, *nthB*, and *phe* were amplified using KOD polymerase and cloned into the pK18 mobSacB vector via blunt end ligation.

Table 9. Plasmid Constructs used in this study

Plasmid Construct	Target Gene	Description
pGemT-ami	<i>ami</i>	GoTaq-amplified <i>ami</i> gene cloned into pre-linearized pGEM®-T Easy via compatible A and T overhangs
pGemT-iaaM	<i>iaaM</i>	GoTaq-amplified <i>iaaM</i> gene cloned into pre-linearized pGEM®-T Easy via compatible A and T overhangs
pGemT-aux	<i>aux</i>	GoTaq-amplified <i>aux</i> gene cloned into prelinearized pGEM®-T Easy via compatible A and T overhangs
pGemT-phe	<i>phe</i>	GoTaq-amplified <i>phe</i> gene cloned into prelinearized pGEM®-T Easy via compatible A and T overhangs
pBS-nthA	<i>nthA</i>	KOD-amplified <i>nthA</i> gene cloned into pBluescript II SK+ between the SacI and HindIII sites via blunt-end ligation
pBS-nthB	<i>nthB</i>	KOD-amplified <i>nthB</i> gene cloned into pBluescript II SK+ between the SacI and HindIII sites via blunt-end ligation
pBS-nit	<i>nit</i>	KOD-amplified <i>nit</i> gene cloned into pBluescript II SK+ between the SacI and HindIII sites via blunt-end ligation
pK18-ami	<i>ami</i>	KOD-amplified <i>ami</i> gene (with deletion) cloned into the SmaI

Plasmid Construct	Target Gene	Description
		site of pK18mobSacB via blunt-end ligation
pK18-iaaM	<i>iaaM</i>	KOD-amplified <i>iaaM</i> gene with deletion) cloned into the SmaI site of pK18mobSacB via blunt-end ligation
pK18-aux	<i>aux</i>	KOD-amplified <i>aux</i> gene with deletion) cloned into the SmaI site of pK18mobSacB via blunt-end ligation
pK18-nthA	<i>nthA</i>	KOD-amplified <i>nthA</i> gene with deletion) cloned into the SmaI site of pK18mobSacB via blunt-end ligation
pK18-nthB	<i>nthB</i>	KOD-amplified <i>nthB</i> gene with deletion) cloned into the SmaI site of pK18mobSacB via blunt-end ligation
pK18-nit	<i>nit</i>	KOD-amplified <i>nit</i> gene with deletion) cloned into the SmaI site of pK18mobSacB via blunt-end ligation

Table 10. Primers and Restriction Enzymes used to make Gene Deletions

Gene	Primer Sequence	Original Size of Amplicon (bp)	Size of Amplicon after Deletion (bp)	Restriction Enzymes used in Sequence Deletion
<i>ami</i>	F-AGCAAATGTTCGAGAGGGATG R- AGTGGATGCTGGGGATACAG	1790	822	SmaI + EheI
<i>iaaM</i>	F- GGTGGTGTCTGTTCGGGC R- ACATTGGTAAAGGGCTACGC	1932	1382	EheI
<i>aux</i>	F- ACGCCAGTGACCTCCATAC R- GCGACGCAGATTACCTACAC	2385	1429	HindIII
<i>ntbA</i>	F-GACCGTGCTAAACCGATGAG R- AGATCGTGAAAGCCATCCAT	692	531	SfoI + PstI
<i>ntbB</i>	F- CCGAGCACATGAGTGAAGAA R- TCATGTCGTTGACGATGACC	923	505	SfoI + EcoRI
<i>nit</i>	F- GAGCAGGTTGAGGTCGATGT R- CAGGGAAATACTCGCTCTGC	1136	599	NruI + NcoI
<i>phe</i>	F- CGCCACCTACCTGTTAGAGC R- TGTTTGGGAGGTCTGTGTCA	1260	778	NruI+ MscI

F= forward primer, R= reverse primer

4.2.3 Bacterial Conjugation & Gene Sequencing

The recombinant pK18 plasmids carrying the truncated IAA-genes were initially transformed into *E. coli* DH5 α using the calcium chloride method described by Sambrook and Russell (2001) (36). The plasmids were then individually transferred from *E. coli* DH5 α into wild-type *Pseudomonas* sp. UW4 by triparental mating using the helper plasmid pRK2013 in *E. coli* HB101 (37). Transconjugants were selected following growth (for 24 h at 30°C) on tryptic soy agar (TSA) medium supplemented with 50 $\mu\text{g mL}^{-1}$ kanamycin (Km) to select for the plasmid. The plasmid was isolated from the positive clones and the insert was mapped by restriction enzyme digestion. Fragment sizes were determined by comparison of migration distance with known DNA markers following agarose gel electrophoresis. To select for transconjugants that had replaced the functional IAA gene in their chromosome with the truncated gene from the plasmid by double crossover between homologous gene sequences, positive colonies growing on TSA+ Km plates were transferred onto TSA+ 10% (w/v) sucrose plates. Colonies that were resistant to the lethal effects of the vector-encoded *sacB* gene product were selected and genomic DNA was extracted and sent to Bio Basic Canada Inc. (Markham, Ontario, Canada) for determination of the nucleotide sequence of the replaced IAA-gene. Primers used for sequencing reactions were the same as those used to amplify the original sequence via PCR. IAA gene deletion mutants were also confirmed by PCR amplification of genomic DNA; the PCR product revealed a single band corresponding to the deleted gene size when analyzed on a 1% agarose gel. Once single-gene knockout mutants were obtained, they were used to make double-gene knockout mutants following the same protocol.

4.2.4 HPLC Analysis

Upon confirmation of the truncated IAA biosynthesis genes' sequences in each respective UW4 mutant via sequencing, the mutant strains along with the wild-type strain were grown in DF minimal media + 500 µg/mL L-tryptophan for 72 hours. The culture supernatants were subjected to HPLC analysis to quantify the amount of IAA secreted by each strain. HPLC analysis was performed using a Waters Alliance 2695 HPLC separation system (Mississauga, Ontario, Canada), which includes a Waters 2996 photodiode array detector. The system was connected to a PC with Empower 2 software (Waters) for data collection and processing. A Sunfire C18 column (50 by 4.6 mm [inner diameter], 2.5 µm pore size; Waters, Ireland) was connected with a Security Guard C18 guard column (4 by 3.0 mm [inner diameter]; Phenomenex, Torrance, CA). Gradient HPLC was performed at room temperature using a mobile phase containing water-acetic acid (1% [vol/vol]) (A) and acetonitrile-acetic acid (1% [vol/vol]) (B). Starting with 80% A, the gradient began at 2 min and reached 60% A at 15 min. The flow rate was 1 ml/min. A 100 µl sample injection volume was used, and the eluent was monitored at 280 nm.

4.2.5 Liquid Chromatography-Tandem Mass Spectrometry (LC-MS-MS)

Liquid Chromatography–Electrospray Ionization–Tandem Mass Spectrometry was used to identify IAA and respective indole intermediates in bacterial cell cultures. Metabolites were identified by mass/charge ratio (m/z) values and the retention time of standard compounds. The protocol followed that described by Lin *et al.*, 2015 (353). Briefly, the bacterial cultures were grown in DF

minimal media for 72 hours at 30°C, with and without Trp (500 µg/mL) supplementation. The cells were collected by centrifugation at 10,000 x g for 10 min and the pellet was discarded. The supernatants were processed by adding 400 µl of cold methanol to 50 µl of culture supernatant. The mixture was vortexed and incubated at ~20°C for 30 min for complete protein precipitation. Samples were centrifuged at 10,000 x g and 4°C for 10 min. The supernatant was dried in a vacuum evaporator (Savant Speed Vac Plus SC110A). The residue was re-dissolved in 100 µl of 0.1% formic acid in water and centrifuged at 10,000 x g and 4°C for 10 min. The final supernatant was transferred to an autosampler vial for LC–MS/MS analysis. The analytical standards (IAA, IAM, IAN, IPyA, IAAld, IAld, ILA, TOL (IEt)) were purchased from Sigma–Aldrich (St. Louis, MO, USA) and stock solutions of each (10 mM) were prepared in methanol.

A Dionex Ultimate 3000 UHPLC system (Thermo Fisher Scientific, USA) coupled with a Q-Exactive Orbitrap mass spectrometer (Thermo Fisher Scientific, USA), equipped with an electrospray ion source, and operated in the positive ion mode was used. A superficially porous particle column (Zorbax 300A, 300Extend-C18, 2.1 mm x 100 mm, 3.5 µm pore) (Agilent Technologies Inc., Santa Clara, CA, USA) with mobile phases A (0.1% formic acid in water) and B (0.1% formic acid in methanol) was used. The column temperature was set at 25°C.

Chromatographic separation was achieved by gradient elution at a flow rate of 0.32 mL/min. The gradient program was as follows: 0–2.5 min, 100% A; 2.5–5.0 min from 0% to 25% B; 5.0–7.5 min from 25% to 40% B; 7.5 - 10 min from 40% to 60% B; 10–12.5 min 60%–80 B; 12.5–15 min 80–100% B, 15–18 min column re-equilibration. The total run time was 18.0 min, and an injection volume of 10 µL was used. The ionization parameter and multiple reaction monitoring (MRM)

transitions for the target analytes were obtained by direct injection of their individual standard solutions with a concentration of 1 mM. The positive ionization mode was used at a spray voltage of 3000 V. Nitrogen was used as the sheath and auxiliary gas at optimal values of 35 and 5 units (arbitrary units). The heated capillary temperature was 300°C. The argon collision gas pressure was set to 1.0 mTorr. The scan time of each MRM transition was set to 3.05 ms.

4.3 Results & Discussion

4.3.1 IAA-Gene Knockout Mutants

Pseudomonas sp. UW4 produces and secretes IAA; however, the complete mechanism through which this pivotal phytohormone is produced is unknown. An initial genomic survey of strain UW4 revealed seven target IAA genes (*ami*, *iaaM*, *aux*, *ntbA*, *ntbB*, *nit*, *pbe*) that compose two possible IAA biosynthesis pathways; the indole acetonitrile (IAN) and the indole acetamide (IAM) pathway. These seven genes were selected for single and double gene knockouts in which a portion of their coding sequence would be deleted. Vector pK18 mobSacB carried the truncated sequence of each IAA gene. This plasmid has an origin of transfer (*oriT*) and *mob* genes from plasmid RP4 (351), enabling transfer of the vector from *E. coli* DH5 α into wild-type strain UW4 via bacterial conjugation. Following transfer of the vector to strain UW4, kanamycin-resistant cells can arise only if the plasmid is taken up and maintained in the cells. Double homologous recombination takes place between the truncated version of the IAA-gene on the plasmid and that on the chromosome, replacing the wild-type gene with the truncated version. In addition, because SacB is encoded on the vector, selection for resistance to the lethal effects of SacB in the presence of sucrose, selects against

the incorporation of the entire plasmid into the genome, an event that would result from a single crossover event. In each case, replacement of the functional IAA biosynthesis gene in the chromosome of strain UW4 with its truncated gene counterpart was confirmed by both PCR and DNA sequencing.

Four of the genes (*ami*, *nthA*, *nthB*, *nit*) have previously been experimentally verified to be involved in IAA biosynthesis in this strain, while the remaining three (*iaaM*, *aux*, *phe*) remain as putative IAA biosynthesis genes based on sequence similarity. In total, eleven mutant UW4 strains referred to herein as “deletion mutants” were obtained. Of the seven target genes, six of them were knocked out (individually); a *phe* mutant could not be obtained. Once these single-gene deletion mutants were obtained, they were used as the starting point for a second deletion in another target gene (double-gene deletion mutants). In total, five double-gene deletion mutants were obtained. All of the UW4 deletion mutants generated in this study are listed in Table 11 and shown in Fig. 21.

Table 11. *Pseudomonas* sp. UW4 IAA-gene Deletion Mutants generated in this study

UW4 Deletion Mutant	Description
<i>ami</i> -	<i>ami</i> single-gene knockout. This gene encodes a functionally characterized amidase that converts IAM into IAA (See Chapter 2)
<i>iaaM</i> -	<i>iaaM</i> single-gene knockout. This gene encodes a putative tryptophan monooxygenase that converts Trp to IAM (see Chapter 5)
<i>aux</i> -	<i>aux</i> single-gene knockout. This gene encodes a putative tryptophan monooxygenase that converts Trp to IAM (see Chapter 5)
<i>nthA</i> -	<i>nthA</i> single-gene knockout. This gene encodes the α -subunit of a functionally characterized nitrile hydratase that converts IAN into IAM (Duca et al., 2014)
<i>nthB</i> -	<i>nthB</i> single-gene knockout. This gene encodes the β -subunit of a functionally characterized nitrile hydratase that converts IAN into IAM (Duca et al., 2014)
<i>nit</i> -	<i>nit</i> single-gene knockout. This gene encodes a functionally characterized nitrilase that converts IAN into IAM and IAA (Duca et al., 2014)
<i>nthB</i> + <i>iaaM</i>	<i>nthB</i> and <i>iaaM</i> double-gene knockout
<i>nthB</i> + <i>nit</i>	<i>nthB</i> and <i>nit</i> double-gene knockout
<i>iaaM</i> + <i>ami</i>	<i>iaaM</i> and <i>ami</i> double-gene knockout
<i>nit</i> + <i>ami</i>	<i>nit</i> and <i>ami</i> double-gene knockout
<i>iaaM</i> + <i>aux</i>	<i>iaaM</i> and <i>aux</i> double-gene knockout

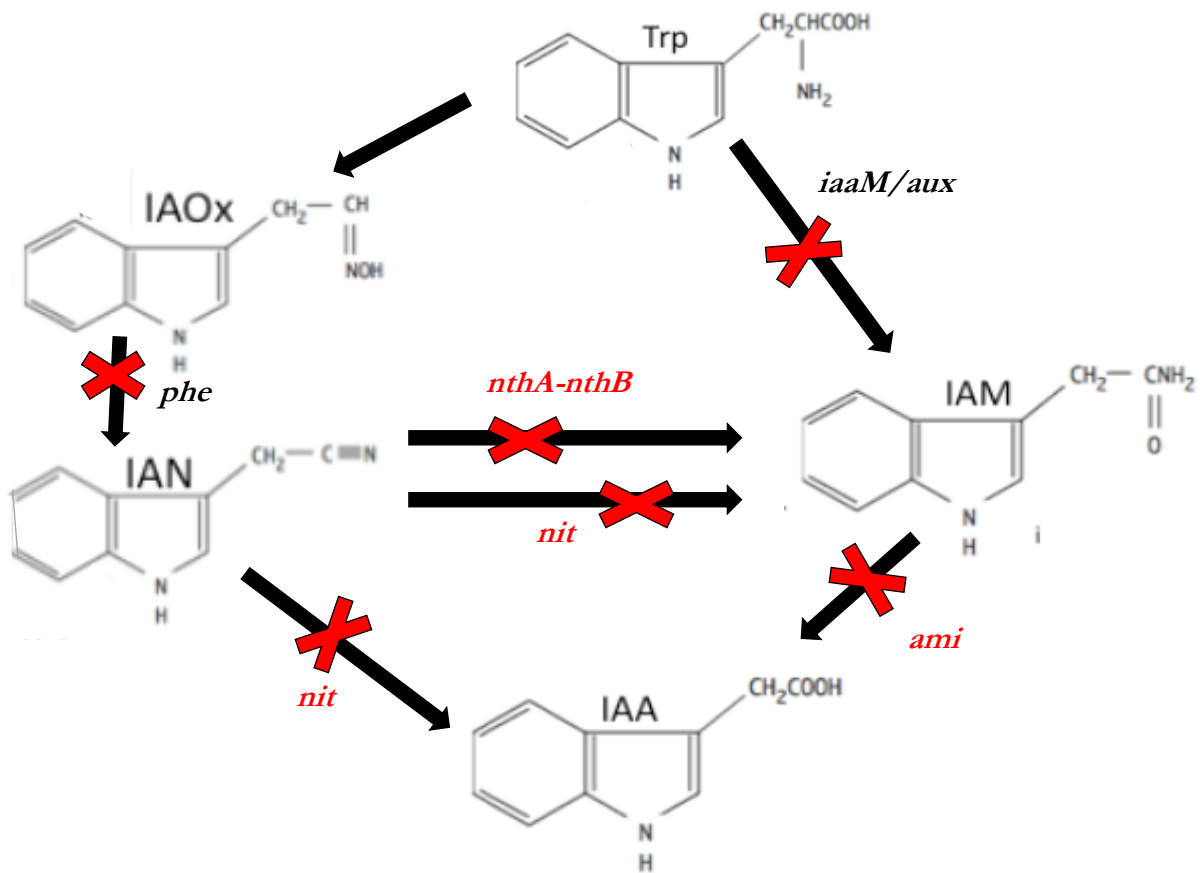


Figure 21. Gene Deletions in IAA biosynthesis pathways in strain UW4

The genes mediating each step of the pathway are shown above each arrow. Those shown in red font have previously been experimentally verified by our lab. Red “x” shows which pathways/genes were disrupted.

4.3.2 Quantification of IAA & Identification of an alternate IAA pathway

Once the deletion mutants were obtained, it was necessary to test the level of IAA that they produced compared to the wild-type when high concentrations of Trp were present. As such, each strain was cultured in DF salts minimal medium with 500 µg/mL Trp and the IAA levels in the

supernatants were measured by high-performance liquid chromatography (HPLC). The results were surprising in that none of the mutants (single and double-gene knockouts) produced significantly less IAA than the wild-type strain (Fig. 22).

This prompted a deeper investigation into why there was no significant decrease in IAA in any of the mutant strains. If both the IAM and IAN pathways are co-operating in strain UW4, then it is expected that if you knock out a gene in one pathway, the other pathway would compensate for that loss. This explanation would account for the results seen for all of the single-gene knockout mutants. However, the double-gene mutant *nit-ami* should not be able to produce IAA as both of these genes mediate the final step of IAA production from each of the two pathways (i.e. this mutant would have both pathways disrupted) (Fig. 21). These findings led to the speculation that a third pathway exists in strain UW4 and perhaps dominates IAA production in strain UW4. The most likely pathway is the IPyA pathway, which was initially ruled out because the typical IPyA pathway genes were not found to be present when UW4's genome was screened. This pathway has been well-characterized in other PGPB, including various *Pseudomonas* species. Since IAA-producing bacteria have the propensity to release intermediate compounds (IPyA, IAM, IAN, ILA, IAAld, IAld etc.) in the surroundings, another approach to detecting the IPyA pathway was taken where LC-MS-MS was used to search for and identify specific IAA-related compounds in the culture supernatant of strain UW4.

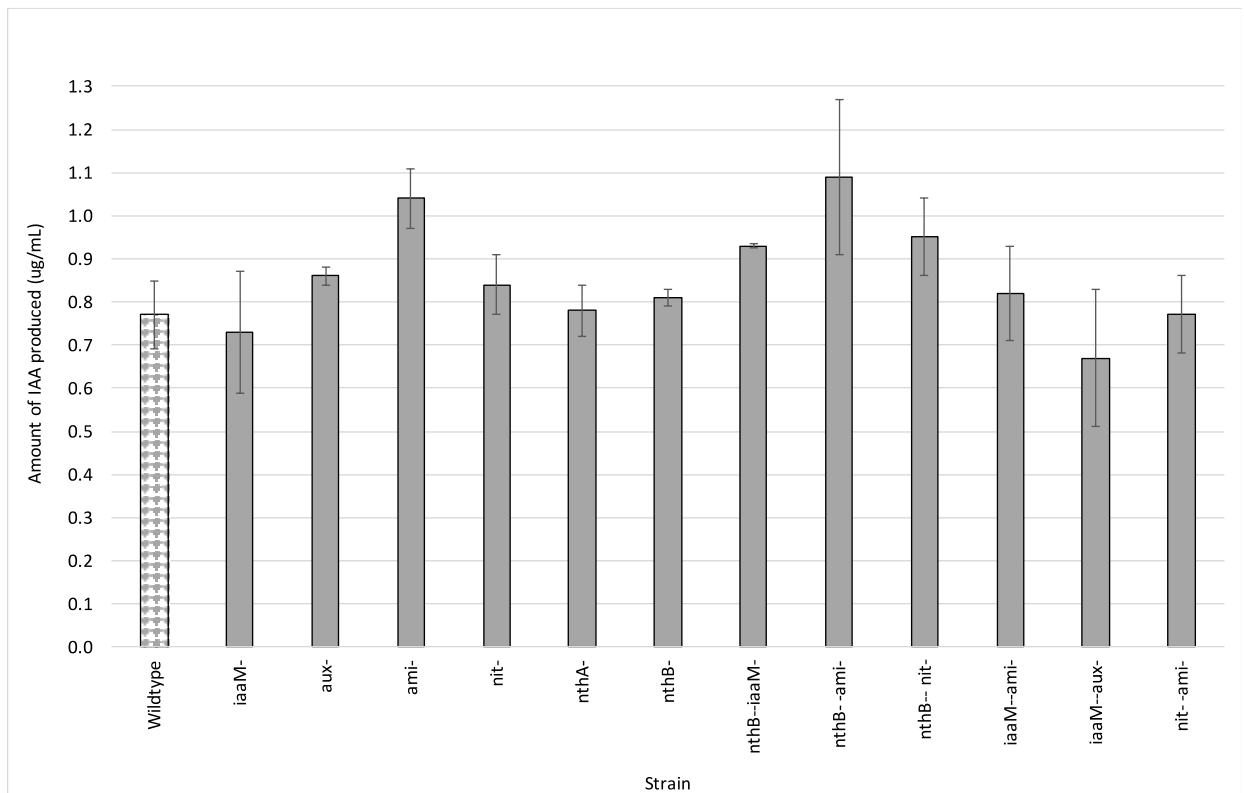


Figure 22. Production of IAA by UW4 wild-type strain and UW4 deletion mutants

Strains were grown for 72 hours in DF minimal media with 500 $\mu\text{g}/\text{mL}$ L-Trp supplementation. The culture supernatant was collected, and IAA was quantified by HPLC. Each value represents the mean of three replicates. Standard error bars are shown.

Wild-type UW4 and two double-gene knockout mutants (*nit-ami* and *iaaM-ami*) were also tested for their ability to produce IAA when fed with the IAM intermediate at 25 or 50 $\mu\text{g}/\text{mL}$. The common denominator between these two mutants is the *ami* gene, which codes for an enzyme that converts IAM into IAA. Therefore, a knockout in this gene is expected to hinder the ability of the strain to convert IAM into IAA. With a doubling of the concentration of IAM, the wild-type strain also produced approximately double the amount of IAA. However, in the case of the two double deletion mutants, IAA levels remained relatively consistent and at negligible amounts, regardless of

the concentration of IAM (Fig. 23). When the *ami*- single gene knockout mutant was tested, IAA production was not detected in the culture at any of the IAM concentrations.

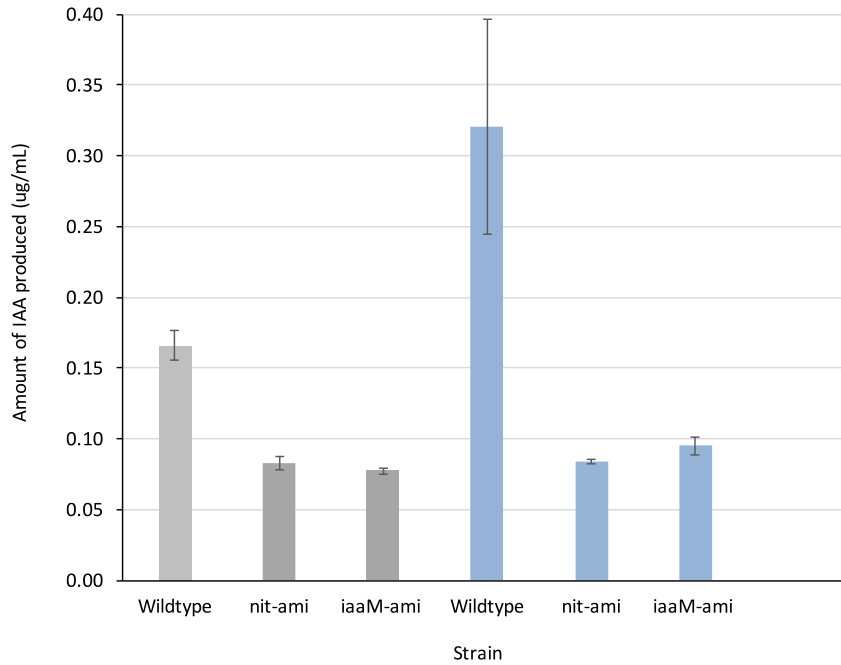


Figure 23. IAA production by wild-type and deletion mutants when fed IAM

Wild-type UW4 and two double-gene knockout mutants (*nit-ami* and *iaaM-ami*) were fed either 25 µg/mL IAM (grey bars) or 50 µg/mL IAM (blue bars). Strains were grown for 72 hours in DF minimal media. The culture supernatant was collected, and IAA was quantified by HPLC. Each value represents the mean of three replicates. Standard error bars are shown.

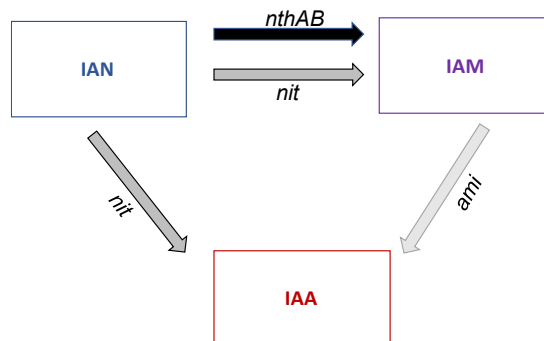


Figure 24. Conversion of IAN to IAM and IAA by *nit*, *nthAB* and *ami*

The *nit* and *nit-ami* deletion mutants were also tested for their ability to convert the IAN intermediate (10, 25, 50 $\mu\text{g}/\text{mL}$) into IAM and IAA. The Nit enzyme has been experimentally shown to convert IAN to both IAM and IAA (Fig. 24) (258). The *nit-ami* mutant produced proportionally more IAM as the concentration of IAN was increased (Fig. 25). In this case, although the *nit* gene was disrupted, another enzyme-nitrile hydratase (NthAB) compensates for that loss and mediates the conversion of IAN into IAM (Fig. 24). This NthAB enzyme has been biochemically verified to perform this reaction (258). Moreover, the proportional increase in IAM as the concentration of IAN is increased, suggests that NthAB is inducible. Indeed, it has been shown that a nitrile hydratase from *Pseudomonas chlororaphis* B23 is induced by its amide product (354). The NthAB from UW4 shares very high sequence identity (87%) with the NthAB from *P. chlororaphis*, thus it is not unreasonable to assume that NthAB is induced by IAM in strain UW4. Since the *ami* gene is also disrupted in this mutant, the IAM product is able to accumulate because it is not converted into IAA by Ami (Fig. 24). However, we still detect negligible amounts of IAA in the culture (Fig. 25), therefore we cannot rule out the possibility that another enzyme besides Ami is also capable of converting IAM into IAA.

For the *nit* deletion mutant, as the concentration of IAN was increased from 10 to 25 $\mu\text{g}/\text{mL}$, the concentration of IAM decreased by $\sim 70\%$ (Fig. 26). At 50 $\mu\text{g}/\text{mL}$ IAN, no IAM could be detected, however IAA was detected in the culture. This suggests that at the highest IAN concentration (50 $\mu\text{g}/\text{mL}$), NthAB converts $\text{IAN} \rightarrow \text{IAM}$ and consecutively Ami rapidly converts $\text{IAM} \rightarrow \text{IAA}$ (Fig. 24). As is seen for nitrile hydratases (NthAB), amidase (Ami) enzymes have also been shown to be induced by their amide substrate (258). Therefore, it is possible that at lower IAN concentrations

(10-25 $\mu\text{g}/\text{mL}$), NthAB produces IAM but perhaps not to the level required for autoinduction or Ami induction. This may be the reason that we do not detect any IAA (Fig. 26). However, at 50 $\mu\text{g}/\text{mL}$ IAN, sufficient amounts of IAM are produced to induce both NthAB and Ami, therefore we are detecting less IAM and more IAA in the culture (Fig. 26).

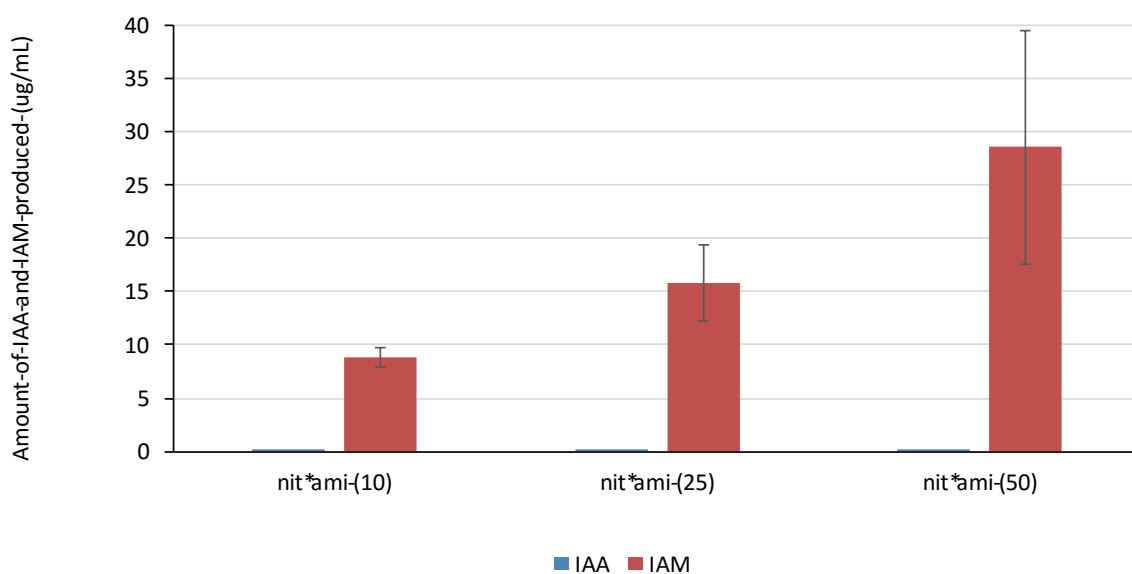


Figure 25. IAA and IAM production by the UW4 deletion mutant *nit-ami*

The UW4 double-gene knockout mutant *nit-ami* was fed IAN at 10, 25 or 50 $\mu\text{g}/\text{mL}$. The strain was grown for 72 hours in DF minimal media. The culture supernatant was collected and IAA/IAM was quantified by HPLC. Each value represents the mean of three replicates. Standard error bars are shown.

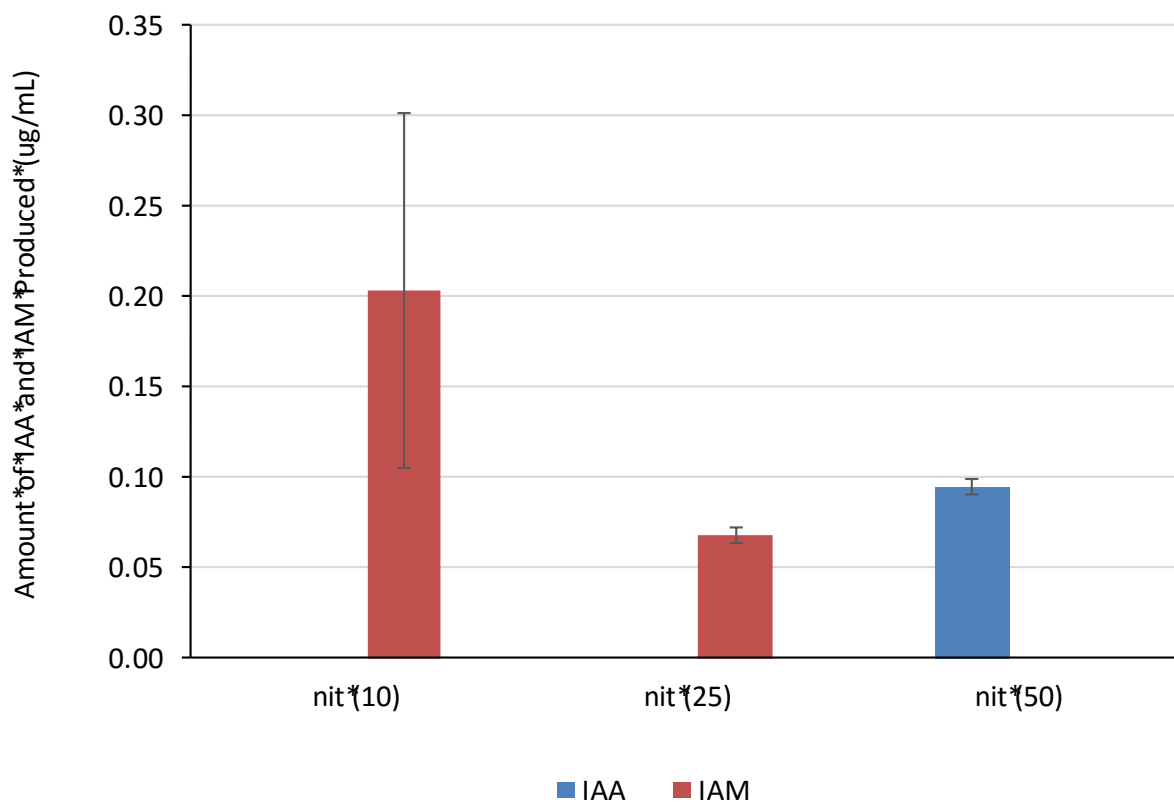


Figure 26. IAA and IAM production by the UW4 deletion mutant *nit*⁻

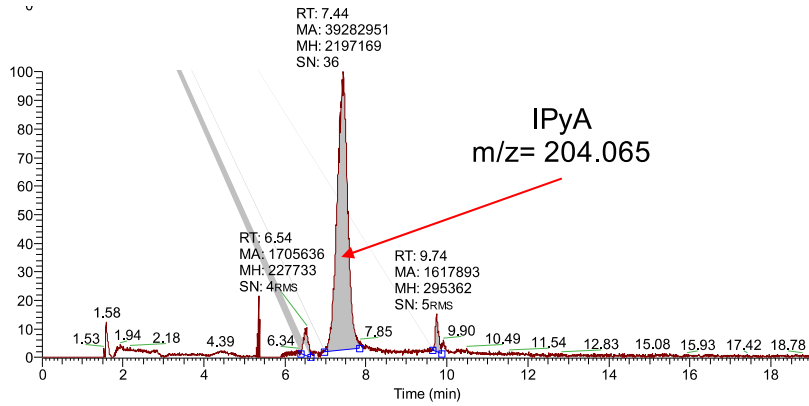
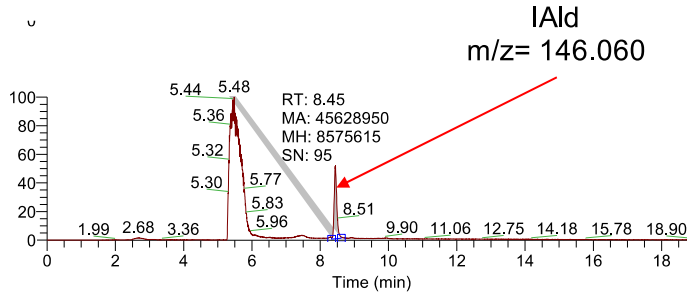
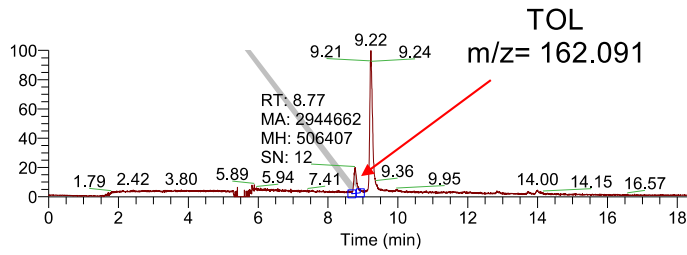
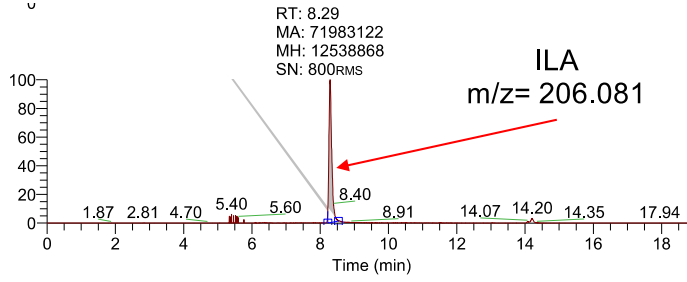
The UW4 single-gene knockout mutant *nit*⁻ was fed either 10, 25 or 50 $\mu\text{g}/\text{mL}$ IAN. The strain was grown for 72 hours in DF minimal media. The culture supernatant was collected, and IAA/IAM was quantified by HPLC. Each value represents the mean of three replicates. Standard error bars are shown

4.3.3 Evidence of the IPyA Pathway

LC-MS-MS analyses of culture extracts from wild-type and mutant UW4 strains was undertaken to identify IAA-related metabolites. The metabolite profiles were the same for wild-type and mutant strains. As expected, IAA and the indole intermediates IAN and IAM were detected. However, this analysis also revealed the presence of compounds indole lactic acid (ILA) and indole-2-ethanol (IEt/TOL), indole-aldehyde (IAld) and indole-pyruvic acid (IPyA), all of which which are intermediates associated with the IPyA pathway (Fig. 27). ILA is a common product of IPyA reduction and IEt is a common product of IAAlde reduction. Indole aldehyde (IAld) is produced non-enzymatically from IPyA.

Figure 27. LC-MS-MS Chromatogram of IPyA pathway metabolites from wild-type UW4

Liquid Chromatography–Electrospray Ionization–Tandem Mass Spectrometry was used to identify indole metabolites in bacterial cell cultures. Metabolites were identified by mass/charge ratio (m/z) values and the retention time (RT) of standard compounds. The bacterial cultures were grown in DF minimal media for 72 hours at 30°, with Trp (500 $\mu\text{g}/\text{mL}$) supplementation. The culture extract was prepared as described in section 4.2.5. The following IPya pathway metabolites were detected: ILA ($m/z=206.081$, RT=8.29 min), IEt (TOL) ($m/z=162.091$, RT=8.77 min), IAld ($m/z=146.060$, RT=8.45 min), IPyA ($m/z=204.065$, RT=7.44 min).



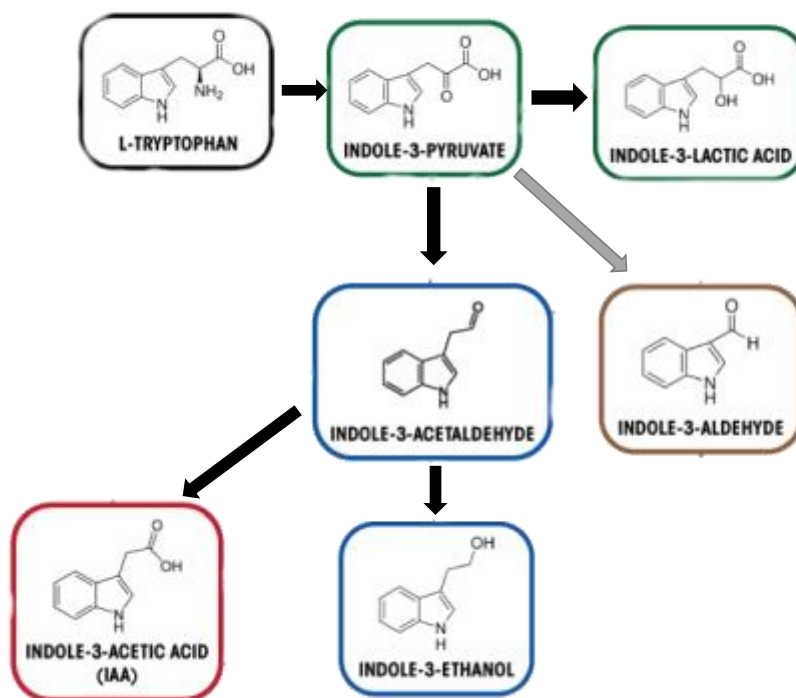


Figure 28. Putative IPyA biosynthesis pathways in *Pseudomonas* sp. UW4

Black arrows represent reactions mediated by enzymes and grey arrows represent non-enzymatic reactions.

4.3.4 The IPyA pathway

In the first step of the IPyA pathway, a transaminase transfers the amino group from tryptophan to α -ketoglutarate forming indole-3-pyruvate and glutamate. Alternatively, IPyA can be produced by oxidative deamination of L-Trp by an L-amino acid oxidase (LAAO) (355). Indolepyruvate decarboxylase (EC 4.1.1.74) then catalyzes the non-oxidative decarboxylation of IPyA to IAAlc, the

rate-limiting step. Finally, the oxidation of IAAld forms IAA by an aldehyde oxidase (Fig. 28) (45). Indolepyruvate decarboxylase and other bacterial α -keto acid decarboxylases are known to have broad substrate specificity. For example, the phenylpyruvate decarboxylase from *Azospirillum brasilense* catalyzes the decarboxylation of both phenyl- and indolepyruvic acid (356). The indolepyruvate decarboxylase homolog KdcA from *Lactococcus lactis* catabolizes α -keto acids derived from aromatic and branched-chain amino acids (357). *Mycobacterium tuberculosis* produces an α -keto acid decarboxylase with similar activities (358). In *Enterobacter cloacae* indolepyruvate decarboxylase can catalyze the decarboxylation of indolepyruvate, pyruvate, benzylformate and seven benzylformic acid analogs (359). The *Enterobacter cloacae* UW5 indolepyruvate decarboxylase acts on tryptophan, tyrosine and phenylalanine (131)(360).

The IPyA pathway may be a pathway for the degradation of tryptophan, and possibly other aromatic amino acids, and may function to supply nitrogen for assimilation. Catabolism of Trp consumes α -ketoglutarate in the transaminase reaction and a decrease in cellular α -ketoglutarate indicates that nitrogen is abundant (361)(362). In fact, IAA levels produced by *A. brasilense* were found to be influenced by the bacterial nitrogen source (214)(211). Moreover, while IPyA is well known as the product of the first step in the IPyA-pathway of IAA biosynthesis, many soil bacteria also use it to produce secondary metabolites such as indolocarbazoles (e.g. staurosporine, rebeccamycin) and indolyquinones (e.g. terrequinone A) (363). The roles of these molecules for their producing organisms are relatively unknown, but they have been suggested to be involved in cell communication and defense (364).

4.3.5 Mining Genes involved in the IPyA Pathway

Since LC-MS-MS analyses of supernatant from strain UW4 grown in Trp-supplemented cultures revealed indole intermediates belonging to the IPyA pathway, efforts were focused on identifying candidate genes encoding enzymes needed to mediate this pathway. However, considering the well-known promiscuous nature of the enzymes involved in this pathway, the genome search was broad. First, the UW4 genome was screened for putative genes based on their functional annotation in the NCBI database; any genes annotated as aminotransferase, α -keto acid/pyruvate decarboxylase and aldehyde oxidase/dehydrogenase were identified. The gene sequences were then screened against genes encoding characterized IPyA pathway enzymes from other bacteria, to determine whether there were any significant sequence similarities (Table 12).

Table 12. Potential UW4 Genes involved in the IPyA Pathway

Organism	Characterized Enzyme	Reaction	Potential Homolog in UW4	% Gene Sequence Similarity to UW4 homolog
<i>Azospirillum brasilense</i> Sp7	Aromatic amino acid transferase (HisC)	oxidative deamination of L-Trp to IPyA	histidinol-phosphate aminotransferase WP_015093981.1	35
			WP_015093507.1	30
			WP_015094384.1	26
<i>Azospirillum brasilense</i> Sp245	aminotransferase		alanine transaminase WP_007974487.1	56
<i>Rhizobium tropici</i> CIAT 899	histidinol-phosphate aminotransferase		histidinol-phosphate transaminase WP_015093507.1	32
			WP_015093981.1	30
			WP_015094384.1	26

Organism	Characterized Enzyme	Reaction	Potential Homolog in UW4	% Gene Sequence Similarity to UW4 homolog
<i>Azospirillum brasilense</i> Yu62	aminotransferases (ArB)		aminotransferase WP_015093046.1	29
	4-aminobutyrate aminotransferase (AtrC)			37
<i>Enterobacter cloacea</i> UW5	indole-3-pyruvate decarboxylase	decarboxylation of indole pyruvate to IAAld	acetolactate synthase WP_015096847.1	23
<i>Mycobacterium tuberculosis</i>		Decarboxylation of indolepyruvate α -ketoisocaproate, α -keto acid derivatives of phenylalanine, valine and isoleucine		22
<i>Pantoea agglomerans</i>		decarboxylation of indolepyruvate to IAAld		26
<i>Paenibacillus polymyxa</i> E681				47
<i>Lactococcus lactis</i>	α -keto acid decarboxylase;	decarboxylation of the α -keto acids derived from leucine, isoleucine, valine, phenylalanine and tryptophan to produce aldehydes	22	
<i>Zymomonas mobilis</i> CP4	pyruvate decarboxylase	decarboxylation of pyruvate	24	
<i>Azospirillum lipoferum</i>	indole-3-pyruvic acid decarboxylase	non-oxidative decarboxylation of IPyA to IAAld	hypothetical protein in the thiamine pyrophosphate	28

Organism	Characterized Enzyme	Reaction	Potential Homolog in UW4	% Gene Sequence Similarity to UW4 homolog
<i>Azospirillum brasilense</i> Sp245			(TPP) enzyme family WP_015095252.1	27
<i>Azospirillum brasilense</i> Yu62	aldehyde dehydrogenase	oxidation of IAAlD to IAA	NAD-dependent aldehyde dehydrogenases WP_015096645.1	66
			WP_015095250.1	66
			WP_015095239.1	66
			WP_015095520.1	67
			WP_015095580.1	67
			WP_015095428.1	75
			WP_015095079.1	76
<i>Bacillus velezensis</i> SQR9			WP_015096991.1	76
			WP_015094433	47
			WP_015095239.1	46
			WP_015097153.1	44
			WP_015095580.1	44
			WP_083884581.1	44
			WP_015095520.1	44

Aminotransferases are members of a large superfamily and they do not exhibit obvious sequence similarities. These enzymes have a diverse functional roles with many different substrate specializations (365). Unfortunately, there are few aminotransferase proteins whose functions have been experimentally validated with respect to their role in IAA biosynthesis. A histidinol-phosphate transaminase is suggested to catalyze Trp transamination to produce IPyA in *Rhizobium tropici* CIAT 899, *Sinorhizobium fredii* NGR234 and *Azospirillum brasilense* Sp7 (355)(148)(129). Three putative histidinol-phosphate transaminase genes are present in the UW4 genome showing 26-32% sequence identity with the *Rhizobium* genes and 26-35% identity with the *Azospirillum* gene (Table 12). Another

characterized aminotransferase from *Azospirillum brasilense* Sp245 (132) shares 56% sequence identity with a UW4 gene annotated as alanine transaminase (Table 12). There are also twelve genes encoding aspartate aminotransferase family proteins, two genes encoding aspartate/tyrosine/aromatic aminotransferases, two genes annotated as general aminotransferases, twenty genes for PLP-dependent aminotransferases, 2 genes for branched-chain amino acid aminotransferases and one gene for adenosylmethionine-8-amino-7-oxononanoate aminotransferase in UW4's genome. One of the general UW4 aminotransferases (WP_015093046.1) has 29% sequence identity with an aminotransferase and 37% identity with a 4-aminobutyrate aminotransferase from *A. brasilense* Yu62 (Table 12) (137). Both of these Yu62 enzymes have been confirmed to be involved in IAA biosynthesis via transposon mutagenesis (137). In total, there are forty-three potential genes encoding an aminotransferase that could facilitate the conversion of Trp into IPyA in the genome of UW4 (Table A4, Appendix A).

Alternatively, IPyA can be produced by an L-amino acid oxidase (LAAO) that catalyzes the oxidative deamination of L-amino acids such as Trp to their respective α -keto acids such as IPyA, generating NH_4^+ and hydrogen peroxide (366)(367). An FAD-containing oxidase from *Lechevalieria aerocolonigenes* was discovered as a key enzyme in the biosynthesis of the antibiotic rebeccamycin. Although 7Cl-Trp is a preferred substrate, it has been shown that this enzyme can also efficiently oxidize Trp to the imine form of IPyA, which readily undergoes non-enzymatic hydrolysis to generate IPyA (366). A search for homologs of this enzyme in UW4's genome, resulted in a hit annotated as an NAD(P)/FAD-dependent oxidoreductase (WP_015097081) sharing 41% sequence identity and 53% query coverage. UW4 also harbors two genes (*iaaM* and *aux*) that code for

predicted FAD-containing amine oxidases showing 26% and 38% identity to the validated L-amino acid oxidase (LAAO) of *Rhodococcus opacus* (AAL14831)(368). Characterization of the enzymes encoded by the *iaaM* and *aux* genes is discussed in Chapter 5.

The next step in the IPyA pathway is the decarboxylation of IPyA into IAAld by indolepyruvate decarboxylase. Homologues of indolepyruvate decarboxylase (IPDC) are present in many diverse groups of bacteria (Patten, 2013). Again, the function of this gene in IAA biosynthesis has been confirmed by mutagenesis in only a few bacteria including *E. cloacae*, *A. brasilense*, and *P. agglomerans* (133)(132)(142)(87)(131). A phylogenetic analysis done by Patten et al., (2013) revealed that the α -keto acid decarboxylase from *Lactococcus* and the phenylpyruvate decarboxylase from *Azospirillum* spp. are closely related to indolepyruvate decarboxylases with overlap in enzymatic activity; they catalyze the decarboxylation of α -keto acids derived from branched-chain and aromatic amino acids. Moreover, known acetolactate synthases are also distantly related homologues of the α -keto acid decarboxylase family (43). When the protein sequences of the experimentally validated indolepyruvate decarboxylase genes were used to search for homologs in the UW4 genome, we found no hits with any significant sequence identity (>30%); suggesting that either IPDC homologs don't exist in UW4 or an alternative enzyme is performing this function. The indolepyruvate decarboxylase from *Enterobacter*, *Mycobacterium* and *Pantoea* were 22-26% identical to an acetolactate synthase from UW4 (Table 12). This acetolactate synthase gene also shared 22% sequence identity with the α -keto acid decarboxylase from *Lactococcus* and 24% sequence identity with the pyruvate decarboxylase from *Zymomonas* (Table 12). Phi et al. (2008) identified an IPDC homolog in the genome of *Paenibacillus polymyxa* E681 that was capable of producing IAAld from

indolepyruvate. Interestingly, this protein lacks the conserved amino acid residues for binding indolepyruvate that are invariant among known indolepyruvate decarboxylases (369)(370). Rather, this protein is more similar to the large subunit of acetolactate synthase that catalyzes the first step in the synthesis of branched-chain amino acids (leucine, isoleucine, and valine) from two molecules of pyruvate (370). Therefore, it is possible that the UW4 acetolactate synthase performs a similar reaction; although the primary function may not be the production of IAA, it may incidentally decarboxylate indolepyruvate into IAAlD. The known indole-3-pyruvic acid decarboxylases that mediate the IPyA pathway in *Azospirillum* spp. shared 27-28% sequence identity with a UW4 protein annotated as “hypothetical” and categorized as a thiamine pyrophosphate (TPP) enzyme family member (Table 12). Given that the thiamine diphosphate binding fold domain is also found in IPDC, pyruvate dehydrogenases and α -keto acid decarboxylases (355), this hypothetical UW4 enzyme is also a good IPDC-candidate. In *Bacillus velezensis* SQR9, inactivation of a gene encoding a 3-polyprenyl-4-hydroxybenzoate decarboxylase (*ycfC*) led to a 55% reduction in IAA production (371). This protein shares 30% sequence identity with a 3-octaprenyl-4-hydroxybenzoate carboxylase (WP_015097311.1) from UW4 (Table 12).

The final step in IAA biosynthesis through the IPyA pathway is IAAlD oxidation to IAA, catalyzed by the enzyme aldehyde dehydrogenase/oxidase. With respect to IAA biosynthesis, almost nothing is known of the bacterial oxidases that catalyze this reaction (43). Aldehyde dehydrogenases are widely distributed in bacterial genomes and are involved in many processes. The involvement of an aldehyde hydrogenase (*aldA*) in IAA biosynthesis in *A. brasilense* Yu62 has been shown by Xie et al. 2005 (137). The *aldA* nucleotide sequence was used as a query against the genome of UW4, revealing

eight putative NAD-dependent aldehyde dehydrogenases that shared 66-76% sequence identity to *aldA* (Table 12). In *Bacillus velezensis* SQR9 inactivation of a gene encoding an indole 3-acetaldehyde dehydrogenase (*dbaS*) decreased IAA production by 77% (371), and this protein showed 44-47% sequence identity with six different putative aldehyde dehydrogenases in UW4 (Table 12).

4.4 Conclusion

This study aimed to assess the function of IAA produced by strain UW4, in the plant-bacterial interaction, and further to determine the contribution of each IAA-gene to the overall production of IAA in this strain. A directed approach was taken, whereby individual IAA-biosynthesis genes were targeted for disruption. The seven genes (*iaaM*, *aux*, *ami*, *nit*, *nthA*, *nthB* and *phe*) encoding enzymes that each catalyze a step in the IAN-IAM pathway for IAA synthesis, were isolated and a portion of each gene was deleted in order to obtain an IAA⁻ mutant with reduced ability to produce IAA. However, the results obtained showed that the mutants did not produce less IAA than the wild-type strain. This prompted an LC-MS-MS analysis of supernatants from both wild-type and mutant bacterial cultures grown in the presence of exogenous Trp, in order to profile the types of IAA-intermediate compounds present. Unexpectedly, we found evidence of the IAA intermediates IPyA, IAAlD, ILA, and IET in the cultures, suggesting the existence of a third IAA biosynthesis pathway-the IPyA pathway. Moreover, it appears that this pathway plays a central role in IAA production by UW4, as mutations in genes of the IAM/IAN pathways did not result in a decrease in IAA. To search for IPyA pathway candidate genes in the UW4 genome, sequences of experimentally verified enzymes were used as queries. An initial genomic survey resulted in 43 potential genes coding for an aminotransferase that could convert Trp to IPyA, from which 9 candidate genes shared highest sequence identity to other characterized aminotransferases (26-56%). From the characterized

decarboxylases that have been explicitly shown to convert IPyA to IAAld, the closest homologue in UW4 was an acetolactate synthase (56% sequence identity). Twelve putative aldehyde dehydrogenases were identified in the genome of UW4, sharing sequence identity with characterized enzymes from *Azospirillum brasilense* Yu62 and *Bacillus velezensis* SQR9. All together, these findings suggest the existence of genes constituting a potential complete IPyA pathway of IAA biosynthesis in strain UW4.

Chapter 5

Deciphering the Role of IaaM and Aux Proteins in *Pseudomonas* sp. UW4

5.1 Introduction

Several decades ago, it was discovered that some bacterial phytopathogens cause hyperplastic symptoms leading to tumor-like outgrowths in plants. The formation of these growths is often a response to the production of high local concentrations of IAA by the pathogen (317). Studies have established that IAA biosynthesis in these phytopathogens, occurs predominantly via the indole acetamide (IAM) pathway (254)(85). The IAM metabolite has also been detected in plant-growth-promoting bacteria (PGPB) such as *Bradyrhizobium japonicum* (227)(372) and *Pseudomonas chloraphis* (217), however this pathway has not been characterized in these strains.

The plant-growth-promoting bacterium *Pseudomonas* sp. UW4 is known to utilize the indole acetonitrile (IAN) and the indole acetamide (IAM) pathway. This is based on the detection of both the IAN and IAM metabolites in Trp-fed cultures, as well as on the biochemical characterization of enzymes involved in these pathways (258)(Refer to Chapter 2). The latter pathway is proposed to be mediated by a tryptophan monooxygenase (TMO) which converts the substrate Trp into IAM. Two genes encoding putative tryptophan monooxygenases (*iaaM* and *aux*) were identified in the genome of strain UW4. Once the IAM intermediate is produced, it is converted into the final product, IAA, by an amidase. Although the IAM metabolite has been detected in UW4 cultures, it can be produced by two different routes. The traditional IAM pathway utilizes a tryptophan monooxygenase (TMO),

and has until now only been characterized in phytopathogens. The alternative route is through a merging of the IAN-IAM pathways whereby IAM is formed from the IAN intermediate via the enzymes nitrilase (*nit*) and nitrile hydratase (*nthAB*). These IAN→IAM enzymes have been biochemically characterized in strain UW4 (258). Therefore, the focus of this chapter is to determine whether the traditional IAM pathway (Trp→IAM→IAA by the consecutive action of TMO and Ami) is also functional in this strain (Fig. 29).

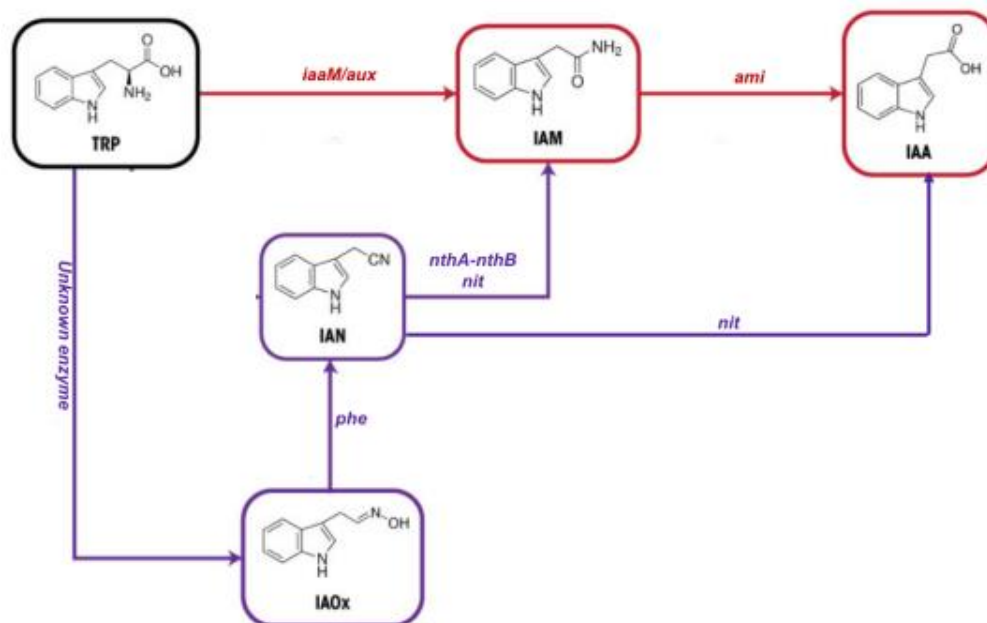


Figure 29. Putative IAN-IAM Biosynthesis Pathways in UW4

iaaM, *aux*= tryptophan monoxygenases, *ami*= IAM-hydrolase/amidase, *nit*= nitrilase, *nthA-nthB*= nitrile hydratase, *phe*= indole acetaldoxime dehydratase

The traditional IAM pathway involves the conversion of tryptophan to IAA in two steps. In the first step, the enzyme tryptophan monooxygenase (TMO) catalyzes the oxidative decarboxylation of L-Trp to indole acetamide (IAM). IAM is subsequently deaminated oxidatively by IAM-hydrolase/amidase yielding IAA and ammonia (Fig. 29). The IAM-hydrolase (Ami) has been functionally characterized in UW4 (refer to Chapter 2), however a TMO has not. This chapter describes the characterization of two putative TMO enzymes from strain UW4. These two enzymes were annotated as TMOs based on sequence similarity to previously characterized TMOs from other bacteria. The first enzyme is referred to as IaaM (accession no. WP_015097081) and the second as Aux (accession no. WP_015096783).

Tryptophan monooxygenase is a flavoprotein that catalyzes the oxidative decarboxylation of the oxidized amine to form an amide in two half-reactions (373). The first is a reductive half-reaction in which a hydride is transferred from the substrate to the flavin cofactor (FAD). This is identical to the reaction of L-amino acid oxidases (LAAOs) and similar to the general reaction of flavoprotein amine oxidases (373). The second is an oxidative half-reaction in which the flavin is reoxidized and the amide product is formed (Fig. 30) (373)(374). The closest paralog to TMO is lysine monooxygenase (LMO), which catalyzes the oxidative decarboxylation of lysine. Other closely related members include phenylalanine oxidase (PAO) and arginine monooxygenase. TMO enzymes share greatest structural similarity with L-amino acid oxidases (LAAOs) and both enzymes can oxidize L-amino acids, despite the low sequence identity between them (~20%)(375)(376). LAAOs are dimeric flavoproteins that catalyze the oxidative deamination of L-amino acids to the corresponding α -keto acids with the release of NH_4^+ and H_2O_2 (377).

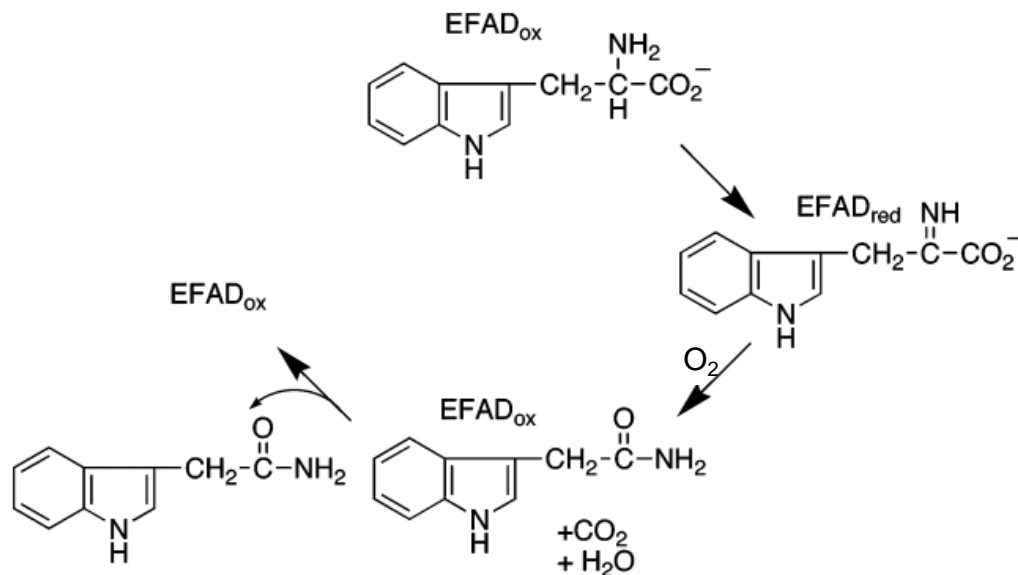


Figure 30. Conversion of Trp into IAM by a TMO Enzyme

Binding of the amino acid Trp to the TMO enzyme is followed by reduction of the flavin (EFAD_{red}) and oxidation of Trp. Subsequently, oxidative decarboxylation of the imino acid to form IAM occurs simultaneously with flavin oxidation (EFAD_{ox}). Figure adapted from Sobrado and Fitzpatrick (2003).

5.2 Methods

5.2.1 Bacterial Strains and Plasmids

E. coli DH5 α (Invitrogen/Life TechnologiesTM) was used as an initial cloning host and *E. coli*

BL21(DE3) (Novagen/Merck, KGaA) was used as the host for recombinant protein expression.

This expression host is designed for expression from pET vectors and contains an IPTG (isopropyl-D-thiogalactopyranoside)-inducible T7 RNA polymerase (Novagen/Merck, KGaA). *Pseudomonas* sp.

UW4 (162) was grown and maintained aerobically at 30°C in tryptic soy broth (Becton-Dickinson™) supplemented with 100 µg/mL of ampicillin. All *E. coli* strains were maintained aerobically at 37°C in Luria-Bertani broth (Fischer Bioreagents). When appropriate, 50 µg/mL of kanamycin to select for the presence of plasmid and 0.1mM IPTG to induce protein expression were added. The plasmid pET30b+ (Novagen®) was used for the expression of IaaM and Aux recombinant proteins. The plasmid constructs generated in the present study are described in detail in Table 13.

Table 13. Plasmids, strains and primers used in this study

Plasmid, Strain or Primer	Sequence (5'-3') or Gene Accession No.	Description
Plasmids		
pET-Iaam	PputUW4_04962	pET30b(+) vector with the <i>iaam</i> gene from UW4 inserted between the NdeI and XhoI sites
pET-Aux	PputUW4_04530	pET30b(+) vector with the <i>iaam</i> gene from UW4 inserted between the NdeI and XhoI sites
Strains		
<i>Pseudomonas</i> sp. UW4	CP003880	Wild-type <i>Pseudomonas</i> sp. UW4 plant-growth-promoting bacterium
<i>E. coli</i> DH5α™		F- Φ80 <i>lacZ</i> ΔM15 Δ(<i>lacZYA-argF</i>)U169 <i>recA1 endA1 hsdR17</i> (rK-, mK+) <i>phoA supE44 λ- thi-1 gyrA96 relA1</i>
<i>E. coli</i> BL21 (DE3)		<i>fhuA2 [lon] ompT gal (λ DE3) [dcm] ΔhsdS λ DE3 = λ sBamHIo ΔEcoRI-B int::(lacI::PlacUV5::T7 gene1) i21 Δnin5</i>
<i>E. coli</i> BL21::pET-Iaam		<i>E. coli</i> BL21 (DE3) carrying pET-Iaam vector
<i>E. coli</i> BL21::pET-Aux		<i>E. coli</i> BL21 (DE3) carrying pET-Aux vector
Primers		
iaaM-F	TAATCATATGACTAT	<i>iaam</i> (NdeI)-fwd
iaaM-R	ATTACTCGAGGGTTTT	<i>iaam</i> (XhoI)-rev
Aux-F	TAATCATATGAACAAG	<i>aux</i> (NdeI)-fwd
Aux-R	ATTACTCGAGCTCGGG	<i>aux</i> -(XhoI)-rev

F= forward primer, R= reverse primer

5.2.2 DNA Extraction and Expression Plasmid Construction

Genomic DNA was isolated using the Wizard Genomic DNA purification kit (Promega, catalog no. A1120). The primer sequences used to amplify *iaaM* and *aux* genes are also given in Table 13. Both the forward and the reverse primer sequences were based on the fully sequenced UW4 genome (GenBank accession no. CP003880). The amplified fragments were subcloned between the NdeI and XhoI sites of pET30b+, resulting in the pET-Iaam and pET-Aux constructs. Hot-start PCR was performed with KOD Hot Start DNA polymerase (Novagen, Mississauga, Ontario, Canada). The reaction mixture (50 µl) was set up on ice and included 5 µl of KOD hot start buffer, 3 µl of 25 mM MgSO₄ (final concentration, 1.5 mM), 5 µl of 2 M deoxynucleoside triphosphates (final concentration, 0.2 mM), 1.5 µl of forward and reverse primer (final concentration, 0.3 mM), 100 ng of template genomic DNA, 1 µl of KOD hot start polymerase and PCR-grade water up to a final volume of 50 µl. The PCR was performed in an Eppendorf MasterCycler gradient machine using the following amplification conditions for *iaaM*: 95°C for 2 min, 95°C for 20 s, 71°C for 10 s, 70°C for 15 s, 70°C for 5 min, and ending at 4°C. For *aux*, the following amplification conditions were used: 95°C for 2 min, 95°C for 20 s, 67°C for 10 s, 70°C for 23 s, 70°C for 5 min, and ending at 4°C.

5.2.3 Expression and Purification of Recombinant IaaM and Aux Proteins in *E. coli*

Following their construction, the expression plasmids were initially transformed into *E. coli* DH5α to maintain recombinant plasmids without any basal protein expression. For over-expression of the recombinant proteins, the plasmids were transformed into *E. coli* BL21(DE3) using the calcium chloride method described by Sambrook and Russell (2001)(304). Cells transformed with pET-IaaM

or pET-Aux were grown in 500 ml of Luria-Bertani (LB) medium containing kanamycin (50 µg/ml) at 37°C with shaking for aeration, until the optical density (OD₆₀₀) reached ~0.5. At this point, the cultures were induced with 0.1 mM IPTG and incubated at 25°C overnight. The cells were collected by centrifugation and resuspended in 100 mL of buffer containing: 0.1 M Tris, 12 mM β-mercaptoethanol, 50 µM IAM, 1 mM EDTA, 1 mM phenylmethylsulfonyl fluoride, 100 µg/mL lysozyme (pH 8.3). The cells were lysed by sonication, 30 times for 30s each time with 10s pauses between each round, keeping the lysate on ice at all times during sonication. The clarified lysate was collected by centrifugation. The recombinant proteins, which have a C-terminal His₆ tag, were purified under native conditions using a His GraviTrap prepacked, single-use gravity-flow column containing precharged Ni Sepharose 6 Fast Flow. The protocol was followed according to the manufacturer's instructions (GE Healthcare, United Kingdom). The purified protein samples were analyzed by SDS-PAGE on a 10% gel (Fig. A6, Appendix A). The eluted fractions were analyzed for protein and flavin content, based on their absorbance values at 280 and 466 nm, respectively.

5.2.4 Removal of bound Indoleacetamide (IAM) from IaaM and Aux

Emanuele et al., (1995) showed that purified TMO from *Pseudomonas savastanoi* contains bound IAM, presumably generated by the enzyme from tryptophan during cell growth (374). The IAM must be removed prior to enzyme assays. Dialysis of the purified enzyme against a buffer containing 20% methanol removes ~95% of the bound IAM, and helps to increase the specific activity of the TMO enzyme (374). The purified IaaM and Aux proteins were dialyzed against 1 liter of 20% methanol, 100 mM Tris-HCl, 1 mM EDTA, 0.5 mM dithiothreitol, 10% glycerol, pH 8.3, dialysis buffer and this was

changed two times over 20 h. Subsequently, the sample was dialyzed against 1 liter of 100 mM Tris-HCl, 1 mM EDTA, 0.5 mM dithiothreitol, 10% glycerol, pH 8.3 for 3 h followed by two 1 liter changes of 50 mM Tris-HCl, 1 mM EDTA, 0.5 mM dithiothreitol, pH 8.3, over 6 h (374).

5.2.5 Protein Determination and SDS-PAGE

Protein concentrations were determined using the Quick Start™ Bradford Protein Assay (BioRad) with bovine serum albumin (BSA) as the reference standard (263, 307). The protein content of chromatography column eluates was monitored at 280 nm. The purity and subunit molecular weight of the proteins were estimated by SDS- PAGE on a 10% gel (Fig A6, Appendix A).

5.2.6 UV-Absorption Spectrum

Flavoproteins have a characteristic UV-absorption spectrum with absorption maxima at 388 and 466 nm wavelengths (374). One milliliter of purified IaaM and Aux enzyme was loaded into a 1.0 ml quartz cuvette and the absorption spectrum was obtained using a simple UV scan method by a Genesys 10S UV-Vis spectrophotometer (Thermo Scientific). To obtain a typical UV spectrum for free FAD, 1 mL of 0.1 mM FAD stock solution was used.

5.2.7 TMO Enzyme Assay

The purified recombinant proteins (Iaam and Aux) were tested for the ability to convert L-Trp into indole acetamide (IAM). Standard enzyme assays were carried out in 50 mM Tris buffer (air saturated), 1 mM EDTA, 0.5 mM dithiothreitol, 1 mM Trp (pH 8.3) at 25 ° C. The reactions were initiated by adding ~50 µg of purified enzyme (IaaM or Aux). Pure oxygen was continuously

injected into the reaction mixture using a manifold. Samples were analyzed by high pressure liquid chromatography (HPLC).

5.2.8 High Performance Liquid Chromatography (HPLC) Analysis

HPLC analysis was performed using a Waters Alliance 2695 HPLC separation system (Mississauga, Ontario, Canada), which includes a Waters 2996 photodiode array detector. The system was connected to a PC with Empower 2 software (Waters) for data collection and processing. A Sunfire C18 column (50 x 4.6 mm [inner diameter], 2.5 μm pore; Waters, Ireland) was connected with a Security Guard C18 guard column (4 x 3.0 mm [inner diameter]; Phenomenex, Torrance, CA). Gradient HPLC was performed at room temperature using a mobile phase containing water-acetic acid (1% [vol/vol]) (A) and acetonitrile-acetic acid (1% [vol/vol]) (B). Starting with 80% A, the gradient began at 2 min and reached 60% A at 15 min. The flow rate was 1 ml/min. A 100 μl sample injection volume was used, and the eluent was monitored at 280 nm.

5.2.9 Liquid Chromatography-Tandem Mass Spectrometry (LC-MS-MS)

Liquid Chromatography–Electrospray Ionization–Tandem Mass Spectrometry was used to identify IAA and respective indole intermediates in bacterial cell cultures. The protocol followed that described by Lin et al., 2015. Briefly, the bacterial cultures were grown in tryptic soy broth (TSB) for 24 hours at 37°C, with and without Trp (500 $\mu\text{g}/\text{mL}$) supplementation. The cells were collected by centrifugation at 10,000 x g for 10 min and the pellet was discarded. The supernatants were processed by adding 400 μl of cold methanol to 50 μl of culture supernatant. The mixture was vortexed and incubated at $\sim 20^\circ\text{C}$ for 30 min for complete protein precipitation. Samples were

centrifuged at 10,000 x g and 4°C for 10 min. The supernatant was dried in a vacuum evaporator (Savant Speed Vac Plus SC110A). The residue was re-dissolved in 100 µL of 0.1% formic acid in water and centrifuged at 10,000 x g and 4°C for 10 min. The final supernatant was transferred to an autosampler vial for LC–MS/MS analysis. The analytical standards, IAA and IAM were purchased from Sigma–Aldrich (St. Louis, MO, USA) and stock solutions of each (10 mM) were prepared in methanol.

A Dionex Ultimate 3000 UHPLC system (Thermo Fisher Scientific, USA) coupled with a Q-Exactive Orbitrap mass spectrometer (Thermo Fisher Scientific, USA), equipped with an electrospray ion source, and operated in the positive ion mode was used. A superficially porous particle column (Zorbax 300A, 300Extend-C18, 2.1 mm x 100 mm, 3.5 µm pore) (Agilent Technologies Inc., Santa Clara, CA, USA) with mobile phases A (0.1% formic acid in water) and B (0.1% formic acid in methanol) was used. The column temperature was set at 25°C.

Chromatographic separation was achieved by gradient elution at a flow rate of 0.32 mL/min. The gradient program was as follows: 0–2.5 min, 100% A; 2.5–5.0 min from 0% to 25% B; 5.0–7.5 min from 25% to 40% B; 7.5 - 10 min from 40% to 60% B; 10–12.5 min 60%–80 B; 12.5–15 min 80–100% B, 15–18 min column re-equilibration. The total run time was 18.0 min, and an injection volume of 10 µL was used. The ionization parameter and multiple reaction monitoring (MRM) transitions for the target analytes were obtained by direct injection of their individual standard solutions with a concentration of 1 mM. The positive ionization mode was used at a spray voltage of 3000 V. Nitrogen was used as the sheath and auxiliary gas at optimal values of 35 and 5 units

(arbitrary units). The heated capillary temperature was 300°C. The argon collision gas pressure was set to 1.0 mTorr. The scan time of each MRM transition was set to 3.05 ms.

5.2.10 Multiple Sequence Alignment & Phylogenetic Analyses

A global multiple sequence alignment was constructed for IaaM, Aux and the following functionally characterized amine oxidase members: five TMOs (*A. tumefaciens*, *P. syringae* pv. *savastanoi*, *P. agglomerans*, *A. rhizogenes* and *D. dadantii*), two LMOs (*P. putida* KT2440 and *Pseudomonas* sp. AIU813) and PAO (*Pseudomonas* sp. P501) using MEGA 7.0 software (264). Each alignment was manually refined, and the regions that could not be aligned reliably were removed. The evolutionary history of IaaM and Aux proteins was inferred by using the Maximum Likelihood method based on the JTT matrix-based model (286). Initial tree(s) for the heuristic search were obtained automatically by applying Neighbor-Join and BioNJ algorithms to a matrix of pairwise distances estimated using a JTT model, and then selecting the topology with superior log likelihood value. One thousand bootstrap replicates were performed to assess the statistical confidence for each clade of the tree. The tree is mid-point rooted; the root is placed at the mid-point of the longest distance between two taxa in a tree. Evolutionary analyses were conducted in MEGA7 (264).

5.3 Results and Discussion

5.3.1 Protein Classification

The IaaM and Aux proteins were implicated in IAA biosynthesis as putative tryptophan monooxygenases (TMOs) based on classification by NCBI's Conserved Domain Database (CDD), which annotates the location of evolutionarily conserved protein domain footprints, and infers

function from such footprints (378). Both IaaM and Aux have the NAD(P)-binding Rossmann-like domain and were classified as members of the flavin-containing amine oxidase superfamily (377). This classification is broad and can include members such as L-amino acid oxidases (LAAO), monoamine oxidases (MAO), tryptophan monooxygenase (TMO), lysine monooxygenase (LMO) and phenylalanine oxidase (PAO) (377).

A Protein BLAST search using IaaM or Aux as the query, results in a large number of related proteins that are annotated as tryptophan monooxygenase (TMO), monoamine oxidase (MAO), or amine oxidase. The vast majority of these proteins have not been functionally characterized. In fact, only five TMO's have been experimentally shown to convert Trp to IAM. These include the TMOs from the plant pathogens: *Agrobacterium tumefaciens* (48), *Pseudomonas syringae* pv. *savastanoi* (146), *Pantoea agglomerans* (49), *Agrobacterium rhizogenes* (271) and *Dickeya dadantii* (245).

5.3.2 UV Spectrum of IaaM and Aux

The spectroscopic properties of the FAD cofactor and its variants allows for reaction monitoring by use of UV absorption. The different isoforms of FAD (i.e., FAD vs. FADH) display distinct absorbance spectra, making for easy observation of changes in oxidation state (374). As IaaM and Aux are putative flavoproteins they should exhibit the characteristic flavoprotein spectrum.

Hutcheson and Kosuge (1985) first demonstrated the UV-absorption spectrum of the well-characterized *P. savastanoi* TMO with both the oxidized and reduced form of the bound FAD cofactor (379). When the bound FAD is in its oxidized form, the UV-spectrum gives two absorbance maxima at wavelengths of 466 and 380 nm (379). When wild-type TMO is mixed with

tryptophan in the absence of oxygen, the absorbance between 350 and 520 nm decreases and that above 520 nm increases. These changes in absorbance occur very rapidly (within milliseconds) and are followed by a slow decrease in absorbance at all wavelengths until the fully reduced enzyme spectrum is formed (380).

When the FAD is in its free form, the absorbance peak at 466 nm shifts to 450 nm (381)(382). Free FAD (0.1 mM) was used to obtain the typical spectrum of the oxidized form with absorbance maxima at 450 and 380 nm wavelengths (Fig. 31). The UV-spectrum of the purified IaaM protein also showed the typical UV-absorption spectrum of a flavoprotein, having absorbance maxima at 466 and 380 nm wavelengths (Fig. 32). Based on the oxidation state, flavins display specific colors when in aqueous solution; FAD (fully oxidized) is yellow and the fully reduced form (FADH₂) is colorless (382). Hutcheson and Kosuge (1985), describe their TMO preparation after isolation, as being yellow in colour, indicating that it contains an oxidized flavin chromophore (379). Our purified IaaM recombinant protein solution also displayed the characteristic yellow colour of an oxidized flavoprotein. Changes in absorbance were observed upon mixing IaaM with Trp (2.5 mM). The reaction was initiated by mixing crude cell lysate from *E. coli* cells over-expressing IaaM with the substrate L-Trp; the absorbance (466nm) was subsequently monitored at 10 second intervals over the course of 2 minutes (Fig. 33). The absorbance decreased over time, indicating that the enzyme-bound FAD was reduced in the reaction and further, that Trp is a substrate for this enzyme.

Purified Aux solution was colorless and the UV spectrum suggested that the bound FAD, if it is present, is in the reduced form (Fig. 32). Hutcheson and Kosuge (1984), report that addition of Trp

to TMO in the absence of oxygen, resulted in a reduction of FAD, and consequently a bleaching of the absorption spectrum (379). The absorption spectrum typical of bound FAD in the oxidized form, could be restored by reintroducing oxygen into the reaction mixture. Ralph et al (2006) report that for TMO, the rates of oxygen consumption at high and low substrate concentrations are independent of the oxygen concentration, consistent with a low K_{O_2} ($< 25 \mu\text{M}$) which allows for the determination of substrate turnover under ambient oxygen concentrations (373). Although Aux was purified and analyzed under atmospheric oxygen concentrations, perhaps the level of dissolved oxygen was not sufficient to oxidize FAD. Furthermore, there were no observed changes in absorbance from mixing crude cell lysate of *E. coli* over-expressing Aux with L-Trp (Fig. 33). The absorbance at 466 nm remained constant throughout the 2-minute monitoring period, suggesting that no reaction had taken place between Aux and Trp.

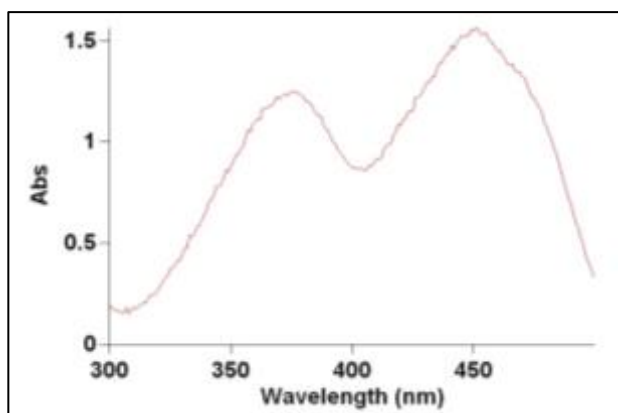


Figure 31. UV Spectrum of free FAD_{OX} in aqueous solution

Stock solution of 0.1 mM FAD dissolved in water under atmospheric conditions. The solution was a yellow colour. The absorption maximas occur at 380 and 450 nm.

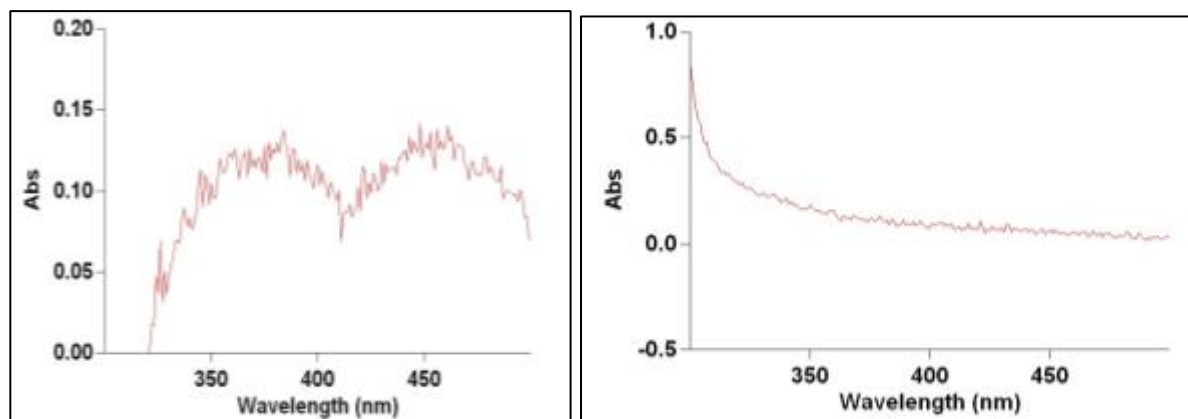


Figure 32. The UV-Absorption Spectrum of purified IaaM and Aux

(Left): purified IaaM in aqueous solution was a yellow colour. The absorption maximas occur at 380 and 466 nm, suggesting that FAD was in the oxidized form.

(Right): purified Aux in aqueous solution was colourless, and the absorption spectrum typical of bound FAD_{OX} was not observed, suggesting that the FAD, if it was present, was in the reduced form.

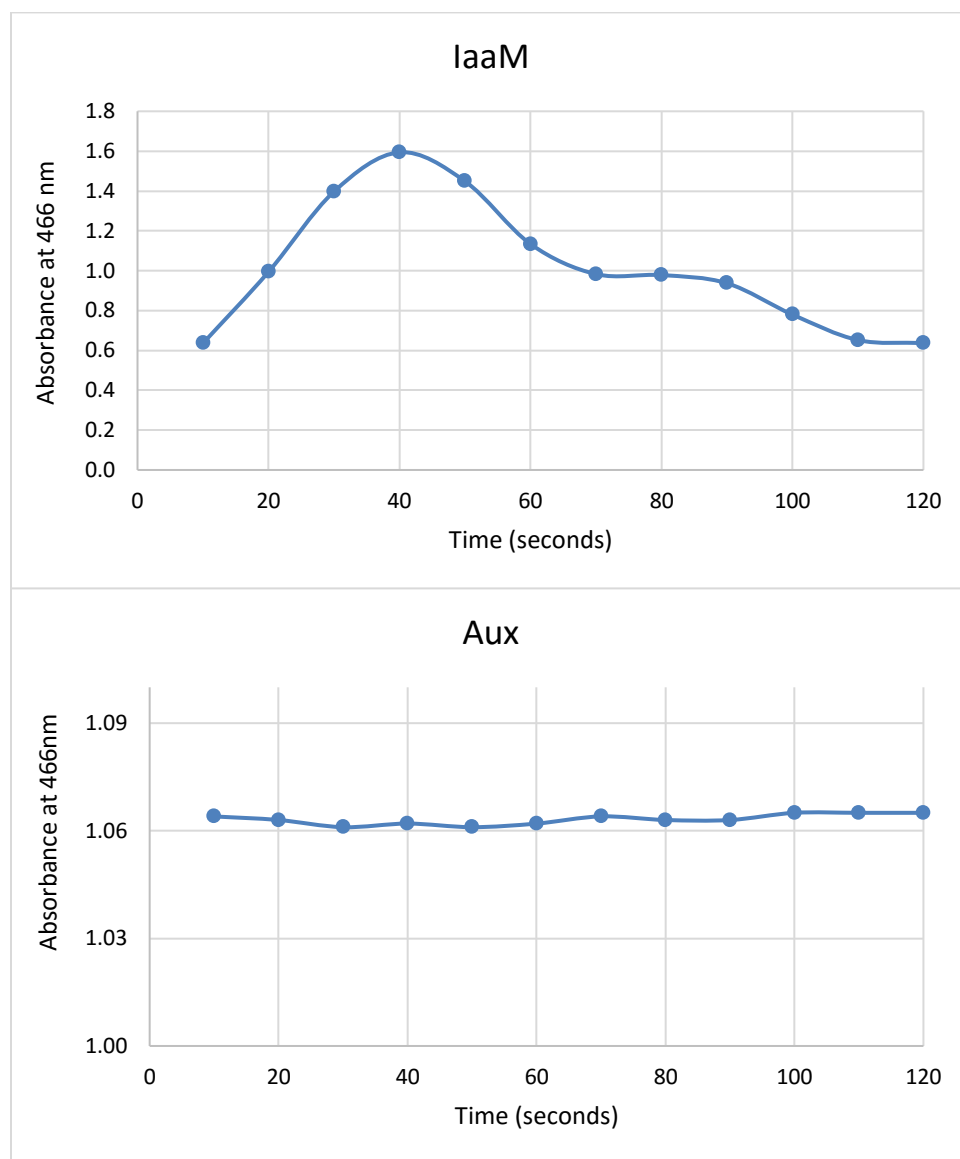


Figure 33. Changes in absorbance of IaaM and Aux in the presence of Trp and FAD

E. coli BL21:pET-IaaM/Aux were grown overnight with 0.1 mM IPTG to induce over-expression of IaaM and Aux, respectively. The crude cell lysates were mixed with 2.5 mM L-Trp and 0.1 mM FAD in Tris buffer pH 8.3, at 25°C, under atmospheric oxygen conditions. The reaction was monitored at 466 nm in real time at 10 second intervals for a duration of two minutes.

5.3.3 TMO Assay

The IaaM and Aux proteins were over-expressed in *E. coli*, purified, and assayed for TMO activity. However, the expected IAM reaction product was not detected by HPLC; therefore, TMO biochemical activity could not be determined. The inability to detect the IAM product does not necessarily mean that IaaM and Aux are not TMOs. It may be that the recombinant proteins are much less active than the proteins in their normal environment. It is possible that the C-terminal His-tag that is added to the recombinant proteins to facilitate purification, hinders the protein's ability to fold into its native conformation or interferes with its catalytic capacity. Moreover, *E. coli* may be a relatively unsuitable host for the heterologous production of these enzymes; in these experiments, most of the IaaM and Aux proteins were expressed in an insoluble form.

Early studies on the *P. savastanoi* TMO, were hindered by the low activity present in cell lysates and by the enzyme's instability (379). TMO activity could be partially stabilized in an alkaline enzyme buffer (pH 8.3) containing 50 μ M IAM. While the addition of IAM may stabilize the protein by preventing partial loss of the FAD cofactor, the enzyme activity is inhibited by both IAM and IAA in a feedback mechanism (379). The addition of high levels of exogenous tryptophan to the culture medium increases the sensitivity of TMO to feedback inhibition by IAM and IAA (379). The IAM must be removed from the enzyme prior to the enzyme assay to allow the Trp substrate to bind (374). Additionally, TMO loses activity when there is a decrease in FAD content; however, assays with the *P. savastanoi* TMO showed that addition of exogenous FAD to the purified enzyme had no effect on either enzyme stability or activity (374).

Since the UW4 IaaM and Aux proteins were expressed in *E. coli* BL21, it was necessary to determine whether this host could produce IAM or IAA natively, which could interfere with recombinant TMO activity. LC-MS-MS analysis of culture extracts from Trp-fed *E. coli* BL21 (untransformed and recombinant), revealed that both IAM and IAA are produced (Table 14, Fig. A7-A9, Appendix A). Therefore, if IaaM and Aux are indeed TMO's, their activity may be inhibited during over-expression in this host. For this reason, the purified enzymes were subjected to a dialysis procedure to remove any bound IAM prior to enzyme assays. Perhaps, the removal of IAM was not sufficient to allow TMO activity, or enzyme activity was lost during the dialysis procedure. For instance, Sobrado and Fitzpatrick (2003) report that in their study, removal of the IAM by dialysis against methanol, the same method used in our study, resulted in the TMO protein losing all activity (380). By using an alternative method in which the IAM-complexed enzyme was reduced several times with excess phenylalanine to displace the IAM, it was possible to obtain the active enzyme. However, this enzyme was unstable in the absence of IAM and had to be used immediately for enzyme assays (380).

Table 14. LC-MS-MS Analysis of *E. coli* BL21 Culture Extracts

Culture Extract	IAA	IAM
<i>E. coli</i> BL21 (untransformed control)– No Trp	-	-
<i>E. coli</i> BL21 (untransformed control) + Trp	+	+
<i>E. coli</i> BL21::pET-Iaam – No Trp	-	-
<i>E. coli</i> BL21::pET-Iaam + Trp	+	+
<i>E. coli</i> BL21::pET-Aux – No Trp	-	-
<i>E. coli</i> BL21::pET-Aux + Trp	+	+

(+) denotes that the indole compound was detected, (-) denotes that the indole compound was not detected by LC-MS-MS.

Alternatively, the possibility exists that IaaM and Aux are not TMOs but rather L-amino acid oxidases (LAAOs). Some LAAOs are expressed as a proenzyme that must be partially digested with proteolytic enzymes to the active form (383). For instance, PAO from *Pseudomonas* sp. P-501 is composed of an α subunit, and β subunit but the ORFs of these subunits are preceded by a prosequence (384). Expression of the gene in *E. coli* showed that without the prosequence, PAO is produced only in a small quantity as a soluble form with no visible absorption, while with the prosequence, proPAO is highly expressed and yellow. The *E. coli* expressed and purified proPAO had no catalytic activity. Treatment of proPAO with a mixture of pronase and trypsin converted the non-catalytic proPAO to the catalytic form (384). Similarly, a putative TMO from *Ralstonia solanacearum* that is homologous with proPAO from *Pseudomonas* sp. P-501, was expressed in *E. coli* but had no catalytic activity. Treatment of the *R. solanacearum* TMO with various proteases, resulted in high activity to oxidize L-Phe, L-Trp, L-Tyr and L-Met. The substrates L-Phe and L-Tyr were

mostly oxygenated, L-Met was mostly oxidized, and both oxygenation and oxidation of L-Trp was observed (385). Although IaaM and Aux do not share significant sequence similarity (26%) with the PAO from *Pseudomonas* sp. P-501, the possibility remains that these enzymes may require a similar type of activation.

Other factors that may affect the activity of LAAO enzymes include bacterial growth phase and pH. Bouvrette and Luong (1993) report that PAO activity in *Morganella morganii* was growth-associated; after 8 h of growth, the cells reached the stationary growth phase and the production of the enzyme decreased sharply (386). Similarly, in *P. chlororaphis* O6 the culture age markedly affected expression of the gene encoding a TMO. The expression of the gene was detected only in log-phase (15-h) and not in stationary-phase (48-h) cell cultures, correlating with the presence of IAM in 15-h but not 48-h cultures (243). Our assays were performed with enzymes from cells grown for ~24 hours, therefore it is possible that enzyme activity was lost by this growth phase. Like other amino acid oxidases, the selectivity of the purified *M. morganii* PAO toward L-amino acids, was pH-dependent. At pH 6.35, the enzyme was more specific for L-leucine, at pH 7.0 toward phenylalanine while at pH 9.4 selectivity shifted towards tryptophan (386). Our enzyme assays were performed at pH 8.3, which may not have been conducive for Trp selectivity.

5.3.4 Sequence Similarity

A phylogenetic analysis by Patten et. al., (2013), showed that “TMO-like” bacterial sequences fall into two clusters of genes; Group I include the TMOs that have been functionally characterized in the plant pathogens and group II which are present in a greater diversity of bacteria including plant-

growth promoting bacteria (PGPB)(43). None of the group II homologs have been studied with respect to a potential role in IAA biosynthesis. Both *iaaM* and *aux* sequences fall into Group II and would thus be among the first TMO's produced by a PGPB to be functionally characterized with respect to IAA biosynthesis. The only sequence of known function in group II is a monooxygenase from *Pseudomonas putida* KT2440 (43)(387). Initially this enzyme was annotated as a TMO, however, it was later experimentally shown to be a lysine monooxygenase (LMO) (387). This prompted a literature search for other functionally characterized paralogs of TMO and led to another LMO from *Pseudomonas* sp. AIU 813 (388) which shares 94% sequence identity with that of KT2440. This LMO exhibits two activities; oxidative deamination (oxidase) and oxidative decarboxylation (monooxygenase) of lysine, arginine and ornithine (388). Another closely related and functionally characterized amine oxidase family member is phenylalanine oxidase (PAO) from *Pseudomonas* sp. P-501, which catalyzes both the oxidative deamination and oxidative decarboxylation of Phe, Tyr and Met (384).

The amino acid sequences of IaaM and Aux were compared with those of functionally characterized amine oxidase members, including five TMOs (*A. tumefaciens*, *P. syringae* pv. *savastanoi*, *P. agglomerans*, *A. rhizogenes* and *D. dadantii*), two LMOs (*P. putida* KT2440 and *Pseudomonas* sp. AIU813) and PAO (*Pseudomonas* sp. P501). The IaaM sequence shared 27-31% identity with the five TMOs, 91% identity with the LMOs and 26% identity with PAO (Table 15).

The Aux sequence shared 24%-32% identity with the TMOs, 20% identity with the LMOs and 26% identity with PAO ((Table 15).

Table 15). A broad-substrate LAAO from *Rhodococcus opacus* DSM 43250 which exhibits higher oxidase activity toward L-Lys and L-Phe, and lower activity with L-Trp (368) was also compared to IaaM and Aux. The *R. opacus* LAAO shared 25% sequence identity with IaaM and 38% identity with Aux (Table 15).

Table 15. Amino Acid Sequence Similarity of Flavin Monoamine Oxidases

Organism	Protein Accession No.	Enzyme Annotation	Substrate	% Sequence Identity to IaaM	% Sequence Identity to Aux
<i>Dickeya dadantii</i> 3937	ADM96599	TMO	Trp	30	25
<i>Pantoea agglomerans</i> pv. <i>gypsophilae</i>	Q47861	TMO	Trp	29	25
<i>Pseudomonas savastanoi</i>	P06617	TMO	Trp	31	24
<i>Agrobacterium fabrum</i> C58	NP_396520	TMO	Trp	30	32
<i>Agrobacterium rhizogenes</i>	Q09109	TMO	Trp	27	25
<i>Pseudomonas</i> sp. AIU 813	BAO51829	LMO	Lys, Arg	91	20
<i>Pseudomonas putida</i> KT2440	NP_742550	LMO	Lys	91	20
<i>Rhodococcus opacus</i>	AAL14831	LAAO	broad substrate	25	38
<i>Pseudomonas</i> sp. P501	Q5W9R9	PAO	Phe	26	26

*Bold text indicates high sequence identity (>90%).

5.3.5 Sequence Analyses and Phylogenetic Tree

Despite the similar structural features and catalytic reactions among members of the flavin-containing amine oxidases, there is a low level of sequence identity across the family (377). To gain insight into the functional activity of IaaM and Aux, a global multiple sequence alignment was constructed to search for conserved domains and critical sites that may be shared between the biochemically characterized TMOs, LMOs, PAO and LAAO shown in Table 15. According to the neutral theory of molecular evolution, residues more relevant for function vary more slowly than less important ones (389). Members of the flavin amine oxidase family possess two conserved sequence motifs at positions crucial for co-factor binding; the “GG” motif (RxGGRxxS/T) and the dinucleotide-binding motif (GxGxxG) that makes up the Rossmann fold that binds the ADP moiety of FAD (390). These two motifs were conserved in all of the eleven sequences in the alignment (Fig. 34). Overall, highest sequence conservation is observed in the N-terminal region (positions 48-135) which encompasses the FAD-binding domain. Outside of this region, there is little sequence conservation (Fig. 34).

Figure 34. Sequence Alignment of Flavin Amine Oxidases

The dinucleotide-binding motif (GxGxxG) which makes up the Rossmann fold that binds FAD and the “GG” motif (RxGGRxxS/T) are show in red boxes. An * (asterisk) indicates positions which have a single, fully conserved residue. A : (colon) indicates conservation between groups of strongly similar properties. A . (period) indicates conservation between groups of weakly similar properties.

Rhodococcus_opacus	GGAGLAYGAMSTLSTAAPARTF-----QPLAAGDLIGKVKGSHSVVVGPPGLCSAFEL
Pseudomonas_sp._P501	SGINYRHPALVSYFVA-----LGRLPAGNY--RIAIVGGGAGGIAALYEL
Pseudomonas_sp._UW4_Aux	IGSSYNYPWAARFPNPDLCFDYRALVEQENGIARATDPQH--KICIGAGVGTGTAAREL
Pseudomonas_sp._UW4_Iaam	MNKNRHPADGKKPITDFFPAFDDWIEHPAGLGSIPENHGAEVAIVGGGIAGLVAAAYEL
Pseudomonas_sp._Aiu_813	MNKNRHPADGKKPITDFFPAFDDWLEHPAGLGSIPAARHGEEVAIVGAGIAGLVAAAYEL
Pseudomonas_putida_KT2440	MNKNRHPADGKKPITDFFPAFDDWLEHPAGLGSIPAARHGEEVAIVGAGIAGLVAAAYEL
Pseudomonas_savastanoi	---MYDHPNS---PSIDILYDYGPFLLKCEGIGSYSAGTPTPRVAIVGAGISGLVAATEL
Dickeya_dadantii_3937	--MSNDASFLANSVPCVDLLYDYPFLQCSERIGYFPPGIPTPRVAIVGAGISGLVAATEL
Pantoea_agglomerans	--MKPHSVFADSLWPSIDLLYDYPFLQCSMHIGFPPGTITPRVAIVGAGISGLVAATEL
Agrobacterium_fabrum_C58	ASSDLSHFSAGSFPTIDLLYDYSFFDQCSRIQGFPPEDVPPKVAIVGAGISGLVVAASEL
Agrobacterium_rhizogenes	ADDDLSHFCSDSFPTVDLLYDYGKFFESCARIQYFPEGVTKPKVAIVGAGFSGVVAASEL
 : : * * * :
Rhodococcus_opacus	QKAGYK-VTVLEARTREGRVWVTARGKCTEGHFYNVGATRIPOSHITL-DYCRELQVEIQ
Pseudomonas_sp._P501	GRLAATDVQIYEAHREGRGIKIKVRLGDPGDTIYEVGAMRFPFIAGLTHWYASAADAAPK
Pseudomonas_sp._UW4_Aux	YRCGFTHITLIEQSRRIQGRRLTVPGSRNSSTPFEMGAMRMEPEGRSLMAYYANQFELAIS
Pseudomonas_sp._UW4_Iaam	MKLGLKPV-VYEAS-KMGGRLRSQAFNGAEGIVAEELGMRFPVSSAFYHYVDKLGLETK
Pseudomonas_sp._Aiu_813	MKLGLKPV-VYEAS-KMGGRLRSQAFNGTDGI IAEELGMRFPVSSAFYHYVDKLGLETK
Pseudomonas_putida_KT2440	MKLGLKPV-VYEAS-KLGGRLRSQAFNGTDGI IAEELGMRFPVSSAFYHYVDKLGLETK
Pseudomonas_savastanoi	LRAGVKDVLVYESRDRIGGRVWSQVFDQTPRYIAEMGAMRFPSPATGLPHYLKFKGISTT
Dickeya_dadantii_3937	LRAGVKDITLFEARDRIGGRVWSQVFDQTPRPHLIAEMGAMRFPSSSETCLFYYLNKLDIATT
Pantoea_agglomerans	LRAGVRDITLFEARDRIGGRVWSQVFDQTPRPHLIAEMGAMRFPSPATGLPHYLNRFSIQTA
Agrobacterium_fabrum_C58	LHAGVDDVTIYEASDRVGGKLSWHAFKDAPSVVAEMGAMRFPSPAASCLFPPFLERYGLSSR
Agrobacterium_rhizogenes	LHAGVDDVTIYEASDRVGGKLSWHAFKDAPSVVAEMGAMRFPSPRESCLFYYLNKLDIATD
 : : * * * :
Rhodococcus_opacus	GFGN--NANTFVNYQSDTSLYRAAK--ADTFGYMSELLKATDQG-----ALD
Pseudomonas_sp._P501	VFPNPGKVPTEFVFGNDRYVWEDPDSPTKVLGVVAGGLVGNQENVAMYPIANVDPAKIA
Pseudomonas_sp._UW4_Aux	NFANPGVSSGTGIYLREQMLIWKNGETPPEELQKVYSKWKAFADRMRTH-----VA
Pseudomonas_sp._UW4_Iaam	FPFNPASGSTVIDLEGQTHYAQKLSDLPALFQEVADAWADALEAGSQFS-----DIQ
Pseudomonas_sp._Aiu_813	FPFNPASRSTVIDLEGQTHYAQKLSDLPALFQEVADAWADALEAGSARFG-----DIQ
Pseudomonas_putida_KT2440	FPFNPASGSTVIDLEGQTHYAQKLSDLPALFQEVADAWADALEAGSQAFA-----DIQ
Pseudomonas_savastanoi	TFPDPGVVDTELHYRGKRYHWPAGKKPELFRVYEGWQSLSEGYLLEGGSLVAPLDIT
Dickeya_dadantii_3937	SFPDPGVVDTELHYRGVRHIIWSAGDPPSFLSRVHEGWVALLNEGYLHNGVPLVAPRIT
Pantoea_agglomerans	SFPDPGIVDTELHYRGVRHLWPAGEQPPALFTRVHNGWRALLYEGCLLDGVSIVLQGIT
Agrobacterium_fabrum_C58	FPFNPPTVDTNLVYQGLRYMNAKAGQPPKLFHRVYSGWRAFLKDGPHGEDIVLASPVAIT
Agrobacterium_rhizogenes	LFPNPGSDVTALFYRGRQYIWKAGEEPPPELFRVHNGWRAPLQDGYLHNGVPLVAPRIT
	* : : :
Rhodococcus_opacus	QVLSREDKDALSEFLSDFGDLSDDGRLGSSRR---GYDSEPGAGLNFTEKKPFAMQEV
Pseudomonas_sp._P501	AILNAATPPADAKYWPEFIAQYDGLTLGAAVRVAFEGTLDPDGVLDVDE-SISELFGFRGF
Pseudomonas_sp._UW4_Aux	ELYASQEWETT---WASIVEKEYESISFRDLVSEAWDGRSPFGGMGTA-QESAIFYAIGI
Pseudomonas_sp._UW4_Iaam	QAIRDVDVPRKELWNTLVPLWDDRTFFYDFVAT-----SKAFAKLSF--HHEVFGQVGF
Pseudomonas_sp._Aiu_813	QAIRDVDVPRKELWNTLVPLWDDRTFFYDFVAT-----SKAFAKLSF--QHREVFGQVGF
Pseudomonas_putida_KT2440	QAIRDVDVPRKELWNTLVPLWDDRTFFYDFVAT-----SRSFALSF--QHREVFGQVGF
Pseudomonas_savastanoi	AMLKSGRLEEAATAWQGLNVFRDCSFYNAIVCIPTGRHPPGGDRWAR-PEDELFGSLGI
Dickeya_dadantii_3937	AMLKSHCFDKARKAWQAWLDAFRDYSFYSALVTMFTSNTPPGVPWRR-PDELFGSLGI
Pantoea_agglomerans	AMLKSERFDEAAEAQIWLNVFRDCSFYSAMVTIFTGTNPPGGIAWER-RDELFGALGI
Agrobacterium_fabrum_C58	QALKSGDIRRAHDSWQTLNRFGRSFSIAIERIFLGTHTPPGGTWSF-PHDDLFKLMGI
Agrobacterium_rhizogenes	DALNLGHLQQAAGHFQSWLTYFERESFSSGIEKMFLGNHPPGGEQWNS-LDDLFLKALGI
 * : :
Rhodococcus_opacus	IRSGIGRNFSDPF-----GYDQAMMPVGGMDRIYYAFQDRI--GTVFG-----AE
Pseudomonas_sp._P501	GTGGFKPLYNISLVEMRLILWDYSNEYTLPTGAGKLVVQVRQERVAASARAQLVPHDQ
Pseudomonas_sp._UW4_Aux	GDGSGWAFYDVCCLYPLRTAIFGFSQLQIHGGLAALDECLLFMAKADHECLERSLTDSS
Pseudomonas_sp._UW4_Iaam	GTGGWDSDFPNSMLEIFRVVMTNCDHQLVVGVEQVPPQGIWRHVPEGTSLSSLAPRTG
Pseudomonas_sp._Aiu_813	GTGGWDSDFPNSMLEIFRVVMTNCDHQLVVGVEQVPPQGIWRHVPEGTSLSSLAPRTG
Pseudomonas_putida_KT2440	GTGGWDSDFPNSMLEIFRVVMTNCDHQLVVGVEQVPPQGIWRDVPEGTSLSLAPRTG
Pseudomonas_savastanoi	GSGGFLPVYQAGFTEILRMVINGYQSDQRLIPDGISSLAARLADQSFQKALRDRVCFSR
Dickeya_dadantii_3937	GSGGFLPVYQAGFTEILRMVINGYEDDQRLIIGGISTLAERLVSKIGDTRLSHEICFNE
Pantoea_agglomerans	GSGGFLPVYQAGFTEILRMVINGYEDDQRLIIGGISTLAERLQAEIRGTTTPGRHVRFSK
Agrobacterium_fabrum_C58	GSGGFGPVFESGFIEILRLVINGYEENQRMCEGISELPRRIATQVNVGVSVSQRIRHVQ
Agrobacterium_rhizogenes	GSGGFGPVFESGFIEILRLVINGYEDNVRLSYEGISELPHRIASQVINGRSIRERTIHVQ
 : * : :

The TMO of *P. savastanoi* and the LMO of *Pseudomonas* sp. AIU813 have been mechanistically and structurally characterized (380)(376)(373)(391). Therefore, the sequences of these two enzymes were used as templates against which to compare IaaM and Aux. The amino acid positions of specific residues involved in cofactor binding, active site formation and catalysis were analyzed, allowing proposals to be made regarding the putative enzymatic function of IaaM and Aux (Table 16, Fig. 35).

➤ **Residues involved in FAD-binding**

In both TMO and LMO, Lys365 is conserved and forms a water-mediated hydrogen bond with the flavin cofactor. This residue is also conserved in IaaM and in Aux (Table 16).

➤ **Residues involved in the active site of TMO**

In the active site of the *P. savastanoi* TMO, Arg98 and Tyr413 interact with the carboxylate of the Trp substrate and Trp519 and Phe476 properly orient the substrate into the active site. These residues are all conserved in IaaM, while only three of the four are conserved in Aux (Arg98, Tyr413 and Trp519) (Table 16). In TMO, the indole ring of the bound IAM product, lies in a hydrophobic pocket made up of Phe244, Val247, Met258, Trp415, Phe476, Leu478. Of these six residues, only two are conserved in IaaM (Trp415, Phe476) and two are conserved in Aux (Trp415, Leu478) (Table 16). Residue Cys511 interacts with the hydroxyl oxygen of the FAD. This position corresponds to Ser511 in the LMO of *Pseudomonas* sp. AIU813. When the TMO Cys511 was mutated to Ser511, there was an 8-fold decrease in the second-order rate constant for binding of the Trp substrate by TMO. In the primary structure of IaaM this position corresponds to Ser511 and in Aux to Asp511.

➤ **Residues involved in substrate specificity**

In the LMO from *Pseudomonas* sp. AIU813, Asp238 forms a ceiling in a long hydrophobic pocket; a structural feature that is consistent with the lysine substrate preference. This Asp238 residue is conserved in Iaam, suggesting that it has lysine substrate specificity (Table 16). In TMO from *P. savastanoi*, Val247 is located at the bottom of the substrate binding pocket and determines the tryptophan substrate specificity. Phenylalanine oxidase (PAO) from *Pseudomonas* sp. P501 contains Leu319 at this position, while the Aux protein contains Phe287.

➤ **Residues involved in deamination and decarboxylation**

Lysine monooxygenase (LMO) and tryptophan monooxygenase (TMO) enzymes can exhibit both oxidase (oxidative deamination) and monooxygenase (oxidative decarboxylation) activities under different conditions (391). The TMO of *P. savastanoi* can be converted from a monooxygenase to an oxidase by introducing mutations at the residues that interact with the carboxylate of the Trp substrate (Tyr413 and Arg98) (374)(376)(380). For the LMO of *Pseudomonas* sp. AIU813, the critical residue for converting between oxidase and monooxygenase activity is Cys254 (391). Matsui et al., (2014) found that the wild-type *Pseudomonas* sp. AIU813 LMO exhibited higher monooxygenase activity than oxidase activity toward L-Lys whereas the site-directed mutation at Cys254 or chemical modification by p-chloromercuribenzoic acid (p-CMB) had the opposite effect (391). Similarly, Yamauchi et al. (1973) also showed that when the sulfhydryl group of the LMO from *P. fluorescens* pf0-1 was modified, monooxygenase activity was inhibited and oxidase activity was induced (393). This suggests that the sulfhydryl group plays a significant role in the oxygenase reaction. In fact, a multiple sequence alignment of the *Pseudomonas* sp. AIU813 LMO and other putative lysine

monooxygenases, reveals five conserved cysteine residues (Cys-254, 280, 331, 342, and 413) (391). These cysteine residues are all conserved in IaaM but none are conserved in Aux or in TMO (Table 16). Koyama et al. (1984) found that phenylalanine oxidase (PAO) performs both the oxidase and monooxygenase activities depending on the substrate used; even a slight difference in the binding position of a substrate can dictate the activity of this type of enzyme as oxidase or monooxygenase (394).

Table 16. Conservation of Critical Residues in TMO and LMO

Structural/Catalytic Feature	Residue	LMO from <i>Pseudomonas</i> sp. AIU813	IaaM from <i>Pseudomonas</i> sp. UW4	Aux from <i>Pseudomonas</i> sp. UW4	TMO from <i>Pseudomonas savasanoi</i>
Residues forming the active site of LMO	Trp418	x	x	x	x
	Trp516	x	x	x	x
Residues that orient the Trp substrate into the active site of TMO	Trp519	x	x	x	x
	Phe476		x		x
Residues forming the active site of TMO	Cys338	x	x		x
	Cys511				x
Residues that form backbone of hydrophobic pocket in TMO	Arg71				x
	Arg77	x	x	x	x
	His464				x
Residues that interact with the carboxylate of the Lys substrate in active site of LMO	Arg102	x	x	x	x
	Tyr416	x	x	x	x
Residues that interact with the carboxylate of the Trp substrate in active site of TMO	Arg98	x	x	x	x
	Tyr413	x	x	x	x
Critical residue for monooxygenase activity in LMO	Cys254	x	x		

Structural/Catalytic Feature	Residue	LMO from <i>Pseudomonas</i> sp. AIU813	IaaM from <i>Pseudomonas</i> sp. UW4	Aux from <i>Pseudomonas</i> sp. UW4	TMO from <i>Pseudomonas savasanoi</i>
Residue that confers Lys substrate specificity	Asp238	x	x		
Residue that confers Trp substrate specificity	Val247				x
Residues that form hydrophobic pocket in which the IAM product is bound in TMO	Phe244				x
	Val 247				x
	Met258				x
	Trp415	x	x	x	x
	Phe476		x		x
	Leu478			x	x
Residues that interact with FAD co-factor	Lys365	x	x	x	x
	Trp466	x	x	x	x
Residues that form a loop that packs against the flavin ring of FAD cofactor in TMO	Glu93	x	x	x	x
	Gly95	x	x	x	x
Residues that form salt bridges between TMO monomers	Arg134			x	x
	Asp350				x
	Arg227				x
	Asp203	x	x		x
	Arg391	x	x		x
	Glu357				x
	His359			x	x
	Asp417				x

“x” denotes the presence of that residue

Figure 35. Multiple Sequence Alignment of IaaM, Aux, TMO and LMO

The protein sequences of IaaM and Aux were compared to the characterized TMO from *P. savastanoi* and LMO from *Pseudomonas* sp. AIU 813. The dinucleotide-binding motif (GxGxxG) and the “GG” motif (RxGGRxxS/T) are shown in red boxes. An * (asterisk) indicates positions which have a single, fully conserved residue. A : (colon) indicates conservation between groups of strongly similar properties. A . (period) indicates conservation between groups of weakly similar properties. The residue that confers substrate specificity is shown in the green box. Residues that interact with the carboxylate of the substrate arg(R)98 and tyr(Y)413 are shown in blue boxes. The critical residue for FAD binding lys(K)365 and for orienting the Trp substrate into the active site are also shown in blue boxes.

Pseudomonas_sp._UW4_Aux Pseudomonas_savastanoi Pseudomonas_sp._UW4_IaaM Pseudomonas_sp._Aiu_813	RFPNP---PDLCFDYRALVEQENGIAR--APQKICII GAGVTGLTAARELYRCGFTHILI NSPSI----DILYDYGPFLLKKEGIGSYSAPTRVAIV GAGISGLVAATELLRAGVKDVLV KKPITIFGPDFPFAFDWDWIEHPAGLGSIPHEGEVAIV GGGIAGLVAAYELMKLGLKPVVY KKPITIFGPDFPFAFDWDWIEHPAGLGSIPHEGEVAIV GAGIAGLVAAYELMKLGLKPVVY . * * * * * : : : : : * : . : * : * : * : * : * * . * . . : :
Pseudomonas_sp._UW4_Aux Pseudomonas_savastanoi Pseudomonas_sp._UW4_IaaM Pseudomonas_sp._Aiu_813	EQSRRIGGRRLTVPGSRNSSHTPFEMGAMR MPEGRSLMAYYANQFELAISNFANPGVSVSTG ESRDRI GGRVWSQVFDQTPRYIAEMGAMR FPPSATGLFHYLKKFGISTTTTFFDPGVVDTE EAS-KMGGRLRSQAFNGAEGIVAELGGMR FVVSSTAFYHYVDKLGLETKPPNPASGSTV EAS-KMGGRLRSQAFNGTDGIIAELGGMR FVVSSTAFYHYVDKLGLETKPPNPASRSTV * . : * * * : : * : * : * : * . : : * : : : . * : * . *
Pseudomonas_sp._UW4_Aux Pseudomonas_savastanoi Pseudomonas_sp._UW4_IaaM Pseudomonas_sp._Aiu_813	IYLREQMLIWKNGETPELQKVYSKWK-AFADRMTVAELYWASIVEKEYESISFRDLVSGR LHYRGKRYHWPAGKKPPLFRVYEGWQSLLESEGYDITAMLWQGLNVFRDCSFYNAIVGR IDLEGQTHYAQKLSDLPLFQEVADAWADALEAGSDIQQAIWNTLVPLWDDRTFFYDFVATS IDLEGQTYAEAADLPLFQEVTDAWADALESGADIQQAIWNTLVPLWDDRTFFYDFVATS : : : * : . * . * : : : * : : : . * : * : *
Pseudomonas_sp._UW4_Aux Pseudomonas_savastanoi Pseudomonas_sp._UW4_IaaM Pseudomonas_sp._Aiu_813	SPFGMGMTAQ-AIFYAIGIGDGSWGAIFYDVCCLYPLRTAIFGFSSQLQIHGGLAALDEC HPPGGDRWARPFELFGLSGLIGSGGFLFVFAQGFTEILRMVINGYQSDQRIPIDGISSLAAR KAFAKLSFHHR-EVFGQVGFQGTGGWSDDFPNSMLEIFRVVMTNCDHGHVVGVEQVPPQG KAFAKLSFQHR-EVFGQVGFQGTGGWSDDFPNSMLEIFRVVMTNCDHGHVVGVEQVPPQG . . : * : * : * * : . : * : : * : :
Pseudomonas_sp._UW4_Aux Pseudomonas_savastanoi Pseudomonas_sp._UW4_IaaM Pseudomonas_sp._Aiu_813	LLFMKADEHCL-ERSLLTDSSVTKLEKQLKIRVYYNWKHDDFDSVIMTLPSWLIETRIK LADQSFQDGLKALRDRVCFSRVG--RISR-EKII IQTEAGERVFDRIVITSRAMQMIHCLDS IWRHVPEGTSL-SSLGAPRTGVKKIAHAGRAVTDNWDREYAAVLTTCQSWLLTTQICD IWRHVPEGTSL-SSLGAPRTGVKRIARAGRLAVTDNWDREYAAVLTTCQSWLLTTQICE : : . * : : : : : * : * : : : .
Pseudomonas_sp._UW4_Aux Pseudomonas_savastanoi Pseudomonas_sp._UW4_IaaM Pseudomonas_sp._Aiu_813	NMLPFETINAYKTAHWETSCKVVFAPLKKSFLSKNNIPQAIVTDSDFIHDVYTYRYNDNYSD EFLSRDVARAVRETHLTGSSKLFILTRTKFWIKNKLPTTIQSDGLVGRGVYCLDYQPDEPG ELFSQKMMWALDRTRYMQSSKTFVMVDRPFWKDKDLMSMTLTDRLTRGTYLFDNGDDKPG ELFSQKMMWALDRTRYMQSSKTFVMVDRPFWKDKDLMSMTLTDRLTRGTYLFDNGDDKPG : : . . * : . * : * * * * . . : : * : . . . * : : . .
Pseudomonas_sp._UW4_Aux Pseudomonas_savastanoi Pseudomonas_sp._UW4_IaaM Pseudomonas_sp._Aiu_813	CILLSYTWEDDATKLASFSDKESKCAEELDRILMNSANPYIGIDQAVVR-WVTDKNALGC VVLLSYTWEDDAQKMLAMPDKKTRCQVLVDDLAAIHPTPVDG YERYVLHDWLTDPHSAGA VICLSYSWMSDALKMLPHPVEK-RVKLALDALKKIYPKDI AAIIGDPITSWEADPHFLGA VICLSYAWMSDALKMLPHPVEK-RVQLALDALKKIYPKDIAGIIGDPITSWEADPHFLGA : * * * * * . * * : . . . : : * : : . . : : * : * : *
Pseudomonas_sp._UW4_Aux Pseudomonas_savastanoi Pseudomonas_sp._UW4_IaaM Pseudomonas_sp._Aiu_813	AKLYRPGTY-YDAVGLMKYNRDL-AHVSGLYLSGESFSVDAQWTEPCFRGAVDVAIHCN FKLNYPGEDVYSQRLFPQMTASPKNKDTGLYLAGCSCSFAGGWIEGAVQ TALNSACAVLR FKGALPGHYRYNQRMYAHFMDMPAEQRGIF IAGDDVSWTPANVEGAVQ TSLNAVWGIMK SKGALPGHYRYNQRMYAHFMDMPAEQRGIF IAGDDVSWTPANVEGAVQ TSLNAVWGIMK * * * * . : * : * * * * . * * * . . . : : . .
Pseudomonas_sp._UW4_Aux Pseudomonas_savastanoi Pseudomonas_sp._UW4_IaaM Pseudomonas_sp._Aiu_813	KTAANGGFSLSDYP--- STGGLKGNPLDCINASY HFGGANPGPGDVFNEIG HFGGANPGPGDVFDEIG * * * *

The putative TMO enzymes (IaaM and Aux) from strain UW4 were used for phylogenetic analyses. Maximum-likelihood (ML) trees were constructed to infer the phylogeny of these proteins (Fig. 36). Since Aux does not share significant sequence similarity with any other characterized flavin amine oxidase proteins, the phylogeny of Aux could not be reliably inferred. Nevertheless, a ML tree was constructed for Aux and is shown in Fig. A10 (Appendix A), however the overall tree topology has low bootstrap support.

The phylogenetic analysis for IaaM includes five biochemically characterized TMOs, and two LMOs. In the IaaM ML tree, all five of the known TMOs cluster together at the top of the tree. The TMO from *D. dadantii*, *P. agglomerans* and *P. savastanoi* form a well-supported clade (96%) (Fig. 36). The two *Agrobacterium* TMOs cluster together with 100% support (Fig. 36). The IaaM protein clusters with the two known *Pseudomonas* spp. LMOs at the bottom of the tree, with 100% bootstrap support (Fig. 36). IaaM and the two LMOs diverged from a common ancestor, suggesting that IaaM is more closely related to LMOs than to TMOs.

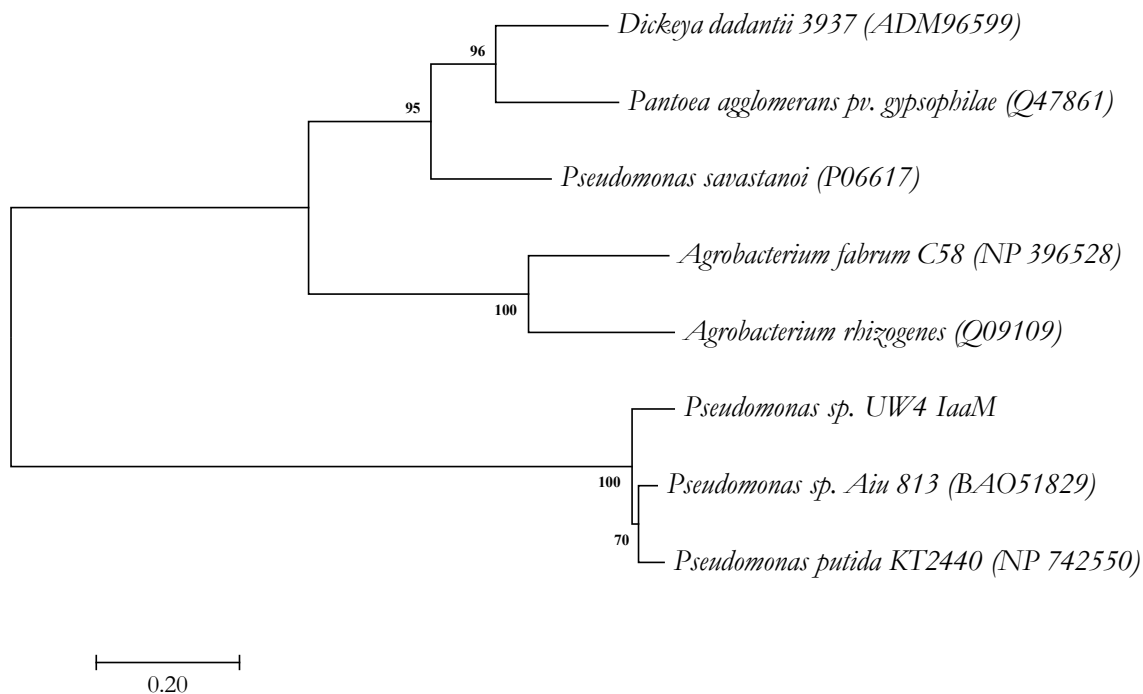


Figure 36. Molecular Phylogenetic Analysis of IaaM by Maximum Likelihood Method

The evolutionary history was inferred by using the Maximum Likelihood method based on the JTT matrix-based model (286). The tree with the highest log likelihood (-5664.5841) is shown. The percentage of trees in which the associated taxa clustered together is shown next to the branches. Initial tree(s) for the heuristic search were obtained automatically by applying Neighbor-Join and BioNJ algorithms to a matrix of pairwise distances estimated using a JTT model, and then selecting the topology with superior log likelihood value. The tree is drawn to scale, with branch lengths measured in the number of substitutions per site. The tree is mid-point rooted; the root is placed at the mid-point of the longest distance between two taxa in a tree. The analysis involved 8 amino acid sequences. All positions containing gaps and missing data were eliminated. There were a total of 499 positions in the final dataset. Evolutionary analyses were conducted in MEGA7 (264).

5.3.6 Structural Analysis

The specific type of oxygenation and selectivity of flavin amine oxidases depends on the shape and chemical nature of the active site and is dictated to some extent by its structural fold (395).

Generally, when a protein shares at least 30% amino acid identity with another protein, the two proteins exhibit similar 3D structures (396). As such, we compared the predicted three-dimensional (3D) structure of IaaM and Aux against the solved structure of other characterized flavoproteins.

The Phyre2 web portal for protein modeling was used to predict the 3D protein structures of IaaM and Aux and to search for other structural homologs in the fold library (397).

The Phyre2 analyses ranks the closest matches to our protein based on the number of aligned residues and the quality of alignment. This in turn is based on the similarity of residue probability distributions for each position, secondary structure similarity and the presence or absence of insertions and deletions (397). The IaaM protein had the highest ranked match with LMO from *Pseudomonas* sp. AIU 813, followed by TMO from *P. savastanoi* and phenylalanine oxidase (PAO) proenzyme from *Pseudomonas* sp. P501, respectively. The predicted secondary structure of IaaM was compared against the structure of its' highest ranked match, the LMO from strain AIU 813 (Fig. 37). The positions of secondary structures (i.e., α -helices and β -strands) are nearly identical between the two sequences, with the exception of an additional α -helix present at position 420 in IaaM (Fig. 37).

The Aux protein had the highest ranked match with PAO proenzyme from *Pseudomonas* sp. P501, followed by LMO from *Pseudomonas* sp. AIU 813 and TMO from *P. savastanoi*. The predicted secondary structure of Aux was compared against the structure of top ranked match, the PAO

proenzyme from *Pseudomonas* sp. P501 (Fig. 38). The Aux sequence has several insertions and deletions relative to the PAO template but the positions of α -helices and β -strands are similar between the two (Fig. 38).

Figure 37. Predicted Secondary Structures of IaaM and LMO

The predicted secondary structure of IaaM (query sequence) vs. the LMO from *Pseudomonas* sp. AIU 813 (template sequence). Confidence level = 100%, Sequence identity= 92%, resolution= 1.9 angstroms, number of aligned residues= 538. Confidence represents the probability (from 0 to 100%) that the match between our sequence and the template is a true homology. Sequence identity is the proportion of our protein residues equivalenced to identical template residues in the generated alignment.



Green helices represent α -helices, blue arrows indicate β -strands and faint lines indicate coil. G = 3-turn helix, I = 5-turn helix, T = hydrogen bonded turn, B = residue in isolated β -bridge (single pair β -sheet hydrogen bond formation), S = bend. Identical residues in the alignment are highlighted with a grey background.

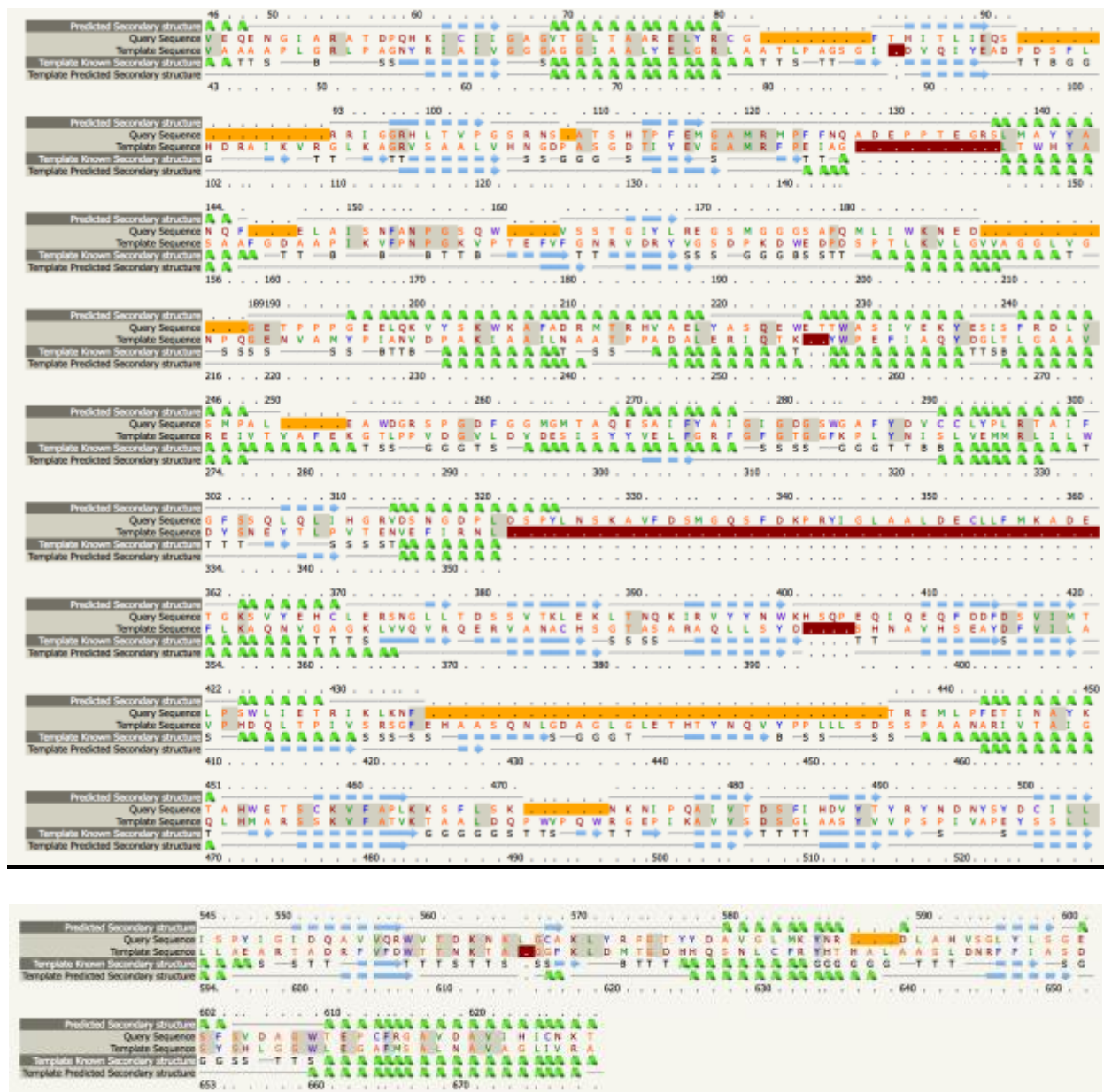
■ Insertion relative to template

Figure 38. Predicted Secondary Structure of Aux and PAO

The predicted secondary structure of Aux (query sequence) vs. the PAO from *Pseudomonas* sp. 501 (template sequence). Confidence level = 100%, Sequence identity= 23%, resolution= 1.35 angstroms, number of aligned residues= 525. Confidence represents the probability (from 0 to 100%) that the match between our sequence and the template is a true homology. Sequence identity is the proportion of our protein residues equivalenced to identical template residues in the generated alignment.

Green helices represent α -helices, blue arrows indicate β -strands and faint lines indicate coil. G = 3-turn helix, I = 5-turn helix, T = hydrogen bonded turn, B = residue in isolated β -bridge (single pair β -sheet hydrogen bond formation), S = bend. Identical residues in the alignment are highlighted with a grey background.

-  Insertion relative to template
-  Deletion relative to template



5.3.7 Genetic organization of *iaaM* and *aux* genes

The *iaaM* gene shares high sequence identity (91%) with the biochemically-characterized LMO of *P. putida* KT2440, which is encoded by the *davB* gene. The DavB protein converts lysine to 5-aminovaleramide. A hydrolase encoded by the *davA* gene subsequently converts the 5-aminovaleramide into 5-aminovalerate (AMV) (398). Thereafter, AMV is converted into glutarate via enzymes encoded by the *davD* and *davT* genes. This energy metabolism pathway is known as the AMV pathway (Fig. 42). The *davD* gene forms an operon with *davT*, the gene order being *davDT* and is located in a different genomic region than the *davBA* cluster. This unlinked chromosomal localization allows the cells to activate different segments of the lysine degradation pathways in response to different nutritional situations (399).

Upon analysis of the *davB-davA* genomic region in *P. putida* KT2440, a striking similarity to that of the *iaaM* genomic region was observed (Fig. 39 and 40). In KT2440, *davA* is found 15 bp upstream of *davB*, and these two genes are co-transcribed. The *davBA* cluster is flanked by several genes involved in the biosynthesis of pyrroloquinoline quinone (PQQ) and by an *asnC* transcriptional regulator (Fig. 40) (399). In *Pseudomonas* sp. UW4, the *iaam* gene is found 13 bp upstream of a hydrolase protein annotated as “nitrilase/cyanide hydratase” (Fig. 39). Given the proximity of these two genes, it is also likely that they are co-transcribed. The UW4 hydrolase gene (WP_015097082) is 64% identical to the *davA* hydrolase (NP_742549). The *aux* gene also has a putative “nitrilase/cyanide hydratase” (WP_015096784) located 12bp downstream, however it only shares 32% sequence identity with *davA* (Fig. 39). The UW4 *iaam*-hydrolase gene cluster is

also flanked by PQQ biosynthesis genes on one side and by an *asnC* transcriptional regulator on the other side (Fig. 39).

To determine whether UW4 also utilizes the AMV energy metabolism pathway, the *davD* and *davT* genes from strain KT2440 were used as BLAST queries against the UW4 genome. The *davD* gene was 90% identical to the *gabD1* of UW4, which is annotated as succinate-semialdehyde dehydrogenase. The *davT* gene is 85% identical to the UW4 *gabT1* gene, which is annotated as 4-aminobutyrate transaminase. Similar to the organization seen in the KT2440 genome, the UW4 *gabD1T1* genes are located in a separate chromosomal region than *iaaM*. Altogether, these observations suggest that UW4 utilizes the AMV pathway and that IaaM may play a role in this pathway as a lysine monooxygenase (Table 17). Bacteria that have the ability to use lysine as the sole carbon and nitrogen source have a selective advantage in the rhizosphere where lysine is released via root exudates.

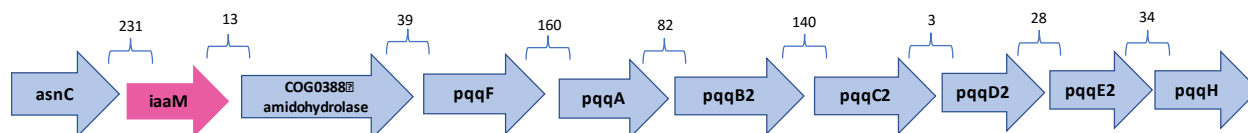


Figure 39. Gene organization of *iaam* in the *Pseudomonas* sp. UW4 genome

AsnC=transcriptional regulator, *iaaM*=putative TMO, COG0388 predicted amidohydrolase=nitrilase/cyanide hydratase and apolipoprotein N-acyltransferase, *pqqF*-*pqqH*= pyrroloquinoline quinone biosynthesis proteins

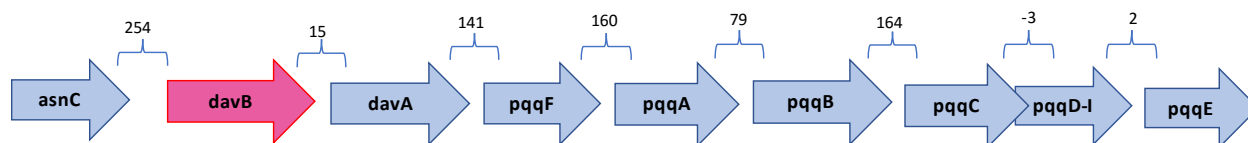


Figure 40. Gene organization of *davB* in the genome of *P. putida* KT2440

AsnC=transcriptional regulator, *davB*=lysine monooxygenase (LMO), *davA*=5-aminopentanamidase, *pqqF*-*pqqE*= pyrroloquinoline quinone biosynthesis proteins

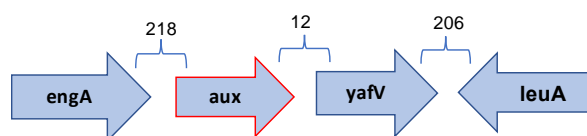


Figure 41. Genetic organization of *aux* in the *Pseudomonas* sp. UW4 genome

engA=COG1160 predicted GTPase, *aux*= putative TMO, *yafV*= nitrilase/cyanide hydratase and apolipoprotein N-acyltransferase, *leuA*= 2-isopropylmalate synthase

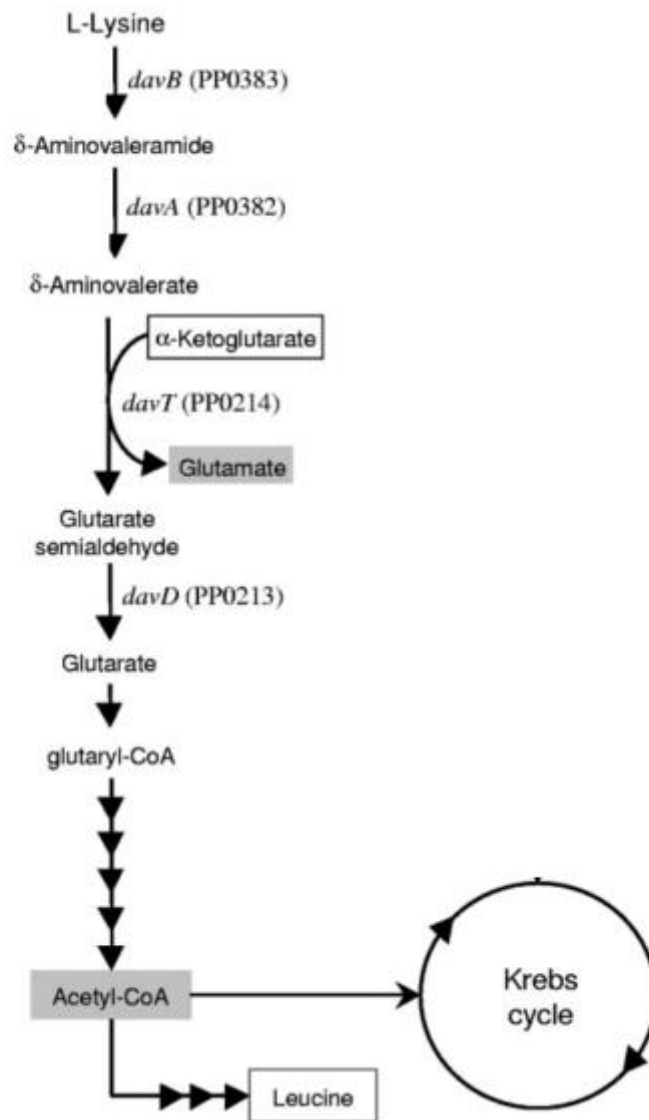


Figure 42. AMV pathway for the degradation of lysine by *Pseudomonas*.

Where they are known, the corresponding gene and the number of its translated product are given. Figure adapted from Revelles et al., (2005).

Table 17. Lysine metabolism genes in *P. putida* KT2440 and homologs in strain UW4

<i>P. putida</i> KT2440 Gene	Characterized Protein Function	<i>Pseudomonas</i> sp. UW4 Gene	Functional Annotation in UW4	% Sequenc e Identity
<i>davD</i> (PP0213)	glutaric semialdehyde dehydrogenase	<i>gabD1</i>	succinate-semialdehyde dehydrogenase	90
<i>davT</i> (PP214)	aminovalerate aminotransferase	<i>gabT1</i>	4-aminobutyrate transaminase	85
<i>davB</i> (PP0383)	lysine monooxygenase	<i>iaaM</i>	tryptophan monooxygenase	91
<i>davA</i> (PP0382)	aminovaleramide amidohydrolase	PputUW4_04963	nitrilase/cyanide hydratase and apolipoprotein N- acyltransferase	64

5.4 Conclusion

The IaaM and Aux protein are both classified as flavin monoamine oxidases (MAOs). Following comparisons of IaaM and Aux to several MAO family members including lysine monooxygenase (LMO), tryptophan monooxygenase (TMO), phenylalanine oxidase (PAO) and L-amino acid oxidase (LAAO); IaaM shared the greatest sequence identity (>90%) and structural similarity with LMO. A phylogenetic analysis also revealed that IaaM is most closely related to LMOs from other *Pseudomonas* spp. Aux shared the highest sequence identity with a broad-spectrum LAAO (38%) and was most structurally similar to TMO. However, a phylogenetic analysis indicated that Aux is most closely related to PAO. Initially, both IaaM and Aux were implicated as putative TMOs, however enzyme assays were not successful in detecting the expected amide product (IAM) formed by the action of TMO. Nevertheless, analysis of the UV-Vis absorption spectrum revealed that Trp was a substrate for IaaM. In order to measure LMO activity in *Pseudomonas* sp. AIU 813, an amide

hydrolase from *Pseudomonas* sp. TPU-A5 was cloned and used in a coupled enzymatic reaction (388). This enzyme coupling results in the production of 5-aminopentanoate and ammonia; LMO activity was measured by the detection of ammonia. Interestingly a comparison of the *Pseudomonas* sp. TPU-A5 amide-hydrolase (BAO51830) to the UW4 amide-hydrolase (Ami; refer to Chapter 2), reveals 82% sequence identity (100% query coverage). If we assume (based on high sequence and structural similarity that IaaM is an LMO enzyme with both oxidase and monooxygenase capacity, then it is capable of producing an amide which then serves as the substrate for the Ami protein. Although Ami was shown to metabolize indoleacetamide (IAM), it is predicted to be a broad substrate enzyme. Based on the preliminary results of this chapter, it is likely that IaaM produces an amide product (i.e., it has monooxygenase activity), however it is unclear whether it acts on Trp, Lys or both.

Chapter 6

General Discussion

6.1 Overview

We do not live in a world with an abundance of nutritious food for everyone. In fact, food security does not exist for nearly one billion people (Lelieveld, 2012). Environmental stresses such as salinity, flooding, drought and temperature fluctuations affect plant growth and decrease crop productivity worldwide. To ensure food security for the increasing world population, total crop production will need to be significantly increased with less arable land and under a range of environmental stresses.

Plants interact with billions of bacteria that colonize the inside as well as outside surfaces, representing an ancient co-evolution. Plant-associated bacteria play a fundamental role in the regulation of plant physiology. As such, plant-growth-promoting bacteria (PGPB) can offer growth promoting effects resulting in high yield and productivity, ensuring food security along with environmental security by reducing the use of hazardous agrochemicals.

PGPB are bio-treasures that provide a rich source of valuable natural products to plants. One of the most valuable compounds is IAA, a key plant-growth regulator and signaling molecule in the plant response/adaptation to environmental stresses. IAA is produced by an interplay of enzymes that mediate multiple interconnected biosynthesis pathways.

Recent genome sequencing of one particularly effective PGPB-*Pseudomonas* sp. UW4-has presented an opportunity to explore the possibility of deciphering the IAA biosynthesis pathways of this strain at the molecular level. Seven putative IAA biosynthesis genes were identified in UW4's genome. Given that the genome annotations are based on similarity to the closest gene sequences rather than precise functional analysis, it was the goal of this work to assign function to these putative proteins. Isolation and characterization of the genes involved in IAA production will enable elucidation of the mechanisms of IAA production in strain UW4. This information is fundamental to the construction of a genetically engineered strain with optimal IAA production that can be used as an inoculant to improve agricultural yield.

6.2 Role of amidase in IAA biosynthesis

My early research elucidated the function of three of the seven putative IAA biosynthesis genes (*nit*, *nthA* and *nthB*). The enzymatic activity of the encoded proteins (Nit and NthAB) is proposed to be coupled with the activity of a putative amidase encoded by the *ami* gene. Altogether these four genes (*nit*, *nthA*, *nthB* and *ami*) constitute a complete IAN-IAM pathway for IAA biosynthesis. The scope of *Chapter 2* was to biochemically characterize this Ami protein. The *ami* gene was cloned into an expression vector, over-expressed in *E. coli*, purified and biochemically characterized. The enzyme was confirmed to catalyze the oxidative deamination of IAM into IAA. Temperature and pH profiles showed optimal activity at 35°C and a pH of 7.5. A multiple sequence alignment showed that Ami contains all of the conserved amino acid residues of the amide-hydrolase catalytic triad as well as the amidase signature (AS) sequence. Phylogenetic analysis of Ami revealed that it is more closely related to wide-spectrum amidases than to known IAM-hydrolases. This suggests that Ami is

capable of hydrolyzing various amides besides IAM; therefore, it likely has or previously had a role beyond IAA biosynthesis. In addition, the *ami* gene is co-located with genes encoding nitrile hydratase and aldoxime dehydratase on the chromosome of strain UW4, an arrangement typical of nitrile-hydrolyzing bacteria. Altogether, these findings suggest that this gene cluster is responsible for IAA production via IAN and IAM and possibly also for other nitrile-degrading activities.

6.3 The effect of increasing UW4's capacity to produce IAA on canola root growth

In the 16th century, Paracelsus taught that “all substances are poisonous, there is none that is not a poison; the right dose differentiates a poison from a remedy.” In the case of IAA, the dose determines the effect on the plant, be it stimulatory or inhibitory. As such, the performance level of PGPB may need fine-tuning to avoid production levels too small or too great (259). By manipulating the levels of IAA produced by bacteria through genetic engineering, it is possible to improve the beneficial effects of PGPB in the rhizosphere. The objective of *Chapter 3* was to develop a deeper understanding of how bacterially synthesized IAA affects plant growth by increasing UW4's capacity to produce IAA. IAA-overproducing transformants of strain UW4 were constructed by introducing a second copy of a target IAA biosynthesis gene on a plasmid. Five different genes were targeted for over-expression (*ami*, *nit*, *nthA*, *nthB*, *phe*) in strain UW4. All transformants produced more IAA than the wild-type bacterium, consistent with the involvement of each of the respective genes in IAA production by strain UW4. Although these data do not enable us to define the specific catabolic role of the uncharacterized Phe enzyme in IAA biosynthesis, over-expression of *phe* by addition of exogenous Trp and consequent overproduction of IAA, strongly suggests the involvement of this gene in IAA synthesis by UW4. Results showed that a 2-3 fold improvement in strain UW4's

capacity to produce IAA, leads to enhanced primary root growth, while shoot growth remains unaffected.

6.4 The contribution of each IAA gene to the production of IAA by strain UW4

It is difficult to establish a direct relationship between altered root growth and bacterial IAA, due to the difficulty of isolating bacterial mutants that are completely deficient in IAA synthesis. While mutants with significantly reduced levels of IAA have been generated by targeting specific genes for mutation, there are no bacterial isolates which are completely devoid of the ability to produce IAA.

The goal of *Chapter 4* was to create mutants that had a reduced capacity to produce IAA in order to delineate which genes/pathways contribute most to overall IAA production in strain UW4. The *seven* genes encoding enzymes that catalyze reactions in the IAN-IAM pathways were selected for single and double gene knockouts by, in each case, deleting a portion of their coding sequence. In total, eleven mutant UW4 strains were obtained; six single-gene deletion mutants and five double-gene deletion mutants. Analysis of bacterial supernatants revealed that none of the mutants produced significantly less IAA than the wild-type strain. When mutagenesis experiments designed to inactivate the IAN-IAM pathway failed to generate mutants deficient in the ability to synthesize IAA, speculation of the presence of a third pathway was ignited. LC-MS-MS analyses of supernatant from bacterial cultures revealed the presence of indole lactic acid (ILA), indole-2-ethanol (IEt) indole aldehyde (IAld) and indole-pyruvic acid (IPyA). These compounds are consistent with the existence of a third pathway in strain UW4, the IPyA pathway, which is compensating for the disruptions made in the IAN-IAM pathways. A search for candidate genes that might encode

enzymes that are part of the IPyA pathway was undertaken and several enzymes with the potential to mediate IPyA pathway reactions were identified based on sequence similarity to other functionally characterized enzymes.

6.5 The role of IaaM and Aux proteins in IAA biosynthesis

The implication of the IAN and IAM pathways in UW4 was based on the detection of the IAN and IAM metabolites in Trp-fed cultures. These two pathways can stand on their own as separate individual pathways (i.e. Trp→IAN→IAA and Trp→IAM→IAA) or merge together as one pathway (Trp→IAN→IAM→IAA). The enzymes (Nit and NthAB) responsible for the conversion of IAN→IAM were experimentally verified in strain UW4 (258). However, there remained the question of whether the IAM pathway can also stand alone in this strain. The previously characterized IAM pathway utilizes a tryptophan monooxygenase (TMO), that converts Trp into IAM and an amidase that converts IAM into IAA. Since the amidase was experimentally validated in *Chapter 2*, the focus of *Chapter 5* was to determine whether a TMO is also functional in this strain. Two genes encoding putative TMOs (*iaaM* and *aux*) were identified in the genome of strain UW4 and were targeted for biochemical characterization.

The IaaM and Aux proteins were both classified as flavin monoamine oxidases (MAOs) based on characteristic sequence motifs. Sequence comparisons of IaaM and Aux to several MAO family members including lysine monooxygenase (LMO), tryptophan monooxygenase (TMO), phenylalanine oxidase (PAO) and L-amino acid oxidase (LAAO), revealed that IaaM shared the greatest sequence identity (>90%) and structural similarity with LMO. A phylogenetic analysis

reinforced this by showing that IaaM is most closely related to LMOs. Aux shared the greatest sequence identity with a broad-spectrum LAAO and was most structurally similar to TMO. However, a phylogenetic analysis indicated that Aux is most closely related to PAO. Although both IaaM and Aux were implicated as putative TMOs, enzyme assays were not successful in detecting the expected amide product (IAM). However, changes in the absorption spectrum of IaaM suggest that both Trp and Lys are substrates. We postulate that the IaaM protein assumes both monooxygenase and oxidase activity, acting on both Trp and Lys, however it is unclear whether its primary role is in IAA biosynthesis.

6.6 Limitations

The effect of IAA, secreted by strain UW4, on canola root growth, is based on the underlying assumption that the measured concentration in the bacterial cultures is available to the target plant tissue. This assumption may be erroneous in view of the fact that plant uptake of bacterial IAA was not measured. IAA is a diffusible bacterial metabolite that alters plant growth depending on the amount that actually reaches the plant cell. However, IAA secreted by the bacteria may be degraded by chemical or enzymatic oxidation before it has a chance to be taken up by the plant.

The range of effective IAA concentrations varies according to the plant species or to the sensitivity of the plant organ to IAA. Generally, only a small window of exogenous IAA (i.e. bacterially secreted) promotes growth. Therefore, the effect that we see for canola seedlings may not translate to the same effect for another plant species. Moreover, if the IAA content within the canola seeds was already optimal prior to inoculation with UW4 or UW4 transformants, then additional IAA

contributed by the bacterium may reach inhibitory levels. Alternatively, depending on the extent of IAA-deficit preexisting in the seed, additional IAA input from the bacteria may not always be enough to optimally stimulate root elongation. Although all seeds were stored and treated in the same manner, the variance in IAA-content between individual seeds was not determined. Increasing the seed sample size might account for that variance and reduce uncertainty with respect to the effect on root elongation.

It is important to note that the amount of IAA produced by the UW4 strains *in vitro*, is a result of the specific experimental conditions under which those cells were cultured at that time (i.e., temperature, pH, growth-phase, oxygen levels, Trp concentration). It is not currently technically possible to determine the amount of IAA that is secreted by the bacteria upon binding to the seed. As such, we cannot accurately define the level of IAA that the inoculated seeds are actually exposed to during the growth pouch assay. This is a function of (1) the number of bacterial cells that successfully colonize the seed and (2) the rate of IAA production and secretion by the cells. The latter is dependent on the conditions under which the bacteria are growing (i.e., pH, temperature, growth phase, Trp, carbon and nitrogen availability). As such, a proportional correlation between the measured IAA concentration in bacterial culture and the resulting plant growth effect upon inoculation with that strain cannot be made precisely.

Pseudomonas sp. UW4 utilizes at least 3 different pathways to produce IAA. The genetic and environmental factors that regulate these pathways are unknown. The relative activities of each IAA pathway may also depend on the associated plant species, and on the developmental state of the

plant. Some of these pathways are constitutively expressed, while others are inducible. Some enzymes involved in IAA biosynthesis are known to be regulated by IAA, as well as by IAA-precursors. Separate pathways may share a common intermediate, merging together from that point, or subsequently separating into different pathways. It is likely that multiple, interacting, and redundant pathways are co-regulated. The promiscuity of the enzymes implicated in IAA biosynthesis (i.e., they catalyze multiple types of reactions distinct from their main function) adds another element of complexity when attempting to decipher their role in IAA biosynthesis. It is possible that although they are able to perform a given reaction *in vitro*, their primary role *in vivo* is not related to the production of IAA.

Single and double-gene disruptions in the IAN-IAM pathway did not produce mutants with a reduced capacity to produce IAA. While this suggests that another biosynthesis pathway exists in UW4, it is also possible that multiple gene copies or alternative IAN-IAM pathway genes may be present. Nevertheless, based on these mutagenesis experiments, the IAN-IAM pathways are believed to contribute relatively little to the measurable levels of IAA produced by strain UW4. However, we cannot determine the contribution of the third pathway until we define the specific catabolic role of candidate IPyA pathway enzymes.

In nature, the complexity of the rhizosphere environment and the intricacies of plant-bacterial interactions alter the outcome that bacterial IAA will have on the plant. From the preceding results, it is evident that levels of IAA produced by strain UW4 are at least partially responsible for the effect of the bacterium on a host plant. However, plant growth is likely regulated not only by IAA but also by other related compounds such as ILA, which can counteract the effect of IAA to some extent.

Furthermore, there is also interaction between IAA and ethylene; therefore, ACC deaminase also contributes to the effect on plant growth. Additionally, our understanding of the effect of bacterial IAA on plants is confounded by the possible production of cytokinins by UW4. It is recognized that IAA and cytokinins interact to regulate a variety of physiological processes in plants and that these interactions may be both antagonistic and synergistic (Coenen and Lomax, 1997). An increase in the concentration of either one of IAA or cytokinin, can decrease the levels of the other in plant tissues (Elkof et al., 1997, Eklof et al., 2000). Since UW4 displays a combination of different modes of plant-growth-promoting actions, we cannot exclude the possibility that a combination of different mechanisms, besides, or in addition to, IAA production, may account for the enhanced plant growth promotion. The crosstalk between the multiple interdependent plant-growth-promoting mechanisms including IAA and its derivatives, ethylene and ACC deaminase remain to be elucidated in detail in UW4.

6.7 Conclusion: Just the Beginning

Today, many studies report stimulation of plant growth following inoculation with an IAA-producing PGPB. However, the specific mode of IAA production by the PGPB is rarely elucidated. In part, this is due to the overwhelming complexity of IAA biosynthesis and regulation. The research reported herein strived to decipher IAA biosynthesis pathways at the genetic and biochemical level in a particularly effective PGPB strain. The work began with an initial genomic screen for putative genes that encode enzymes involved in IAA biosynthesis. This screen identified six candidate enzymes (Nit, NthAB, Ami, Phe, IaaM and Aux). The role of Nit, NthAB and Ami in the IAN-IAM pathway was experimentally verified through biochemical assays. The implication of

Phe in IAA biosynthesis is based on the over-production of IAA resulting from the over-expression of the *phe* gene. However, its catalytic role as aldoxime dehydratase that converts IAOx into IAN remains to be verified. The IaaM and Aux enzymes were implicated in the IAM pathway as putative TMOs. Our results suggest that IaaM has both monooxygenase and oxidase activity and can act on tryptophan and lysine. The Aux enzyme is likely a general L-amino acid oxidase, whose primary role is not in IAA biosynthesis. Biochemical evidence of the IPyA pathway was also found and candidate IPyA pathway genes coding for an aminotransferase, α -keto acid decarboxylase and aldehyde oxidase were identified. The functional role of these genes remains to be determined. If indeed IaaM has oxidase activity, it would produce IPyA and therefore be involved in that pathway instead of the IAM pathway. To date, the majority of research on IAA biosynthesis describes three separate pathways classified in terms of their intermediates- IAN, IAM and IPyA. Each of these pathways is mediated by a set of enzymes, many of which are traditionally assumed to exist for that specific catalytic role. This lends the possibility of missing other, novel, enzymes that may also incidentally serve that function, if looking only for a traditional "IAA gene". For instance, as this work has shown, genes annotated as TMOs may in fact be LAAOs, or both. Nitrilases traditionally implicated in the IAN pathway, also serve in IAM pathway, bridging the two. The presence of IPyA in bacterial cultures does not necessarily imply that the bacterium utilizes the traditional IPDC enzyme. UW4 does not have an IPDC homologue, therefore a novel enzyme may perform that role. Perhaps, discrete separation of the different pathways doesn't need to be made. In other words, all three pathways are interconnected and one enzyme can act in more than one pathway.

References

1. Hardoim PR, Overbeek LS van, Berg G, Pirttilä AM, Compant S, Campisano A, Döring M, Sessitsch A. 2015. The Hidden World within Plants: Ecological and Evolutionary Considerations for Defining Functioning of Microbial Endophytes. *Microbiol Mol Biol Rev* 79:293–320.
2. Bacon CW, White JF. 2016. Functions, mechanisms and regulation of endophytic and epiphytic microbial communities of plants. *Symbiosis*. 68: 1-3.
3. Glick B, Penrose D, Li J. 1998. A model for the lowering of plant ethylene concentrations by plant growth-promoting bacteria. *J Theor Biol* 190:63–8.
4. Duca D, Lorv J, Patten CL, Rose D, Glick BR. 2014. Indole-3-acetic acid in plant–microbe interactions. *Antonie Van Leeuwenhoek* 106:85–125.
5. Kennedy IR, Pereggerk LL, Wood C, Deaker R, Gilchrist K. 2006. Biological nitrogen fixation in non-leguminous field crops: Facilitating the evolution of an effective association between *Azospirillum* and wheat. *Plant Soil* 194:65–79.
6. Kennedy IR, Choudhury ATMA, Kecskés ML. 2004. Non-symbiotic bacterial diazotrophs in crop-farming systems: Can their potential for plant growth promotion be better exploited *Soil Biology and Biochemistry*.1229:1244
7. Cattelan AJ, Hartel PG, Fuhrmann JJ. 1999. Screening for Plant Growth-Promoting Rhizobacteria to Promote Early Soybean Growth. *Soil Sci Soc Am J* 63:1670–1680.
8. Pal K.K. 2001. Suppression of maize root diseases caused by *Macrophomina phaseolina*, *Fusarium moniliforme* and *Fusarium graminearum* by plant growth promoting rhizobacteria. *Microbiol Res* 156:209–223.
9. Glick, B. R., & Bashan, Y. 1997. Genetic manipulation of plant growth-promoting bacteria to enhance biocontrol of phytopathogens. *Biotechnology advances*, 2: 353-378.
10. Rodríguez H, Fraga R. 1999. Phosphate solubilizing bacteria and their role in plant growth promotion. *Biotechnol Adv* 17:319–339.
11. Alvarez MI, Sueldo RJ, Barassi CA. 1996. Effect of *Azospirillum* on coleoptile growth in wheat seedlings under water stress. *Cereal Res Commun* 24:101–107.

12. Saleem M, Arshad M, Hussain S, Bhatti AS. 2007. Perspective of plant growth promoting rhizobacteria (PGPR) containing ACC deaminase in stress agriculture. *J Ind Microbiol Biotechnol.* 10: 635-648.
13. Forni C, Duca D, Glick BR. 2016. Mechanisms of plant response to salt and drought stress and their alteration by rhizobacteria. *Plant Soil* 1–22.
14. Stajner D, Kevresan S, Gasic O, Mimica-Dukic N, Zongli H. 1997. Nitrogen and *Azotobacter chroococcum* enhance oxidative stress tolerance in sugar beet. *Biol Plant* 39:441–445.
15. Revillas JJ, Rodelas B, Pozo C, Martínez-Toledo M V., González-López J. 2000. Production of B-group vitamins by two *Azotobacter* strains with phenolic compounds as sole carbon source under diazotrophic and adiazotrophic conditions. *J Appl Microbiol* 89:486–493.
16. Sierra S, Rodelas B, Martínez-Toledo M V., Pozo C, González-López J. 1999. Production of B-group vitamins by two *Rhizobium* strains in chemically defined media. *J Appl Microbiol* 86:851–858.
17. Vessey J. 2003. Plant growth promoting rhizobacteria as biofertilizers. *Plant Soil* 255:571–586.
18. Compant S, Clément C, Sessitsch A. 2010. Plant growth-promoting bacteria in the rhizo- and endosphere of plants: Their role, colonization, mechanisms involved and prospects for utilization. *Soil Biol Biochem.*5:669-678
19. Walker TS, Bais HP, Grotewold E, Vivanco JM. 2003. Root exudation and rhizosphere biology. *Plant Physiol* 132:44–51.
20. Foley J a. 2011. Can We Feed the World & Sustain the Planet? *Sci Am* 305:60–65.
21. Berg G. 2009. Plant-microbe interactions promoting plant growth and health: Perspectives for controlled use of microorganisms in agriculture. *Appl Microbiol Biotechnol.*1:11-18.
22. Miller SA, Beed FD, Harmon CL. 2009. Plant disease diagnostic capabilities and networks. *Annu Rev Phytopathol* 47:15–38.
23. Morrissey JP, Dow JM, Mark GL, O’Gara F. 2004. Are microbes at the root of a solution to world food production? Rational exploitation of interactions between microbes and plants can help to transform agriculture. *EMBO Rep* 5:922–926.
24. Glick BR. 2014. Bacteria with ACC deaminase can promote plant growth and help to feed the world. *Microbiol Res* 169:30–39.
25. Timmusk S, Behers L, Muthoni J, Muraya A, Aronsson A-C. 2017. Perspectives and Challenges of Microbial Application for Crop Improvement. *Front Plant Sci* 8.

26. Marrone PG. 2014. The market and potential for biopesticides, In ACS Symposium Series. p. 245–258
27. Bashan Y, de-Bashan LE, Prabhu SR, Hernandez JP. 2014. Advances in plant growth-promoting bacterial inoculant technology: Formulations and practical perspectives (1998-2013). *Plant Soil*.2:1-33.
28. Bhau BS, Phukon P, Ahmed R, Gogoi B, Borah B, Baruah J, Sharma DK, Wann SB. 2016. Microbial Inoculants in Sustainable Agricultural Productivity. *Microb Inoculants Sustain Agric Product Vol 2 Funct Appl* 253–270.
29. Berg G, Eberl L, Hartmann A. 2005. The Rhizosphere as a Reservoir for Opportunistic Human Pathogenic Bacteria. *Environ Microbiol* 7:1672–1685.
30. Teale WD, Paponov I a., Palme K. 2006. Auxin in action: signalling, transport and the control of plant growth and development. *Nat Rev Mol Cell Biol* 7:847–859.
31. Grossmann K. 2010. Auxin herbicides: Current status of mechanism and mode of action. *Pest Manag Sci.* 2: 113-120
32. Halliday KJ, Martínez-García JF, Josse EM. 2009. Integration of light and auxin signaling. *Cold Spring Harb Perspect Biol.* 1(6), a001586.
33. Paque S, Weijers D. 2016. Auxin: the plant molecule that influences almost anything. *BMC Biol* 14:67.
34. Petersson S V, Johansson AI, Kowalczyk M, Makoveychuk A, Wang JY, Moritz T, Grebe M, Benfey PN, Sandberg G, Ljung K. 2009. An auxin gradient and maximum in the *Arabidopsis thaliana* root apex shown by high-resolution cell-specific analysis of IAA distribution and synthesis. *Plant Cell* 21:1659–1668.
35. Petrasek J, Friml J. 2009. Auxin transport routes in plant development. *Development* 136:2675–2688.
36. Tromas A, Perrot-Rechenmann C. 2010. Recent progress in auxin biology. *Comptes Rendus - Biol* 333:297–306.
37. Ljung K, Hull AK, Celenza J, Yamada M, Estelle M, Normanly J, Sandberg G. 2005. Sites and regulation of auxin biosynthesis in *Arabidopsis thaliana* roots. *Plant Cell* 17:1090–104.
38. Reid AE, Kim SW, Seiner B, Fowler FW, Hooker J, Ferrieri R, Babst B, Fowler JS. 2011. Radiosynthesis of C-11 labeled auxin (3-indolyl[1- ¹¹C]acetic acid) and its derivatives from gramine. *J Label Compd Radiopharm* 54:433–437.

39. Pencík A, Simonovik B, Petersson S V, Henyková E, Simon S, Greenham K, Zhang Y, Kowalczyk M, Estelle M, Zazímalová E, Novák O, Sandberg G, Ljung K. 2013. Regulation of auxin homeostasis and gradients in *Arabidopsis thaliana* roots through the formation of the indole-3-acetic acid catabolite 2-oxindole-3-acetic acid. *Plant Cell* 25:3858–70.
40. Boerjan W, Cervera MT, Delarue M, Beeckman T, Dewitte W, Bellini C, Caboche M, Van Onckelen H, Van Montagu M, Inzé D. 1995. Superroot, a recessive mutation in *Arabidopsis thaliana*, confers auxin overproduction. *Plant Cell* 7:1405–1419.
41. Stepanova AN, Robertson-Hoyt J, Yun J, Benavente LM, Xie DY, Doleval K, Schlereth A, Jurgens G, Alonso JM. 2008. TAA1-Mediated Auxin Biosynthesis Is Essential for Hormone Crosstalk and Plant Development. *Cell* 133:177–191.
42. Okada K, Ueda J, Komaki MK, Bell CJ, Shimura Y. 1991. Requirement of the Auxin Polar Transport System in Early Stages of *Arabidopsis thaliana* Floral Bud Formation. *Plant Cell* 3:677–684.
43. Patten CL, Blakney AJC, Coulson TJD. 2013. Activity, distribution and function of indole-3-acetic acid biosynthetic pathways in bacteria. *Crit Rev Microbiol* 39:395–415.
44. Sergeeva E, Liaimer A, Bergman B. 2002. Evidence for production of the phytohormone indole-3-acetic acid by cyanobacteria. *Planta* 215:229–238.
45. Patten CL, Glick BR. 1996. Bacterial biosynthesis of indole-3-acetic acid. *Can J Microbiol* 42:207–220.
46. Spaepen S, Vanderleyden J, Remans R. 2007. Indole-3-acetic acid in microbial and microorganism-plant signaling. *FEMS Microbiol Rev* 31:425–448.
47. Zambryski PC. 1992. Chronicles from the *Agrobacterium*-Plant Cell DNA Transfer Story. *Annu Rev Plant Physiol Plant Mol Biol* 43:465–490.
48. Thomashow LS, Reeves S, Thomashow MF. 1984. Crown gall oncogenesis: evidence that a T-DNA gene from the *Agrobacterium* Ti plasmid pTiA6 encodes an enzyme that catalyzes synthesis of indoleacetic acid. *Proc Natl Acad Sci U S A* 81:5071–5.
49. Clark E, Manulis S, Ophir Y, Barash I, Gafni Y. 1993. Cloning and characterization of *iaaM* and *iaaH* from *Erwinia herbicola* pathovar *gypsophylae*. *Phytopathology*. 2:234-240.
50. Rodríguez-Moreno L, Barceló-Muñoz A, Ramos C. 2008. In vitro Analysis of the Interaction of *Pseudomonas savastanoi* pvs. *savastanoi* and *nerii* with Micropropagated Olive Plants. *Phytopathology* 98:815–822.

51. Cerboneschi M, Decorosi F, Biancalani C, Ortenzi MV, Macconi S, Giovannetti L, Viti C, Campanella B, Onor M, Bramanti E, Tegli S. 2016. Indole-3-acetic acid in plant-pathogen interactions: a key molecule for in planta bacterial virulence and fitness. *Res Microbiol* 167:774–787.
52. Yang S, Zhang Q, Guo J, Charkowski AO, Glick BR. 2007. Global Effect of Indole-3-Acetic Acid Biosynthesis on Multiple Virulence Factors of *Erwinia*. *Applied and environmental microbiology*. 4:1079-1088.
53. Aragón IM, Pérez-Martínez I, Moreno-Pérez A, Cerezo M, Ramos C. 2014. New insights into the role of indole-3-acetic acid in the virulence of *Pseudomonas savastanoi* pv. *savastanoi*. *FEMS Microbiol Lett* 356:184–192.
54. Fu J, Liu H, Li Y, Yu H, Li X, Xiao J, Wang S. 2011. Manipulating broad-spectrum disease resistance by suppressing pathogen-induced auxin accumulation in rice. *Plant Physiol* 155:589–602.
55. Alfano JR, Collmer A. 2004. Type III secretion system effector proteins: double agents in bacterial disease and plant defense. *Annu Rev Phytopathol* 42:385–414.
56. González-Lamothe R, El Oirdi M, Brisson N, Bouarab K. 2012. The Conjugated Auxin Indole-3-Acetic Acid-Aspartic Acid Promotes Plant Disease Development. *Plant Cell* 24:1–17.
57. Cui F, Wu S, Sun W, Coaker G, Kunkel B, He P, Shan L. 2013. The *Pseudomonas syringae* type III effector AvrRpt2 promotes pathogen virulence via stimulating *Arabidopsis thaliana* auxin/indole acetic acid protein turnover. *Plant physiology*.2:1018-1029.
58. Chen Z, Agnew JL, Cohen JD, He P, Shan L, Sheen J, Kunkel BN. 2007. *Pseudomonas syringae* type III effector AvrRpt2 alters *Arabidopsis thaliana thaliana* auxin physiology. *Proc Natl Acad Sci U S A* 104:20131–20136.
59. Navarro L, Dunoyer P, Jay F, Arnold B, Dharmasiri N, Estelle M, Voinnet O, Jones JDG. 2006. A plant miRNA contributes to antibacterial resistance by repressing auxin signaling. *Science* 312:436–9.
60. Ding X, Cao Y, Huang L, Zhao J, Xu C, Li X, Wang S. 2008. Activation of the indole-3-acetic acid-amido synthetase GH3-8 suppresses expansin expression and promotes salicylate- and jasmonate-independent basal immunity in rice. *Plant Cell* 20:228–40.
61. Cernadas RA, Benedetti CE. 2009. Role of auxin and gibberellin in citrus canker development and in the transcriptional control of cell-wall remodeling genes modulated by *Xanthomonas axonopodis* pv. *citri*. *Plant Sci* 177:190–195.
62. Leveau JHJ, Lindow SE. 2005. Utilization of the plant hormone indole-3-acetic acid for growth by *Pseudomonas putida* strain 1290. *Appl Environ Microbiol* 71:2365–2371.

63. Robert-Seilaniantz A, Grant M, Jones JDG. 2011. Hormone Crosstalk in Plant Disease and Defense: More Than Just Jasmonate-Salicylate Antagonism. *Annu Rev Phytopathol* 49:317–343.
64. Gepstein S, Glick BR. 2013. Strategies to ameliorate abiotic stress-induced plant senescence. *Plant Mol Biol* 82:623–633.
65. Park JE, Seo PJ, Lee AK, Jung JH, Kim YS, Park CM. 2007. An *Arabidopsis thaliana* GH3 gene, encoding an auxin-conjugating enzyme, mediates phytochrome B-regulated light signals in hypocotyl growth. *Plant Cell Physiol* 48:1236–1241.
66. Wang D, Pajerowska-Mukhtar K, Culler AH, Dong X. 2007. Salicylic Acid Inhibits Pathogen Growth in Plants through Repression of the Auxin Signaling Pathway. *Curr Biol* 17:1784–1790.
67. Kazan K, Manners JM. 2009. Linking development to defense: auxin in plant-pathogen interactions. *Trends Plant Sci.*7:373-382.
68. Mutka AM, Fawley S, Tsao T, Kunkel BN. 2013. Auxin promotes susceptibility to *Pseudomonas syringae* via a mechanism independent of suppression of salicylic acid-mediated defenses. *Plant J* 74:746–754.
69. Pontier D, Balagué C, Roby D. 1998. The hypersensitive response. A programmed cell death associated with plant resistance. *C R Acad Sci III* 321:721–734.
70. Gopalan S. 2008. Reversal of an immunity associated plant cell death program by the growth regulator auxin. *BMC Res Notes* 1:126.
71. Rayle DL. 1973. Auxin-induced hydrogen-ion secretion in *Avena* coleoptiles and its implications. *Planta* 114:63–73.
72. Rayle DL, Cleland RE. 1992. The Acid Growth Theory of auxin-induced cell elongation is alive and well. *Plant Physiol* 99:1271–1274.
73. Cleland RE. 1992. Auxin-induced growth of *Avena* coleoptiles involves two mechanisms with different pH optima. *Plant Physiol* 99:1556–1561.
74. Fry SC, Smith RC, Renwick KF, Martin DJ, Hodge SK, Matthews KJ. 1992. Xyloglucan endotransglycosylase, a new wall-loosening enzyme activity from plants. *Biochem J* 282 (Pt 3:821–8.
75. Catala C. 2000. Auxin-Regulated Genes Encoding Cell Wall-Modifying Proteins Are Expressed during Early Tomato Fruit Growth. *Plant Physiol* 122:527–534.
76. Kochar M, Upadhyay A, Srivastava S. 2011. Indole-3-acetic acid biosynthesis in the biocontrol strain *Pseudomonas fluorescens* Psd and plant growth regulation by hormone overexpression. *Res Microbiol* 162:426–435.

77. Albert M, Werner M, Proksch P, Fry SC, Kaldenhoff R. 2004. The cell wall-modifying xyloglucan endotransglycosylase/hydrolase LeKTH1 is expressed during the defence reaction of tomato against the plant parasite *Cuscuta reflexa*. *Plant Biol* 6:402–407.
78. Patten CL, Glick BR. 2002. Role of *Pseudomonas putida* indoleacetic acid in development of the host plant root system. *Appl Environ Microbiol* 68:3795–801.
79. Arshad M, Frankenberger WT. 1991. Microbial production of plant hormones. *Plant Soil* 133:1–8.
80. Reed RC, Brady SR, Muday GK. 1998. Inhibition of auxin movement from the shoot into the root inhibits lateral root development in *Arabidopsis thaliana*. *Plant Physiol* 118:1369–1378.
81. Thimann K V. 1939. Auxins and the inhibition of plant growth. *Biol Rev* 14:314–337.
82. Baudoin E, Lerner A, Mirza MS, El Zembrany H, Prigent-Combaret C, Jurkevich E, Spaepen S, Vanderleyden J, Nazaret S, Okon Y, Moëgne-Loccoz Y. 2010. Effects of *Azospirillum brasilense* with genetically modified auxin biosynthesis gene ipdC upon the diversity of the indigenous microbiota of the wheat rhizosphere. *Res Microbiol* 161:219–226.
83. Apine OA, Jadhav JP. 2011. Optimization of medium for indole-3-acetic acid production using *Pantoea agglomerans* strain PVM. *J Appl Microbiol* 110:1235–1244.
84. Comai L, Kosuge T. 1983. Transposable element that causes mutations in a plant pathogenic *Pseudomonas* sp. *J Bacteriol* 154:1162–1167.
85. Liu ST, Perry KL, Schardl CL, Kado CI. 1982. *Agrobacterium* Ti plasmid indoleacetic acid gene is required for crown gall oncogenesis. *Proc Natl Acad Sci U S A* 79:2812–6.
86. Dobbelaere S, Croonenborghs A, Thys A, Vande Broek A, Vanderleyden J. 1999. Phytostimulatory effect of *Azospirillum brasilense* wild type and mutant strains altered in IAA production on wheat. *Plant Soil* 6:155–164.
87. Malhotra M, Srivastava S. 2008. An ipdC gene knock-out of *Azospirillum brasilense* strain SM and its implications on indole-3-acetic acid biosynthesis and plant growth promotion. *Antonie van Leeuwenhoek, Int J Gen Mol Microbiol* 93:425–433.
88. Patten CL, Glick BR. 2002. Regulation of indoleacetic acid production in *Pseudomonas putida* GR12-2 by tryptophan and the stationary-phase sigma factor RpoS. *Can J Microbiol* 48:635–642.
89. Barbieri P, Galli E. 1993. Effect on wheat root development of inoculation with an *Azospirillum brasilense* mutant with altered indole-3-acetic acid production. *Res Microbiol* 144:69–75.

90. Beyeler M, Keel C, Michaux P, Haas D. 1999. Enhanced production of indole-3-acetic acid by a genetically modified strain of *Pseudomonas fluorescens* CHA0 affects root growth of cucumber, but does not improve protection of the plant against *Pythium* root rot. FEMS Microbiol Ecol 28:225–233.
91. Bianco C, Defez R. 2010. A *Sinorhizobium meliloti* IAA-overproducing strain improves phosphate solubilization and Medicago plant yield. Appl Env Microbiol AEM.02756-09.
92. Malhotra M, Srivastava S. 2006. Targeted engineering of *Azospirillum brasilense* SM with indole acetamide pathway for indoleacetic acid over-expression. Can J Microbiol 52:1078–84.
93. Sarwar M, Kremer RJ. 1995. Enhanced suppression of plant-growth through production of L-tryptophan derived compounds by deleterious rhizobacteria. Plant Soil 172:261–269.
94. Suzuki S, He Y, Oyaizu H. 2003. Indole-3-acetic acid production in *Pseudomonas fluorescens* HP72 and its association with suppression of creeping bentgrass brown patch. Curr Microbiol 47:138–143.
95. Xie H, Pasternak JJ, Glick BR. 1996. Isolation and characterization of mutants of the plant growth promoting rhizobacterium *Pseudomonas putida* GR12-2 that overproduce indoleacetic-acid. Curr Microbiol 32:67–71.
96. Dubeikovskiy AN, Mordukhova EA, Kochetkov V V., Polikarpova FY, Boronin AM. 1993. Growth promotion of blackcurrant softwood cuttings by recombinant strain *Pseudomonas fluorescens* BSP53a synthesizing an increased amount of indole-3-acetic acid. Soil Biol Biochem 25:1277–1281.
97. Jangu OP, Sindhu SS. 2011. Differential Response of Inoculation with Indole Acetic Acid Producing *Pseudomonas* Sp. In Green Gram (*Vigna radiata* L.) and Black Gram (*Vigna mungo* L.). Microbiol J 1:159–173.
98. Badenoch-Jones J, Summons RE, Rolfe BG, Letham DS. 1984. Phytohormones, *Rhizobium* mutants, and nodulation in legumes. IV. Auxin metabolites in pea root nodules. J Plant Growth Regul 3:23–39.
99. Mathesius U, Schlaman HRM, Spaik HP, Sautter C, Rolfe BG, Djordjevic MA. 1998. Auxin transport inhibition precedes root nodule formation in white clover roots and is regulated by flavonoids and derivatives of chitin oligosaccharides. Plant J 14:23–34.
100. Lambrecht M, Okon Y, Vande Broek A, Vanderleyden J. 2000. Indole-3-acetic acid: A reciprocal signalling molecule in bacteria-plant interactions. Trends Microbiol.7:298-300.
101. Defez R, Esposito R, Angelini C, Bianco C. 2016. Overproduction of indole-3-acetic acid in free-living rhizobia induces transcriptional changes resembling those occurring in nodule bacteroids. Mol Plant-Microbe Interact 29:484–495.

102. Defez R, Andreozzi A, Bianco C. 2017. The Overproduction of Indole-3-Acetic Acid (IAA) in Endophytes Upregulates Nitrogen Fixation in Both Bacterial Cultures and Inoculated Rice Plants. *Microb Ecol.* p.1-12.
103. Kim YC, Leveau J, McSpadden Gardener BB, Pierson EA, Pierson LS, Ryu CM. 2011. The multifactorial basis for plant health promotion by plant-associated bacteria. *Appl Environ Microbiol.* 5: 1548-1555.
104. Halda-Alija L. 2003. Identification of indole-3-acetic acid producing freshwater wetland rhizosphere bacteria associated with *Juncus effusus* L. *Can J Microbiol* 49:781–787.
105. Wakagi T, Fukuda E, Ogawa Y, Kino H, Matsuzawa H. 2002. A novel bifunctional molybdo-enzyme catalyzing both decarboxylation of indolepyruvate and oxidation of indoleacetaldehyde from a thermoacidophilic archaeon, *Sulfolobus* sp. strain 7. *FEBS Lett* 510:196–200.
106. Chung KT, Anderson GM, Fulk GE. 1975. Formation of indoleacetic acid by intestinal anaerobes. *J Bacteriol* 124:573–575.
107. Imperlini E, Bianco C, Lonardo E, Camerini S, Cermola M, Moschetti G, Defez R. 2009. Effects of indole-3-acetic acid on *Sinorhizobium meliloti* survival and on symbiotic nitrogen fixation and stem dry weight production. *Appl Microbiol Biotechnol* 83:727–738.
108. Nwodo UU, Green E, Okoh AI. 2012. Bacterial exopolysaccharides: Functionality and prospects. *Int J Mol Sci.* 11;14002-14015.
109. Ruas-Madiedo P, Hugenholtz J, Zoon P. 2002. An overview of the functionality of exopolysaccharides produced by lactic acid bacteria. In *International Dairy Journal.* p. 163–171
110. Nichols CM, Lardière SG, Bowman JP, Nichols PD, Gibson JAE, Guézennec J. 2005. Chemical characterization of exopolysaccharides from Antarctic marine bacteria. *Microb Ecol* 49:578–589.
111. Junge K, Eicken H, Deming JW. 2004. Bacterial Activity at -2 to -20 degrees C in Arctic wintertime sea ice. *Appl Environ Microbiol* 70:550–557.
112. Bianco C, Imperlini E, Defez R. 2009. Legumes like more IAA. *Plant Signal Behav* 4:763–5.
113. Donati AJ, Lee HI, Leveau JHJ, Chang WS. 2013. Effects of Indole-3-Acetic Acid on the Transcriptional Activities and Stress Tolerance of *Bradyrhizobium japonicum*. *PLoS One* 8:1–11.
114. Masuda S, Mizusawa K, Narisawa T, Tozawa Y, Ohta H, Takamiya KI. 2008. The bacterial stringent response, conserved in chloroplasts, controls plant fertilization. *Plant Cell Physiol* 49:135–141.

115. Chowdhury N, Kwan BW, Wood TK. 2016. Persistence Increases in the Absence of the Alarmone Guanosine Tetraphosphate by Reducing Cell Growth. *Sci Rep* 6:20519.
116. Srivatsan A, Wang JD. 2008. Control of bacterial transcription, translation and replication by (p)ppGpp. *Curr Opin Microbiol.* 2: 100-105.
117. Barker MM, Gaal T, Gourse RL. 2001. Mechanism of regulation of transcription initiation by ppGpp. II. Models for positive control based on properties of RNAP mutants and competition for RNAP. *J Mol Biol* 305:689–702.
118. Navarro Llorens JM, Tormo A, Martinez-Garcia E. 2010. Stationary phase in gram-negative bacteria. *FEMS Microbiol Rev.* 4:476-495.
119. Bianco C, Imperlini E, Calogero R, Senatore B, Amoresano A, Carpentieri A, Pucci P, Defez R. 2006. Indole-3-acetic acid improves *Escherichia coli*'s defences to stress. *Arch Microbiol* 185:373–382.
120. Scott JC, Greenhut I V., Leveau JHJ. 2013. Functional Characterization of the Bacterial *iac* Genes for Degradation of the Plant Hormone Indole-3-Acetic Acid. *J Chem Ecol* 39:942–951.
121. Krell T, Lacal J, Muñoz-Martínez F, Reyes-Darias JA, Cadirci BH, García-Fontana C, Ramos JL. 2011. Diversity at its best: Bacterial taxis. *Environ Microbiol.*5:1115-1124.
122. Parales RE, Luu RA, Chen GY, Liu X, Wu V, Lin P, Hughes JG, Nesteryuk V, Parales J V., Ditty JL. 2013. *Pseudomonas putida* F1 has multiple chemoreceptors with overlapping specificity for organic acids. *Microbiol (United Kingdom)* 159:1086–1096.
123. Drogue B, Doré H, Borland S, Wisniewski-Dyé F, Prigent-Combaret C. 2012. Which specificity in cooperation between phytostimulating rhizobacteria and plants? *Res Microbiol* 163:500–510.
124. Monier JM, Lindow SE. 2005. Aggregates of resident bacteria facilitate survival of immigrant bacteria on leaf surfaces. *Microb Ecol* 49:343–352.
125. Spaepen S, Das F, Luyten E, Michiels J, Vanderleyden J. 2009. Indole-3-acetic acid-regulated genes in *Rhizobium etli* CNPAF512: Research Letter. *FEMS Microbiol Lett* 291:195–200.
126. Zúñiga A, Poupin MJ, Donoso R, Ledger T, Guiliani N, Gutiérrez R a, González B. 2013. Quorum sensing and indole-3-acetic acid degradation play a role in colonization and plant growth promotion of *Arabidopsis thaliana* by *Burkholderia phytofirmans* PsJN. *Mol Plant-Microbe Interact* 26:546–53.
127. Matsukawa E, Nakagawa Y, Iimura Y, Ñ MH. 2007. Stimulatory effect of indole-3-acetic acid on aerial mycelium formation and antibiotic production in *Streptomyces* spp . *Actinomycetologica* 21:32–39.

128. Liu P, Nester EW. 2006. Indoleacetic acid, a product of transferred DNA, inhibits vir gene expression and growth of *Agrobacterium tumefaciens* C58. *Proc Natl Acad Sci U S A* 103:4658–4662.
129. Kittell BL, Helinski DR, Ditta GS. 1989. Aromatic aminotransferase activity and indoleacetic acid production in *Rhizobium meliloti*. *J Bacteriol* 171:5458–5466.
130. Pedraza RO, Ramírez-Mata A, Xiqui ML, Baca BE. 2004. Aromatic amino acid aminotransferase activity and indole-3-acetic acid production by associative nitrogen-fixing bacteria. *FEMS Microbiol Lett* 233:15–21.
131. Ryu RJ, Patten CL. 2008. Aromatic amino acid-dependent expression of indole-3-pyruvate decarboxylase is regulated by *tyrR* in *Enterobacter cloacae* UW5. *J Bacteriol* 190:7200–7208.
132. Costacurta a, Keijers V, Vanderleyden J. 1994. Molecular cloning and sequence analysis of an *Azospirillum brasilense* indole-3-pyruvate decarboxylase gene. *Mol Gen Genet* 243:463–472.
133. Koga J, Adachi T, Hidaka H. 1991. IAA Biosynthetic Pathway from Tryptophan via Indole-3-pyruvic Acid in *Enterobacter cloacae*. *Agric Biol Chem* 55:701–706.
134. Panke S, Held M, Wubbolts M. 2004. Trends and innovations in industrial biocatalysis for the production of fine chemicals. *Curr Opin Biotechnol*.4: 272-279.
135. Trinchant JC, Rigaud J. 1974. Lactate Dehydrogenase from *Rhizobium*. Purification and Role in Indole Metabolism. *Enzyme* 32:394–399.
136. Idris EE, Iglesias DJ, Talon M, Borriss R. 2007. Tryptophan-dependent production of indole-3-acetic acid (IAA) affects level of plant growth promotion by *Bacillus amyloliquefaciens* FZB42. *Mol Plant Microbe Interact* 20:619–626.
137. Xie B, Xu K, Hong XZ, San FC. 2005. Isolation of transposon mutants from *Azospirillum brasilense* Yu62 and characterization of genes involved in indole-3-acetic acid biosynthesis. *FEMS Microbiol Lett* 248:57–63.
138. Gomez-Manzo S, Chavez-Pacheco JL, Contreras-Zentella M, Sosa-Torres ME, Arreguan-Espinosa R, Perez De La Mora M, Membrillo-Hernandez J, Escamilla JE. 2010. Molecular and catalytic properties of the aldehyde dehydrogenase of *Gluconacetobacter diazotrophicus*, a quinoxaline protein containing pyrroloquinoline quinone, cytochrome b, and cytochrome c. *J Bacteriol* 192:5718–5724.
139. Narumiya S, Takai K, Tokuyama T, Noda Y, Ushiro H, Hayaishi O. 1979. A new metabolic pathway of tryptophan initiated by tryptophan side chain oxidase. *J Biol Chem* 254:7007–7015.

140. Lee S, Flores-Encarnación M, Contreras-Zentella M, Garcia-Flores L, Escamilla JE, Kennedy C. 2004. Indole-3-acetic acid biosynthesis is deficient in *Gluconacetobacter diazotrophicus* strains with mutations in cytochrome c biogenesis genes. *J Bacteriol* 186:5384–5391.
141. Manulis S, Valinski L, Gafni Y, Hershenhorn J. 1991. Indole-3-acetic acid biosynthetic pathways in *Erwinia herbicola* in relation to pathogenicity on *Gypsophila paniculata*. *Physiol Mol Plant Pathol* 39:161–171.
142. Brandl MT, Lindow SE. 1996. Cloning and characterization of a locus encoding an indolepyruvate decarboxylase involved in indole-3-acetic acid synthesis in *Erwinia herbicola*. *Appl Environ Microbiol* 62:4121–4128.
143. Brandl M, Clark EM, Lindow SE. 1996. Characterization of the indole-3-acetic acid (IAA) biosynthetic pathway in an epiphytic strain of *Erwinia herbicola* and IAA production in vitro. *Can J Microbiol* 42:586–592.
144. Oberhänsli T, Dfago G, Haas D. 1991. Indole-3-acetic acid (IAA) synthesis in the biocontrol strain CHA0 of *Pseudomonas fluorescens*: role of tryptophan side chain oxidase. *J Gen Microbiol* 137:2273–2279.
145. Whistler CA, Corbell NA, Sarniguet A, Ream W, Loper JE. 1998. The two-component regulators GacS and GacA influence accumulation of the stationary-phase sigma factor(s) and the stress response in *Pseudomonas fluorescens* Pf-5. *J Bacteriol* 180:6635–6641.
146. Comai L, Kosuge T. 1982. Cloning and characterization of *iaaM*, a virulence determinant of *Pseudomonas savastanoi*. *J Bacteriol* 149:40–46.
147. Sekine M, Watanabe K, Syono K. 1989. Molecular cloning of a gene for indole-3-acetamide hydrolase from *Bradyrhizobium japonicum*. *J Bacteriol* 171:1718–1724.
148. Theunis M, Kobayashi H, Broughton WJ, Prinsen E. 2004. Flavonoids, NodD1, NodD2, and nod-box NB15 modulate expression of the y4wEFG locus that is required for indole-3-acetic acid synthesis in *Rhizobium* sp. strain NGR234. *Mol Plant Microbe Interact* 17:1153–1161.
149. Schroder G, Waffenschmidt S, Weiler EW, Schroder J. 1984. The T-region of Ti plasmids codes for an enzyme synthesizing indole-3-acetic acid. *Eur J Biochem* 138:387–391.
150. Glickmann E, Gardan L, Jacquet S, Hussain S, Elasri M, Petit A, Dessaux Y. 1998. Auxin Production Is a Common Feature of Most Pathovars of *Pseudomonas syringae*. *Mol Plant-Microbe Interact* 11:156–162.
151. Manulis S, Haviv-Chesner A, Brandl MT, Lindow SE, Barash I. 1998. Differential Involvement of Indole-3-Acetic Acid Biosynthetic Pathways in Pathogenicity and Epiphytic Fitness of *Erwinia herbicola* pv. *gypsophila*. *Mol Plant-Microbe Interact* 11:634–642.

152. Manulis S, Shafrir H, Epstein E, Lichter A, Barash I. 1994. Biosynthesis of indole-3-acetic acid via the indole-3-acetamide pathway in *Streptomyces* spp. *Microbiology* 140:1045–1050.
153. Lehmann T, Hoffmann M, Hentrich M, Pollmann S. 2010. Indole-3-acetamide-dependent auxin biosynthesis: A widely distributed way of indole-3-acetic acid production? *Eur J Cell Biol.* 12:895-905.
154. Vega-Hernández MC, León-Barrios M, Pérez-Galdona R. 2002. Indole-3-acetic acid production from indole-3-acetonitrile in *Bradyrhizobium*. *Soil Biol Biochem* 34:665–668.
155. Coffey L, Owens E, Tambling K, O'Neill D, O'Connor L, O'Reilly C. 2010. Real-time PCR detection of Fe-type nitrile hydratase genes from environmental isolates suggests horizontal gene transfer between multiple genera. *Antonie van Leeuwenhoek, Int J Gen Mol Microbiol* 98:455–463.
156. Blakey AJ, Colby J, Williams E, O'Reilly C. 1995. Regio- and stereo-specific nitrile hydrolysis by the nitrile hydratase from *Rhodococcus* AJ270. *FEMS Microbiol Lett* 129:57–61.
157. O'Mahony R, Doran J, Coffey L, Cahill OJ, Black GW, O'Reilly C. 2005. Characterisation of the nitrile hydratase gene clusters of *Rhodococcus erythropolis* strains AJ270 and AJ300 and *Microbacterium* sp. AJ115 indicates horizontal gene transfer and reveals an insertion of IS1166. *Antonie van Leeuwenhoek, Int J Gen Mol Microbiol* 87:221–232.
158. Asano Y, Tani Y, Yamada H. 1980. A new enzyme “Nitrile hydratase” which degrades acetonitrile in combination with amidase. *Agric Biol Chem* 44:2251–2252.
159. Yamada H, Kobayashi M. 1996. Nitrile hydratase and its application to industrial production of acrylamide. *Biosci Biotechnol Biochem* 60:1391–400.
160. Watanabe I, Satoh Y, Enomoto K. 1987. Screening, isolation and taxonomical properties of microorganisms having acrylonitrile-hydrating activity. *Agric Biol Chem.* 12:3193-3199.
161. Song L, Yuan H-J, Coffey L, Doran J, Wang M-X, Qian S, O'Reilly C. 2008. Efficient expression in *E. coli* of an enantioselective nitrile hydratase from *Rhodococcus erythropolis*. *Biotechnol Lett* 30:755–762.
162. Duan J, Jiang W, Cheng Z, Heikkila JJ, Glick BR. 2013. The Complete Genome Sequence of the Plant Growth-Promoting Bacterium *Pseudomonas* sp. UW4. *PLoS One* 8:e58640.
163. Kim SH, Oriel P. 2000. Cloning and expression of the nitrile hydratase and amidase genes from *Bacillus* sp. BR449 into *Escherichia coli*. *Enzyme Microb Technol* 27:492–501.
164. Nishiyama M, Horinouchi S, Kobayashi M, Nagasawa T, Yamada H, Beppu T. 1991. Cloning and characterization of genes responsible for metabolism of nitrile compounds from *Pseudomonas chlororaphis* B23. *J Bacteriol* 173:2465–2472.

165. Mayaux JF, Cerbelaud E, Soubrier F, Faucher D, Petre D. 1990. Purification, cloning, and primary structure of an enantiomer-selective amidase from *Brevibacterium* sp. strain R312: Structural evidence for genetic coupling with nitrile hydratase. *J Bacteriol* 172:6764–6773.
166. Tauber MM, Cavaco-Paulo A, Robra KH, Gübitz GM. 2000. Nitrile hydratase and amidase from *Rhodococcus rhodochrous* hydrolyze acrylic fibers and granular polyacrylonitriles. *Appl Environ Microbiol* 66:1634–1638.
167. Gilligan T, Yamada H, Nagasawa T. 1993. Production of S-(+)-2-phenylpropionic acid from (R,S)-2-phenylpropionitrile by the combination of nitrile hydratase and stereoselective amidase in *Rhodococcus equi* TG328. *Appl Microbiol Biotechnol* 39:720–725.
168. Stolz A, Trott S, Binder M, Bauer R, Hirrlinger B, Layh N, Knackmuss HJ. 1998. Enantioselective nitrile hydratases and amidases from different bacterial isolates. In *Journal of Molecular Catalysis - B Enzymatic*. p. 137–141.
169. Cantarella M, Cantarella L, Gallifuoco A, Frezzini R, Spera A, Alfani F. 2004. A study in UF-membrane reactor on activity and stability of nitrile hydratase from *Microbacterium imperiale* CBS 498-74 resting cells for propionamide production. In *Journal of Molecular Catalysis B: Enzymatic*. p. 105–113
170. Bhalla TC, Kumar H. 2005. *Nocardia globerula* NHB-2: a versatile nitrile-degrading organism. *Can J Microbiol* 51:705–708.
171. Zheng YG, Chen J, Liu ZQ, Wu MH, Xing LY, Shen YC. 2008. Isolation, identification and characterization of *Bacillus subtilis* ZJB-063, a versatile nitrile-converting bacterium. *Appl Microbiol Biotechnol* 77:985–993.
172. Brando PFB, Clapp JP, Bull AT. 2003. Diversity of Nitrile Hydratase and Amidase Enzyme Genes in *Rhodococcus erythropolis* Recovered from Geographically Distinct Habitats. *Appl Environ Microbiol* 69:5754–5766.
173. Xie SX, Kato Y, Komeda H, Yoshida S, Asano Y. 2003. A Gene Cluster Responsible for Alkylaldoxime Metabolism Coexisting with Nitrile Hydratase and Amidase in *Rhodococcus globerulus* A-4. *Biochemistry* 42:12056–12066.
174. Kato Y, Yoshida S, Xie S-X, Asano Y. 2004. Aldoxime dehydratase co-existing with nitrile hydratase and amidase in the iron-type nitrile hydratase-producer *Rhodococcus* sp. N-771. *J Biosci Bioeng* 97:250–259.
175. Kato Y, Nakamura K, Sakiyama H, Mayhew SG, Asano Y. 2000. Novel heme-containing lyase, phenylacetaldoxime dehydratase from *Bacillus* sp. strain OxB-1: Purification, characterization, and molecular cloning of the gene. *Biochemistry* 39:800–809.

176. Kato Y, Asano Y. 2006. Molecular and enzymatic analysis of the “aldoxime-nitrile pathway” in the glutaronitrile degrader *Pseudomonas* sp. K-9. *Appl Microbiol Biotechnol* 70:92–101.
177. Kobayashi M, Suzuki T, Fujita T, Masuda M, Shimizu S. 1995. Occurrence of enzymes involved in biosynthesis of indole-3-acetic acid from indole-3-acetonitrile in plant-associated bacteria, *Agrobacterium* and *Rhizobium*. *Proc Natl Acad Sci U S A* 92:714–718.
178. Mikkelsen MD, Hansen CH, Wittstock U, Halkier BA. 2000. Cytochrome P450 CYP79B2 from *Arabidopsis thaliana* catalyzes the conversion of tryptophan to indole-3-acetaldoxime, a precursor of indole glucosinolates and indole-3-acetic acid. *J Biol Chem* 275:33712–33717.
179. Kato Y, Ryoko O, Asano Y. 2000. Distribution of aldoxime dehydratase in microorganisms. *Appl Environ Microbiol* 66:2290–2296.
180. Howden AJM, Preston GM. 2009. Nitrilase enzymes and their role in plant-microbe interactions. *Microb Biotechnol.* 4: 441-451.
181. Brenner C, Pace HC, Brenner C. 2016. The nitrilase superfamily : Classification , structure and function The nitrilase superfamily : classification , structure and function 1–9.
182. Asano Y, Kato Y. 1998. Z-phenylacetaldoxime degradation by a novel aldoxime dehydratase from *Bacillus* sp. strain OxB-1. *FEMS Microbiol Lett* 158:185–190.
183. Kobayashi M, Izui H, Nagasawa T, Yamada H. 1993. Nitrilase in biosynthesis of the plant hormone indole-3-acetic acid from indole-3-acetonitrile: Cloning of the *Alcaligenes* gene and site-directed mutagenesis of cysteine residues. *Proc Natl Acad Sci* 90:247–251.
184. Howden AJM, Rico A, Mentlak T, Miguet L, Preston GM. 2009. *Pseudomonas syringae* pv. *syringae* B728a hydrolyses indole-3-acetonitrile to the plant hormone indole-3-acetic acid. *Mol Plant Pathol* 10:857–865.
185. O’Reilly C, Turner PD. 2003. The nitrilase family of CN hydrolysing enzymes - A comparative study. *J Appl Microbiol* 95:1161–1174.
186. Kato Y, Yoshida S, Asano Y. 2005. Polymerase chain reaction for identification of aldoxime dehydratase in aldoxime- or nitrile-degrading microorganisms. *FEMS Microbiol Lett* 246:243–249.
187. Feil H, Feil WS, Chain P, Larimer F, Dibartolo G, Copeland A, Lykidis A, Trong S, Nolan M, Goltsman E, Thiel J, Malfatti S, Loper JE, Lapidus A, Detter JC, Land M, Richardson PM, Kyrpides NC, Ivanova N, Lindow SE. 2005. Comparison of the complete genome sequences of *Pseudomonas syringae* pv. *syringae* B728a and pv. *tomato* DC3000. *PNAS* 102:11064–11069.

188. Stepanova AN, Alonso JM. 2016. Auxin catabolism unplugged: Role of IAA oxidation in auxin homeostasis. *Proc Natl Acad Sci* 113:10742–10744.
189. Ali B, Sabri AN, Hasnain S. 2010. Rhizobacterial potential to alter auxin content and growth of *Vigna radiata* (L.). *World J Microbiol Biotechnol* 26:1379–1384.
190. Costacurta A, Vanderleyden J. 1995. Synthesis of phytohormones by plant-associated bacteria. *Crit Rev Microbiol* 21:1–18.
191. Ernstsén A, Sandberg G, Crozier A, Wheeler CT. 1987. Endogenous indoles and the biosynthesis and metabolism of indole-3-acetic acid in cultures of *Rhizobium phaseoli*. *Planta* 171:422–428.
192. Brandl MT, Lindow SE. 1997. Environmental Signals Modulate the Expression of an Indole-3-Acetic Acid Biosynthetic Gene in *Erwinia herbicola*. *Mol Plant-Microbe Interact* 10:499–505.
193. Sitbon F, Hennion S, Sundberg B, Little CH, Olsson O, Sandberg G. 1992. Transgenic Tobacco Plants Coexpressing the *Agrobacterium tumefaciens* *iaaM* and *iaaH* Genes Display Altered Growth and Indoleacetic Acid Metabolism. *Plant Physiol* 99:1062–1069.
194. Glass NL, Kosuge T. 1988. Role of indoleacetic acid-lysine synthetase in regulation of indoleacetic acid pool size and virulence of *Pseudomonas syringae* subsp. *savastanoi*. *J Bacteriol* 170:2367–2373.
195. Glass NL, Kosuge T. 1986. Cloning of the gene for indoleacetic acid-lysine synthetase from *Pseudomonas syringae* subsp. *savastanoi*. *J Bacteriol* 166:598–603.
196. Tam YY, Epstein E, Normanly J. 2000. Characterization of auxin conjugates in *Arabidopsis thaliana*. Low steady-state levels of indole-3-acetyl-aspartate, indole-3-acetyl-glutamate, and indole-3-acetyl-glucose. *Plant Physiol* 123:589–596.
197. Chou JC, Mulbry WW, Cohen JD. 1998. The gene for indole-3-acetyl-L-aspartic acid hydrolase from *Enterobacter agglomerans*: Molecular cloning, nucleotide sequence, and expression in *Escherichia coli*. *Mol Gen Genet* 259:172–178.
198. Hangarter RP, Good NE. 1981. Evidence That IAA Conjugates Are Slow-Release Sources of Free IAA in Plant Tissues 1. *Plant Physiol* 68:1424–1427.
199. Cohen JD, Bandurski RS. 1982. Chemistry and physiology of the bound auxins. *Annu Rev Plant Physiol* 33:403–430.
200. Seidel C, Walz A, Park S, Cohen JD, Ludwig-Müller J. 2006. Indole-3-acetic acid protein conjugates: Novel players in auxin homeostasis. *Plant Biol*. 3:340-345.

201. Ebenau-Jehle C, Thomas M, Scharf G, Kockelkorn D, Knapp B, Schühle K, Heider J, Fuchs G. 2012. Anaerobic metabolism of indoleacetate. *J Bacteriol* 194:2894–2903.
202. Jensen JB, Egsgaard H, Vanonckelen H, Jochimsen BU. 1995. Catabolism of Indole-3-Acetic-Acid and 4-Chloroindole-3-Acetic and 5-Chloroindole-3-Acetic Acid in *Bradyrhizobium-japonicum*. *J Bacteriol* 177:5762–5766.
203. Egebo LA, Nielsen SVS, Jochimsen BU. 1991. Oxygen-dependent catabolism of indole-3-acetic acid in *Bradyrhizobium japonicum*. *J Bacteriol* 173:4897–4901.
204. Leveau JHJ, Gerards S. 2008. Discovery of a bacterial gene cluster for catabolism of the plant hormone indole 3-acetic acid. In *FEMS Microbiology Ecology*. p. 238–250
205. Lin GH, Chen HP, Huang JH, Liu TT, Lin TK, Wang SJ, Tseng CH, Shu HY. 2012. Identification and characterization of an indigo-producing oxygenase involved in indole 3-acetic acid utilization by *Acinetobacter baumannii*. *Antonie van Leeuwenhoek, Int J Gen Mol Microbiol* 101:881–890.
206. Donoso R, Leiva-Novoa P, Zúñiga A, Timmermann T, Recabarren-Gajardo G, González B. 2016. Biochemical and genetic basis of indole-3-acetic acid (auxin phytohormone) degradation by the plant growth promoting rhizobacterium *Paraburkholderia phytofirmans* PsJN. *Appl Environ Microbiol.* 83(1), e01991-16.
207. Loper JE, Schroth MN. 1986. Influence of Bacterial Sources of Indole-3-acetic Acid on Root Elongation of Sugar Beet. *Phytopathology.* 4:386-389.
208. Prinsen E, Chauvaux N, Schmidt J, John M, Wieneke U, De Greef J, Schell J, Van Onckelen H. 1991. Stimulation of indole-3-acetic acid production in *Rhizobium* by flavonoids. *FEBS Lett* 282:53–55.
209. Abbas-Akbari G, Mehdi Arab S, Alikhani H a, Allahdadi I, Arzanesh MH. 2007. Isolation and Selection of Indigenous *Azospirillum* spp. and the IAA of Superior Strains Effects on Wheat Roots. *World J Agric Sci* 3:523–529.
210. Sergeeva E, Hirkala DLM, Nelson LM. 2007. Production of indole-3-acetic acid, aromatic amino acid aminotransferase activities and plant growth promotion by *Pantoea agglomerans* rhizosphere isolates. *Plant Soil* 297:1–13.
211. Shokri D, Emtiazi G. 2010. Indole-3-acetic acid (IAA) production in symbiotic and non-symbiotic nitrogen-fixing bacteria and its optimization by taguchi design. *Curr Microbiol* 61:217–225.
212. O'Brien PJ, Siraki AG, Shangari N. 2005. Aldehyde sources, metabolism, molecular toxicity mechanisms, and possible effects on human health. *Crit Rev Toxicol* 35:609–662.

213. Ellis EM. 2007. Reactive carbonyls and oxidative stress: Potential for therapeutic intervention. *Pharmacol Ther.* 1:13-14.
214. Malhotra M, Srivastava S. 2009. Stress-responsive indole-3-acetic acid biosynthesis by *Azospirillum brasilense* SM and its ability to modulate plant growth. *Eur J Soil Biol* 45:73–80.
215. Sridevi M, Mallaiah K V. 2007. Production of indole-3-acetic acid by *Rhizobium* isolates from *Sesbania* species. *African J Microbiol Res* 1:125–128.
216. Omay SH, Schmidt WA, Martin P, Bangerth F. 1993. Indoleacetic acid production by the rhizosphere bacterium *Azospirillum brasilense* Cd under in vitro conditions. *Can J Microbiol* 39:187–192.
217. Dimkpa CO, Zeng J, McLean JE, Britt DW, Zhan J, Anderson AJ. 2012. Production of indole-3-acetic acid via the indole-3-acetamide pathway in the plant-beneficial bacterium *Pseudomonas chlororaphis* O6 is inhibited by ZnO nanoparticles but enhanced by CuO nanoparticles. *Appl Environ Microbiol* 78:1404–1410.
218. Dimkpa CO, Svatoš A, Dabrowska P, Schmidt A, Boland W, Kothe E. 2008. Involvement of siderophores in the reduction of metal-induced inhibition of auxin synthesis in *Streptomyces* spp. *Chemosphere* 74:19–25.
219. Kamnev AA, Tugarova A V., Antonyuk LP, Tarantilis PA, Polissiou MG, Gardiner PHE. 2005. Effects of heavy metals on plant-associated rhizobacteria: Comparison of endophytic and non-endophytic strains of *Azospirillum brasilense*. In *Journal of Trace Elements in Medicine and Biology*. p. 91–95
220. Mohite B. 2013. Isolation and characterization of indole acetic acid (IAA) producing bacteria from rhizospheric soil and its effect on plant growth. *J soil Sci plant Nutr.* 3:638-649.
221. Khamna S, Yokota A, Peberdy JF, Lumyong S. 2010. Indole-3-acetic acid production by *Streptomyces* sp. isolated from some Thai medicinal plant rhizosphere soils. *EurAsian J Biosci* 23–32.
222. Vessey JK, Henry LT, Chaillou S, Raper CD. 1990. Root-zone acidity affects relative uptake of nitrate and ammonium from mixed nitrogen sources. *J Plant Nutr* 13:95–116.
223. Vande Broek A, Gysegom P, Ona O, Hendrickx N, Prinsen E, Van Impe J, Vanderleyden J. 2005. Transcriptional Analysis of the *Azospirillum brasilense* Indole-3-Pyruvate Decarboxylase Gene and Identification of a cis-Acting Sequence Involved in Auxin Responsive Expression. *Mol Plant Microbe Interact* 18:311–323.
224. Booth IR. 1985. Regulation of cytoplasmic pH in bacteria. *Microbiol Rev* 49:359–378.

225. Prasad S, Raj J, Bhalla TC. 2009. Purification of a hyperactive nitrile hydratase from resting cells of *Rhodococcus rhodochrous* PA-34. *Indian J Microbiol* 49:237–242.
226. Leinhos V. 1994. Effects of pH and glucose on auxin production of phosphate-solubilizing rhizobacteria in vitro. *Microbiol Res* 149:135–138.
227. Bar T, Okon Y. 1993. Tryptophan conversion to indole-3-acetic acid via indole-3-acetamide in *Azospirillum brasilense* Sp7. *Can J Microbiol* 39:81–86.
228. Ona O, Van Impe J, Prinsen E, Vanderleyden J. 2005. Growth and indole-3-acetic acid biosynthesis of *Azospirillum brasilense* Sp245 is environmentally controlled. *FEMS Microbiol Lett* 246:125–32.
229. Hartmann a., Singh M, Klingmüller W. 1983. Mutants Excreting High Amounts of Indoleacetic Acid. *Can J Microbiol* 29:916–923.
230. Ona O, Van Impe J, Prinsen E, Vanderleyden J. 2005. Growth and indole-3-acetic acid biosynthesis of *Azospirillum brasilense* Sp245 is environmentally controlled. *FEMS Microbiol Lett* 246:125–132.
231. Zimmer W, Roeben K, Bothe H. 1988. An alternative explanation for plant growth promotion by bacteria of the genus *Azospirillum*. *Planta* 176:333–342.
232. Saleh SS, Glick BR. 2001. Involvement of *gacS* and *rpoS* in enhancement of the plant growth-promoting capabilities of *Enterobacter cloacae* CAL2 and UW4. *Can J Microbiol* 47:698–705.
233. Liu X, Wu Y, Chen Y, Xu F, Halliday N, Gao K, Chan KG, Cámara M. 2016. RpoS differentially affects the general stress response and biofilm formation in the endophytic *Serratia plymuthica* G3. *Res Microbiol* 167:168–177.
234. Boyer M, Bally R, Perrotto S, Chaintreuil C, Wisniewski-Dyé F. 2008. A quorum-quenching approach to identify quorum-sensing-regulated functions in *Azospirillum lipoferum*. *Res Microbiol* 159:699–708.
235. Liu X, Jia J, Popat R, Ortori CA, Li J, Diggle SP, Gao K, Cámara M. 2011. Characterisation of two quorum sensing systems in the endophytic *Serratia plymuthica* strain G3: differential control of motility and biofilm formation according to life-style. *BMC Microbiol* 11:26.
236. Müller H, Westendorf C, Leitner E, Chernin L, Riedel K, Schmidt S, Eberl L, Berg G. 2009. Quorum-sensing effects in the antagonistic rhizosphere bacterium *Serratia plymuthica* HRO-C48. *FEMS Microbiol Ecol* 67:468–478.
237. Mazzola M, White FF. 1994. A mutation in the indole-3-acetic acid biosynthesis pathway of *Pseudomonas syringae* pv. *syringae* affects growth in *Phaseolus vulgaris* and syringomycin production. *J Bacteriol* 176:1374–1382.

238. Gentry DR, Hernandez VJ, Nguyen LH, Jensen DB, Cashel M. 1993. Synthesis of the stationary-phase sigma factor(s) is positively regulated by ppGpp. *J Bacteriol* 175:7982–7989.
239. Hengge-Aronis R. 2002. Signal Transduction and Regulatory Mechanisms Involved in Control of the S (RpoS) Subunit of RNA Polymerase. *Microbiol Mol Biol Rev* 66:373–395.
240. Oh SA, Kim JS, Park JY, Han SH, Dimkpa C, Anderson AJ, Kim YC. 2013. The RpoS sigma factor negatively regulates production of IAA and siderophore in a biocontrol rhizobacterium, *Pseudomonas chlororaphis* O6. *Plant Pathol J* 29:323–329.
241. Blumer C, Heeb S, Pessi G, Haas D. 1999. Global GacA-steered control of cyanide and exoprotease production in *Pseudomonas fluorescens* involves specific ribosome binding sites. *Proc Natl Acad Sci* 96:14073–14078.
242. Kitten T, Kinscherf TG, McEvoy JL, Willis DK. 1998. A newly identified regulator is required for virulence and toxin production in *Pseudomonas syringae*. *Mol Microbiol* 28:917–929.
243. Kang BR, Yang KY, Cho BH, Han TH, Kim IS, Lee MC, Anderson AJ, Kim YC. 2006. Production of indole-3-acetic acid in the plant-beneficial strain *Pseudomonas chlororaphis* O6 is negatively regulated by the global sensor kinase gacS. *Curr Microbiol* 52:473–476.
244. Rothballer M, Schmid M, Fekete A, Hartmann A. 2005. Comparative in situ analysis of ipdC-gfpmut3 promoter fusions of *Azospirillum brasilense* strains Sp7 and Sp245. *Environ Microbiol* 7:1839–1846.
245. Yang S, Perna NT, Cooksey D a, Okinaka Y, Lindow SE, Ibekwe a M, Keen NT, Yang C-H. 2004. Genome-wide identification of plant-upregulated genes of *Erwinia chrysanthemi* 3937 using a GFP-based IVET leaf array. *Mol Plant Microbe Interact* 17:999–1008.
246. Brandl MT, Quiñones B, Lindow SE. 2001. Heterogeneous transcription of an indoleacetic acid biosynthetic gene in *Erwinia herbicola* on plant surfaces. *Proc Natl Acad Sci U S A* 98:3454–3459.
247. Fett WF, Osman SF, Dunn MF. 1987. Auxin production by plant-pathogenic pseudomonads and xanthomonads. *Appl Environ Microbiol* 53:1839–1845.
248. Yang S, Zhang Q, Guo J, Charkowski AO, Glick BR, Ibekwe AM, Cooksey DA, Yang CH. 2007. Global effect of indole-3-acetic acid biosynthesis on multiple virulence factors of *Erwinia chrysanthemi* 3937. *Appl Environ Microbiol* 73:1079–1088.
249. Gaffney TD, Silva OC, Yamada T, Kosuge T. 1990. Indoleacetic acid operon of *Pseudomonas syringae* subsp. *syringae*: Transcription analysis and promoter identification. *J bacteriol* 172:5593–5601.

250. Brandl MT, Lindow SE. 1998. Contribution of indole-3-acetic acid production to the epiphytic fitness of *Erwinia herbicola*. *Appl Environ Microbiol* 64:3256–3263.
251. Barbieri P, Zannelli T, Galli E, Zanetti G. 1986. Wheat inoculation with *Azospirillum brasilense* Sp6 and some mutants altered in nitrogen fixation and indole-3-acetic acid production. *Fems Microbiol Lett* 36:87–90.
252. Kaneshiro T, Kwolek WF. 1985. Stimulated nodulation of soybeans by *Rhizobium japonicum* mutant (B-14075) that catabolizes the conversion of tryptophan to indol-3-yl-acetic acid. *Plant Sci* 42:141–146.
253. Somers E, Ptacek D, Gysegom P, Srinivasan M, Vanderleyden J. 2005. *Azospirillum brasilense* Produces the Auxin-Like Phenylacetic Acid by Using the Key Enzyme for Indole-3-Acetic Acid Biosynthesis. *Appl Environ Microbiol* 71:1803–1810.
254. Palm CJ, Gaffney T, Kosuge T. 1989. Cotranscription of genes encoding indoleacetic acid production in *Pseudomonas syringae* subsp. *savastanoi*. *J Bacteriol* 171:1002–1009.
255. Vande Broek A, Lambrecht M, Eggermont K, Vanderleyden J. 1999. Auxins upregulate expression of the indole-3-pyruvate decarboxylase gene in *Azospirillum brasilense*. *J Bacteriol* 181:1338–1342.
256. Komeda H, Hori Y, Kobayashi M, Shimizu S. 1996. Transcriptional regulation of the *Rhodococcus rhodochrous* J1 *nitA* gene encoding a nitrilase. *Proc Natl Acad Sci U S A* 93:10572–10577.
257. Cheng Z, Park E, Glick BR. 2007. 1-Aminocyclopropane-1-carboxylate deaminase from *Pseudomonas putida* UW4 facilitates the growth of canola in the presence of salt. *Can J Microbiol* 53:912–918.
258. Duca D, Rose DR, Glick BR. 2014. Characterization of a nitrilase and a nitrile hydratase from *Pseudomonas* sp. strain UW4 that converts indole-3-acetonitrile to indole-3-acetic acid. *Appl Environ Microbiol* 80:4640–4649.
259. Vacheron J, Desbrosses G, Bouffaud M-L, Touraine B, Moënne-Loccoz Y, Muller D, Legendre L, Wisniewski-Dyé F, Prigent-Combaret C. 2013. Plant growth-promoting rhizobacteria and root system functioning. *Front Plant Sci* 4:356.
260. Spaepen S, Vanderleyden J. 2011. Auxin and plant-microbe interactions. *Cold Spring Harb Perspect Biol* 3:1–13.
261. Yue J, Hu X, Huang J. 2014. Origin of plant auxin biosynthesis. *Trends Plant Sci*. 12:764-770.
262. Duan J, Heikkilä JJ, Glick BR. 2010. Sequencing a bacterial genome : an overview. *Curr Res Technology Educ Top Applied Microbiol Microb Biotechnol* 1443–1451.

263. Bradford MM. 1976. A rapid and sensitive method for the quantitation of microgram quantities of protein utilizing the principle of protein-dye binding. *Anal Biochem* 72:248–254.
264. Kumar S, Stecher G, Tamura K. 2016. MEGA7: Molecular Evolutionary Genetics Analysis version 7.0 for bigger datasets. *Mol Biol Evol* msw054.
265. Tamura K, Peterson D, Peterson N, Stecher G, Nei M, Kumar S. 2011. MEGA5: Molecular evolutionary genetics analysis using maximum likelihood, evolutionary distance, and maximum parsimony methods. *Mol Biol Evol* 28:2731–2739.
266. Fournand D, Bigey F, Arnaud A. 1998. Acyl transfer activity of an amidase from *Rhodococcus* sp. strain R312: Formation of a wide range of hydroxamic acids. *Appl Environ Microbiol* 64:2844–2852.
267. Chebrou H, Bigey F, Arnaud A, Galzy P. 1996. Study of the amidase signature group. *Biochim Biophys Acta - Protein Struct Mol Enzymol* 1298:285–293.
268. Bhatia RK, Bhatia SK, Mehta PK, Bhalla TC. 2014. Biotransformation of nicotinamide to nicotinyl hydroxamic acid at bench scale by amidase acyl transfer activity of *Pseudomonas putida* BR-1. *J Mol Catal B Enzym* 108:89–95.
269. Trott S, Bürger S, Calaminus C, Stolz A. 2002. Cloning and heterologous expression of an enantioselective amidase from *Rhodococcus erythropolis* strain MP50. *Appl Environ Microbiol* 68:3279–3286.
270. Martinková L, Křen V. 2002. Nitrile- and Amide-converting Microbial Enzymes: Stereo-, Regio- and Chemoselectivity. *Biocatal Biotransformation* 20:73–93.
271. Camilleri C, Jouanin L. 1991. The TR-DNA region carrying the auxin synthesis genes of the *Agrobacterium rhizogenes* agropine-type plasmid pRiA4: nucleotide sequence analysis and introduction into tobacco plants. *Mol Plant Microbe Interact* 4:155–162.
272. Finn RD, Attwood TK, Babbitt PC, Bateman A, Bork P, Bridge AJ, Chang H-Y, Dosztányi Z, El-Gebali S, Fraser M, Gough J, Haft D, Holliday GL, Huang H, Huang X, Letunic I, Lopez R, Lu S, Marchler-Bauer A, Mi H, Mistry J, Natale DA, Necci M, Nuka G, Orengo CA, Park Y, Pesseat S, Piovesan D, Potter SC, Rawlings ND, Redaschi N, Richardson L, Rivoire C, Sangrador-Vegas A, Sigrist C, Sillitoe I, Smithers B, Squizzato S, Sutton G, Thanki N, Thomas PD, Tosatto SCE, Wu CH, Xenarios I, Yeh L-S, Young S-Y, Mitchell AL. 2016. InterPro in 2017-beyond protein family and domain annotations. *Nucleic Acids Res.* 45(D1), D190-D199.
273. Gough J, Karplus K, Hughey R, Chothia C. 2001. Assignment of homology to genome sequences using a library of hidden Markov models that represent all proteins of known structure1. *J Mol Biol* 313:903–919.

274. Gasteiger E, Hoogland C, Gattiker A, Duvaud S, Wilkins MR, Appel RD, Bairoch A. 2005. The Proteomics Protocols Handbook. The Proteomics Protocols Handbook.
275. Kyte J, Doolittle RF. 1982. A simple method for displaying the hydropathic character of a protein. *J Mol Biol* 157:105–132.
276. Smialowski P, Martin-Galiano AJ, Mikolajka A, Girschick T, Holak TA, Frishman D. 2007. Protein solubility: Sequence based prediction and experimental verification. *Bioinformatics* 23:2536–2542.
277. Ciskanik LM, Wilczek JM, Fallon RD. 1995. Purification and characterization of an enantioselective amidase from *Pseudomonas chlororaphis* B23. *Appl Environ Microbiol* 61:998–1003.
278. Kobayashi M, Komeda H, Nagasawa T, Nishiyama M, Horinouchi S, Beppu T, Yamada H, Shimizu S. 1993. Amidase coupled with low-molecular-mass nitrile hydratase from *Rhodococcus rhodochromus* J1. Sequencing and expression of the gene and purification and characterization of the gene product. *Eur J Biochem* 217:327–336.
279. Mayaux JF, Cerbelaud E, Soubrier F, Yeh P, Blanche F, Petre D. 1991. Purification, cloning, and primary structure of a new enantiomer-selective amidase from a *Rhodococcus* strain: Structural evidence for a conserved genetic coupling with nitrile hydratase. *J Bacteriol* 173:6694–6704.
280. Hirrlinger B, Stolz A, Knackmuss HJ. 1996. Purification and properties of an amidase from *Rhodococcus erythropolis* MP50 which enantioselectively hydrolyzes 2-arylpropionamides. *J Bacteriol* 178:3501–3507.
281. Fournand D, Arnaud A, Galzy P. 1998. Study of the acyl transfer activity of a recombinant amidase overproduced in an *Escherichia coli* strain. Application for short-chain hydroxamic acid and acid hydrazide synthesis. *J Mol Catal - B Enzym* 4:77–90.
282. Canaday J, Gérard JC, Crouzet P, Otten L. 1992. Organization and functional analysis of three T-DNAs from the vitopine Ti plasmid pTiS4. *MGG Mol Gen Genet* 235:292–303.
283. Yamada T, Palm CJ, Brooks B, Kosuge T. 1985. Nucleotide sequences of the *Pseudomonas savastanoi* indoleacetic acid genes show homology with *Agrobacterium tumefaciens* T-DNA. *Proc Natl Acad Sci U S A* 82:6522–6526.
284. Hashimoto Y, Nishiyama M, Ikehata O, Horinouchi S, Beppu T. 1991. Cloning and characterization of an amidase gene from *Rhodococcus* species N-774 and its expression in *Escherichia coli*. *BBA - Gene Struct Expr* 1088:225–233.
285. Ohtaki A, Murata K, Sato Y, Noguchi K, Miyatake H, Dohmae N, Yamada K, Yohda M, Odaka M. 2010. Structure and characterization of amidase from *Rhodococcus* sp. N-771: Insight into

the molecular mechanism of substrate recognition. *Biochim Biophys Acta - Proteins Proteomics* 1804:184–192.

286. Jones DT, Taylor WR, Thornton JM. 1992. The rapid generation of mutation data matrices from protein sequences. *Bioinformatics* 8:275–282.

287. Zhao N, Ferrer J-L, Ross J, Guan J, Yang Y, Pichersky E, Noel JP, Chen F. 2008. Structural, biochemical, and phylogenetic analyses suggest that indole-3-acetic acid methyltransferase is an evolutionarily ancient member of the SABATH family. *Plant Physiol* 146:455–67.

288. Kato Y, Tsuda T, Asano Y. 1999. Nitrile hydratase involved in aldoxime metabolism from *Rhodococcus* sp. strain YH3-3. Purification and characterization. *Eur J Biochem* 263:662–670.

289. Okamoto S, Eltis LD. 2007. Purification and characterization of a novel nitrile hydratase from *Rhodococcus* sp. RHA1. *Mol Microbiol* 65:828–838.

290. Dudnik A, Dudler R. 2014. Genomics-Based Exploration of Virulence Determinants and Host-Specific Adaptations of *Pseudomonas syringae* strains Isolated from Grasses. *Pathogens* 3:121–148.

291. Ljung K. 2013. Auxin metabolism and homeostasis during plant development. *Development* 140:943–950.

292. Kramer EM, Ackelsberg EM. 2015. Auxin metabolism rates and implications for plant development. *Front Plant Sci* 6:150.

293. Mayak S, Tirosh T, Glick BR. 1999. Effect of Wild-Type and Mutant Plant Growth-Promoting Rhizobacteria on the Rooting of Mung Bean Cuttings. *J Plant Growth Regul* 18:49–53.

294. Leyser O. 2003. Regulation of shoot branching by auxin. *Trends Plant Sci.*11: 541-545.

295. Mller D, Leyser O. 2011. Auxin, cytokinin and the control of shoot branching. *Ann Bot.*7:1303-1212.

296. Abel S, Nguyen MD, Chow W, Theologis A. 1995. ASC4, a primary indoleacetic acid-responsive gene encoding 1-aminocyclopropane-1-carboxylate synthase in *Arabidopsis thaliana*: Structural characterization, expression in *Escherichia coli*, and expression characteristics in response to auxin. *J Biol Chem* 270:19093–19099.

297. Ruzicka K, Ljung K, Vanneste S, Podhorska R, Beeckman T, Friml J, Benkova E. 2007. Ethylene Regulates Root Growth through Effects on Auxin Biosynthesis and Transport-Dependent Auxin Distribution. *Plant Cell Online* 19:2197–2212.

298. Burg SP, Burg EA. 1966. The interaction between auxin and ethylene and its role in plant growth. *Proc Natl Acad Sci* 55:262–269.

299. Czarny JC, Shah S, Glick BR. 2007. Response of canola plants at the transcriptional level to expression of a bacterial ACC deaminase in the roots. *Adv plant Ethyl Res* 377–382.
300. Glick BR, Cheng Z, Czarny J, Duan J. 2007. Promotion of plant growth by ACC deaminase-producing soil bacteria. *New Perspect Approaches Plant Growth-Promoting Rhizobacteria Res* 329–339.
301. Stearns JC, Woody OZ, McConkey BJ, Glick BR. 2012. Effects of Bacterial ACC Deaminase on *Brassica napus* Gene Expression. *Mol Plant-Microbe Interact MPMI* 668:668–676.
302. Glick BR. 2014. Bacteria with ACC deaminase can promote plant growth and help to feed the world. *Microbiol Res* 169:30–39.
303. Keen NT, Tamaki S, Kobayashi D, Trollinger D. 1988. Improved broad-host-range plasmids for DNA cloning in Gram-negative bacteria. *Gene* 70:191–197.
304. Sambrook J, Russell DW. 2001. *Molecular Cloning - Sambrook & Russel - Vol. 1, 2, 3*. Cold Spring Harb Lab Press 3rd Edition.
305. Figurski DH, Helinski DR. 1979. Replication of an origin-containing derivative of plasmid RK2 dependent on a plasmid function provided in trans. *Proc Natl Acad Sci U S A* 76:1648–52.
306. Penrose DM, Glick BR. 2003. Methods for isolating and characterizing ACC deaminase-containing plant growth-promoting rhizobacteria. *Physiol Plant* 118:10–15.
307. Wu L, Yang B, Bi J, Wang J. 2011. Development of bovine serum albumin certified reference material. *Anal Bioanal Chem* 400:3443–3449.
308. Livak KJ, Schmittgen TD. 2001. Analysis of relative gene expression data using real-time quantitative PCR and the $\Delta\Delta CT$ Method. *Methods* 25:402–408.
309. Lifshitz R, Kloepper JW, Kozlowski M, Simonson C, Carlson J, Tipping EM, Zaleska I. 1987. Growth promotion of canola (rapeseed) seedlings by a strain of *Pseudomonas putida* under gnotobiotic conditions. *Can J Microbiol* 33:390–395.
310. Glick BR. 1995. Metabolic load and heterogenous gene expression. *Biotechnol Adv* 13:247–261.
311. Pérez-Galdona R, Corzo J, León-Barrios MA, Gutiérrez-Navarro AM. 1992. Characterization of an aromatic amino acid aminotransferase from *Rhizobium leguminosarum* biovar *trifolii*. *Biochimie* 74:539–544.
312. Normanly J, Bartel B. 1999. Redundancy as a way of life - IAA metabolism. *Curr Opin Plant Biol.* 3:207-213.

313. Shah S, Li J, Moffatt B a, Glick BR. 1998. Isolation and characterization of ACC deaminase genes from two different plant growth-promoting rhizobacteria. *Can J Microbiol* 44:833–843.
314. Tang W, Pasternak JJ, Glick BR. 1995. Persistence in soil of the plant growth promoting rhizobacterium *Pseudomonas putida* GR12-2 and genetically manipulated derived strains. *Can J Microbiol* 41:445–451.
315. Sun Y, Cheng Z, Glick BR. 2009. The presence of a 1-aminocyclopropane-1-carboxylate (ACC) deaminase deletion mutation alters the physiology of the endophytic plant growth-promoting bacterium *Burkholderia phytofirmans* PsJN. *FEMS Microbiol Lett.*1:131-136.
316. Sprunck S, Jacobsen HJ, Reinard T. 1995. Indole-3-lactic acid is a weak auxin analogue but not an anti-auxin. *J Plant Growth Regul* 14:191–197.
317. Korber H, Strizhov N, Staiger D, Feldwisch J, Olsson O, Sandberg G, Palme K, Schell J, Koncz C. 1991. T-DNA gene 5 of *Agrobacterium* modulates auxin response by autoregulated synthesis of a growth hormone antagonist in plants. *Embo J* 10:3983–3991.
318. Hilbert M, Voll LM, Ding Y, Hofmann J, Sharma M, Zuccaro A. 2012. Indole derivative production by the root endophyte *Piriformospora indica* is not required for growth promotion but for biotrophic colonization of barley roots. *New Phytol* 196:520–534.
319. Yang Y, Xu R, Ma C-J, Vlot a C, Klessig DF, Pichersky E. 2008. Inactive methyl indole-3-acetic acid ester can be hydrolyzed and activated by several esterases belonging to the AtMES esterase family of *Arabidopsis thaliana*. *Plant Physiol* 147:1034–1045.
320. Overvoorde P, Fukaki H, Beeckman T. 2010. Auxin control of root development. *Cold Spring Harb Perspect Biol.* 2(6), a001537.
321. Smalle J, Haegman M, Kurepa J, Van Montagu M M Van, Straeten D V. 1997. Ethylene can stimulate *Arabidopsis thaliana* hypocotyl elongation in the light. *Proc Natl Acad Sci U S A* 94:2756–61.
322. Vandenbussche F, Vriezen WH, Smalle J, Laarhoven LJJ, Harren FJM, Van Der Straeten D. 2003. Ethylene and auxin control the *Arabidopsis thaliana* response to decreased light intensity. *Plant Physiol* 133:517–27.
323. Pitts RJ, Cernac A, Estelle M. 1998. Auxin and ethylene promote root hair elongation in *Arabidopsis thaliana*. *Plant J* 16:553–560.
324. Lehman A, Black R, Ecker JR. 1996. *Hookless1* an ethylene response gene, is required for differential cell elongation in the *Arabidopsis thaliana* hypocotyl. *Cell* 85:183–194.

325. Lee JS, Chang W-K, Evans ML. 1990. Effects of ethylene on the kinetics of curvature and auxin redistribution in gravistimulated roots of *Zea mays*. *Plant Physiol* 94:1770–5.
326. Buer CS, Sukumar P, Muday GK. 2006. Ethylene modulates flavonoid accumulation and gravitropic responses in roots of *Arabidopsis thaliana*. *Plant Physiol* 140:1384–1396.
327. Pickett FB, Wilson a K, Estelle M. 1990. The aux1 Mutation of *Arabidopsis thaliana* Confers Both Auxin and Ethylene Resistance. *Plant Physiol* 94:1462–1466.
328. Rahman a, Amakawa T, Goto N, Tsurumi S. 2001. Auxin is a positive regulator for ethylene-mediated response in the growth of *Arabidopsis thaliana* roots. *Plant Cell Physiol* 42:301–307.
329. Stepanova AN, Hoyt JM, Hamilton AA, Alonso JM. 2005. A Link between ethylene and auxin uncovered by the characterization of two root-specific ethylene-insensitive mutants in *Arabidopsis thaliana*. *Plant Cell* 17:2230–42.
330. Woodward AW, Bartel B. 2005. Auxin: Regulation, action, and interaction. *Ann Bot.* 5:707-735.
331. Chadwick a V, Burg SP. 1967. An explanation of the inhibition of root growth caused by indole-3-acetic Acid. *Plant Physiol* 42:415–420.
332. Burg SP, Burg EA. 1967. Inhibition of Polar Auxin Transport by Ethylene'. *Plant Physiol* 42:1224–1228.
333. Lewis DR, Negi S, Sukumar P, Muday GK. 2011. Ethylene inhibits lateral root development, increases IAA transport and expression of PIN3 and PIN7 auxin efflux carriers. *Development* 138:3485–3495.
334. Negi S, Ivanchenko MG, Muday GK. 2008. Ethylene regulates lateral root formation and auxin transport in *Arabidopsis thaliana thaliana*. *Plant J* 55:175–187.
335. Velocchia A, Fattorini L, Della Rovere F, Sofo A, D'angeli S, Betti C, Falasca G, Altamura MM. 2016. Ethylene and auxin interaction in the control of adventitious rooting in *Arabidopsis thaliana thaliana*. *J Exp Bot* 67:6445–6458.
336. Bruex A, Kainkaryam RM, Wieckowski Y, Kang YH, Bernhardt C, Xia Y, Zheng X, Wang JY, Lee MM, Benfey P, Woolf PJ, Schiefelbein J. 2012. A gene regulatory network for root epidermis cell differentiation in *Arabidopsis thaliana*. *PLoS Genet* 8.
337. Masucci JD, Schiefelbein JW. 1994. The rhd6 Mutation of *Arabidopsis thaliana thaliana* Alters Root-Hair Initiation through an Auxin- and Ethylene-Associated Process. *Plant Physiol* 106:1335–1346.

338. Strader LC, Chen GL, Bartel B. 2010. Ethylene directs auxin to control root cell expansion. *Plant J* 64:874–884.
339. Battesti A, Majdalani N, Gottesman S. 2011. The RpoS-mediated general stress response in *Escherichia coli*. *Annu Rev Microbiol* 65:189–213.
340. Subsin B, Thomas MS, Katzenmeier G, Shaw JG, Tungpradabkul S, Kunakorn M. 2003. Role of the Stationary Growth Phase Sigma Factor RpoS of *Burkholderia pseudomallei* in Response to Physiological Stress Conditions. *J Bacteriol* 185:7008–7014.
341. Sun Y, Cheng Z, Glick BR. 2009. The presence of a 1-aminocyclopropane-1-carboxylate (ACC) deaminase deletion mutation alters the physiology of the endophytic plant growth-promoting bacterium *Burkholderia phytofirmans* PsJN. *FEMS Microbiol Lett* 296:131–136.
342. Landini P, Egli T, Wolf J, Lacour S. 2014. sigmaS, a major player in the response to environmental stresses in *Escherichia coli*: Role, regulation and mechanisms of promoter recognition. *Environ Microbiol Rep* 6:1–13.
343. López-Bucio J, Campos-Cuevas JC, Hernández-Calderón E, Velásquez-Becerra C, Farías-Rodríguez R, Macías-Rodríguez LI, Valencia-Cantero E. 2007. *Bacillus megaterium* rhizobacteria promote growth and alter root-system architecture through an auxin- and ethylene-independent signaling mechanism in *Arabidopsis thaliana thaliana*. *Mol Plant Microbe Interact* 20:207–217.
344. Coenen C, Lomax TL. 1997. Auxin-cytokinin interactions in higher plants: old problems and new tools. *Trends Plant Sci* 2:351–6.
345. Eklöf S, Astot C, Blackwell J, Moritz T, Olsson O, Sandberg G. 1997. Auxin-Cytokinin Interactions in Wild-Type and Transgenic Tobacco. *Plant Cell Physiol* 38:225–235.
346. Eklöf S, Åstot C, Sitbon F, Moritz T, Olsson O, Sandberg G. 2000. Transgenic tobacco plants co-expressing *Agrobacterium iaa* and *ipt* genes have wild-type hormone levels but display both auxin- and cytokinin-overproducing phenotypes. *Plant J* 23:279–284.
347. Wang KL-C, Yoshida H, Lurin C, Ecker JR. 2004. Regulation of ethylene gas biosynthesis by the *Arabidopsis thaliana* ETO1 protein. *Nature* 428:945–950.
348. Chae HS, Faure F, Kieber JJ. 2003. The *eto1*, *eto2*, and *eto3* mutations and cytokinin treatment increase ethylene biosynthesis in *Arabidopsis thaliana* by increasing the stability of ACS protein. *Plant Cell* 15:545–559.
349. Comai L, Kosuge T. 1980. Involvement of plasmid deoxyribonucleic acid in indoleacetic acid synthesis in Involvement of Plasmid Deoxyribonucleic Acid in Indoleacetic Acid Synthesis in *Pseudomonas savastanoi*. *J Bacteriol* 143:950–957.

350. Dworkin M, Foster JW. 1958. Experiments with some microorganisms which utilize ethane and hydrogen. *J Bacteriol* 75:592–603.
351. Schäfer A, Tauch A, Jäger W, Kalinowski J, Thierbach G, Pühler A. 1994. Small mobilizable multi-purpose cloning vectors derived from the *Escherichia coli* plasmids pK18 and pK19: selection of defined deletions in the chromosome of *Corynebacterium glutamicum*. *Gene* 145:69–73.
352. Gay P, Le Coq D, Steinmetz M, Berkelman T, Kado CI. 1985. Positive selection procedure for entrapment of insertion sequence elements in gram-negative bacteria. *J Bacteriol* 164:918–921.
353. Lin G-H, Chang C-Y, Lin H-R. 2015. Systematic profiling of indole-3-acetic acid biosynthesis in bacteria using LC–MS/MS. *J Chromatogr B* 988:53–58.
354. Sakashita T, Hashimoto Y, Oinuma KI, Kobayashi M. 2008. Transcriptional regulation of the nitrile hydratase gene cluster in *Pseudomonas chlororaphis* B23. *J Bacteriol* 190:4210–4217.
355. Imada EL, Rolla dos Santos AA de P, Oliveira ALM de, Hungria M, Rodrigues EP. 2017. Indole-3-acetic acid production via the indole-3-pyruvate pathway by plant growth promoter *Rhizobium tropici* CIAT 899 is strongly inhibited by ammonium. *Res Microbiol* 168:283–292.
356. Spaepen S, Versées W, Gocke D, Pohl M, Steyaert J, Vanderleyden J. 2007. Characterization of phenylpyruvate decarboxylase, involved in auxin production of *Azospirillum brasilense*. *J Bacteriol* 189:7626–7633.
357. Smit BA, van Hylckama Vlieg JET, Engels WJM, Meijer L, Wouters JTM, Smit G. 2005. Identification, cloning, and characterization of a *Lactococcus lactis* branched-chain alpha-keto acid decarboxylase involved in flavor formation. *Appl Environ Microbiol*. 1:301-311.
358. Werther T, Spinka M, Tittmann K, Schütz A, Golbik R, Mrestani-Klaus C, Hübner G, König S. 2008. Amino acids allosterically regulate the thiamine diphosphate-dependent α -keto acid decarboxylase from *Mycobacterium tuberculosis*. *J Biol Chem* 283:5344–5354.
359. Schütz A, Golbik R, König S, Hübner G, Tittmann K. 2005. Intermediates and transition states in thiamine diphosphate-dependent decarboxylases. A kinetic and NMR study on wild-type indolepyruvate decarboxylase and variants using indolepyruvate, benzoylformate, and pyruvate as substrates. *Biochemistry* 44:6164–6179.
360. Coulson TJD, Patten CL. 2015. The TyrR transcription factor regulates the divergent akr-ipdC operons of *Enterobacter cloacae* UW5. *PLoS One* 10.
361. Goyal S, Yuan J, Chen T, Rabinowitz JD, Wingreen NS. 2010. Achieving optimal growth through product feedback inhibition in metabolism. *PLoS Comput Biol* 6:1–12.

362. Parsons C V., Harris DMM, Patten CL. 2015. Regulation of indole-3-acetic acid biosynthesis by branched-chain amino acids in *Enterobacter cloacae* UW5. FEMS Microbiol Lett. 362(18).
363. Asamizu S, Kato Y, Igarashi Y, Furumai T, Onaka H. 2006. Direct formation of chromopyrrolic acid from indole-3-pyruvic acid by StaD, a novel hemoprotein in indolocarbazole biosynthesis. Tetrahedron Lett 47:473–475.
364. Ryan KS, Drennan CL. 2009. Divergent Pathways in the Biosynthesis of Bisindole Natural Products. Chem Biol. 4: 351-364.
365. Jensen RA, Gu W. 1996. Evolutionary recruitment of biochemically specialized subdivisions of family I within the protein superfamily of aminotransferases. J Bacteriol 178:2161–2171.
366. Nishizawa T, Aldrich CC, Sherman DH. 2005. Molecular analysis of the rebeccamycin L-amino acid oxidase from *Lechevalieria aerocolonigenes* ATCC 39243. J Bacteriol 187:2084–2092.
367. Faust A, Niefind K, Hummel W, Schomburg D. 2007. The Structure of a Bacterial L-Amino Acid Oxidase from *Rhodococcus opacus* Gives New Evidence for the Hydride Mechanism for Dehydrogenation. J Mol Biol 367:234–248.
368. Geueke B, Hummel W. 2002. A new bacterial L-amino acid oxidase with a broad substrate specificity: Purification and characterization. Enzyme Microb Technol 31:77–87.
369. Schütz A, Sandalova T, Ricagno S, Hübner G, König S, Schneider G. 2003. Crystal structure of thiamindiphosphate-dependent indolepyruvate decarboxylase from *Enterobacter cloacae*, an enzyme involved in the biosynthesis of the plant hormone indole-3-acetic acid. Eur J Biochem 270:2312–2321.
370. Phi QT, Park YM, Ryu CM, Park SH, Ghim SY. 2008. Functional identification and expression of indole-3-pyruvate decarboxylase from *Paenibacillus polymyxa* E681. J Microbiol Biotechnol 18:1235–1244.
371. Shao J, Li S, Zhang N, Cui X, Zhou X, Zhang G, Shen Q, Zhang R. 2015. Analysis and cloning of the synthetic pathway of the phytohormone indole-3-acetic acid in the plant-beneficial *Bacillus amyloliquefaciens* SQR9. Microb Cell Fact 14:130.
372. Sekine M, Ichikawa T, Kuga N, Kobayashi M, Sakurai A, Syōno K. 1988. Detection of the IAA Biosynthetic Pathway from Tryptophan via Indole-3-Acetamide in *Bradyrhizobium* spp. Plant Cell Physiol 29:867–874.
373. Ralph E, Anderson M, Cleland W, Fitzpatrick P. 2006. Mechanistic Studies of the Flavoenzyme Tryptophan 2- Monooxygenase: Deuterium and 15 N Kinetic Isotope Effects on Alanine Oxidation by an L-Amino Acid Oxidase. Biochemistry 45:15844–15852.

374. Emanuele J, Heasley C, Fitzpatrick P. 1995. Purification and characterization of the flavoprotein tryptophan 2-monooxygenase expressed at high levels in *Escherichia coli*. Arch Biochem Biophys. 1: 241-248.
375. Sobrado P, Fitzpatrick PF. 2002. Analysis of the roles of amino acid residues in the flavoprotein tryptophan 2-monooxygenase modified by 2-oxo-3-pentynoate: Characterization of His338, Cys339, and Cys511 mutant enzymes. Arch Biochem Biophys 402:24–30.
376. Sobrado P, Fitzpatrick PF. 2003. Identification of Tyr413 as an Active Site Residue in the Flavoprotein Tryptophan 2-Monooxygenase and Analysis of Its Contribution to Catalysis. Biochemistry 42:13833–13838.
377. Gaweska H, Fitzpatrick PF. 2011. Structures and mechanism of the monoamine oxidase family. Biomol Concepts. 5:365-377.
378. Marchler-Bauer A, Bo Y, Han L, He J, Lanczycki CJ, Lu S, Chitsaz F, Derbyshire MK, Geer RC, Gonzales NR, Gwadz M, Hurwitz DI, Lu F, Marchler GH, Song JS, Thanki N, Wang Z, Yamashita RA, Zhang D, Zheng C, Geer LY, Bryant SH. 2017. CDD/SPARCLE: Functional classification of proteins via subfamily domain architectures. Nucleic Acids Res 45:D200–D203.
379. Hutcheson SW, Kosuge T. 1985. Regulation of 3-indoleacetic acid production in *Pseudomonas syringae* pv. *savastanoi*. Purification and properties of tryptophan 2-monooxygenase. J Biol Chem 260:6281–6287.
380. Sobrado P, Fitzpatrick PF. 2003. Analysis of the Role of the Active Site Residue Arg98 in the Flavoprotein Tryptophan 2-Monooxygenase, a Member of the L-Amino Oxidase Family. Biochemistry 42:13826–13832.
381. Gadda G, Fitzpatrick PF. 1998. Biochemical and physical characterization of the active FAD-containing form of nitroalkane oxidase from *Fusarium oxysporum*. Biochemistry 37:6154–6164.
382. Kim HJ, Winge DR. 2013. Emerging concepts in the flavinylation of succinate dehydrogenase. Biochim Biophys Acta - Bioenerg. 5: 627-636.
383. Ida K, Kurabayashi M, Suguro M, Hiruma Y, Hikima T, Yamamoto M, Suzuki H. 2008. Structural basis of proteolytic activation of L-phenylalanine oxidase from *Pseudomonas* sp. P-501. J Biol Chem 283:16584–16590.
384. Suzuki H, Higashi Y, Asano M, Suguro M, Kigawa M, Maeda M, Katayama S, Mukoyama EB, Uchiyama K. 2004. Sequencing and expression of the L-phenylalanine oxidase gene from *Pseudomonas* sp. p-501. Proteolytic activation of the proenzyme. J Biochem 136:617–627.
385. Kurosawa N, Hirata T, Suzuki H. 2009. Characterization of putative tryptophan monooxygenase from *Ralstonia solanasearum*. J Biochem 146:23–32.

386. Bouvrette P, Luong JHT. 1994. Isolation, purification and further characterization of an L-Phenylalanine Oxidase from *Morganella morganii*. *Appl Biochem Biotechnol* 48:61–74.
387. Revelles O, Espinosa-urgel M, Fuhrer T, Sauer U, Ramos JL. 2005. Multiple and Interconnected Pathways for L -Lysine Catabolism in *Pseudomonas putida* KT2440. *J Bacteriol* 187:7500–7510.
388. Isobe K, Sugawara A, Domon H, Fukuta Y, Asano Y. 2012. Purification and characterization of an l-amino acid oxidase from *Pseudomonas* sp. AIU 813. *J Biosci Bioeng* 114:257–261.
389. Kimura M, Ota T. 1974. On some principles governing molecular evolution. *Proc Natl Acad Sci U S A* 71:2848–2852.
390. Dym O, Eisenberg D. 2001. Sequence-structure analysis of FAD-containing proteins. *Protein Sci* 10:1712–1728.
391. Matsui D, Im DH, Sugawara A, Fukuta Y, Fushinobu S, Isobe K, Asano Y. 2014. Mutational and crystallographic analysis of l-amino acid oxidase/monooxygenase from *Pseudomonas* sp. AIU 813: Interconversion between oxidase and monooxygenase activities. *FEBS Open Bio* 4:220–228.
392. Matsui D, Im DH, Sugawara A, Fukuta Y, Fushinobu S, Isobe K, Asano Y. 2014. Mutational and crystallographic analysis of l-amino acid oxidase/monooxygenase from *Pseudomonas* sp. AIU 813: Interconversion between oxidase and monooxygenase activities. *FEBS Open Bio* 4:220–228.
393. Takashi Yamauchi, Shozo Yamamoto AO, Hayashi. 1973. Reversible Conversion of Lysine Monooxygenase to an Oxidase by Modification of Sulfhydryl Groups. *J Biol Chem* 248:3750–3752.
394. Koyama H. 1984. Oxidation and Oxygenation from *Pseudomonas* of L-Amino Acids Catalyzed by a L-Phenylalanine Oxidase (Deaminating and Decarboxylating). *J Biochem* 96:421–427.
395. Van Berkel WJH, Kamerbeek NM, Fraaije MW. 2006. Flavoprotein monooxygenases, a diverse class of oxidative biocatalysts. *J Biotechnol* 124:670–689.
396. Fitch WM. 1987. Of urfs and orfs: A primer on how to analyze derived amino acid sequences. *Cell* 50:329.
397. Kelley LA, Mezulis S, Yates CM, Wass MN, Sternberg MJE. 2015. The Phyre2 web portal for protein modeling, prediction and analysis. *Nat Protoc* 10:845–858.
398. Liu P, Zhang H, Lv M, Hu M, Li Z, Gao C, Xu P, Ma C. 2014. Enzymatic production of 5-aminovalerate from l-lysine using l-lysine monooxygenase and 5-aminovaleramidase. *Sci Rep* 4.

399. Revelles O, Espinosa-Urgel M, Fuhrer T, Sauer U, Ramos JL. 2005. Multiple and interconnected pathways for l-lysine catabolism in *Pseudomonas putida* KT2440. *J Bacteriol* 187:7500–7510.
400. Thrupp LA. 2000. Linking Agricultural Biodiversity and Food Security: The Valuable Role of Sustainable Agriculture. *Int Aff (Royal Inst Int Aff 1944-)* 76:265–281.
401. Patten CL, Glick BR. 2002. Regulation of indoleacetic acid production in *Pseudomonas putida* GR12-2 by the stationary phase sigma factor RpoS. *Can J Microbiol.* 260:6281–6287.

Appendix A

Tables:

Table A 1. Sequence conservation in global multiple sequence alignment of uncharacterized amidases

Alignment Block	Consensus Sequence
1 (amidase signature sequence)	L-x-G-x5-K-x25-A-x2-V-x2-L-x3-G-A-x3-G-x22-N-P-x7- <u>G-G-S-S</u> -x-G-x4-V-A-x8-G-x-D-x-G-G- S -x-R-x-P-A-x2- C -G-x2-G-x2-P- T -x-G-x5-G-x8-D-x2-G-x3-R-x-V-x-D-x9-G-x-D-G-x-D-P-R
2 (C-terminal)	G-x-P-x2-S-x-P-x6-L-P-x-G-x13-L-x6-E

Conserved sites toggled at 90% level. Amino acid residues highlighted in grey are conserved in all 445 amidase sequences that were aligned. The GGSS motif is underlined. Boldface letters represent the catalytic triad. “x” represents variable residues.

Table A 2. Results of Amidase (Ami) Enzyme Assay

Reaction	IAA (ug/mL)	Temperature (°C)
1	132.8	5
2	142.4	10
3	145.2	20
4	153.7	30
5	156.1	35
6	153.3	40
7	146.2	45
8	91.4	50

Reaction	IAA (ug/mL)	pH
1	1240	5.0
2	1704	6.0
3	2297	7.5
4	1455	8.0
5	1101	8.5
6	1115	9.0

The enzyme activity was assayed in a 1ml reaction mixture containing 50 µg of purified Ami, 1 mM IAM substrate, and 50 mM KH₂PO₄ (pH 7.5) buffer. Reaction mixtures were allowed to proceed for 1 h. Samples were analyzed by high pressure liquid chromatography (HPLC).

Table A 3. IAA Production by wild-type and mutant *Pseudomonas* sp. UW4 strains

Sample	[IAA] ug/mL
Wild-type	0.77 ±0.08
<i>iaaM</i>	0.73 ±0.14
<i>aux^c</i>	0.86 ±0.02
<i>ami</i>	1.04 ±0.07
<i>nit</i>	0.84 ±0.07
<i>nthA</i>	0.78 ±0.06
<i>nthB</i>	0.81 ±0.02
<i>nthB-iaaM</i>	0.93 ±0.004
<i>nthB-ami</i>	1.09 ±0.18
<i>nthB-nit</i>	0.95 ±0.09
<i>iaaM-ami</i>	0.82 ±0.11
<i>iaaM-aux^c</i>	0.67 ±0.16
<i>nit-ami</i>	0.77 ±0.09

Production of IAA by wild-type and IAA deletion mutants of *Pseudomonas* sp. UW4. Strains were grown for 72 hours in DF minimal media with 500 ug/mL L-Trp. The culture supernatant was collected for HPLC analysis. Each value represents the mean of three replicates ± standard error.

Table A 4. Potential IPyA pathway aminotransferase enzymes identified in the genome of UW4

Functional Annotation	NCBI Accession No.
aspartate aminotransferase family protein	WP_007975624.1
	WP_015093348.1
	WP_015093516.1
	WP_015093588.1
	WP_015094192.1
	WP_015094945.1
	WP_015095251.1
	WP_015095646.1
	WP_015096501.1
	WP_015096948.1
	WP_015097089.1
	WP_015097273.1
aspartate/tyrosine/aromatic aminotransferase	WP_015095910.1
	WP_015096285.1
aminotransferase	WP_015093046.1
	WP_041474860.1
PLP-dependent aminotransferase	WP_015093563.1
	WP_015093574.1
	WP_015093632.1

Functional Annotation	NCBI Accession No.
	WP_015093951.1 WP_007973513.1 WP_015094110.1 WP_015094166.1 WP_015094803.1 WP_015095047.1 WP_015095189.1 WP_015095305.1 WP_015095334.1 WP_015095393.1 WP_015095795.1 WP_015096115.1 WP_015096424.1 WP_015096564.1 WP_015096856.1 WP_015097357.1 WP_015097406.1
branched-chain amino acid aminotransferase	WP_041474782.1 WP_015095447.1
adenosylmethionine-8-amino-7-oxononanoate aminotransferase	WP_015097184.1

Figures:

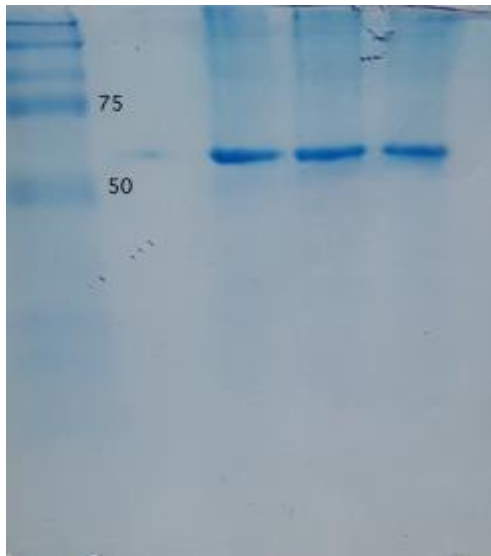


Figure A 1. SDS-PAGE of purified Ami from *Pseudomonas* sp. UW4

The amidase (Ami) from UW4 was overexpressed in *E. coli* BL21 and purified using Ni affinity chromatography. The eluted protein was analyzed on a 10% gel. The left lane contains a protein size marker. All three lanes contain Ami protein samples. The estimated protein size is ~54 kDa.

Figure A 2. Conserved Residues in global multiple sequence alignment of uncharacterized amidases

Only the Ami protein sequence is shown here. Sites highlighted in black represent show residues that are conserved in 90% of the 445 amidases in the alignment, while an asterisk (*) denotes residues that are conserved in all of the amidases in the alignment. The GGSS motif is boxed in red. The highest sequence conservation is seen in amidase signature sequence region highlighted with the blue line. The numbers show the positions/length of the sequence.

40 AVDLVDELDTFVYQESGKRFSDSHLELHAWYVTEVIRGAREGILASKTVALLKDRISLADVIFKIDLSAATLEQFVAKFGATVYKLEEDG 132

133 VTLEKATCEHYGLDQDQHTSDFAPVHVFYFHQFALDQDLSQSAALVAQVVDLAVQDQDQDLEITAFGQTYQWKTTHQLVYVTDVYKLE 224

225 FTIDHAGQITRNVDHMLNLEVNAADQDLDVFKRATGVDAVCOLENSVQLRVDLCEQSLAMGGRVADQVFAKLEVLDQAFVEEYK 318

319 AEHLLAGSEWYIQCEDLTHQWMTQVQASFRWKGLEVDQLLQKQAWVEQDLEKSLKLNHFQDYLQLEHYRQVFLKQGNIAKFRAGVDFAD 413

414 ETVDLVHPTVPIAQRHAFGGCSITEVVAKALEMIGNIFKQDTGHLAMSTFGGLVVDLFLQLEFVQKHFAEGTIYQAAAFEATDQWATL 505

Figure A 3. Predicted secondary structure of amidase from strain UW4 and *Rhodococcus* sp. N771

The predicted secondary structure of Ami (query sequence) vs. the amidase from *Rhodococcus* sp. N771 (template sequence). Confidence level = 100%, Sequence identity= 47%, resolution= 2.32 angstroms, number of aligned residues= 501. Confidence represents the probability (from 0 to 100%) that the match between our sequence and the template is a true homology. Sequence identity is the proportion of our protein residues equivalenced to identical template residues in the generated alignment.

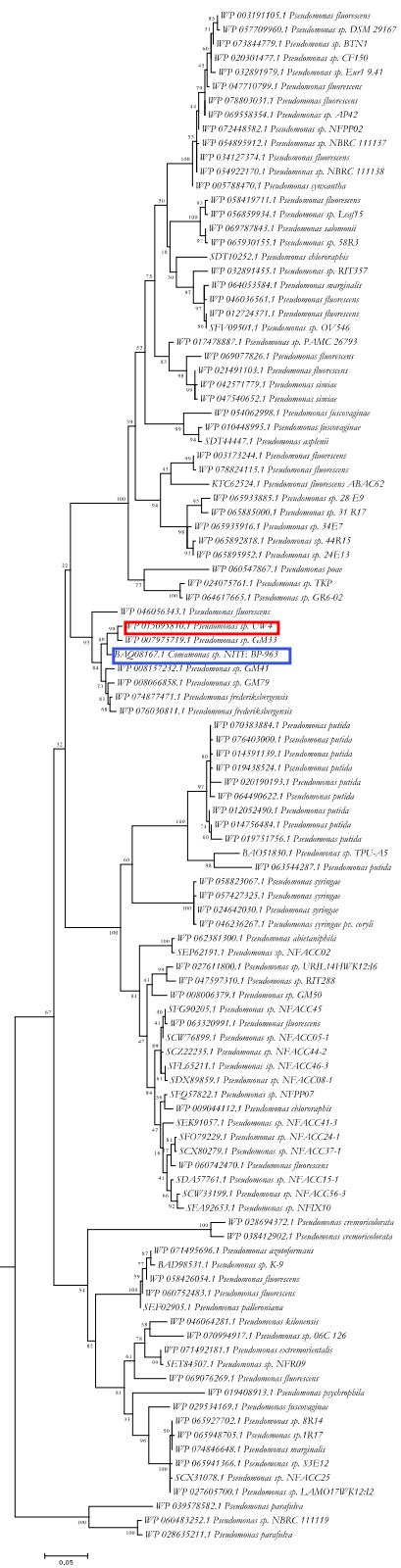
Green helices represent α -helices, blue arrows indicate β -strands and faint lines indicate coil. G = 3-turn helix, I = 5-turn helix, T = hydrogen bonded turn, B = residue in isolated β -bridge (single pair β -sheet hydrogen bond formation), S = bend. Identical residues in the alignment are highlighted with a grey background.

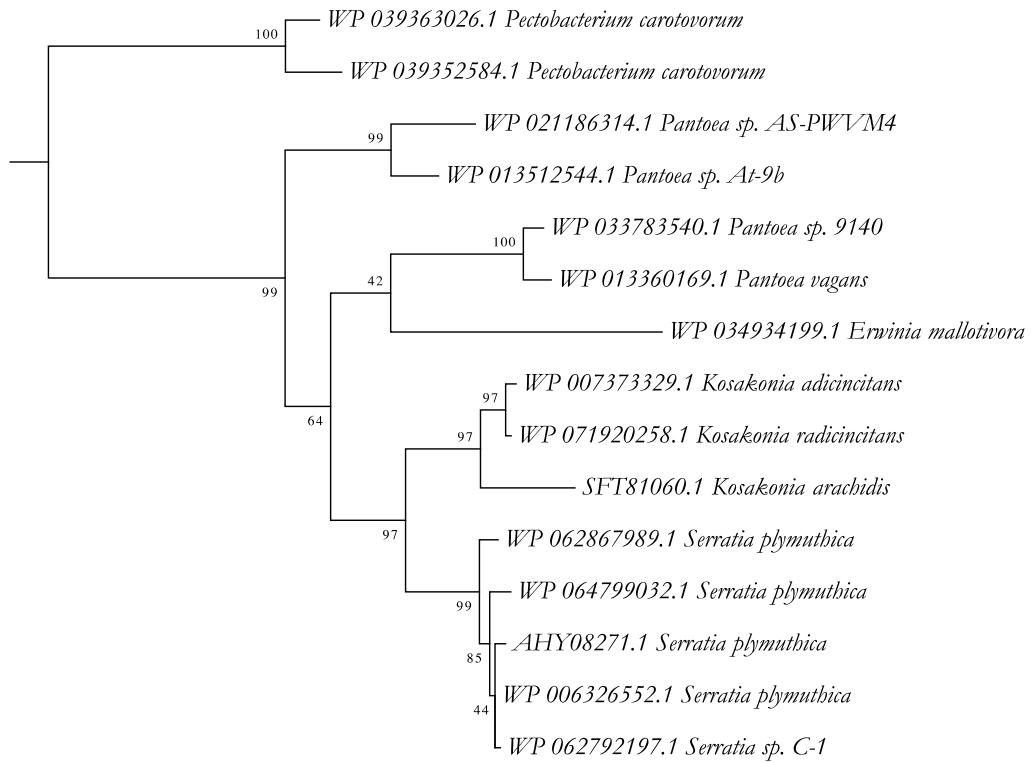
 Deletion relative to template



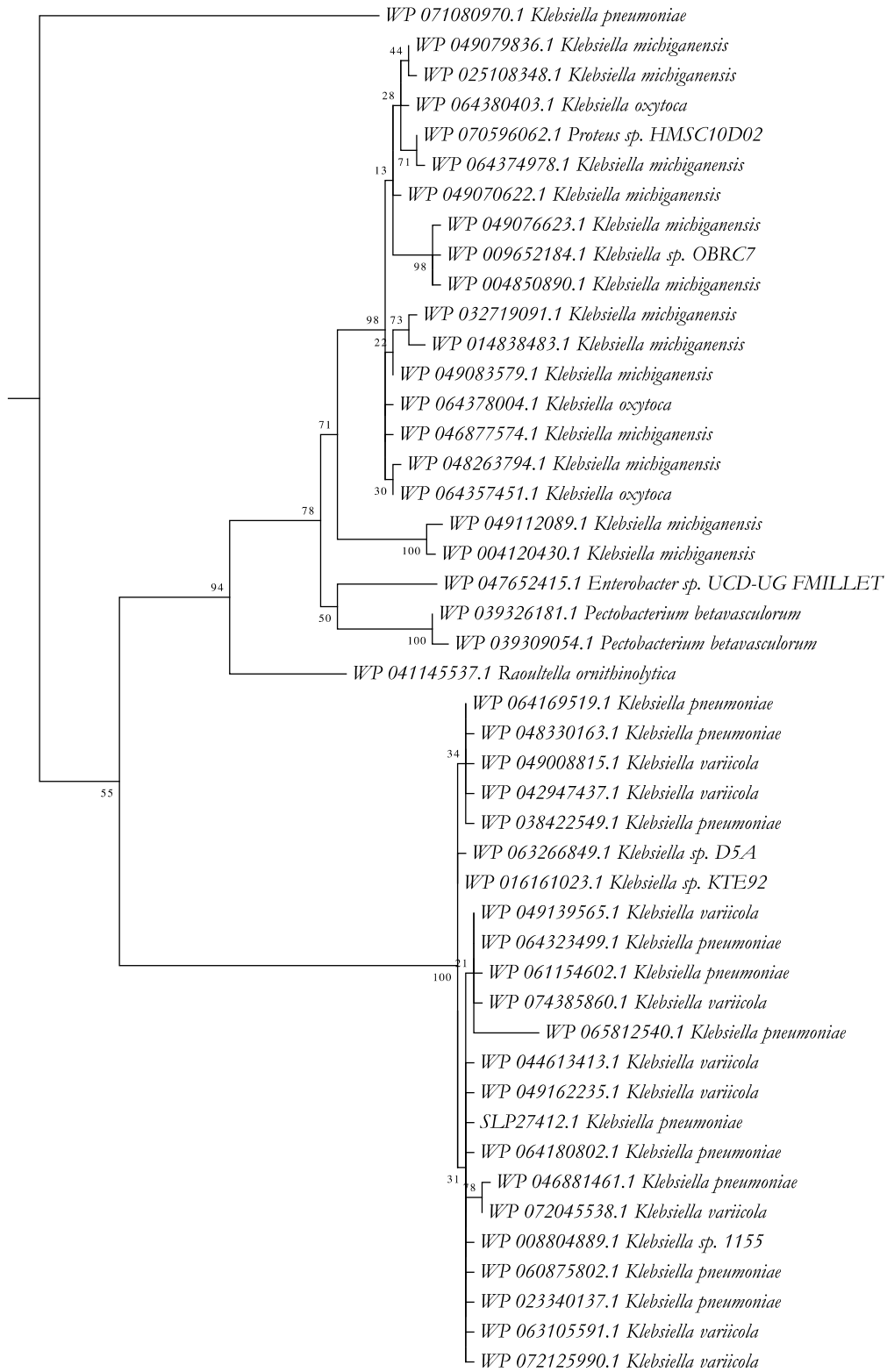
Figure A 4. Molecular Phylogenetic Analysis of uncharacterized Amidases

The figure shows several sub-trees of the main ML tree. The evolutionary history was inferred by using the Maximum Likelihood (ML) method based on the JTT matrix-based model (286). The percentage of trees in which the associated taxa clustered together is shown next to the branches. Initial tree(s) for the heuristic search were obtained automatically by applying Neighbor-Join and BioNJ algorithms to a matrix of pairwise distances estimated using a JTT model, and then selecting the topology with superior log likelihood value. The tree is drawn to scale, with branch lengths measured in the number of substitutions per site. The tree is mid-point rooted. The analysis involved 445 amino acid sequences. All positions containing gaps and missing data were eliminated. There were a total of 420 positions in the final dataset. Evolutionary analyses were conducted in MEGA7 (265)

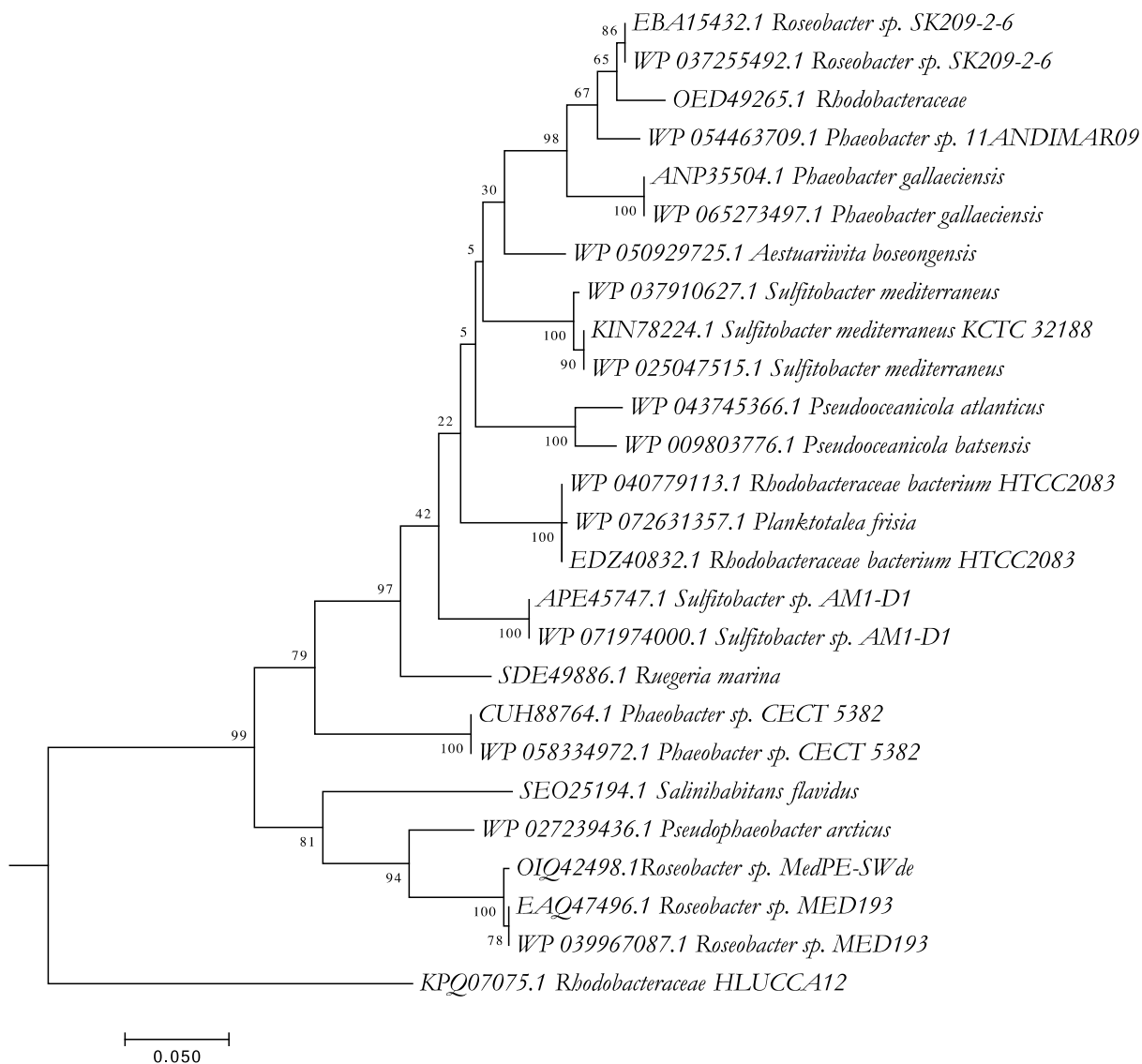


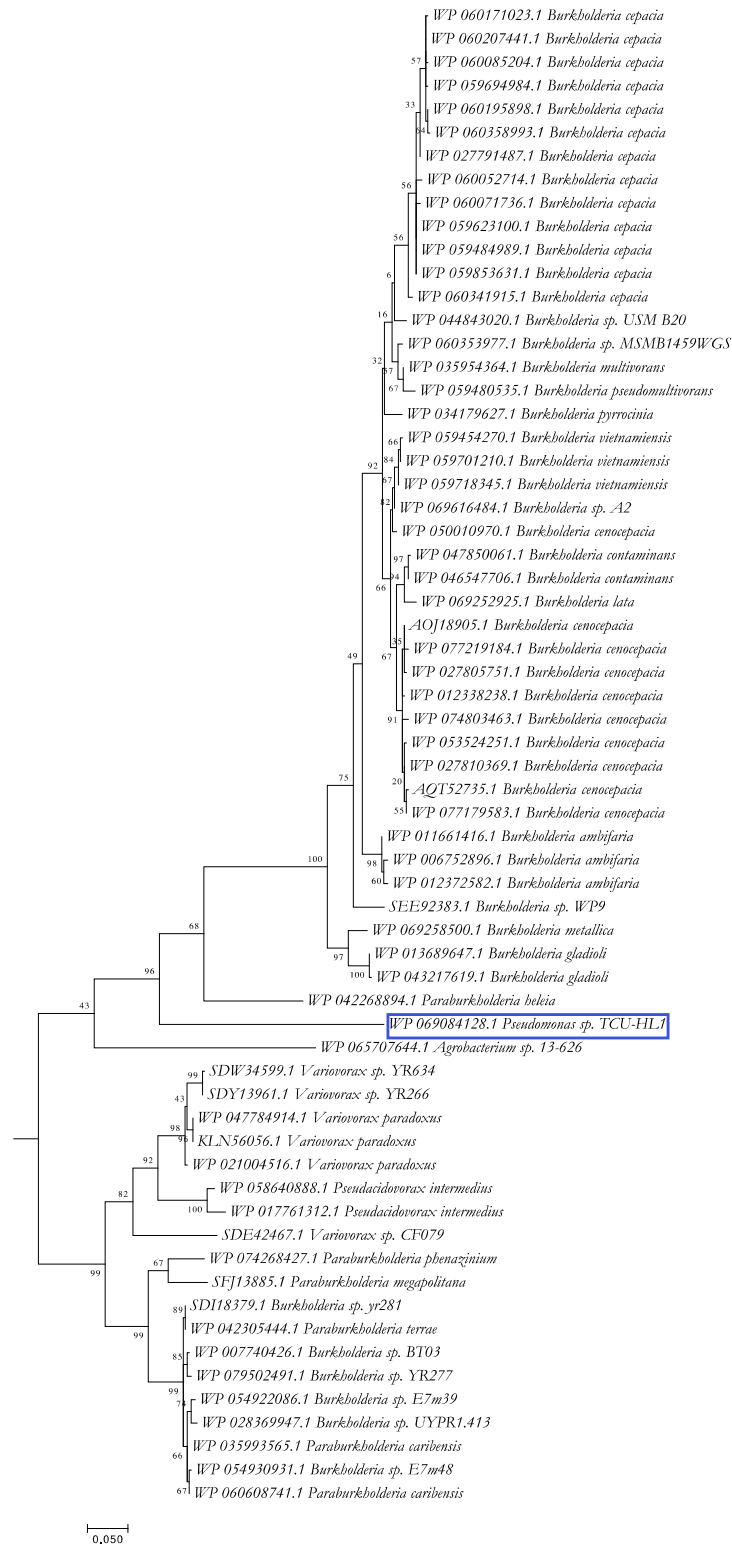


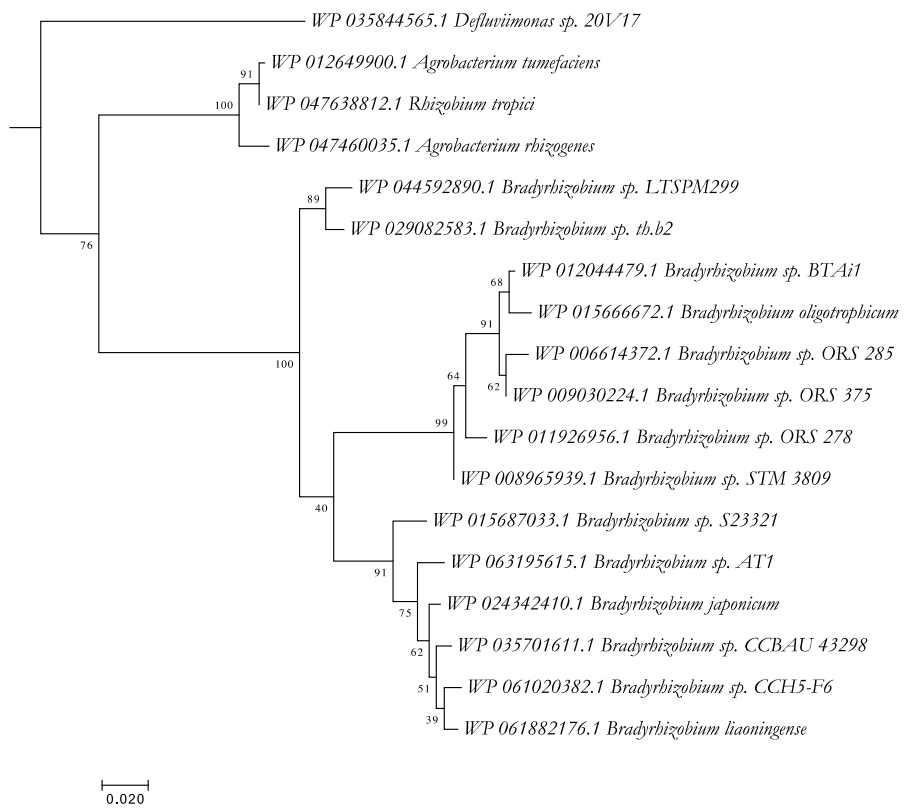
0.050

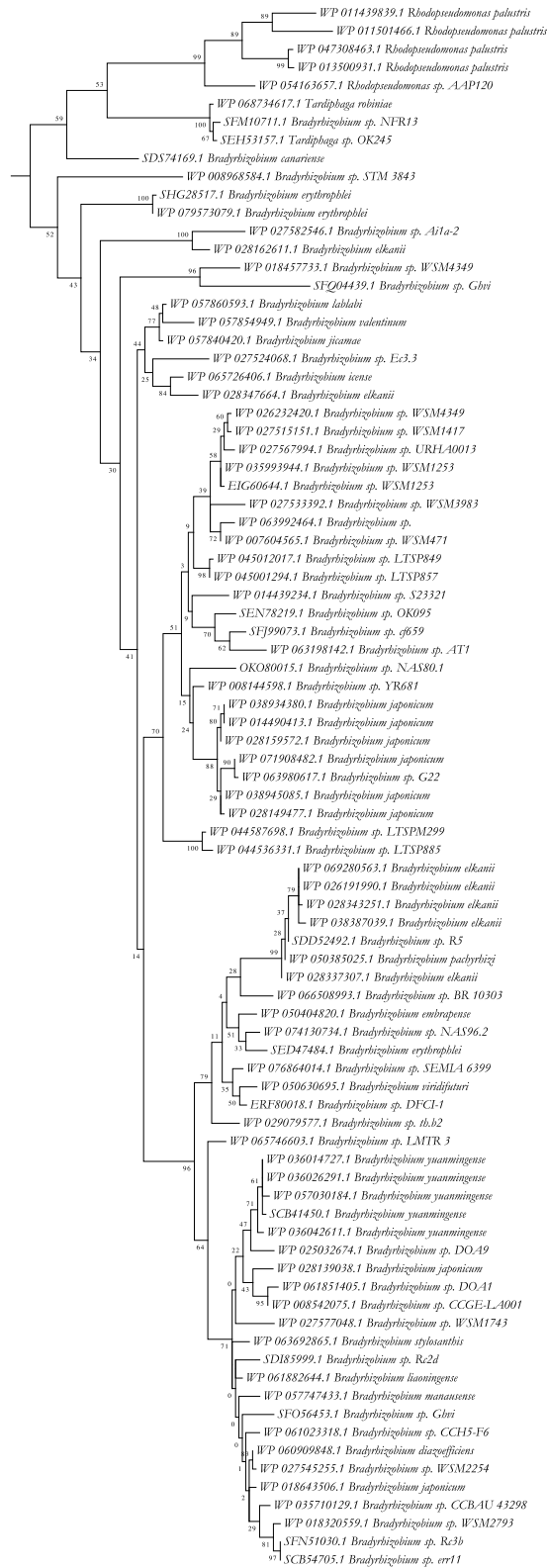


0.020









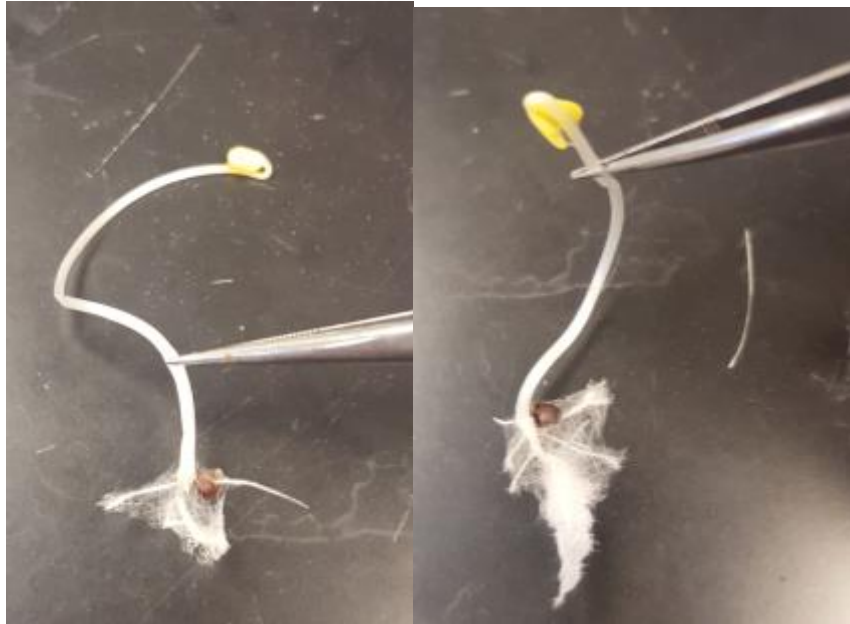


Figure A 5. Root hair growth of Canola Seedlings

Root hair growth of canola seedlings were inoculated with wild-type UW4 (left) and UW4:nit, a transformant strain (right) which contains a second copy of the *nit* gene expressed from a plasmid. The transformant produces ~3-fold more IAA than the wild-type in the presence of exogenous tryptophan (500 $\mu\text{g}/\text{mL}$). Seedlings were grown for 3 days in growth pouches as described in Chapter 3, section 3.2.8.

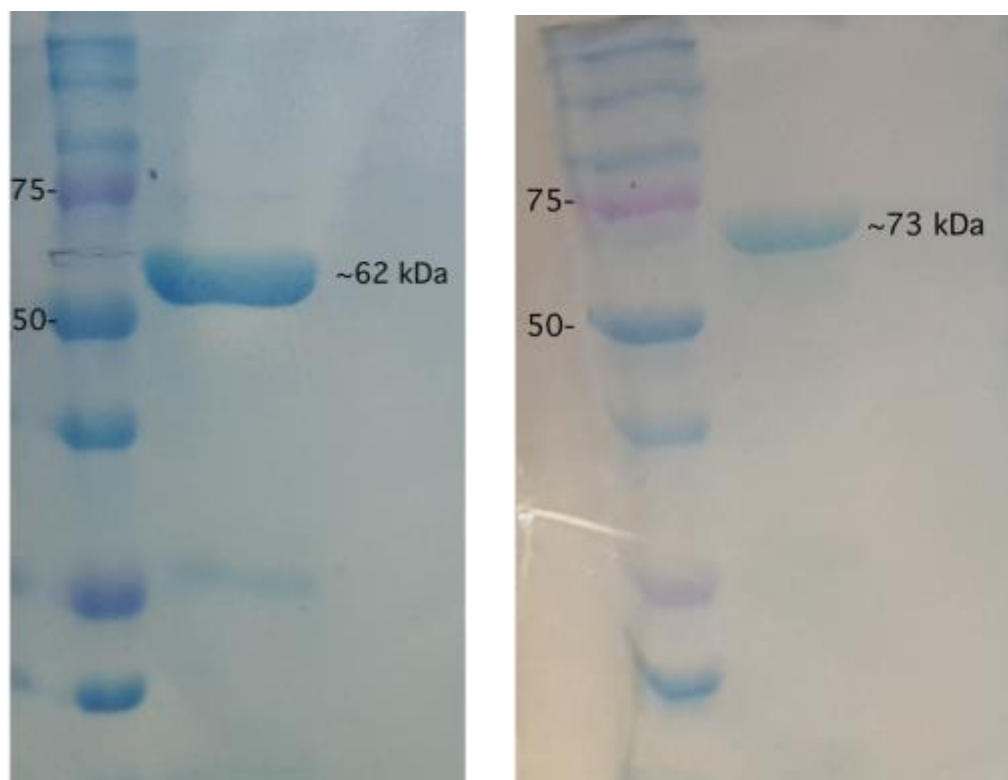
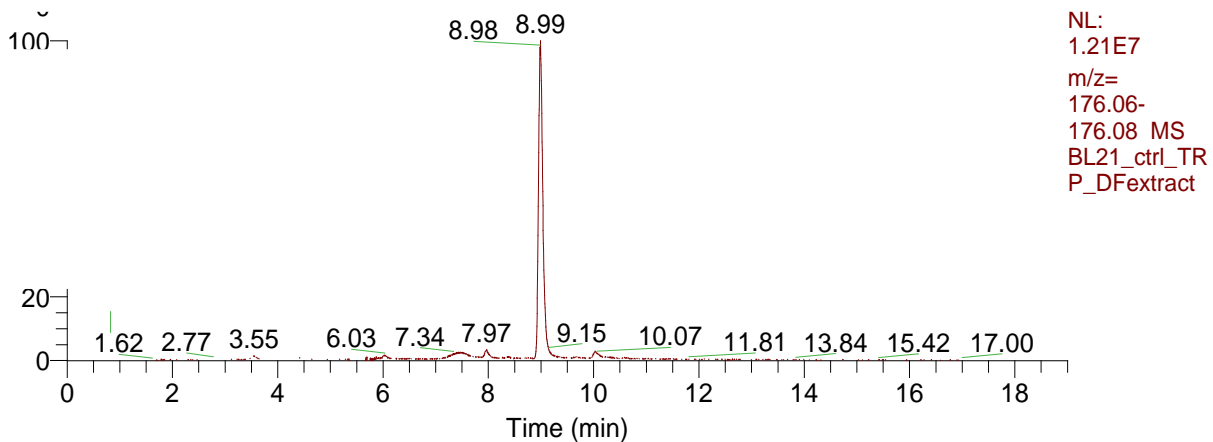


Figure A 6. SDS PAGE of purified IaaM and Aux

IaaM (left) and Aux (right) proteins from UW4 were overexpressed in *E. coli* BL21 and purified using Ni-affinity chromatography. The eluted proteins were analyzed on a 10% SDS gel. The left lane contains a protein size marker. The estimated protein size of IaaM is ~62 kDa and Aux is ~73 kDa.

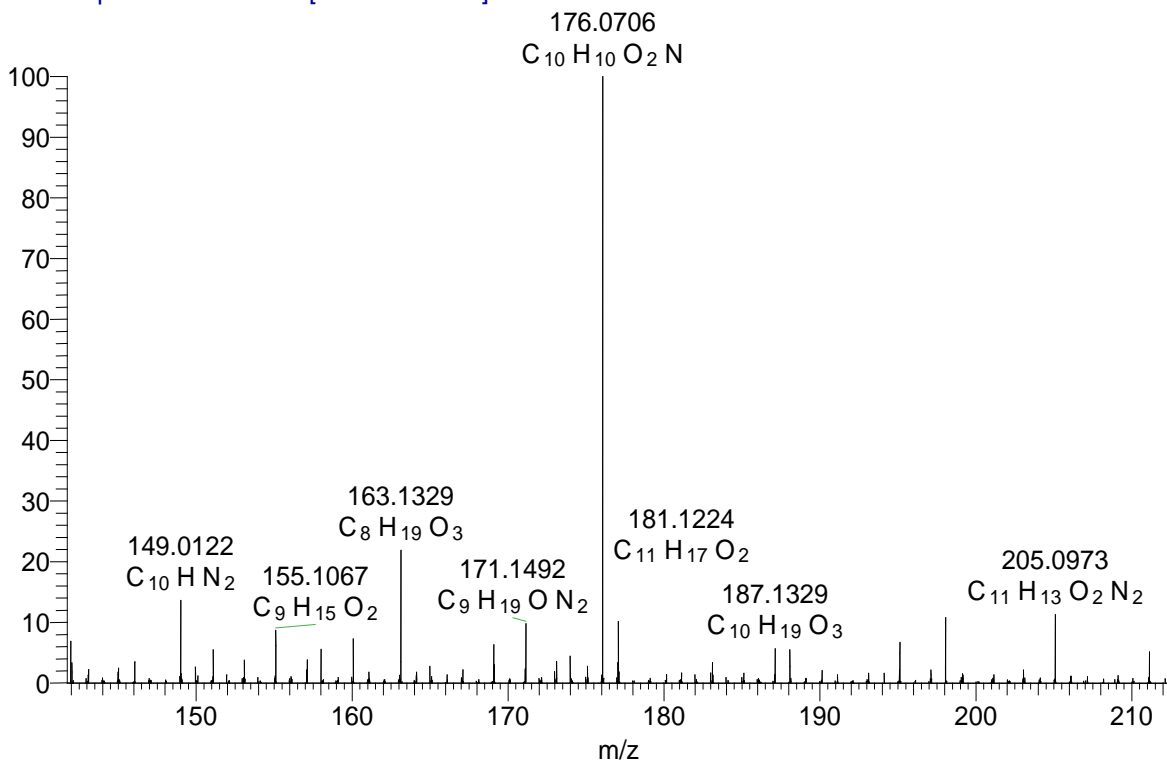
Figure A 7. LC-MS-MS chromatogram for *E. coli* BL21 Control

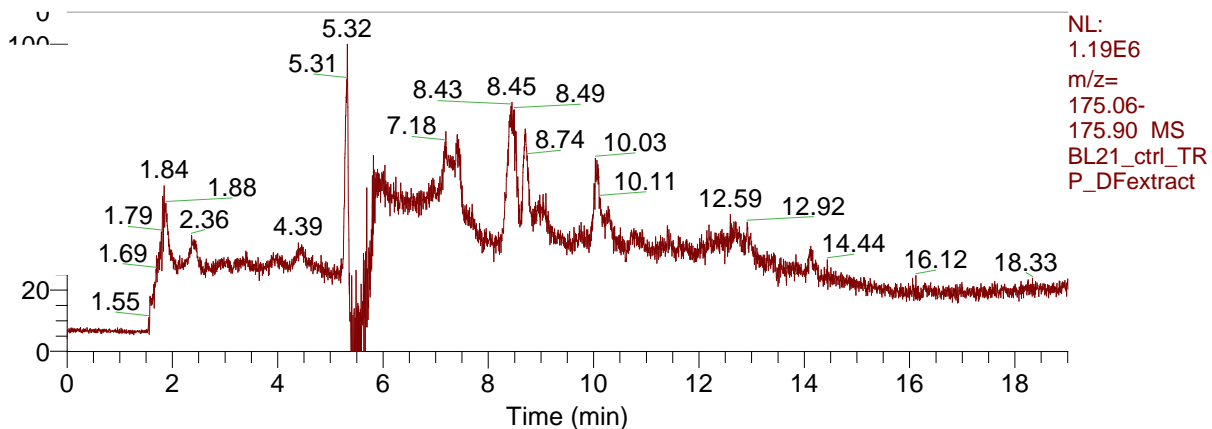
The bacterial cultures were grown in tryptic soy broth (TSB) for 24 hours at 37°, with Trp (500 µg/mL) supplementation. The culture extract was prepared as described in Section 5.2.9 and analyzed by LC-MS-MS. Both IAA (m/z = 176.0706, retention time=8.98 min) and IAM (m/z= 175.0867, retention time= 7.12 min) were detected.



NL:
1.21E7
m/z=
176.06-
176.08 MS
BL21_ctrl_TR
P_DFextract

BL21_ctrl_TRP_DFextract #2019 RT: 9.00 AV: 1 NL: 1.14E7
T: FTMS + p ESI Full lock ms [140.00-500.00]





NL:
1.19E6
m/z=
175.06-
175.90 MS
BL21_ctrl_TR
P_DFextract

BL21_ctrl_TRP_DFextract #1578-1691 RT: 7.03-7.53 AV: 114 NL: 2.54E5
T: FTMS + p ESI Full lock ms [140.00-500.00]

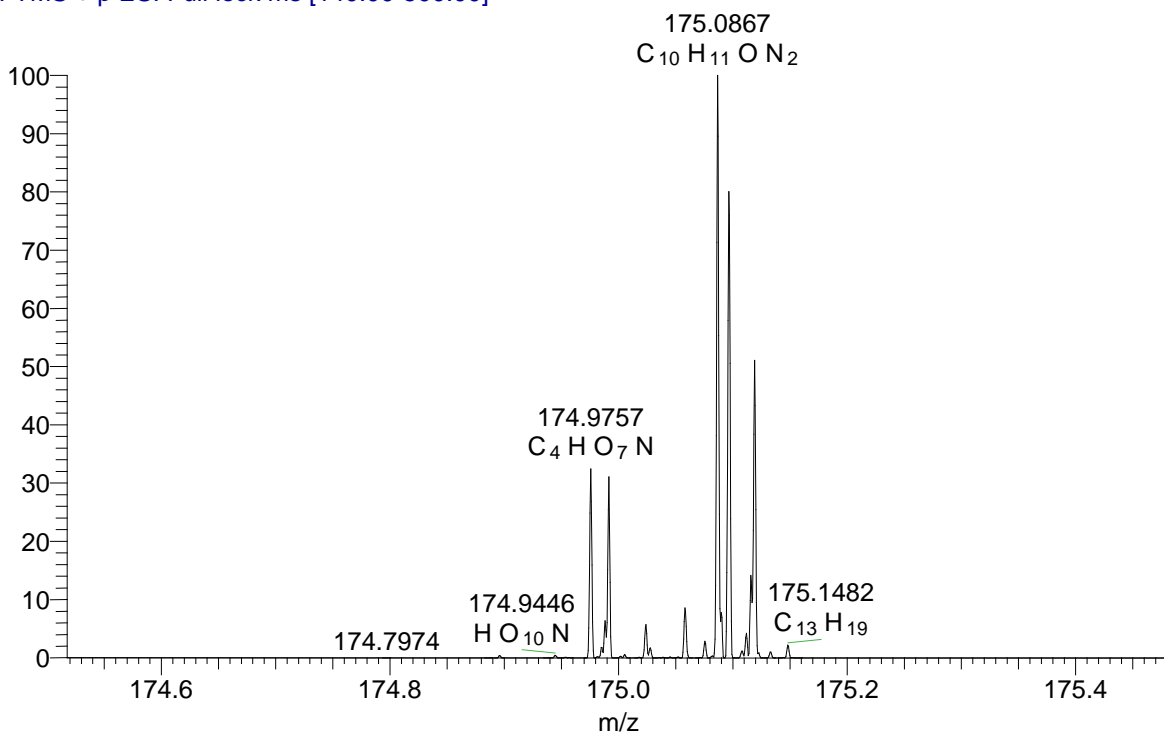
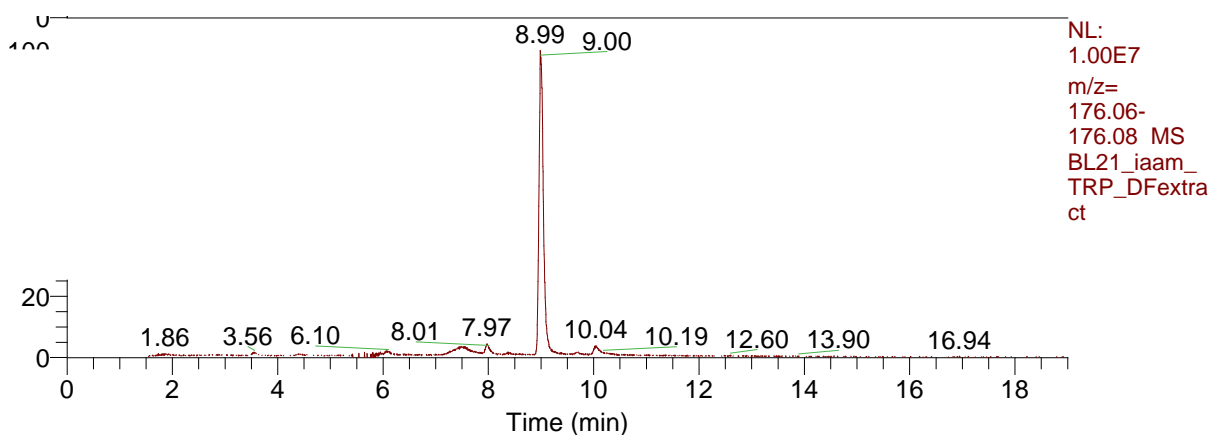
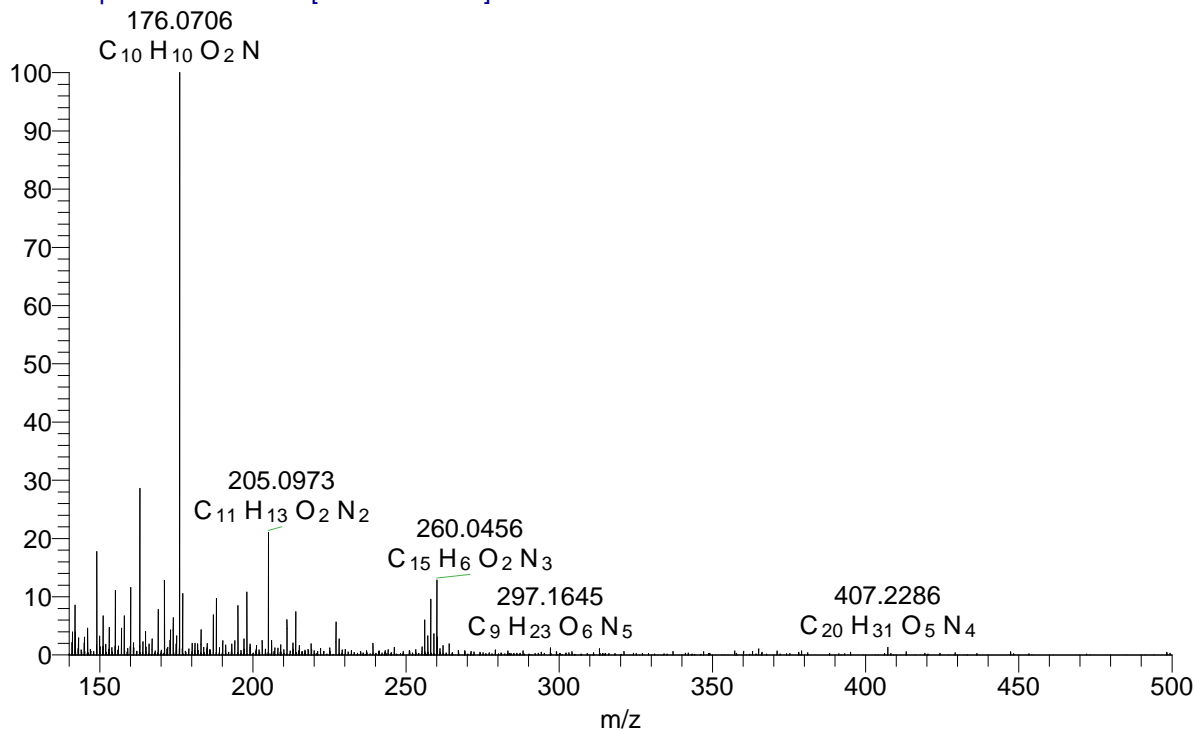


Figure A 8. LC-MS-MS chromatogram for *E. coli* BL21:IaaM

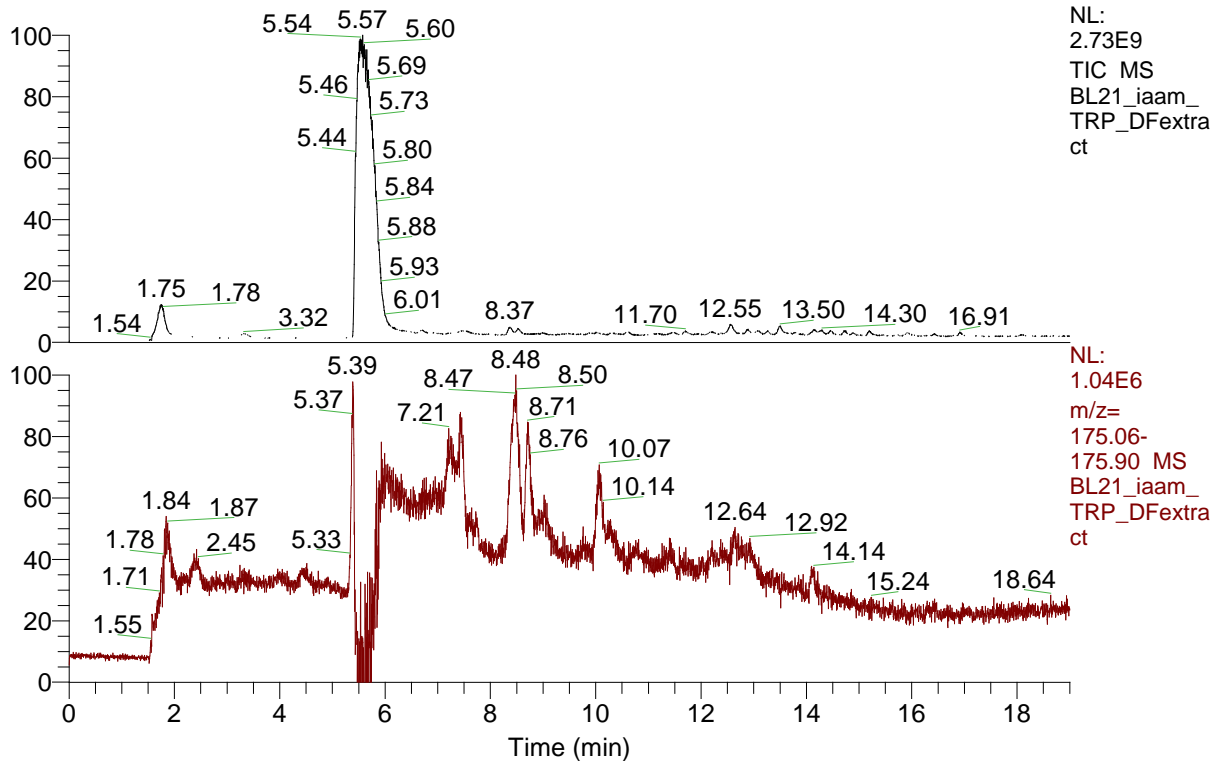
The bacterial cultures were grown in tryptic soy broth (TSB) for 24 hours at 37°, with Trp (500 ug/mL) supplementation. The culture extract was prepared as described in Section 5.2.9 and analyzed by LC-MS-MS. Both IAA (m/z = 176.0706, retention time=8.98 min) and IAM (m/z= 175.0867, retention time= 7.12 min) were detected.



BL21_iaam_TRP_DFextract #2021 RT: 9.01 AV: 1 NL: 9.53E6
T: FTMS + p ESI Full lock ms [140.00-500.00]



RT: 0.00 - 19.00



BL21_iaam_TRP_DFextract #1580-1689 RT: 7.04-7.53 AV: 110 NL: 2.77E5
T: FTMS + p ESI Full lock ms [140.00-500.00]

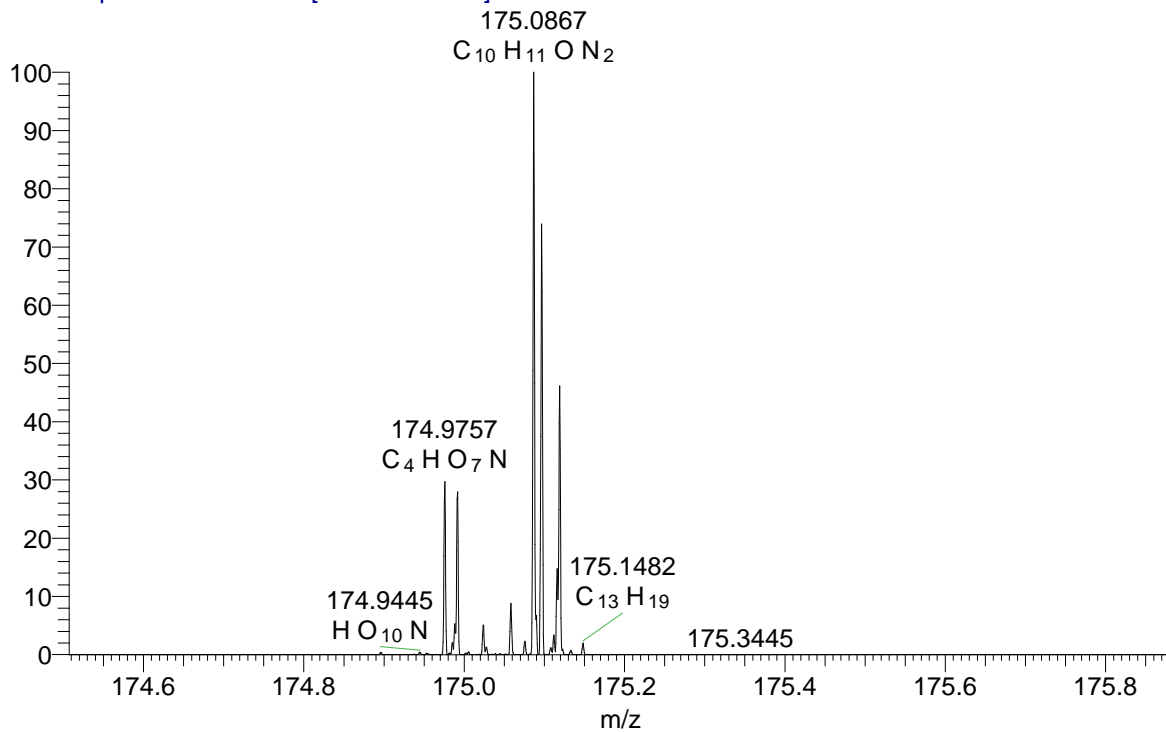
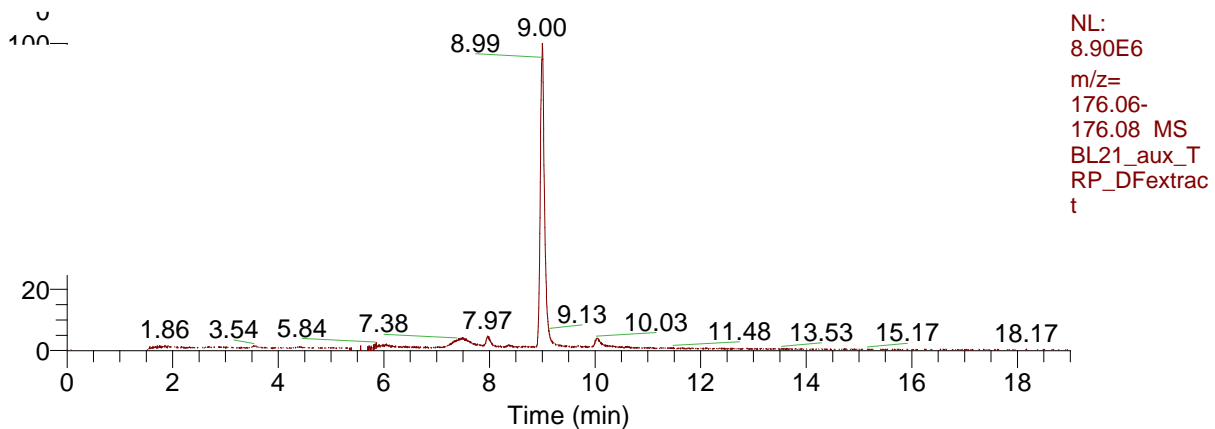


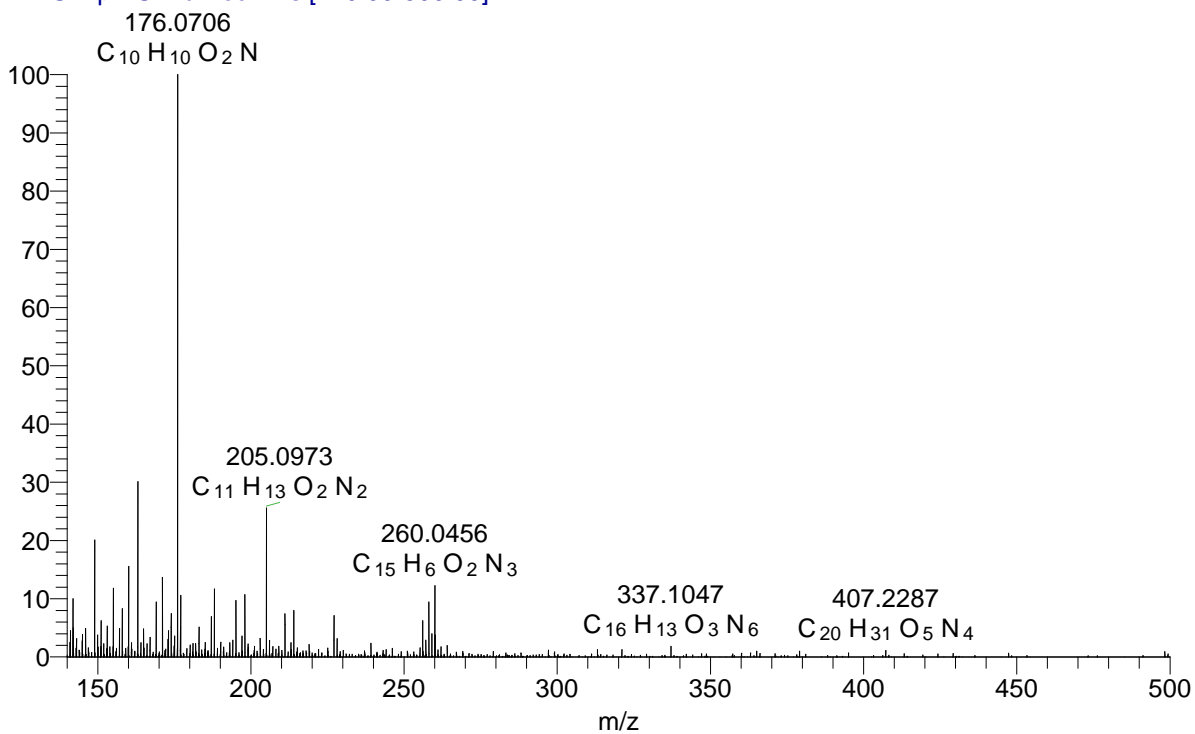
Figure A 9. LC-MS-MS chromatogram for *E. coli* BL21:Aux

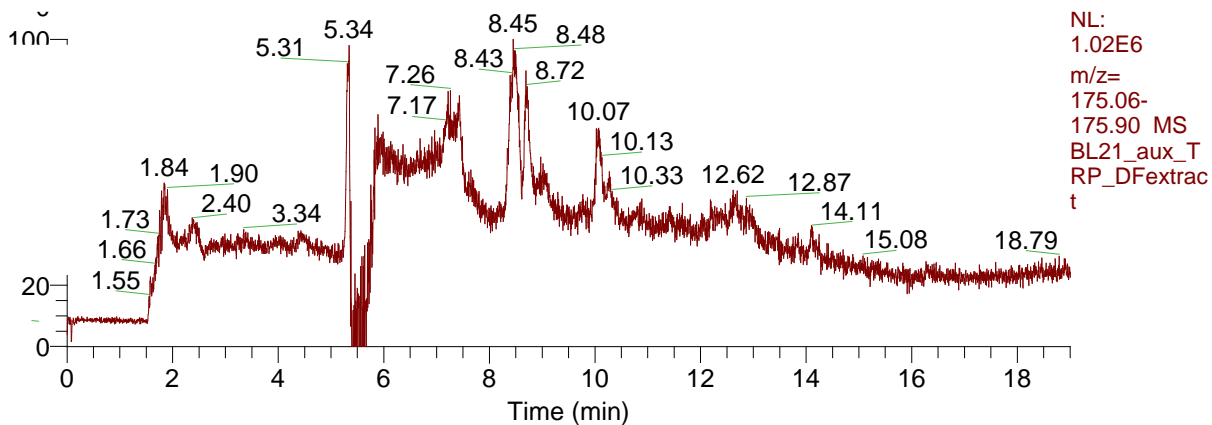
The bacterial cultures were grown in tryptic soy broth (TSB) for 24 hours at 37°, with Trp (500 µg/mL) supplementation. The culture extract was prepared as described in Section 5.2.9 and analyzed by LC-MS-MS. Both IAA (m/z = 176.0706, retention time=8.98 min) and IAM (m/z= 175.0867, retention time= 7.12 min) were detected.



NL:
8.90E6
m/z=
176.06-
176.08 MS
BL21_aux_T
RP_DFextrac
t

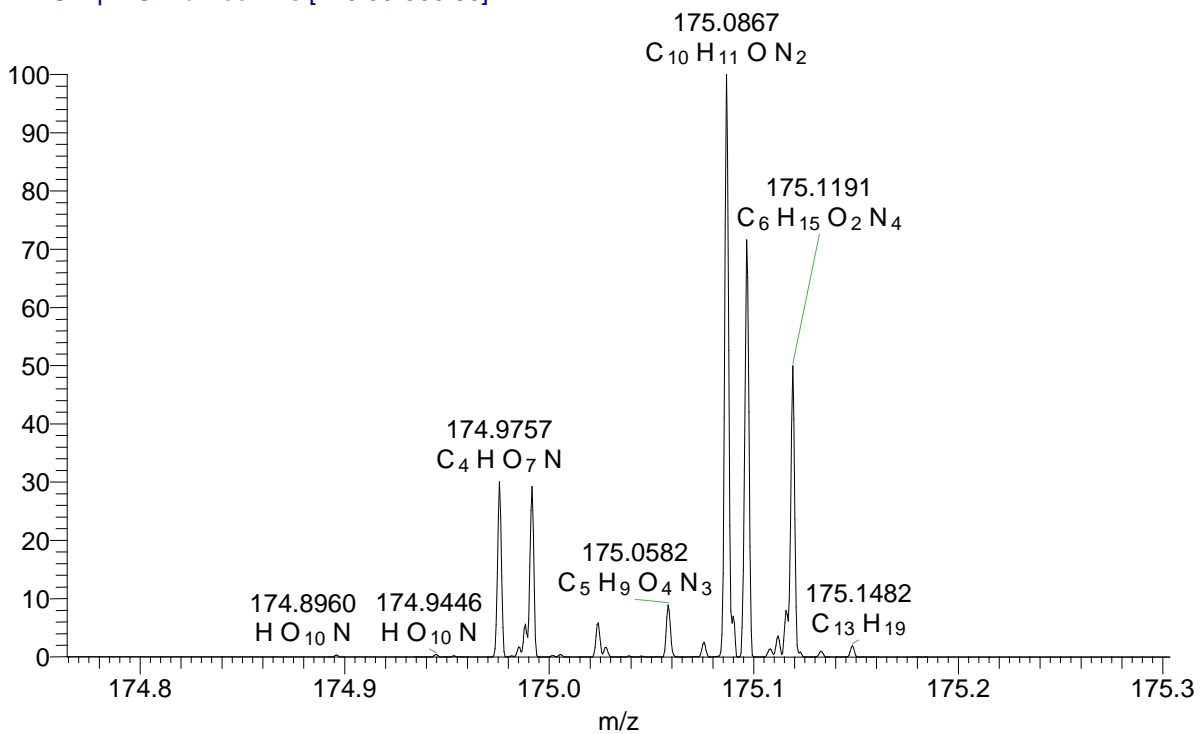
BL21_aux_TRP_DFextract #2022 RT: 9.01 AV: 1 NL: 8.41E6
T: FTMS + p ESI Full lock ms [140.00-500.00]





NL:
1.02E6
m/z=
175.06-
175.90 MS
BL21_aux_T
RP_DFextrac
t

BL21_aux_TRP_DFextract #1576-1686 RT: 7.02-7.51 AV: 111 NL: 2.74E5
T: FTMS + p ESI Full lock ms [140.00-500.00]



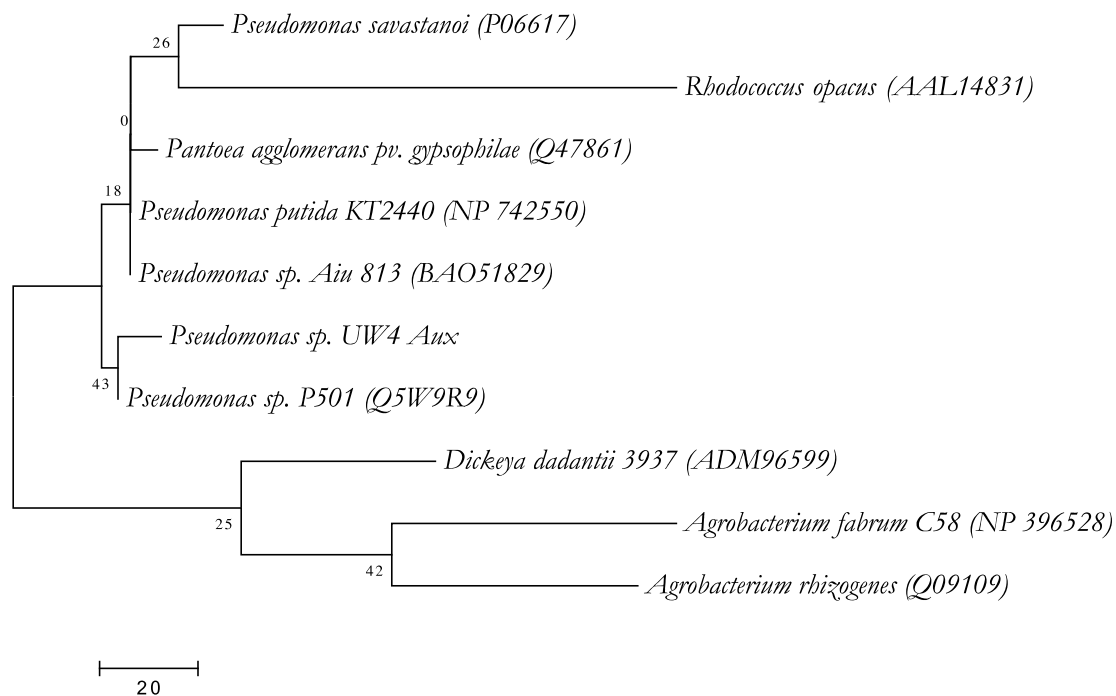


Figure A10. Maximum Likelihood Tree for Aux Protein

The evolutionary history for Aux was inferred by using the Maximum Likelihood method based on the JTT matrix-based model. The tree with the highest log likelihood (-14117.4089) is shown. The percentage of trees in which the associated taxa clustered together is shown next to the branches. Initial tree(s) for the heuristic search were obtained automatically by applying Neighbor-Join and BioNJ algorithms to a matrix of pairwise distances estimated using a JTT model, and then selecting the topology with superior log likelihood value. The tree is drawn to scale, with branch lengths measured in the number of substitutions per site. The tree is mid-point rooted. The analysis involved 10 amino acid sequences. All positions containing gaps and missing data were eliminated. There were a total of 534 positions in the final dataset. Evolutionary analyses were conducted in MEGA7.